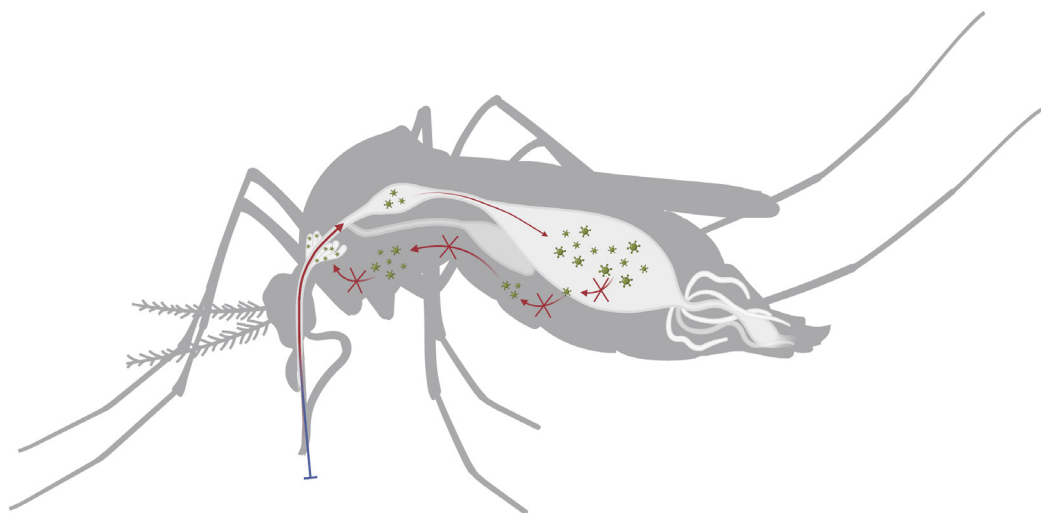




DOCTORAL THESIS NO. 2022:18
FACULTY OF VETERINARY MEDICINE AND ANIMAL SCIENCE

Insect-specific viruses as control measures for West Nile virus infection of animals and humans

PONTUS ÖHLUND



Insect-specific viruses as control measures for West Nile virus infection of animals and humans

Pontus Öhlund

Faculty of Veterinary Medicine and Animal Science
Department of Biomedical Sciences and Veterinary Public Health
Uppsala



SWEDISH UNIVERSITY
OF AGRICULTURAL
SCIENCES

DOCTORAL THESIS

Uppsala 2022

Acta Universitatis Agriculturae Sueciae
2022:18

Cover: A mosquito immune to arbovirus-infection via a viremic blood meal.
(Biorender.com)

Cover: Description of photograph (if any)
(photo: N. Name)

ISSN 1652-6880

ISBN (print version) 978-91-7760-911-7

ISBN (electronic version) 978-91-7760-912-4

© 2022 Pontus Öhlund, Swedish University of Agricultural Sciences

Uppsala

Print: SLU Grafisk Service, Uppsala 2022

Insect-specific viruses as control measures for West Nile virus infection of animals and humans

Abstract

Mosquitoes serve as vector for many medically important viruses and their associated diseases cause a major health burden across the globe. Mosquito-borne viruses are often maintained in nature through an enzootic cycle, in which the mosquito acquire the virus through a viremic blood meal of a vertebrate reservoir. Furthermore, the virus need to establish a systemic infection in the mosquito and replicate in the salivary glands before it can be transmitted to a new host during a blood meal. This is key for developing novel control strategies that target the mosquito's ability to carry and transmit pathogenic viruses. However, the interaction between viruses and their mosquito host and its antiviral defence mechanisms remain unclear. The overall aim of this thesis was to investigate the use of a group of viruses known as insect-specific viruses (ISVs) to manipulate the mosquito antiviral immunity and elucidate important antiviral mechanisms, with the ultimate goal to increase the mosquito host's resistance to infection of medically important viruses. A viral metagenomic approach has initially been used to characterize the virome of mosquitoes collected in mid-east Sweden, revealing a broad range of viral families. Furthermore, the ISV interaction and effect on the mosquito host was studied in a mosquito-derived cell line. This showed that the two studied ISVs (Lammi- and Hanko virus) triggered a robust RNA-interference mediated antiviral immune response and a broad range of heat-shock proteins during acute infection. A prior ISV (Lammi virus) infection was shown to interfere with the replication of a secondary arbovirus-infection (West Nile virus) and potential gene targets for modification were identified.

Keywords: Insect-specific virus, mosquito, transmission, control strategies

Author's address: Pontus Öhlund, SLU, Department of Biomedical Sciences and Veterinary Public Health, Box 7028, 750 07, Uppsala, Sweden

Insekt-specifika virus som kontrollåtgärd för West Nile virus infektion hos djur och människor

Sammanfattning

Myggor tjänar som vektor för många medicinskt viktiga virus och dem associerade virussjukdomarna orsakar en stor hälsobörda över hela världen. Myggburna virus bibehålls i naturen genom en enzootisk cykel, där myggan förvärvar viruset genom ett viremiskt blodmål från ett infekterat ryggradsdjur. Dessutom så måste viruset etablera en systemisk infektion i myggan samt infektera och replikera i spottkörtlarna innan viruset kan överföras till en ny värd via ett blodmål. Detta är centralt för nya kontrollstrategier som riktar in sig på myggans förmåga att bära och överföra patogena virus. Dock, så är interaktionen mellan myggvärderna och viruset samt viktiga antivirala försvarsmekanismer hos myggan fortfarande oklara. Det övergripande målet med denna avhandling var att undersöka användningen av en grupp av virus som kallas insekt-specifika virus (ISVs) för att manipulera myggans antivirala immunitet och belysa viktiga antiviral mekanismer i myggan, med målet att öka myggvärdens motståndskraft mot medicinskt viktiga myggburna virus. Ett viralt metagenomiskt tillvägagångssätt har använts för att karakterisera viromet hos myggor som samlats in i östra Svealand, vilket visade ett brett spektrum av virus från många olika virusfamiljer. Dessutom, studerades effekten av en akut infektion av ISVs (Lammi- och Hanko virus) i en myggcellinje, vilket visade att de ISVs utlöste ett robust RNA-interferens medierat antiviralt immunsvar samt en rad olika värmechocksproteiner i myggvärderna. Dessutom visades att myggceller infekterade med ett ISV (Lammi virus) hindrade virusreplikation av en sekundär arbovirusinfektion (West Nile virus) och potentiella gener för modifiering i myggan upptäcktes.

Keywords: Insekt-specifika virus, myggor, spridning, kontrollstrategier

Författarens adress: Pontus Öhlund, SLU, Institutionen för biomedicin och veterinär folkhälsovetenskap, Box 7028, 750 07, Uppsala, Sweden

Dedication

For a world were mosquitoes are no longer deadly, just annoying

Contents

List of publications.....	9
Publications not included in this thesis.....	11
Abbreviations	13
1. Introduction.....	15
1.1 Mosquito-borne virus transmission	15
1.2 Mosquito's antiviral immunity.....	16
1.2.1 RNA-interference (RNAi) pathways.....	17
1.2.2 JAK-STAT, Toll and Imd pathways.....	19
1.2.3 Other innate immune responses	21
1.3 Insect-specific viruses.....	22
1.3.1 Insect-specific flavivirus.....	23
1.4 West Nile virus.....	26
1.5 Control strategies.....	28
1.5.1 Wolbachia as a biocontrol agent	29
1.5.2 Genetically modified vectors.....	29
1.5.3 ISVs in control strategies.....	30
2. Aims of this thesis.....	33
3. Material and Methods	35
3.1 Mosquito collection (Paper I).....	35
3.2 Metagenomic pre-sequencing preparation (Paper I).....	36
3.3 Metagenomic sequencing and analysis (Paper I).....	37
3.4 Mosquito cell lines and culture conditions (Paper II and III)	38
3.5 Viruses (Paper II and III).....	38
3.6 <i>In vitro</i> infections (Paper II and III).....	39
3.7 Quantification of viral RNA copies of virus stocks and supernatant (Paper II and III).....	39
3.8 Small and large RNA extraction (Paper I and II).....	40
3.9 Small RNA sequencing and analysis (Paper II).....	40

3.10	Transcriptomics sequencing and analysis (Paper III)	41
4.	Results and discussion	43
4.1	Mosquito collection	43
4.2	The Swedish mosquito virome	44
4.3	Characterization of RNA viruses discovered	46
4.4	Small RNA sequencing	47
4.5	RNAi-mediated immunity to ISFV infection	48
4.6	Transcriptomics of ISFV and arbovirus infection	51
4.7	Altered gene expression upon LamV infection	52
4.8	Altered gene expression upon WNV infection	54
4.9	Altered gene expression in Dual-infected cells	55
4.10	Prior LamV-infection interference of WNV	57
5.	Conclusion	61
6.	Future perspectives	63
	References	65
	Popular science summary	81
	Populärvetenskaplig sammanfattning	83
	Acknowledgements	85

List of publications

This thesis is based on the work contained in the following papers, referred to by Roman numerals in the text:

- I. **Öhlund P**, Hayer J, Lunden H, Hesson J C, Blomstrom A L (2019). Viromics reveal a number of novel RNA viruses in Swedish mosquitoes. *Viruses*, 11 (11), 1027.
- II. **Öhlund P**, Hayer J, Hesson J C, Blomstrom A L (2021). Small RNA response to infection of the insect-specific Lammi virus and Hanko virus in an *Aedes albopictus* cell line. *Viruses*, 13 (11), 2181.
- III. **Öhlund P**, Delhomme N, Hayer J, Hesson J C, Blomstrom A L (2022). Transcriptome analysis of an *Aedes albopictus* cell line single- and dual-Infected with Lammi virus and WNV. *Int. J. Mol. Sci*, 23 (2), 875.

Papers I-III are reproduced with the permission of the publishers.

The contribution of Pontus Öhlund to the papers included in this thesis was as follows:

- I. Planned the study together with co-authors. Performed the collection, laboratory experiments and analyzed the data. Wrote the manuscript with support from the co-authors.
- II. Planned the study together with co-authors. Performed the laboratory experiments and analyzed the data. Wrote the manuscript with support from the co-authors
- III. Planned the study together with co-authors. Performed the laboratory experiments and analyzed the data. Wrote the manuscript with support from the co-authors

Publications not included in this thesis

- IV. **Öhlund P**, Lunden H, Blomstrom A L (2019). Insect-specific virus evolution and potential effects on vector competence. *Virus genes*, 55, pp. 127-137.
- V. Blomstrom A L, Luz R H, **Öhlund P**, Lukenge M, Brandão P E, Labruna M B, Berg M (2019). Novel viruses found in *Antricola* Ticks collected in bat caves in the western Amazonia of Brazil. *Viruses*, 12 (1), 48

Abbreviations

<i>Ae</i>	<i>Aedes</i>
CPE	Cytopathic effect
<i>Cq</i>	<i>Coquillettidia</i>
<i>Cx</i>	<i>Culex</i>
DE	Differently expressed
dpi	Days post infection
EVEs	Endogenous viral elements
GMVs	Genetically modified vectors
HakV	Hanko virus
hpi	Hours post infection
ISFV	Insect-specific flavivirus
ISV	Insect-specific virus
LamV	Lammi virus
miRNA	Micro RNA
NIRVS	Non-retroviral integrated RNA virus sequences
piRNA	Piwi RNA
RNAi	RNA interference
siRNA	Small interfering RNA
sRNA	Small RNA

vpiRNA	Virus-derived piwi RNA
vsiRNA	Virus-derived small interfering RNA
vsRNA	Virus-derived small RNA
WNV	West Nile virus

1. Introduction

1.1 Mosquito-borne virus transmission

Mosquitoes serve as vectors for many medically important arthropod-borne viruses (arboviruses) such as West Nile Virus (WNV), Dengue virus (DENV), Zika virus (ZIKV) and chikungunya virus (CHIKV). Their associated diseases cause a major health burden across the globe in both animals and humans. Arboviruses are often maintained in nature through an enzootic cycle (sylvatic), that includes a vertebrate reservoir host such as birds, rodents or non-human primates and a primary mosquito vector. Human and domestic animal infections are often considered spillover events with no further spread, however, outbreaks resulting in an urban transmission cycle occurs from time to time (Weaver & Barrett 2004). The frequency of these arbovirus outbreaks are believed to increase with global trade, urbanization and increasing temperatures (Simon *et al.* 2008).

There are only a handful of mosquito species responsible for the majority of arbovirus transmissions in animals and humans. *Aedes (Ae) aegypti* and *Ae. albopictus* are closely related and serve as vectors for many arboviruses, but mainly CHIKV, DENV, ZIKV and yellow fever virus (YFV). *Ae. aegypti* originates from sub-Saharan Africa and was probably introduced to the New World via the African slave trade between 15th and 17th centuries, and further spread to Asia and later Australia from Europe during the opening of the Suez Canal in the year 1869 (Smith 1956; Powell *et al.* 2018). *Ae. albopictus* originates from tropical forests in South-East Asia and until the late 1970s was restricted to a limited region, however, in only a few decades, *Ae. albopictus* has conquered all continents except Antarctica. The fast spread was partially due to increased human mobility and trade, but also *Ae.*

albopictus ability to survive in both tropical and temperate regions (Benedict *et al.* 2007; Caminade *et al.* 2012). The *Culex (Cx) pipiens* complex, which include species such as *Cx. pipiens* and *Cx. quinquefasciatus* are geographically distributed over the whole world and are thought to be key vector for arboviruses such as WNV, Japanese encephalitis virus (JEV) and St. Louis encephalitis virus (SLEV) (Farajollahi *et al.* 2011).

1.2 Mosquito's antiviral immunity

Most of the medically important arboviruses are horizontally transmitted, which means that the mosquito needs to acquire the viral infection by a viremic blood meal from a vertebrate host. Once an infectious blood meal is ingested by a female mosquito, the virus needs to conquer tissue barriers and antiviral immune responses before successful establishment. The first barrier is the midgut epithelium, where the virus particles must initiate an infection and replicate before dissemination to the hemocoel. In the hemocoel the virus can spread systemically to the rest of the body including the salivary glands, where sufficiently high viral titers need to be achieved in the mosquito saliva before transmission to a new host during blood feeding (Franz *et al.* 2015) (Figure 1).

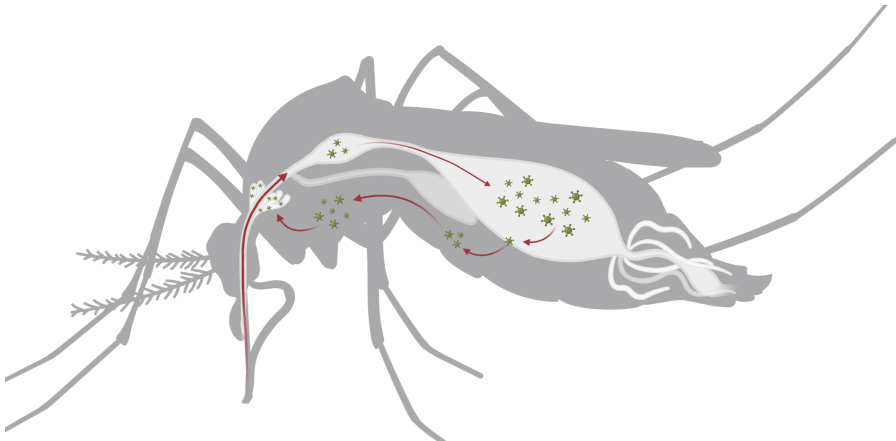


Figure 1. Ingestion of a viremic blood meal and the routes of infection before successful establishment and transmission. The figure was generated using the webtool Biorender.com.

Unlike the mammalian immune system, mosquitoes lack a lymphocyte-mediated adaptive immunity and the interferon response, where no orthologs have been identified in insects (Lemaitre & Hoffmann 2007). Instead, mosquitoes rely on their innate immune system to fight viral infections, which is composed of both cellular and humoral immune responses (Souza-Neto *et al.* 2009; Ramirez & Dimopoulos 2010; Satyavathi *et al.* 2014). The invading virus is recognized by a variety of pattern-recognition receptors (PRRs), that can identify pathogen-associated molecular patterns (PAMPs) resulting in the activation of an array of molecular signaling pathways and immune effector proteins to control the infection (Zhang *et al.* 2015). The main immune pathways are thought to be the RNA interference (RNAi) pathway, the toll pathway, the immune deficiency (Imd) pathway and the Janus kinase-signal transducer (JAK/STAT) pathway (Lee *et al.* 2019).

1.2.1 RNA-interference (RNAi) pathways

The RNAi-pathway includes three major types of small RNAs (sRNAs): small interfering RNA (siRNA), microRNA (miRNA), and P-element-induced wimpy testis (piwi)-interacting RNA (piRNA) (Figure 2).

The siRNA pathway is considered the main antiviral immune response. Many mosquito-borne viruses are single-stranded RNA viruses, and upon viral replication double-stranded RNA (dsRNA) will form as replicative intermediates in the cytoplasm (Blair 2011). These foreign (exogenous) dsRNA interact with the Dicer2-R2D2 complex and is subsequently cleaved by the RNase III enzyme Dicer2, to generate siRNAs of 21 nucleotides (nt) in length. The siRNAs are then incorporated with a multiprotein known as the RNA-induced silencing complex (RISC), where one of the strands is degraded and the remaining guide strand is used as a template to bind complementary target RNAs, that is cleaved and degraded by Argonaute-2 (Ago2) in a sequence specific manner (Matranga *et al.* 2005; Rand *et al.* 2005; Galiana-Arnoux *et al.* 2006).

The primary function of the miRNA pathway is post-transcriptional regulation of gene expression. Unlike siRNAs, miRNAs (20-25 nt) are derived from endogenous hairpin transcripts, which are first transcribed into primary miRNA (pri-miRNA) by host polymerase II and are processed into precursor miRNA (pre-miRNA) by Drosha in the nucleus. The pre-miRNAs are further processed in the cytosol by Dicer-1 to generate mature miRNA,

which are incorporated into the RISC complex, which facilitates target specific cleavage of mRNA by Ago-1 (Lee *et al.* 2004; Bavia *et al.* 2016).

The piRNA pathway is the least understood of all RNAi pathways, but the main function is believed to silence transposons and maintain the integrity of the germline (Ku & Lin 2014). Interestingly, virus-derived piRNA (vpiRNA) have been observed in mosquitoes and mosquito derived cell lines infected with different viruses, suggesting an antiviral immune function (Miesen *et al.* 2015). The *Aedes* genome encode eight proteins involved in the piRNA pathway, Piwi 1-7 and Ago3 (Girardi *et al.* 2017). The general biogenesis of piRNAs (24-30 nt), starts with the synthesis of primary piRNAs from single stranded precursors. These precursors are believed to originate from different sources such as viral single stranded RNA in the cytosol, repetitive genomic sequences called piRNA clusters, endogenous viral elements (EVEs) or non-retroviral integrated RNA virus sequences (NIRVS). The precursors are processed by a helicase and endonuclease that cleave the precursor at a uridine (U) in the 5'-end, these are then loaded onto a Piwi protein and are further trimmed from their 3'-end to the size of mature piRNA by an unknown exonuclease (Liu *et al.* 2016). The piRNA can then undergo an alternative amplification process known as the ping-pong amplification cycle. This amplification of piRNAs is a two-step amplification mechanism where the Piwi-5 protein, loaded with a piRNA cleaves a complementary target RNA. The resulting 3'-cleavage product is transferred to Ago-3 and used as a template to cleave a complementary target RNA, which in turn generates a new piRNA precursor for the Piwi-5 protein, which give rise to the same piRNA sequence that initiated the amplification. This amplification processes give a characteristic ping-pong nucleotide bias where piRNAs derived from the antisense strand show a U at the first position (Piwi-5 bound) and piRNAs derived from the sense strand show an Adenine (A) in the 10th position (Ago-3 bound). The ping-pong amplification also predicts an even distribution of piRNAs derived from the sense- and antisense-strand (Girardi *et al.* 2017). The processed piRNA is then either transported back to the nucleus to silence transposons or is associated with a multiprotein known as piRISC that facilitates piRNA-mediated silencing in the cytosol (Siomi *et al.* 2011).

Interestingly, virus-derived DNA (vDNA) (linear and circular) have been observed in mosquitoes and mosquito derived cell lines infected by different RNA viruses (Nag *et al.* 2016; Nag & Kramer 2017). These vDNAs are

believed to be generated by host cellular reverse transcriptase during viral replication, and this is supported by the fact that the vDNA production is stopped when the reverse transcriptase inhibitor, azidothymidine (AZT) is added to infected cells (Goic *et al.* 2013). The vDNA are thought to play an important role in the RNAi-mediated immunity and is connected to viral tolerance and persistent infection (Goic *et al.* 2016). Furthermore, vDNAs have been observed to integrate into the host chromosomes as NIRVS (Crochu *et al.* 2004), and are often located in piRNA cluster regions of the genomes suggesting that they help in the production of vpiRNAs and subsequently piRNA-mediated silencing (Blair 2011). If the NIRVS are integrated into the germline as EVEs the RNAi-mediated immunity is maintained in the population through vertical transmission (Katzourakis & Gifford 2010) (Figure 2).

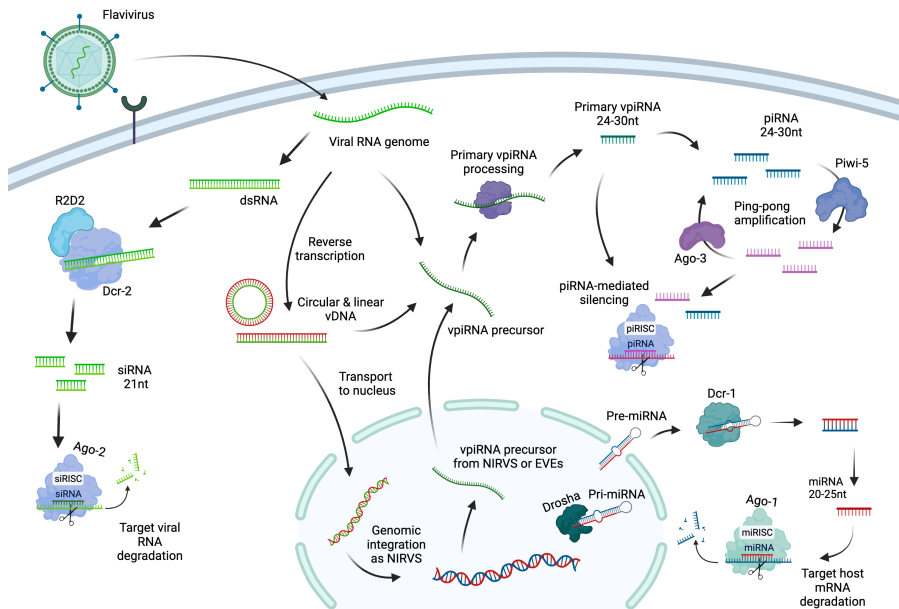


Figure 2. RNA-interference pathways and generation of vDNA, NIRVS and vpiRNA. The figure was generated using the webtool Biorender.com.

1.2.2 JAK-STAT, Toll and Imd pathways

The signaling pathways JAK-STAT, Toll and Imd play essential roles in mosquito immunity and are activated upon recognition of PAMPs through a

variety of different PRRs such as Toll, peptidoglycan-recognition protein (PGRPs), fibrinogen-related protein, scavenger receptors and C-type lectins. Activation of these pathways initiates a downstream signaling cascade of different protein kinases leading to the expression and synthesis of effector molecules such as antimicrobial peptides (AMPs), reactive oxygen species (ROS), virus-induced RNAs and components of the phenoloxidase cascade (Kumar *et al.* 2018).

The JAK-STAT pathway is activated upon binding of the Unpaired ligand (Upd) to the Dome receptor, resulting in a conformational change and self-phosphorylation of the tyrosine kinase Hopscotch (Hop/JAK). Activated Hop/JAK in turn phosphorylates Dome leading to the recruitment and phosphorylation of signal transducers and activators of transcription (STATs). The phosphorylated STATs dimerize and translocate to the nucleus and activate transcription of specific effector genes such as *vir-1* (Souza-Neto *et al.* 2009) (Figure 3). The JAK/STAT pathways seem to play an essential role in the antiviral defense. Over expression of the JAK/STAT pathway in the midgut of *Ae. aegypti* mosquitoes decreased replication of DENV, while knockdown of the Dome receptors or the Hop/JAK protein resulted in enhanced replication of DENV (Jupatanakul *et al.* 2017). Furthermore, a secretory protein known as Vago have shown to activate the JAK/STAT pathway via an unknown receptor, and this protein was shown to be upregulated upon WNV-infection in *Culex* mosquitoes and restricted WNV infection by activating the JAK/STAT pathway (Paradkar *et al.* 2012).

Cleavage and maturation of the cytokine Spätzle (Spz) initiates the Toll pathway by binding to the Toll transmembrane receptor. This activates the MyD88, Tube and Pelle proteins that phosphorylates the negative regulator Cactus, which is subsequently degraded. Without Cactus, the NF- κ B-like transcription factor Relish-1 (Rel-1) is released and translocated to the nucleus where it increase the expression of many AMPs genes (Shin *et al.* 2006) (Figure 3). The Toll pathway is most known for its role in innate immunity against Gram-positive bacteria and fungi (Lemaitre *et al.* 1996; Michel *et al.* 2001). However, an upregulation of genes controlled by Rel-1, such as defensin, have shown to aid in the control/neutralization of DENV in *Ae. aegypti* mosquitoes (Xi *et al.* 2008).

The Imd pathway works in a similar way as the Toll pathway, where binding of a ligand to PGRPs on the cell surface leads to activation of the

Imd, FADD and Dredd proteins which phosphorylates and inhibits the negative regulator Caspar, resulting in the release and translocation of phosphorylated Relish-2 (Rel-2) to the nucleus, which promotes expression of different AMPs genes (Kim *et al.* 2006) (Figure 3). The Imd pathway is thought to be the major immune response against the malaria parasite *Plasmodium*, and overexpression of Rel-2 resulted in complete resistance to *Plasmodium falciparum* in *Anopheles (An)* mosquitoes (Garver *et al.* 2009). The Imd pathway is also important for immunity against Gram-negative and Gram-positive bacteria (Meister *et al.* 2005). Furthermore, expression of Rel-2 controlled genes has shown antiviral effects against WNV infection in *Culex* mosquitoes (Paradkar *et al.* 2012).

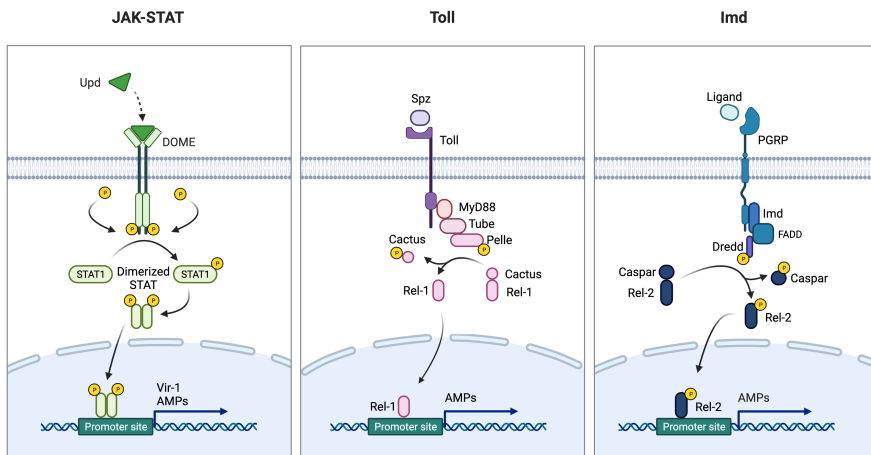


Figure 3. Schematic representation of the mosquito JAK-STAT, Toll and Imd pathways. The figure was generated using the webtool Biorender.com.

1.2.3 Other innate immune responses

Hemocytes are cells that circulate within the hemolymph and are involved in the cellular immune response that include phagocytosis, nodulation and encapsulation of pathogens. But they are also involved in the humoral response such as initiation of signaling cascades, production of AMPs and melanization (Satyavathi *et al.* 2014). There are three types of hemocytes in mosquitoes: prohemocytes, granulocytes and oenocytoids (Castillo *et al.* 2006). Granulocytes are the most abundant (80-95%) of all hemocytes and upon activation they adhere to and engulf pathogens (Hillyer & Strand 2014).

Oenocytoids constitute 10% of circulating hemocytes and are the main producer of components of the phenoloxidase cascade (Nakatogawa *et al.* 2009). Together with the serine proteases, such as the CLIP proteases they initiate the phenoloxidase cascade upon recognition av PAMPs leading to the formation of melanin around invading pathogens (Rodriguez-Andres *et al.* 2012).

1.3 Insect-specific viruses

The first described insect-specific virus (ISV) was the cell fusing agent virus (CFAV) by Stollar and Thomas back in the 1975. They observed the formation of syncytia in an *Ae. aegypti* derived cell line and managed to isolate the causing virus, which was named CFAV. Furthermore, when CFAV was inoculated on different vertebrate cell lines no cytopathic effect (CPE) was observed and the virus could not be re-isolated, which suggested that the virus must be insect-specific (Stollar & Thomas 1975). Since then, a large number of novel ISVs have been discovered, which is not surprising considering that insects belong to the largest phylum Arthropoda, which account for over 80% of all animal species (Giribet & Edgecombe 2019). The majority of ISVs have been discovered through surveillance for pathogenic viruses in hematophagous vectors, particularly mosquitoes. Advances in sequencing technology, cost efficiency and bioinformatic tools have intensified the frequency of novel ISV discoveries over the past decade (Calisher & Higgs 2018).

As their name implies, ISVs only replicate in insect cells and are identified as a component of the insect's natural microbiome (Bolling *et al.* 2015). Unlike arboviruses, that have a dual-host tropism and a transmission cycle between a vertebrate reservoir host and a mosquito vector, the ISVs are thought to be maintained in nature through vertical transmission in which the virus is passed transovarially, from mother to their offspring. This is supported by transmission studies where offspring from ISV-infected female mosquitoes have tested positive for the same virus (Bolling *et al.* 2011; Saiyasombat *et al.* 2011; Haddow *et al.* 2013). However, knowledge of other potential routes of transmission is lacking, such as venereal transmission or environmental transmission from *e.g.* the aquatic environment during early development.

Many ISVs belong to viral families associated with medically and veterinary important arboviruses such as *Peribunyaviridae*, *Reoviridae*, *Togaviridae* and *Flaviviridae* (Öhlund et al. 2019). Furthermore, phylogenetic analyses of sequence identities between ISVs and arboviruses suggest that ISVs are ancestral to the pathogenic arboviruses (Marklewitz et al. 2015). This makes ISVs the perfect model to study virus evolution and the transition from single- to dual-host tropism. The reverse genetics approach have proven to be a valuable tool, by generating chimeric viruses with genes from ISVs and arboviruses of the same taxa. This has elucidated genetic factors that may allow ISVs to cross the host barrier. Generally, ISVs must overcome several bottlenecks to gain dual-host tropism, such as: immune system evasion, viral attachment and entry, interaction with multiple host factors for successful replication, tolerance to temperature differences and more (Nasar et al. 2015; Junglen et al. 2017; Piyasena et al. 2017).

The same reverse genetic approach has been utilized as a platform for vaccine development, where chimeric viruses express the structural proteins of an arbovirus and non-structural proteins of an ISV. These chimeric viruses can replicate in mammalian cells but do not produce infectious virions, *i.e.* offering the possibility of a safe and efficient novel vaccine platform (Erasmus et al. 2017; Hobson-Peters et al. 2019). Furthermore, in recent years, the interest for ISVs has increased due to their potential to be utilized in novel control strategies that target the mosquitoes ability to carry and transmit arboviruses, which is further discusses in chapter 1.4.

1.3.1 Insect-specific flavivirus

Some of the most recognized and important arboviruses belong to the genus *flavivirus* such as WNV, DENV, ZIKV, yellow fever virus (YFV) and Japanese encephalitis virus (JEV). These are all examples of dual-host flaviviruses, however, a large number of the ISVs also belong to the same genus and are referred to as insect-specific flaviviruses (ISFVs) (Blitvich & Firth 2015).

The Flavivirus family comprises a large number of viruses that are enveloped and possess a single-stranded, positive-sense RNA genome of approximately 11 kb. The genome encodes a single open reading frame (ORF) that is flanked by a 5'- and a 3'-untranslated region (UTR). The ORF

encodes a large polyprotein that is processed by viral and cellular proteases to produce viral structural proteins, designated capsid (C), pre-membrane/membrane protein (prM/M), envelope (E) protein, and seven non-structural (NS) proteins (NS1, NS2A, NS2B, NS3, NS4A, NS4B and NS5) (Best 2016).

The ISFVs can further be divided into two distinct phylogenetic subgroups. One subgroup, that is known as the classical ISFVs and is phylogenetically distinct from all other flaviviruses. The other subgroup is phylogenetically affiliated with dual-host flaviviruses but have the insect-specific phenotype and is known as dual-host affiliated ISFVs (Figure 4) (Blitvich & Firth 2015). The classical ISFVs have been isolated from mosquitoes in every continent except the Antarctica and include thirteen viruses to our knowledge (Table 1). However, some classical ISFVs have been assigned multiple names due to their simultaneous discoveries, although they share >84% nucleotide identity and should have been classified within the same species according to the cut-offs proposed in (Kuno *et al.* 1998). For example, Hango virus (HakV), Ochlerotatus flavivirus (OcfV) and Spanish Ochlerotatus flavivirus (SOcfV) are likely to be strains of the same virus species (Calzolari *et al.* 2012; Huhtamo *et al.* 2012; Vazquez *et al.* 2012; Ferreira *et al.* 2013). Among the dual-host affiliated ISFVs there are nine isolated viruses to our knowledge (Table 2). The phylogenetic placement of these viruses indicates that they have a dual-host tropism, however, the replicative abilities have been assessed in numerous vertebrate cell lines and no study supports viral replication. It is suggested that the dual-host affiliated ISFVs have evolved from dual-host flaviviruses and lost their ability to infect vertebrates (Blitvich & Firth 2015).

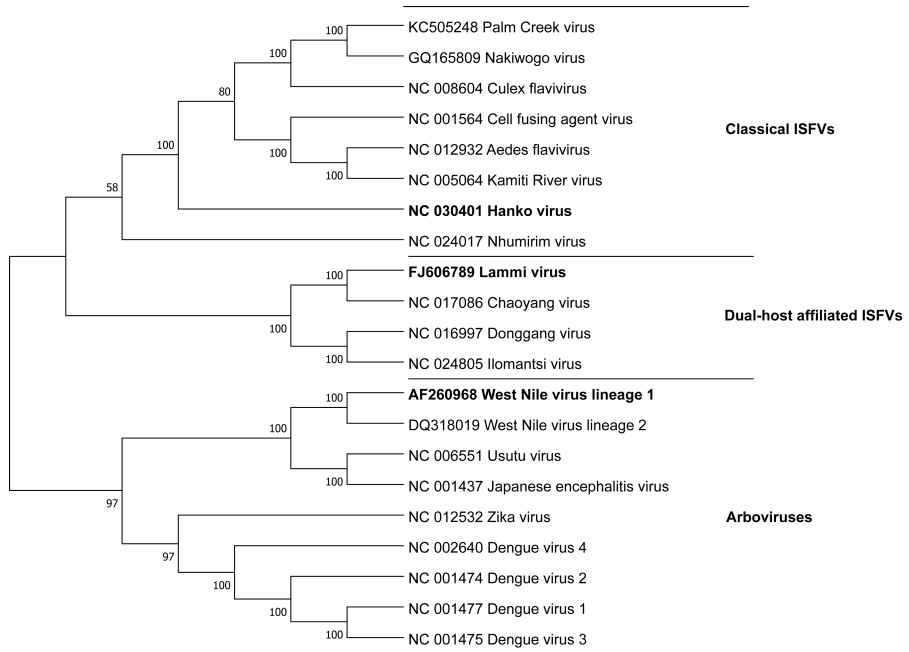


Figure 4. Phylogenetic tree of flaviviruses from the categories arbovirus, classical ISFV and dual-host affiliated ISFV. Complete polyprotein amino acid sequences were aligned using MUSCLE (Edgar 2004). A maximum-likelihood phylogenetic tree was generated using the default settings in MEGA-11 (Tamura *et al.* 2021) with 500 bootstraps.

Table 1. Classical insect-specific flaviviruses

Viruses	Gene bank accession No
Cell fusing agent virus (CFAV)	NC_001564
Hanko virus (HakV)	JQ268258
Culex flavivirus (CvFV)	NC_008604
Kamiti River virus (KRV)	NC_005064
Nakiwogo virus (NAKV)	GQ165809
Palm Creek virus (PCV)	KC505248
Aedes flavivirus (AEFV)	NC_012932
Aedes galloisi flavivirus (AGFV)	AB639347
Calbertado virus (CLBOV)	EU569288
Quang Binh virus (QBV)	NC_012671
Culex theileri flavivirus (CTFV)	HE574574
Nienokoue virus (NIEV)	NC_024299

Viruses	Gene bank accession No
Parramatta River virus (PaRV)	NC_027817

Table 2. Dual-host affiliated insect-specific flaviviruses

Viruses	Gene bank accession No
Lammi virus (LamV)	FJ606789
Barkedji virus (BJV)	MG214905
Chaoyang virus (CHAOV)	NC_017086
Donggang virus (DONV)	NC_016997
Ilomantsi virus (ILOV)	NC_024805
Marisma mosquito virus (MMV)	MF139576
Nanay virus (NANV)	NC_040610
Nhumirim virus (NHUV)	NC_024017
Nounané virus (NOUV)	NC_033715

1.4 West Nile virus

The first known isolation of WNV was from the blood of a febrile Ugandan woman in 1937 (Smithburn 1940). Further isolations were reported in sera of Egyptian children a couple of years later (Melnick *et al.* 1951). In the summer of 1953, a significant outbreak of WNV was reported in Israel, that caused a relatively mild, self-limiting febrile illness known as West Nile fever (Goldblum *et al.* 1954). It was later connected to neuroinvasive disease in elderly Israeli patients (Spigland *et al.* 1958). WNV arrived to Europe in the late 1950s (Bardos *et al.* 1959), and have since then caused sporadic outbreaks, with increased intensity during the late 1990s (Murgue *et al.* 2002). The introduction of WNV in the Western Hemisphere started with the New York city outbreak in 1999 (Lanciotti *et al.* 1999), and by 2005 WNV had reached across the U.S. and into Canada and Latin America (Kramer *et al.* 2008). Today, WNV is the most geographically widespread arbovirus and the leading cause of arboviral encephalitis (Turell *et al.* 2005; Jansen *et al.* 2008; Kramer *et al.* 2008; Fros *et al.* 2015).

There are two main genetic lineages of WNV responsible for severe neurological disease worldwide. Lineage 1 that is circulating on all continents except Antarctica and is the dominant lineage of WNV in North America (Kramer *et al.* 2008). Lineage 2 of WNV was mainly associated to

sub-Saharan Africa and Madagascar but was introduced to Europe via Hungary in 2004, and have since then rapidly spread throughout Europe and is now responsible for the majority of seasonal outbreaks (Bakonyi *et al.* 2013).

The dominant transmission cycle of WNV is predominantly between *Culex* mosquitoes and birds (Hurlbut *et al.* 1956), with over 300 species of birds identified as competent hosts (CDC 2016). Although *Culex* mosquito species are believed to be the main vector for WNV, several other mosquito species have proven to be competent vectors, including *Ae. albopictus* and *Coquillettidia (Cq) richardii*. Humans and horses are considered dead-end hosts (Figure 5).

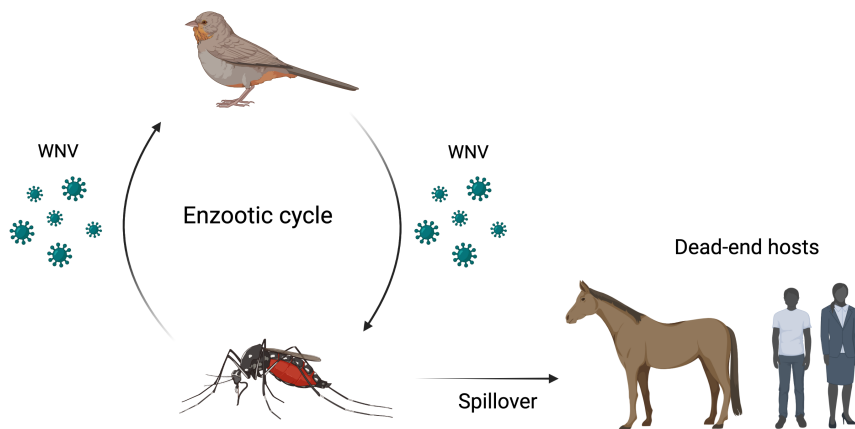


Figure 5. Schematic illustration of the transmission cycle of WNV. The figure was generated using the webtool Biorender.com.

WNV is responsible for mild fever to severe, lethal neuroinvasive disease in humans, horses, birds, reptiles and other wildlife animals (Habarugira *et al.* 2020). To date, there is no approved vaccines or antiviral drugs against WNV for use in human, however (Volz *et al.* 2016), there are two approved and commercially available vaccine for veterinary use. These vaccines have shown good protective immunity in horses after two initial doses, however, both vaccines requires a booster dose every six months to maintain a fully protective response (Davidson *et al.* 2005).

The Nordic regions of Europe such as Sweden, have to our knowledge no circulation of WNV today, although the competent mosquito vectors and birds are relatively common species in these areas. However, there is an

increasing possibility for an introduction of WNV into these nonendemic regions. Factor such as environmental changes with higher temperatures and rainfall are fundamental drivers of mosquito abundance and amplification of WNV, and have been linked to outbreaks in endemic areas (Hartley *et al.* 2012). Furthermore, globalization, travel and trade could introduce WNV-infected birds or mosquitoes via *e.g.* ships, planes and bird trade (Kilpatrick *et al.* 2006). To reduce the spread of WNV in Europe and other parts of the world, novel control strategies and vaccines are required.

1.5 Control strategies

For many of the pathogenic mosquito-borne viruses there are no licensed vaccines or therapeutic drugs available, and today, the main method for reducing the transmission of arboviruses are focused on reducing mosquito populations. These strategies are utilizing everything from the bacteria *Bacillus thuringiensis israelensis* (Bti), to aquatic animals and insecticides to kill larvae and/or adult mosquito populations (Walton 2007; Anderson *et al.* 2011; Bonds 2012). However, these approaches are only able to temporarily limit the arbovirus transmission and are often bad for the environment, cumbersome and costly due to the constant need to repeat the treatments, monitor levels of larvae and/or adults and the dependence on community participation to access hidden breeding sites. Furthermore, with increasing levels of insecticide resistance, these strategies are becoming less effective (Luz *et al.* 2011). Novel control strategies are needed and the development of strategies that target the vector competence (mosquitoes ability to acquire, carry and transmit pathogenic arboviruses) are among the proposed methods. The vector competence is one of many factors that determine the vectorial capacity of a hematophagous vector. Other factors include: vector abundance, host specificity, vector longevity, blood feeding frequency and the extrinsic incubation period. All of these factors have an impact on the vectorial capacity and can be calculated with the equation:

$$C = (ma^2)(pn)(b) / -\log(p)$$

where C is the vectorial capacity, b is the vector competence, p is the daily probability of vector survival, n is the extrinsic incubation period and ma^2 is a combined value of blood feeding frequency with human biting rate (Delatte *et al.* 2010; Ciota & Kramer 2013).

In the development of strategies that target the vector competence, many methods are being developed, such as the use of the endosymbiotic bacterium *Wolbachia*, ISVs or genetically modified vectors (GMVs). All of these novel strategies involve large-scale releases of modified mosquitoes in local regions to replace the population with mosquitoes that are refractory to pathogen transmission.

1.5.1 *Wolbachia* as a biocontrol agent

The *Wolbachia*-based control approach is the most studied and utilized strategy that targets the vector competence. *Wolbachia* is a maternally inherited bacterial endosymbiont that occurs naturally in many arthropod species (Caragata *et al.* 2021). *Ae. aegypti* is not a natural host for *Wolbachia* and artificial transinfection of *Wolbachia* in mosquitoes makes use of two manipulation of host biology: cytoplasmic incompatibility (CI) and pathogen blocking. CI is a reproductive manipulation that occurs when *Wolbachia*-infected males mate with uninfected females, resulting in eggs failing to hatch. This has been used in population suppression strategies (Yen & Barr 1973). However, *Wolbachia*-infected female mosquitoes are capable of reproducing successfully with partners of either infection status and vertically transmit *Wolbachia* to their offspring. This phenomenon is very usefully in population replacement strategies (Caragata *et al.* 2021). The pathogen blocking mechanism of *Wolbachia* is still unclear, but *Wolbachia*-infected mosquitoes have proven to reduce transmission of important arboviruses such as DENV, ZIKV, CHKV and YFV (Moreira *et al.* 2009; van den Hurk *et al.* 2012; Dutra *et al.* 2016). The *Wolbachia*-based mosquito-control intervention is now widespread and at least ten countries, including Australia, Brazil and Indonesia have released *Wolbachia*-infected *Ae. aegypti* into the wild to control arbovirus transmission. Results have shown a major impact on DENV transmission with 40-100% reduction in incidence. Furthermore, the *Wolbachia*-infection rate of targeted mosquito populations has proven to remain high several years post release (Caragata *et al.* 2021).

1.5.2 Genetically modified vectors

The use of genetically modified vectors (GMVs) have the potential to be an effective and powerful tool in limiting arbovirus transmission through the expression of transgenes that block arbovirus infection/transmission. Today there are many GMVs systems for population suppression, but no system

that have been used in the field that target the vector competence for arboviruses (Flores & O'Neill 2018). However, the search for potential gene targets is facilitated with increased knowledge of mosquito-virus interactions and host factors important for arbovirus replication. Once a good gene target is found, the CRISPR-Cas9 technology has proven to be a robust system to genetically modify various organisms including mosquitoes (Doudna & Charpentier 2014). Furthermore, to increase the sustainability of the GMVs, various gene-driver systems have been developed. These are often inspired by natural gene drivers, and work through biased inheritance in their favor. Like the homing endonuclease genes, which can be placed within their target gene leading to conversion of heterozygotes into homozygotes, drastically increasing the inheritance frequency (Traver *et al.* 2009). Furthermore, some GMVs with an increased resistance to DENV-infection have been investigated; such as insertion of miRNA cassettes targeting DENV-3, which reduced viral transmission rate (Yen *et al.* 2018), or overexpression of the JAK/STAT pathway to increase resistance to DENV-2 and DENV-4 (Jupatanakul *et al.* 2017). Perhaps the most radical GMV study, inserted a transgene expressing a modified monoclonal antibody 1C19, which neutralizes all major DENV serotypes. The modified 1C19 gene was placed next to a carboxypeptidase promoter, which induces gene expression in the midgut following blood ingestion. Results showed a significant reduction of all four DENV serotypes in midgut, carcass and saliva when challenged with a DENV containing blood meal (Buchman *et al.* 2020).

1.5.3 ISVs in control strategies

Similarly to *Wolbachia*, ISVs could potentially be utilized as a biocontrol agent to reduce arbovirus transmission in targeted mosquito populations. As mentioned earlier, ISVs are vertically transmitted, which would sustain the pathogen blocking effect in the population. Furthermore, many ISVs are within the same viral family as the pathogenic arboviruses, and a prior infection of some ISVs has proven to block or interfere with a secondary infection of an arbovirus of the same viral family (Ohlund *et al.* 2019). The mechanism of interference is still unknown but is thought to be through priming of the immune response and/or superinfection exclusion, hindering establishment of the secondary arbovirus. The molecular mechanisms of superinfection exclusion are hypothesized to involve competition or

modification of cellular resources required for: viral entry, RNA replication, translation and viral particle assembly (Lee *et al.* 2005).

Cx. annulirostris mosquitoes pre-infected with the ISFV Palm creek virus (PCV) showed a significantly lower WNV-infection rate compared to PCV negative *Cx. annulirostris* when orally exposed to WNV via a blood meal (Hall-Mendelin *et al.* 2016). Similar interference effects of arboviruses have been observed in mosquito-derived cell lines infected with the ISFV Nhumirim virus (NHUV) and in cells dual-infected with CFAV and an insect-specific phasivirus named Phasi Charoen like virus (PCLV) (Kenney *et al.* 2014; Schultz *et al.* 2018). However, the arbovirus interference effect seems to be specific to some ISVs, and a prior infection of the CxFV or CFAV did not significantly reduce replication of a pathogenic flavivirus (Kent *et al.* 2010; Kuwata *et al.* 2015; Schultz *et al.* 2018). Further studies are needed to find good candidates, that can establish a persistent infection in the mosquito host and block secondary infections of arboviruses. Many of the ISFVs have not been evaluated for this, especially among the dual-host affiliated ISFVs.

Novel control strategies should aim to be inexpensive, effective, environmentally friendly, safe and self-sustaining. The strategies described above tick most if not all of these boxes. However, they all require communities to have high levels of trust to willingly participate. The health benefits need to be promoted and overpower the fear and mistrust towards genetic modification technology, government and industry.

2. Aims of this thesis

The overall aim of the present thesis was to investigate the use of a group of viruses known as insect-specific viruses (ISVs) to manipulate the mosquito antiviral immunity and elucidate important antiviral mechanisms, with the goal to increase the mosquito host resistance to infection of medically important viruses with a focus on West Nile virus (WNV).

The specific aims were to:

- ⇒ Characterise the virome of mosquitoes collected in Sweden (Paper I)
- ⇒ Investigate the RNA interference (RNAi) response to insect-specific flavivirus infection (ISFV) in the mosquito host (Paper II)
- ⇒ Investigate the altered gene expression upon acute ISFV and arbovirus infection in the mosquito host to elucidate virus-host interactions (Paper III)
- ⇒ Investigate the effect of ISFV infection on the vector competence for WNV and elucidate potential mechanism of WNV restriction (Paper III)

3. Material and Methods

This section provides an overview of the methods and materials used in the three papers, with comments to why they were chosen. Detailed descriptions on the material and methods are found in the individual papers I-III.

3.1 Mosquito collection (Paper I)

The first part of the thesis work (Paper I) aimed to investigate the virome of Swedish mosquitoes. Therefore, mosquitoes were collected in the summer of 2017 at two different geographic locations in mid-east Sweden. The first location was close to a town named Flen (coordinate: 59°04'08.6" N 16°31'14.1" E), where mosquito collections took place once every second week from May to the end of August. At this location, two different types of traps were used, four dry-ice-baited CDC miniature light traps and five CDC gravid traps (JohnW. Hock company) (Figure 6). The CDC miniature light traps were used with blocks of dry ice (releasing CO₂) to attract female mosquitoes searching for a blood meal (Sriwichai *et al.* 2015). The CDC gravid traps are designed to attract gravid *Culex* female mosquitoes searching for a water source to lay their eggs, where a fermented hay water mix is used as the bait (Lee & Kokas 2004). Traps were placed at a minimum distance of 500 meters from each other and at various environments such as forest, tree-lines and near livestock animals to maximise the chances of collecting different mosquito species. Traps were setup in the evening and emptied in the morning the day after. The other location for mosquito collection was in the nature reserve Hammarskog, close to Uppsala (coordinate: 59°46'31.9" N 17°35'01.3" E), where a Mosquito Magnet® was used from Monday to Friday (emptied every 24 h) every second week from July to August (Figure 6). The Mosquito Magnet® attract female mosquitoes searching for a blood meal with CO₂ and Octenol. The Mosquito Magnet® was placed close to a bird breeding ground, to increase the chances of collecting mosquitoes with a bird-feeding preference, such as *Culex*

mosquitoes. Collected mosquitoes were euthanized and stored at -80°C and later identified to species based on morphological characteristics, using a taxonomic key (Becker *et al.* 2010), stereomicroscope and a cold table, to keep the cold chain and prevent viral genome degradation.

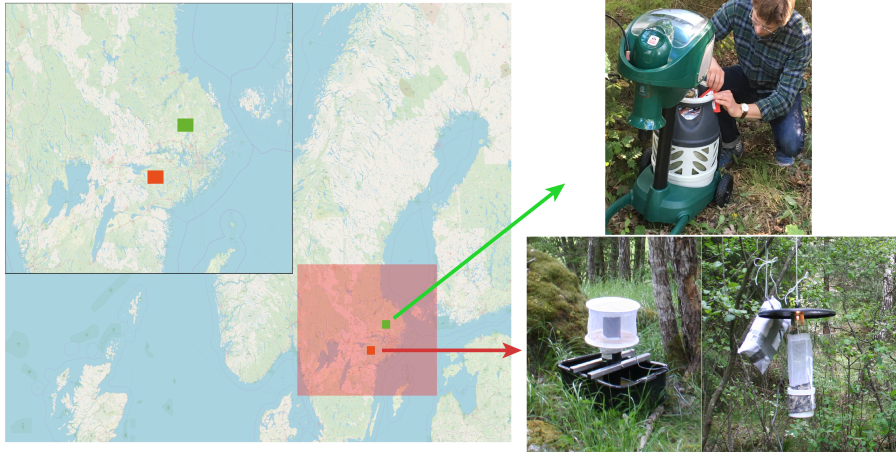


Figure 6. Map of the two different geographic locations where the mosquito collection took place, and the different traps used at each location. Green squares and arrow represent Hammarskog and red squares and arrow represent Flen.

3.2 Metagenomic pre-sequencing preparation (Paper I)

Collected mosquitoes were pooled based on species, location and time of collection, which generated 109 pools of 9-12 mosquitoes per pool. These 109 pools were further processed for RNA extraction, starting with removal of surface microorganisms by dipping the individual mosquitoes once in 70% ethanol and then twice in milliQ water. Pools were then homogenized mechanically (bead beating) using a Precellys® evolution (Bertin instruments) and Precellys® tubes (soft tissue homogenization CK14). In addition, to keep the temperature at 10°C a Cryolys (Bertin instruments) cooled with liquid nitrogen was coupled to the Precellys® evolution. The homogenates were centrifuged and supernatant were collected, one part was used for total RNA extraction and the other part was kept at -80°C for potential virus isolations. For the RNA extractions we used a mixed protocol starting with TRIzol™ extraction and further purification of the aqueous phase using GeneJet spin columns (Thermo Fisher Scientific). To keep the high-throughput sequencing cost-efficient, the 109 pools of extracted RNA

were further pooled into 12 pools that still had the species, location and for some pools the time of collection information. The remaining RNA from the 109 RNA pools were kept and used to backtrack potential virus discoveries. RNA from the 12 pools were further processed by DNase treatment using RNAeasy mini elute kit and RNase-Free DNase set (Qiagen). To increase the proportion of viral RNA, ribosomal RNA was removed using the Ribo-Zero Gold (epidemiology) rRNA Removal Kit (Illumina) and the non-ribosomal RNA was randomly amplified with the Ovation® RNA-Seq System V2 (NuGEN Technology).

3.3 Metagenomic sequencing and analysis (Paper I)

The amplified RNA was submitted to SciLifeLab in Uppsala for library preparation and sequencing using the Ion 530 Chip kit (Thermo Fisher scientific). The 12 pools were divided on four Ion 530 Chips and sequencing was carried out with an Ion S5 XL sequencing system running the protocol for 400 bp-long reads.

The resulting Ion S5 XL sequence data was analysed in a metagenomics pipeline starting with quality control using FastQC (v1.2.1) (Bioinformatics 2021b), reads of low quality were trimmed with sickle (version 1.210) (Joshi NA 2011) using a cut-off PHRED score of 20. The mean read lengths after trimming were 359–380 nt. The good quality reads were de-novo assembled using MEGAHIT (v1.1.2) (Li *et al.* 2015). Both good quality reads that did not assemble, and the de-novo assembled contigs were taxonomically assigned using Diamond (v0.9.10) (Buchfink *et al.* 2015), with the blastx option using the default settings (e-value cut-off 0.001 and one top hit) and the NCBI non-redundant protein (nr) database from October 2018. In order to visualize the results with the R-package Pavian (v0.8.4) (Breitwieser & Salzberg 2020), the output format taxonomy (102) was used in Diamond. This option performs a LCA (Last Common Ancestor) algorithm to assign the taxonomy of each read and output a tabulated file. For the de-novo assembled contigs, an additional Diamond run was performed to output a DAA (Direct Access Archive) format that could be imported into MEGAN6 (version 6.15.2) (Huson *et al.* 2007), for further investigation. Potential viral sequences were analysed with NCBI's ORF finder, functional annotation of ORFs were performed using NCBI's BLASTp, EMBL-EBI's protein sequence analysis and classification tool InterProScan (Mitchell *et al.* 2019), and Phobius (Kall *et al.* 2007). Phylogenetic analyses were performed on the RNA-dependent RNA polymerase (RdRp) amino acid sequences for the novel viruses and related sequences in the GenBank database with >20%

amino acid (aa) identity. Sequence alignment and phylogenetic tree building were performed in MEGA 7 (Kumar *et al.* 2016). MUSCLE was used for multiple sequence alignment of the amino acid (aa) sequences (Le & Gascuel 2008). The phylogenetic trees were computed with the maximum-likelihood method using 500 bootstraps replicates. The raw sequence reads are available at the NCBI sequence read archive (SRA) under Bioproject accession PRJNA574583.

3.4 Mosquito cell lines and culture conditions (Paper II and III)

The mosquito cell lines used in paper II and III are both derived from *Ae. albopictus* larvae. The C6/36 cell line (Sigma-Aldrich), was used to propagate ISFVs stocks, due to its defective RNAi response, which exhibit susceptibility to a wide range of mosquito viruses and increased virus replication (Brackney *et al.* 2010). The U4.4 cell line (kindly provided by Associate Professor G. Pijlman, Wageningen University) is immunocompetent and was therefore used in the different infection studies (Goertz *et al.* 2019). Both cell lines were cultured at 28 °C without CO₂ in Leibovitz L-15 medium (Gibco) supplemented with 10% fetal bovine serum (FBS; Gibco), 10% tryptose phosphate broth (TPB; Gibco), Amphoterecin (250 ug/mL; Gibco) and Pen Strep (penicillin 100 U/mL and streptomycin 100 ug/mL; Gibco).

3.5 Viruses (Paper II and III)

To study the effect of ISFVs infection on the mosquito host, HakV (Strain: 2005/FI/UNK) and LamV (Strain: 2009/FI/Original) were obtained from the European Virus Archive—Global (EVAg). Both of these ISFVs were first isolated from mosquitoes in Finland and HakV belong to the classical ISFV (Huhtamo *et al.* 2012), while LamV belong to the dual-host affiliated ISFV (Huhtamo *et al.* 2009). Stocks of HakV and LamV were propagated in the C6/36 cell line until a clear cytopathic effect (CPE) was shown (4 days post infection (dpi)), and then supernatant was collected, centrifuged, and frozen at -80 °C. The ISFVs stock titers could not be obtained with traditional methods. Thus, to quantify the virus stocks, plasmid standards containing the PCR target region of the virus were ordered (GeneScript Biotech). Plasmids were used to construct qPCR standard curves and stock concentrations were calculated as RNA copies/mL. WNV (lineage 1) used in paper III was kindly provided by Professor Åke Lundkvist (Department of Medical Biochemistry

and Microbiology/Zoonosis Science Center, Uppsala University, Uppsala, Sweden). The WNV stock was propagated in Vero E6 cells (African green monkey clone E6) and supernatant was collected when clear cytopathic effect (CPE) was observed at three days post infection (dpi). The WNV stock titer was determined by a plaque assay, as described in (Brien *et al.* 2013).

3.6 *In vitro* infections (Paper II and III)

To study the small RNA response upon acute ISFVs infection (Papers II) and the overall gene expression upon single- or dual-infection with an ISFV and/or WNV (Paper III), the immunocompetent U4.4 cell line was infected with either HakV, LamV, WNV or a dual-infection scheme, whereby U4.4 cells were pre-infected with LamV 24 h before being challenged with WNV. On the day of infection, 24-well plates with U4.4 cells at a confluency of 85–90% (approximately 350,000 cells per well) were used. WNV-infected cells were inoculated at a multiplicity of infection (MOI) of 0.1. HakV-infected cells were inoculated with 35,000 HakV RNA copies and the LamV-infected cells were infected with either 35,000 LamV RNA copies (Paper II) or 175,000 LamV RNA copies (Paper III). For all infections, the inoculum was incubated for one hour at 28 °C, it was then discarded and replaced with growth medium. Each infection and timepoint were performed in triplicate, mock-infected cells were used as control. Cells and supernatant were sampled every 24 h post-infection (hpi) for qPCR and sequencing. All experiments were performed in the Biosafety level-3 facility at the Zoonosis Science Center, Uppsala University, Uppsala, Sweden.

3.7 Quantification of viral RNA copies of virus stocks and supernatant (Paper II and III)

To quantify the amount of viral RNA copies in stocks or supernatant of infected cells, RNA was extracted from 200 uL stock/supernatant using the same protocol as described in section 3.2, which includes TRIzol™ extraction and further purification of the aqueous phase using GeneJet spin columns.

First-strand cDNA was generated using the SuperScript™ III Reverse Transcription kit (Thermo Fisher Scientific) with Random Hexamers (Thermo Fisher Scientific) following the manufacturer's instructions. The qPCR was performed using the iTaq Universal SYBR® Green Supermix (Bio-Rad laboratories Inc) with 2 uL of template cDNA and 0.5 uM of each corresponding virus primer in a total volume of 20 uL per reaction. We used

three technical replicates and the qPCR was carried out using the Bio-Rad® CFX96 real-time PCR system (Bio-Rad laboratories Inc). Primer pairs for the qPCR were designed using virus genomes obtained from NCBI and the software Primer3 (Rozen & Skaletsky 2000), to generate a product between 170 and 200 bp long and a T_m of 60 °C.

3.8 Small and large RNA extraction (Paper I and II)

Small RNA used for high-throughput small RNA sequencing (paper II) and large RNA used for transcriptomics (paper III) was isolated from U4.4 cells infected as described in section 3.6. Cells were collected every 24 h post infection by pipetting 750 uL of TRIzol™ in the respective wells of 24-well plates. The RNA containing aqueous phase obtained after the addition of chloroform and subsequent centrifugation step was collected and the RNA was further purified using the mirVana™ PARIS™ Kit (Thermo Fisher Scientific), according to the protocol to isolate and separate, large RNA (>200 nt) and small RNA (<200 nt) provided by the manufacturer.

3.9 Small RNA sequencing and analysis (Paper II)

Small RNA isolated from the infected U4.4 cells was quantified and quality controlled with the 4150 TapeStation System using the RNA ScreenTape Analysis kit (Agilent Technologies). Triplicates from each timepoint (24-72 h) and infection (HakV, LamV or mock) were pooled and submitted to SciLifeLab (Stockholm, Sweden) for library preparation using the QIAseq miRNA low input kit (QIAGEN). The libraries were then sequenced on one flow cell of the NextSeq 2000 with a 101nt (Read1)-8nt(Index1) setup using the ‘P20’ flow cell, which generated 10–20 million reads per sample with a read length of 1 x 100 base pairs (bp).

The generated small RNA sequence data (FASTQ files) were analysed with a pipeline including the trimming of adaptors and the removal of bad quality reads using Trim Galore! (v0.6.6) (Babraham-Bioinformatics 2021a), with a setting to discard all reads below 17 nt and above 40 nt. The trimmed reads were mapped to the LamV (FJ606789) genome and the HakV (NC030401) genome using Bowtie (v1.2.3) (Langmead *et al.* 2009), allowing for one mismatch. We used the -a, -best, -strata, and -all flags, which instructed Bowtie to only report those alignments in the best alignment stratum and to generate a FASTQ file of the mapped reads in addition to the SAM file. The FASTQ files were used to analyse the size distribution of the mapped reads, which was visualized with the R package ggplot2. The SAM output files were further analysed with the MISIS-2 software (v2.6) to

visualize the alignment and polarity distribution of small RNA to the viral genomes (Seguin *et al.* 2016). The ping-pong signatures of 27–30 nt piRNA were analysed with WebLogo (Crooks *et al.* 2004).

3.10 Transcriptomics sequencing and analysis (Paper III)

Large RNA isolated from the single- and dual-infected U4.4 cells was quantified and quality-controlled in the same way as described in section 3.9. Triplicates for each infection and timepoint were submitted to SciLifeLab for library preparation using the Illumina Truseq Stranded mRNA (poly-A selection) kit. Libraries were sequenced on an Illumina NovaSeq 6000 sequencer using one lane of a S4 flow cell to a depth of 30–40 million reads per sample with a read length of 2 x 151 bp.

The raw transcriptomic FASTQ files were analysed with the bioinformatic Nextflow pipeline *nf-core/rnaseq* (v3.0) (Ewels *et al.* 2020). The pipeline included quality control (FastQC v0.11.9) (Bioinformatics 2021a), adapter and quality trimming (Trim Galore! V0.6.6) (Bioinformatics 2021b), removal of ribosomal RNA (SortMeRNA v4.2.0) (Kopylova *et al.* 2012), and pseudo-alignment and quantification (Salmon v1.4.0) (Patro *et al.* 2017), using the reference *Ae. albopictus* Foshan genome sequence and annotation (version Aalo1.2) retrieved from Vectorbase (Giraldo-Calderon *et al.* 2015). The resulting Salmon quant.sf files were further analysed with an inhouse script in R (<https://github.com/Pooh0001/Salmon/tree/V1.0>). This script includes a quality control of the data, normalization and DESeq2 analysis. Every infection group was compared with mock-infected cells at the corresponding time point, using the parameters of p-adjusted value of 0.01 and log₂ FC of 0.5 as cut-offs, following the recommendations found in (Schurch *et al.* 2016). Lists of significant differentially expressed (DE) transcripts were further analysed and transcript IDs were transferred to VectorBase for gene description and Gene Ontology (GO) enrichment analysis (Giraldo-Calderon *et al.* 2015). The latter was focused on the sole biological process aspect.

4. Results and discussion

4.1 Mosquito collection

Metagenomic studies have shown that mosquitoes harbor a far more complex virome than just the medically important arboviruses, including a broad range of viral families and host specificities. However, the majority of metagenomic studies have used mosquitoes collected in tropical regions and the knowledge of viruses harbored by mosquitoes in the Nordic region are less known. Therefore, in paper I, mosquitoes were collected in mid-east Sweden resulting in a total of 1428 mosquitoes (920 mosquitoes from Flen and 508 mosquitoes from Uppsala (Hammarskog). The most abundant mosquito species were *Coquillettidia Cq. richardii* (433), *Ae. cantans* (407), *Ae. communis* (106) and *Ae. annulipes* (72). Unfortunately, despite all efforts to collect *Culex* mosquitoes (primary vector of WNV), only a small sample size of 22 *Cx. pipiens* and four *Cx. torrentium* were obtained (Figure 7). Our collection show similar mosquito species patterns as was described by a more detailed study performed over 11 full seasons in the province of Uppland, with *Culex* mosquitoes being less abundant than for example *Cq. richardii* and *Ae. communis* (Lundström *et al.* 2013).

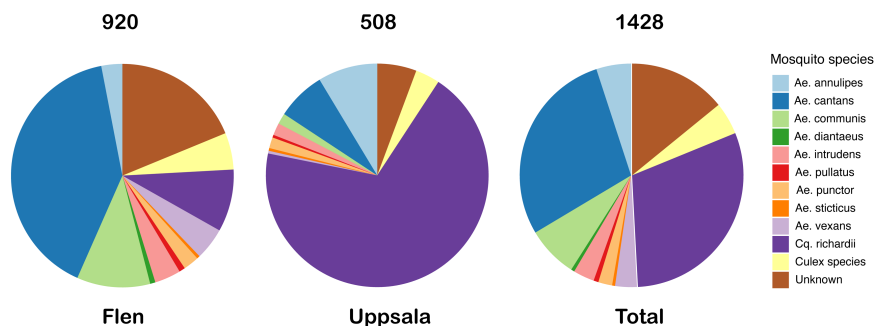


Figure 7. Distribution of all mosquito species collected in Flen and Uppsala. Mosquito species are represented by different colors. The figure is taken from the published article (Öhlund *et al.* 2019a).

4.2 The Swedish mosquito virome

A viral metagenomic approach was used to characterize the virome of 953 female mosquitoes, divided into 12 pools representing six mosquito species and two geographic locations (Table 3). High-throughput sequencing resulted in 1.4-9.2 million reads per pool, of which 1.4-42.6% were classified as mosquito/diptera reads, 13.2-56.2% as microbial reads and 1.4-12.5% as viral reads (Table 3).

Table 3. Summary of the mosquito pools that were sequenced.

Pool	Mosquito spp	Sample location	Time point	Diptera reads (%)	Microbial reads (%)	Viral reads (%)
1	<i>Cx. pipiens</i>	Mix	Mix	7.6%	27.55%	8.76%
2	<i>Cx. torrentium</i>	Mix	Mix	42.65%	56.21%	4.86%
3	<i>Ae. communis</i>	Mix	Mix	1.43%	13.78%	1.44%
4	<i>Ae. annulipes</i>	Mix	Mix	5.42%	27.65%	12.47%
5	<i>Ae. cantans</i>	Flen	May/ June	5.35%	24.75%	11.00%
6	<i>Ae. cantans</i>	Flen	July	3.3%	13.23%	5.43%
7	<i>Ae. cantans</i>	Flen	August	5.11%	19.73%	8.48%
8	<i>Ae. cantans</i>	Uppsala	Mix	6.5%	23.54%	8.00%
9	<i>Cq. richardii</i>	Uppsala	June	14.02%	26.8%	3.13%
10	<i>Cq. richardii</i>	Uppsala	July	12.6%	26.37%	5.39%
11	<i>Cq. richardii</i>	Uppsala	August	9.19%	27.73%	10.4%
12	<i>Cq. richardii</i>	Flen	Mix	12.2%	29.19%	5.81%

The viral reads were further analyzed by homology searches and a large proportion of viral reads in most of the mosquito pools were labeled as unclassified RNA viruses (Figure 8A). These unclassified viral RNAs showed close to distant similarity (28-96% amino acids (aa) identity) to viruses previously identified through large metagenomic surveys of invertebrates (Li *et al.* 2015a; Shi *et al.* 2016; Sadeghi *et al.* 2018). If the analysis were repeated today, the proportion of classified viral reads would probably be higher due to an extended viral taxonomy. Furthermore, among the classified viral reads, multiple viral families were detected, and the majority of the studied mosquito pools showed a highly diverse virome (Table 8B). The exceptions were the two *Culex* mosquito pools, which had few but very abundant viruses, one that represented more than half of the total viral reads in the *Cx. pipiens* pool. This is probably because of the small sample size, but further investigation with a larger sample size is needed to draw any conclusion. If the sequence depth and number of mosquitoes in each pool is disregarded, some differences between the mosquito genera and the viruses they harbored could be observed in this dataset; *e.g.* the *Aedes* mosquito pools, seemed to harbor a more diverse negative RNA virus virome, compared to the *Culex* and *Coquillettidia* pools, and the *Coquillettidia* mosquito pools had many viral hits among the unclassified RNA viruses. Some viral hits could only be observed in one of the mosquito genera or species, indicating a host specificity. No significant difference between the locations and time points could be observed. However, the mosquito sampling was biased between the species collected and the location, *e.g.* 350/433 of the *Cq. richardii* were collected in Uppsala and 371/407 of the *Ae. cantans* were collected in Flen (Figure 6). To draw any conclusion regarding local difference and time of the season, we would need a bigger sampling size of each mosquito species from each location and timepoint.

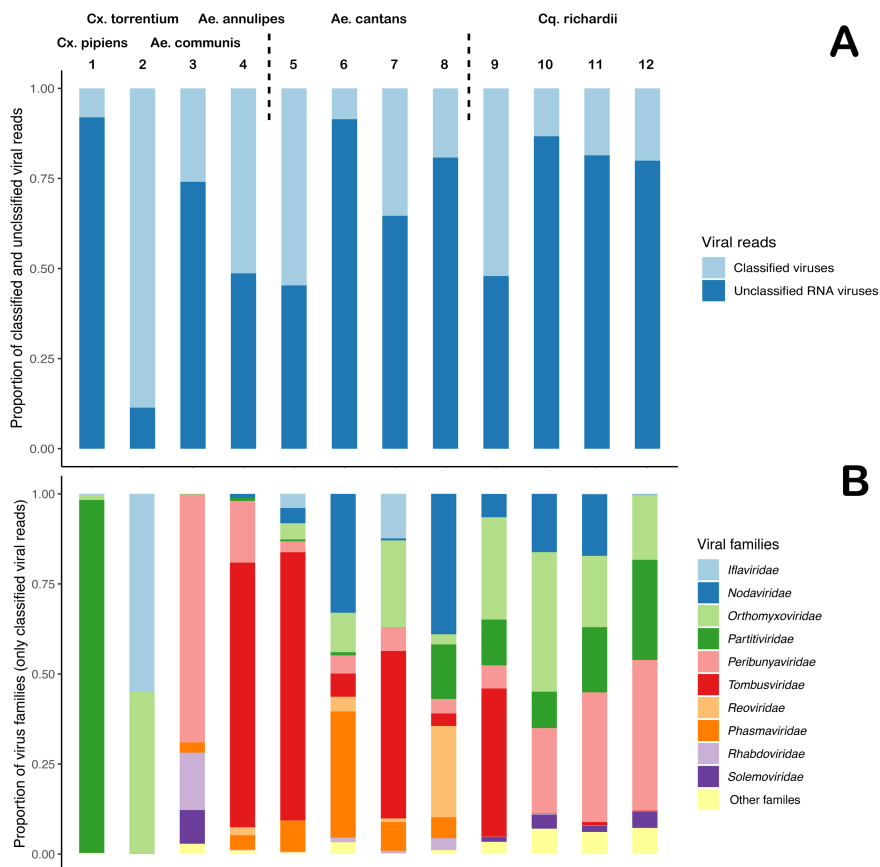


Figure 8. Annotation of viral reads in the different pools of mosquitoes. Each bar represents a mosquito pool – designated 1-12 and are described in table 3. (A) proportion of classified viral reads and unclassified RNA viral reads. (B) Proportion of virus families of the classified viral reads. The figure is taken from the published article (Öhlund *et al.* 2019a).

4.3 Characterization of RNA viruses discovered

De novo assembly of viral reads, resulted in nine near-complete viral genomes in the orders *Picornavirales*, *Tymovirales*, *Articulavirales*, *Bunyavirales*, *Mononegavirales*, *Nodamuvirales* and *Martellivirales* (Table 4). All of these viruses showed close association to viruses previously detected in mosquitoes or in other invertebrates when analyzed with nucleotide blast and through the phylogenetic analysis. Four of the near-complete genomes detected in this study (MN513381, MN513378, MN513379 and MN513374-76) showed close association to the Yongsan

picorna-like virus 3, Yongsan bunyavirus 1 and Yongsan tombus-like virus 1, which were discovered in mosquitoes collected at the Yongsan U.S army Garrison, in the Republic of Korea (Hang *et al.* 2016; Sanborn *et al.* 2019). The close phylogenetic relation to other viruses detected in insects, indicates that these might be insect-specific, however, infection studies in different vertebrate cell lines are needed to confirm this.

The two tombus-like viruses detected in this study (MN513378 and MN513379) showed close association to viruses in the order *Tymovirales*, which is mainly associated with plant and fungi viruses (Nagy 2016). Since whole mosquitoes were used in this study, plant viruses from their diet or viruses from commensal organisms residing inside or on the mosquito may get detected. However, when raw reads from respective mosquito pool were mapped to the viral genomes, a significant amount of reads mapped. This indicates a rather high abundance of the virus and possibly viral replication. To confirm replication in mosquitoes, *in vitro* infection studies of these two tombus-like viruses are needed.

This study has shown the diversity of viruses harbored by the investigated mosquito species collected in Mid-East Sweden.

Table 4. Summary of the characterized near-complete viral genomes discovered.

Virus	Viral order	Mosquito spp	Accession
Hammarskog picorna-like virus	<i>Picornavirales</i>	<i>Cq. richardii</i>	MN513381
Flen tombus-like virus	<i>Tymovirales</i>	<i>Ae. cantans</i>	MN513378
Hammarskog tombus-like virus	<i>Tymovirales</i>	<i>Cq. richardii</i>	MN513379
Flen picorna-like virus	<i>Picornavirales</i>	<i>Ae. cantans</i>	MN513377
Culex orthomyxo-like virus	<i>Articulavirales</i>	<i>Cx. torrentium</i>	MN513370-74
Flen bunya-like virus	<i>Bunyavirales</i>	<i>Ae. cantans</i>	MN513374-76
Culex mononega-like virus 2	<i>Mononegavirales</i>	<i>Cx. torrentium</i>	MN513369
Hammarskog noda-like virus	<i>Nodamuvirales</i>	<i>Cq. richardii</i>	MN513380
Hammarskog virga-like virus	<i>Martellivirales</i>	<i>Cx pipiens</i>	MN513382

4.4 Small RNA sequencing

Since no flavivirus was discovered in the Swedish mosquitoes in Paper I, the ISFVs, HakV and LamV were obtained from the EVAg for the subsequent studies. Both of these viruses were first isolated from mosquitoes collected in Finland and belong to different subcategories of ISFVs. HakV was isolated from *Ae. caspius* mosquitoes and belong to the classical ISFVs (Huhtamo *et al.* 2012), while LamV was isolated from *Ae. cinerus*

mosquitoes and belong to the dual-host affiliated ISFVs (Huhtamo *et al.* 2009).

The knowledge on the virus interaction between the mosquito host and ISVs is very sparse, and much of the current information is based on studies done with human pathogenic arboviruses. Therefore, the thesis work progressed by investigating the RNAi-mediated antiviral immunity to acute infection of the ISFVs HakV and LamV. The immunocompetent *Ae albopictus* derived cell line U4.4 was infected with either HakV or LamV at a concentration of 35,000 RNA copies/mL. Cells were collected at 24 h, 48 h and 72 h post-infection (hpi) and processed for small RNA sequencing. The retrieved sequence data had between 10,4-16,9 million reads per sample and a read length between 17 and 40 nt, after trimmed from adapters and removal of bad quality reads.

4.5 RNAi-mediated immunity to ISFV infection

To investigate the RNAi-induced production of virus-derived small RNAs (vsRNAs) the trimmed sequence data from respective infection was mapped to the corresponding viral genome. Results from HakV- and LamV-infected cells showed a low production of vsRNA at the early timepoint which gradually increased over time, probably due to increased infection rates and higher concentrations of viral genomes in the cells. The proportion of vsRNA to total sRNA was between, 0.01-0.001% at 24 hpi, 0.06% at 48 hpi and 0.17-0.08% at 72 hpi. Interestingly, the increased proportion of vsRNA correlated with the plateau of the virus growth curves, which could indicate RNAi-induced interference with virus replication (Figure 9G).

Furthermore, when analyzing the distribution of vsRNA across the viral genomes, both HakV and LamV derived sRNAs mapped along the whole genome, however, some differences could be observed. vsRNA from HakV-infected cells were evenly distributed from the sense and antisense strand and had slightly more coverage at the 3'-end, which correspond to the NS5 gene region (Figure 9C). vsRNA from LamV-infected cells were mainly derived from the antisense genome and had four hotspots located in genome regions corresponding to the capsid protein, NS2A, NS4A and the 3'-UTR (Figure 9D). The bias for antisense-derived vsRNA is a bit enigmatic, but could indicate that the source for vsRNA production is not primarily dsRNA in the cytosol.

The siRNA pathway is thought to be the primary antiviral defense in mosquitoes, and when analyzing the read length distribution of vsRNA, siRNA was the most abundant population (21 nt) of vsRNA in both HakV- and LamV-infected cells. The LamV-infected cells had a virus-derived

siRNA (vsiRNA) proportion between 32,2-36,7%, and the HakV-infected cells had a slightly higher proportion of 48,4-66,5% (Figure 9E and F). However, although, robust siRNA response has been observed in both arbovirus- and ISV-infections (Goertz *et al.* 2019), mosquitoes are usually persistently infected with little or no fitness cost and it has been postulated that this is enabled by the siRNA response. The siRNA pathway keeps the viral load in the host cell at a tolerable level, thereby sustaining a persistent infection (Goic *et al.* 2016). Our data, suggest that the persistent infection of ISFV in mosquitoes, could at least partially be due to the siRNA response induced by the ISFVs.

Interestingly, vsRNA in the size range of piRNA (24-30 nt) were only observed in the LamV-infected cells (Figure 9E and F), which suggest that the biogenesis of virus-derived piRNAs (vpiRNAs) is virus-dependent. One can speculate that a virus-specific sequence element or structure is needed for the production of vpiRNA, which is absent in the classical ISFV but present in the dual-host affiliated ISFV. It would be interesting to further investigate if similar results are observed during infection of other classical and dual-host affiliated ISFVs.

Furthermore, the vpiRNAs observed in the LamV-infected cells did not show the typical signatures for ping-pong amplified piRNAs. Ping-pong amplification would predict an even distribution of piRNA from both strands, with a nucleotide bias of an U in the first position of those derived from the antisense and an A in the tenth position of those derived from the sense strand (Girardi *et al.* 2017). However, the vpiRNA observed in the LamV-infected cells were mainly derived from the antisense strand, with a nucleotide bias of a U at the first position, which is also characteristic for primary piRNA. However, the few vpiRNA derived from the sense strand did not contain the A bias in the tenth position. Similar results have been observed in U4.4 cells infected with WNV (Goertz *et al.* 2019), and Aag2 cells infected with ZIKV (Varjak *et al.* 2017). These observations suggest that the identified vpiRNAs could be primary piRNAs and one can hypothesize that they are derived from vDNA in the cytosol or integrated NIRVS (Houe *et al.* 2019), which are more likely to have a biased production of precursors mainly from the antisense strand (Tassetto *et al.* 2019). Furthermore, the Piwi-4 protein in Aag2 cell infected with Sinbis virus (SINV) was shown to specifically bind to antisense vpiRNA produced from NIRVS/EVEs leading to methylation of the 3'-end (maturation) protecting them from beta-elimination (Tassetto *et al.* 2019).

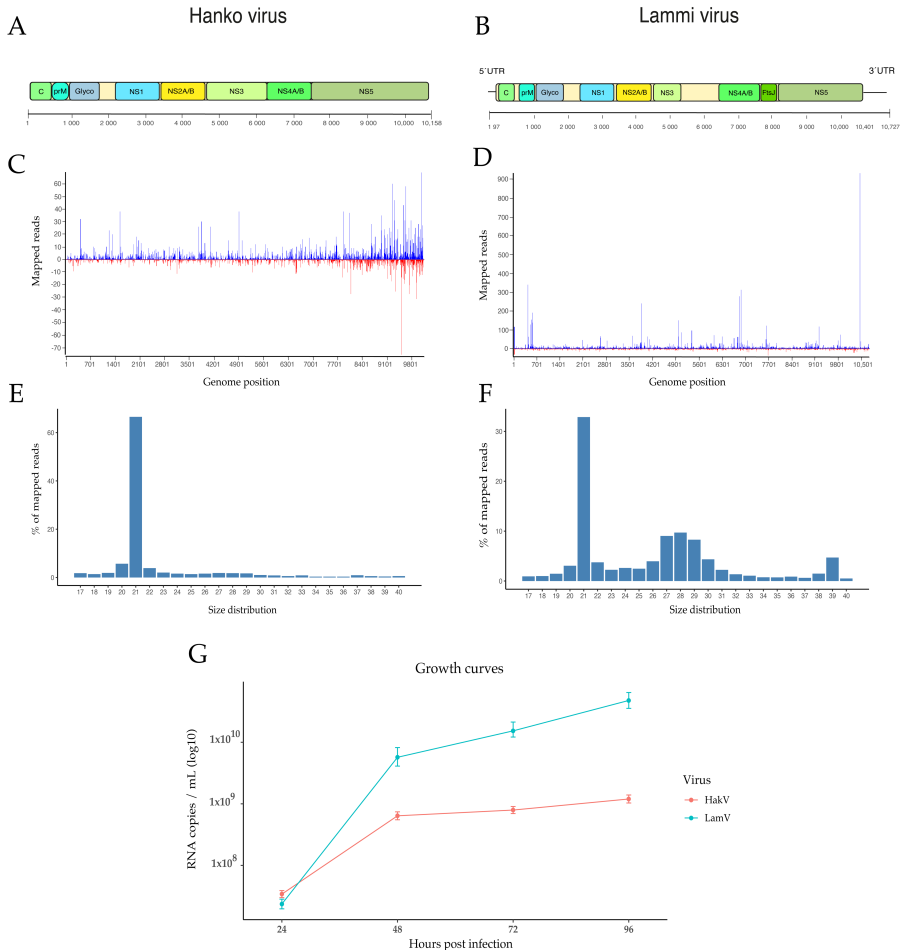


Figure 9. Viral small RNA profiles of U4.4 cells after LamV or HakV infection. (A) Schematic representation of HakV genome and (B) LamV genome. (C) Distribution of vsRNA along the HakV genome at 72 hpi. (D) Distribution of vsRNA along the LamV genome at 72 hpi. (E) Length distribution of HakV-specific vsRNA at 72 hpi. (F) Length distribution of HakV-specific vsRNA at 72 hpi. (G) Growth curve of HakV and LamV, shown as RNA copies/mL over time. Dots show mean RNA copy number with a standard deviation between biological replicates. The figure consists of several figures from the published article (Öhlund *et al.* 2021).

4.6 Transcriptomics of ISFV and arbovirus infection

Understanding the flavivirus infection process and interactions with the mosquito host is important and fundamental in the search for novel arbovirus control strategies and interruption of flavivirus transmission by mosquitoes (Figure 10).

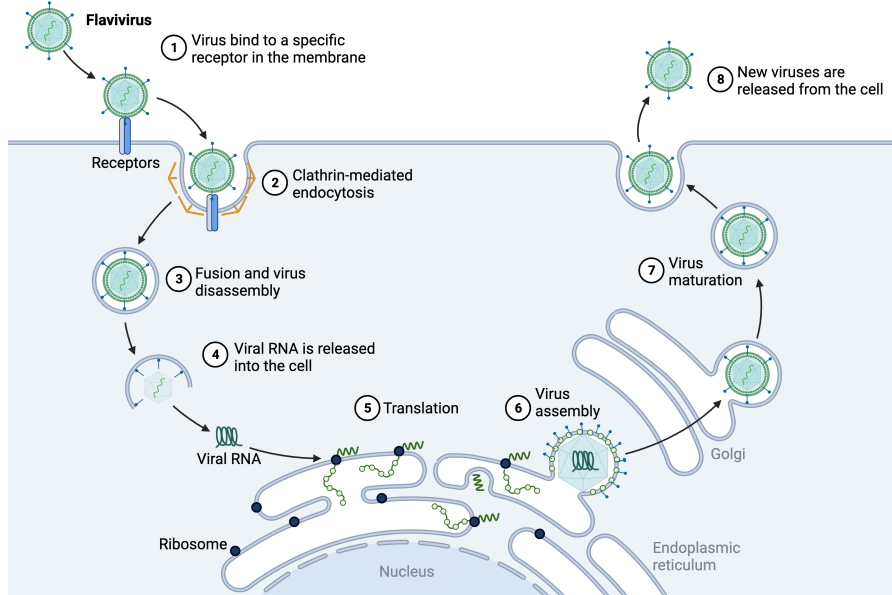


Figure 10. Schematic illustration of the flavivirus infection cycle in the cell.

In Paper II, the insect-specific LamV was shown to effectively replicate in the *Ae albopictus* derived cell line U4.4 and to mount a robust RNAi-mediated immune response. To further investigate the virus-host interaction and altered gene expression upon flavivirus-infection, RNA-sequencing was conducted on poly(A)-enriched RNA extracted from U4.4 cells infected with either LamV or WNV. In addition, we included an infection scheme whereby cells were pre-infected with LamV 24 h before being challenged with WNV, to study the interference effect of prior ISFV-infection on the replication of a secondary arbovirus infection. Cells were collected between 24 hpi to 72 hpi as biological triplicates, including mock-infected cells. A total of 30 RNA-seq libraries were created, which generated between 31,1 to 50,9 million paired-end reads per sample.

4.7 Altered gene expression upon LamV infection

When comparing the altered gene expression of LamV-infected cells to mock controls at 24 h to 72 hpi, 13 (13 up-regulated), 102 (84 up- and 18 down-regulated) and 359 (180 up- and 179 down-regulated) transcripts were significantly differently expressed (DE) in each respective timepoint. Only two transcripts very commonly DE at all time points and these transcripts were up-regulated and coding for a 40S ribosomal protein S21 (Figure 11 and Table 5).

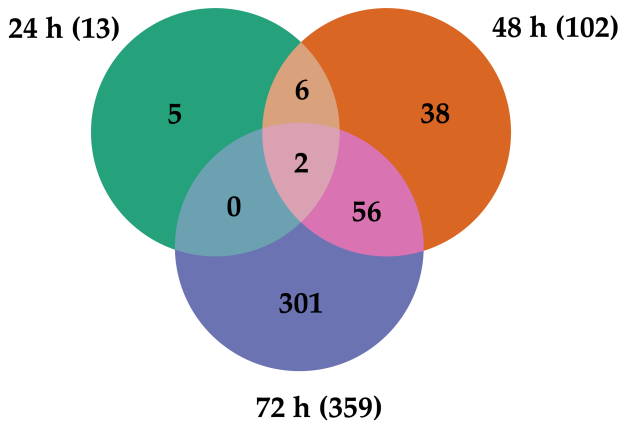


Figure 11. Venn diagram representing the number of significantly DE at the different time points of LamV-infected U4.4 cells. The figure is taken from the published article (Öhlund *et al.* 2022).

Furthermore, when focusing on the most highly DE transcripts at either direction, many genes coding for different heat-shock proteins (HSPs) were observed to be up-regulated. The HSPs are a family of proteins that are expressed by cells in response to stressful conditions, such as heat-shock, wound healing and during pathogen infections. Many of the HSPs perform chaperone functions by guiding and ensuring correct folding of proteins (Zhao *et al.* 2009). Among the up-regulated HSPs, we observed endoplasmic reticulum chaperone, also known as HSP-90, two HSP-40 proteins, a HSP-70 protein known as Bip/GRP-79, two proteins of the GRP-E family, which act as co-chaperons for the HSP-70 proteins (Table 5). Two proteins within the family *lethal(2)-essential-for-life (l(2)efl)* were up-regulated and are known as HSP-20 proteins. The *l(2)efl* family have been observed to be up-regulated during DENV-2 infection in *Ae. aegypti* mosquitoes, and suppression of *l(2)efl* genes in the mosquito cell line CCL-125 resulted in increased replication of DENV-2, while enhanced expression of *l(2)efl* genes resulted in reduced DENV-2 replication in the same cell line (Runtuwene *et al.* 2020). Among

the most down-regulated transcripts, two histone H2A and three histone H2B were observed (Table 5). This down-regulation of histones is a bit enigmatic, and the opposite has been observed, where the DENV capsid protein was shown to bind to core histones and act as a histone mimic, possibly to favor viral replication. The host cells responded to this by increasing the production of histones (Colpitts *et al.* 2011). To conclude, no known immune effect proteins were observed among the DE transcripts, which suggests that LamV does not evoke the signaling immune pathways or induce a higher expression of RNAi-pathway proteins. However, the active viral infection and replication induced a strong stress response in the cells with an increased expression of different HSPs.

Table 5. DE transcripts described in the text above following LamV infection. The cut-offs used were *p*-adjusted value of ≤ 0.01 and log₂ fold change of ≥ 0.5 . Bold numbers have significant *p*-adjust value.

Transcript ID	Protein	Log2 fold change 24 hpi	Log2 fold change 48 hpi	Log2 fold change 72 hpi
AALF005471	40S ribosomal protein S21	1.0562	1.1301	0.85
AALF002626	40S ribosomal protein S21	1.0391	0.9034	0.0978
AALF011939	HSP-90	-0.0125	1.0744	0.787
AALF010569	HSP-40	1.4235	3.7625	3.09
AALF013640	HSP-40	0.2059	1,4541	2.2194
AALF021835	HSP-70	0.0521	1.3414	1.2567
AALF026344	GRP-E family	0.2767	0.6026	1.3522
AALF026694	GRP-E family	0.2329	0.7675	1.3438
AALF005663	<i>l(2)efl</i>	0.441	1.3782	1.2391
AALF015016	<i>l(2)efl</i>	0.14489	0.9516	1.2629
AALF007138	H2A	0.1922	0.2182	-1.9303
AALF010649	H2A	0.6116	0.1366	-2.0894
AALF010137	H2B	0.3631	-0.3504	-2.1733
AALF014537	H2B	0.0576	-0.4323	-2.3487
AALF010648	H2B	0.1482	-0.3246	-2.5371

4.8 Altered gene expression upon WNV infection

The analysis and comparison of WNV-infected cells to mock controls showed 108 (65 up- and 43 down-regulated) and 138 (85 up- and 53 down-regulated) significantly DE transcripts at 24 hpi and 48 hpi. Comparison of the transcriptome profiles, showed 23 overlapping DE transcripts between the two timepoints (Figure 12). Many of the up-regulated overlapping transcripts were related to immune effector proteins, and when further analyzing the most highly DE transcripts, a cascade of up-regulated immune-related genes were observed. Many of these have previously been described during arbovirus infection of mosquitoes and mosquito-derived cell lines (Shin *et al.* 2014; Etebari *et al.* 2017; Shrinet *et al.* 2017; Li *et al.* 2020; Li *et al.* 2021). Among the uppermost up-regulated immune-related transcripts observed in this study, we found C-type lysozyme, C-type lectin, defensin, leucine-rich immune protein, cecropin-A2, prophenoloxidase, clip-domain serine protease family B and peptidoglycan-recognition protein (Table 6). Interestingly, among the most down-regulated transcript we could observe genes that belong to the same protein-family as some of the up-regulated immune genes, such as C-type lectin, Serine protease and clip-domain serine protease family D (Table 6). However, the down-regulated genes showed very low similarity to the up-regulated counterpart, and we speculate that these down-regulated proteins have a negative-regulating function in controlling the immune activity under normal conditions. A down-regulation of these proteins may increase the expression or activity of an immune effector protein within the same family.

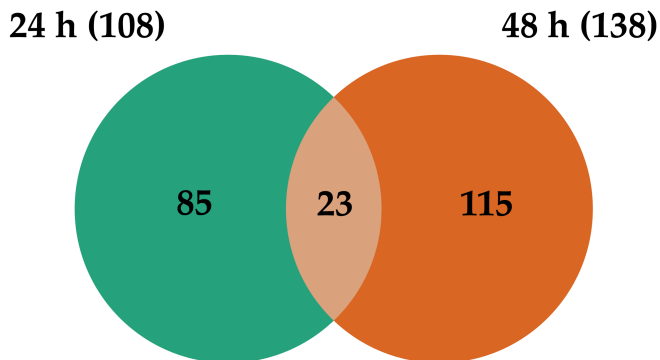


Figure 12. Venn diagram representing the number of significantly DE at the different time points of WNV-infected U4.4 cells. The figure is taken from the published article (Öhlund *et al.* 2022).

Table 6. DE transcripts described in the text above following WNV infection. The cut-offs used were p -adjusted value of ≤ 0.01 and \log_2 fold change of ≥ 0.5 . Bold numbers have significant p -adjust value.

Transcript ID	Protein	Log2 fold change 24 hpi	Log2 fold change 48 hpi
AALF021807	C-type lysozyme	2.6372	0.8026
AALF016234	C-type lectin	1.9185	1.2493
AALF008821	defensin	1.6614	1.7614
AALF016505	leucine-rich immune protein	1.2261	0.4717
AALF000656	cecropin-A2	1.2251	1.4427
AALF012716	prophenoloxidase	0.9904	0.3324
AALF019859	clip-domain serine protease family B	1.6947	0.9666
AALF020197	clip-domain serine protease family B	1.1833	-0.07211
AALF020799	peptidoglycan-recognition protein	1.1608	1.0099
AALF009202	C-type lectin	-1.8152	0.1942
AALF013937	Serine protease	-1.7158	-0,3632
AALF015014	clip-domain serine protease family D	-2.3914	-0.4714

4.9 Altered gene expression in Dual-infected cells

The mRNA expression profiles of U4.4 cells dual-infected with WNV 24 h post-infection with LamV, showed the highest amount of significantly DE transcripts with 117 (70 up- and 47 down-regulated) and 577 (300 up- and 277 down-regulated) at 24 h and 48 h post WNV-infection. Between the two timepoints 55 overlapping transcripts were observed (Figure 13), 22 up-regulated transcripts in both timepoints of which many were immune-related genes. Three transcripts that were up-regulated at 24 hpi but down-regulated at 48 hpi, which were also related to immune genes. Among the 30 down-regulated transcripts in common, some were related to immune processes and DNA metabolic processes, but a large proportion was not annotated and no function information is available.

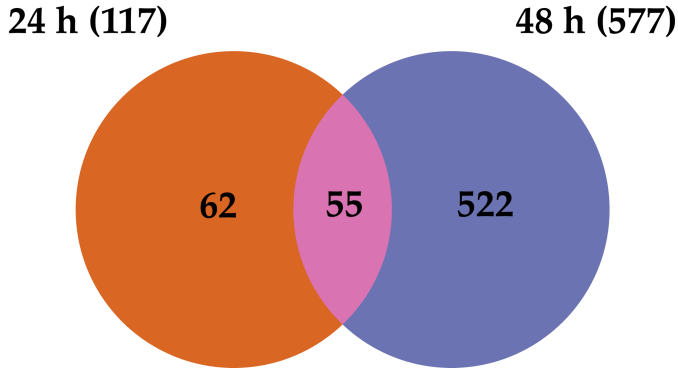


Figure 13. Venn diagram representing the number of significantly DE at the different time points of dual-infected U4.4 cells. The figure is taken from the published article (Öhlund *et al.* 2022).

Furthermore, the transcriptome profiles of the dual-infected cells, showed a mix of altered gene expression triggered by both LamV and WNV. Although, cells were pre-infected with LamV before challenged with WNV, their transcriptome profile were more similar to the one of WNV-only infected cells at 24 hpi (Figure 15A). They had 102 DE in common, of which many were immune-related genes that were expressed at similar levels. However, at 48 h post WNV challenge, the transcriptome profile were more similar to the LamV-only infected cells at 72 hpi (Figure 15B), with 291 DE transcripts in common, such as an up-regulation of HSPs and down-regulation of histone proteins. Furthermore, at the late time point, 254 DE transcripts were only observed in the dual-infected cells. Among this group of transcripts, two mitogen-activated protein kinases (MAPK) were highly up-regulated (Table 7). The MAPK is known to regulate a broad range of cellular processes, such as growth, metabolism, apoptosis and innate immune responses through various signaling cascades. However, the function of MAPK in mosquitoes has a very limited understanding (Horton *et al.* 2011), and with such range of potential functions it is hard to draw any conclusions. Unfortunately, a large proportion of the 254 DE transcripts, lacked annotation in the database and we were unable to infer a functional role for these.

Table 7. DE transcripts described in the text above following WNV infection. The cut-offs used were p -adjusted value of ≤ 0.01 and \log_2 fold change of ≥ 0.5 . Bold numbers have significant p -adjust value.

Transcript ID	Protein	Log2 fold change 24 hpi with WNV	Log2 fold change 48 hpi with WNV
AALF018203	MAPK	0.2228	2.167
AALF011886	MAPK	0.5439	1.6377

4.10 Prior LamV-infection interference of WNV

Supernatant from each infection group was collected to investigate the possible interfering effect of a prior LamV-infection on WNV replication. Extracted RNA was used to follow the infections over time with a qPCR-analysis. Results showed that the level of LamV RNA copies were similar between cells infected only with LamV and dual-infected cells (Figure 14A). However, the level of WNV RNA copies were significantly lower in those cells pre-infected with LamV compared to those only-infected with WNV (Figure 14B).

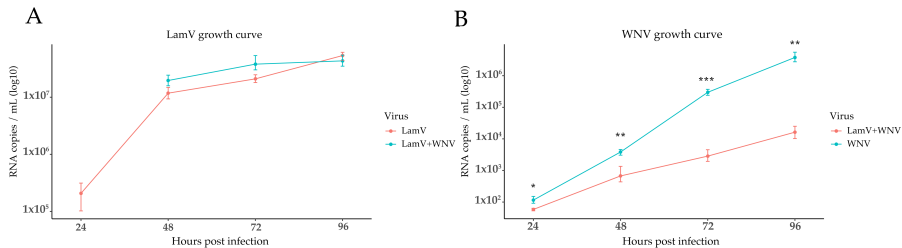
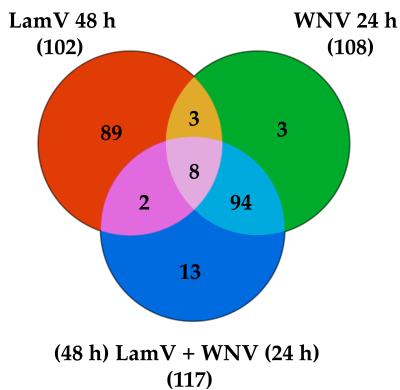


Figure 14. Growth curve of virus replication in supernatant shown as RNA copies/mL, dots show mean RNA copy number with a standard deviation between biological replicates. (A) after LamV-infection (B) after WNV-infection. * $p < 0.05$, ** $p < 0.01$, *** $p < 0.001$. The figure is taken from the published article (Öhlund *et al.* 2022).

Since a prior LamV-infection seemed to restrain the secondary WNV infection, potential gene targets for modification in mosquitoes to reduce transmission of flaviviruses were investigated. These potential genes would most likely be among the DE transcripts in the LamV-only and dual-infected cells, that do not overlap with the DE transcripts of WNV-only infected cells (Figure 15C and D). Therefore, these groups of DE transcripts were further analyzed as potential genes for modification, and among these transcripts many of the HSPs described in 4.7 were commonly up-regulated, such as the

HSP-90, the HSP-70, the HSP-40 and the GRP-E family co-chaperon (Table 8). Unfortunately, for a large proportion of transcripts that could be potential gene targets of modification, we were unable to infer a functional role, due to lack of annotation in the databases. This was especially problematic among the DE transcripts in the dual-infected cells. Interestingly, among the overlapping transcripts between all infection groups, an up-regulation of transcripts related to protein processing in the endoplasmic reticulum were observed, including the signal peptidase complex (SPC) proteins, SPC 25 kDa subunit, SPC subunit 3 and SPC subunit SEC11 (Table 9). These proteins have shown to be important for proper cleavage of the flavivirus structural (PrM and E) needed for assembly and secretion of viral particles. Silencing of the SPC 1, 2 or 3 in *Drosophila* DL1 cells resulted in reduced infection of WNV and DENV-2 without affecting the cell viability. Similar results were observed when SPC-2 was silenced in the *Ae. aegypti* derived cell line Aag2 (Zhang *et al.* 2016).

A



B

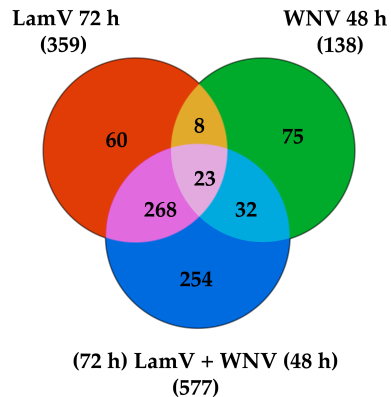


Figure 15. Venn diagram representing the number of significantly DE transcripts among the infection schemes. (A) LamV at 48 hpi, WNV at 24hpi and the dual-infection 48 hpi with LamV and 24 hpi with WNV. (B) LamV at 72 hpi, WNV at 48hpi and the dual-infection 72 hpi with LamV and 48 hpi with WNV. The figure is taken from the published article (Öhlund *et al.* 2022).

Table 8. DE transcripts of HSPs at 72 hpi with LamV and 48 hpi with WNV. The cut-offs used were p -adjusted value of ≤ 0.01 and log2 fold change of ≥ 0.5 . Bold numbers have significant p -adjust value.

Transcript ID	Protein	Log2 fold change 72 hpi with LamV	Log2 fold change 48 hpi with WNV	Log2 fold change dual-infected 48 hpi with WNV
AALF011939	HSP-90	0.787	0.0881	1.1134
AALF021835	HSP-70	1.2567	0.0139	1.5011
AALF013640	HSP-40	2.2194	-0.072	2.2416
AALF026344	GRP-E family	1.3522	0.6782	1.5012
AALF026694	GRP-E family	1.3438	0.6295	1.46

Table 9. DE transcripts of SPC proteins in common between all infection at 48 hpi with LamV and 24 hpi with WNV. The cut-offs used were p -adjusted value of ≤ 0.01 and log2 fold change of ≥ 0.5 . Bold numbers have significant p -adjust value.

Transcript ID	Protein	Log2 fold change 48 hpi with LamV	Log2 fold change 24 hpi with WNV	Log2 fold change dual-infected 24 hpi with WNV
AALF006247	SPC 25 kDa subunit	1.2853	0.9409	0.9406
AALF003192	SPC subunit 3	1.1982	0.8185	0.8181
AALF019423	SPC subunit SEC11	0.9981	0.7226	0.722

The results presented in Paper III, only give an overview of the altered gene expression upon acute infection of the different infection schemes in cell culture. Further *in vivo* studies are needed to validate the possible interference effect of LamV on WNV transmission. The potential gene targets for modification also need to be validated through knockdown or overexpression studies both *in vitro* and *in vivo* to investigate the effects on virus transmission and host viability.

5. Conclusion

This thesis has investigated a group of viruses known as insect-specific flaviviruses (ISFVs) with the focus on how they affect the mosquito host and if ISFVs can be used to manipulate the mosquito antiviral immunity to increase host's resistance to infection of medically important arboviruses, with a specific focus on WNV. First, it investigated viruses harbored by mosquitoes collected in mid-east Sweden, which revealed a highly diverse virome, composed of a broad range of viral families in most of the mosquito species studied. Some differences between the mosquito genera and the viruses they harbored could be observed, such as that *Aedes* mosquitoes seem to harbor more negative RNA viruses and *Coquillettidia* mosquitoes had many viral hits among the unclassified viruses. Furthermore, nine near-complete viral genomes were detected and characterized, which were phylogenetically affiliated to viruses previously described from large metagenomic studies of insects. However, further studies are needed to confirm host specificity.

Acute infection of the ISFVs LamV or HakV in an *Ae. albopictus* derived cell line induces a strong RNAi mediated immune response. The siRNA-pathway elicited the strongest response, where vsiRNAs were the largest proportion of sRNA in both infections. The siRNA-pathway has been associated with persistent viral infection in the mosquito, by controlling the viral replication but not clearing the infection. This suits the viral growth shown in Paper II, which display a plateau with increasing amounts of vsiRNAs, but do not inhibit the viral replication. Furthermore, in the cells infected with LamV, which is closely related to the dual-host flaviviruses, a production of vpiRNA was observed, while in cells infected with HakV, which is more distantly related to the dual-host flaviviruses, no vpiRNA was observed. This suggests that the biogenesis of vpiRNAs is virus-dependent.

Furthermore, the vpiRNAs observed in the LamV-infected cells did not show the typical signatures for ping-pong amplified piRNAs, and we speculate that these could be primary piRNAs derived from vDNA in the cytosol or integrated NIRVS.

The analysis and comparison of mRNA expression profiles of WNV-infected cells to mock controls showed a cascade of up-regulated immune genes, while in the LamV-infected cells, no up-regulation of immune-related genes was observed, however, the active viral infection induced a strong stress response in the cells, with an increased expression of different HSPs. Furthermore, the transcriptome profiles of the dual-infected cells had the highest amount of DE transcripts, which was a mix of up- and down-regulated genes triggered by both LamV and WNV, which was more similar to the one of only WNV-infected cells at the early time points, but switched and was more similar to the one of only LamV-infected cells at the late time point.

Results from the qPCR analysis of supernatant collected over time, revealed that the level of WNV RNA copies were significantly lower in those cells pre-infected with LamV compared to those only-infected with WNV, which suggest that a prior LamV-infection restrains the secondary WNV-infection. Because of this, a panel of potential gene targets for modification in mosquitoes to reduce transmission of medically important flaviviruses was suggested. Among these, five different HSPs and three SPC proteins were selected. The five HSPs were only significantly DE in the LamV- and dual-infected cells, while the SPC proteins were significantly DE among all infection groups and have shown to be important for proper cleavage of flavivirus structural proteins and secretion of viral particles.

Overall, this thesis provides knowledge that could aid in the development of novel control strategies that aim to reduce the vector transmission of arboviruses.

6. Future perspectives

- Further investigation of the biogenesis of vpiRNAs during ISFV-infection is required to elucidate virus-dependent factors needed to trigger the production, the source of vpiRNA precursors and host proteins involved in the biogenesis of vpiRNA.
- LamV-Infection studies in mosquitoes are needed to elucidate viral tropism, vertical transmission, host viability and the effect on secondary arbovirus-infections and transmission. All this information is crucial to validate LamV as a potential biocontrol agent.
- The potential gene targets for modification needs to be validated through knockdown or overexpression studies both *in vitro* and *in vivo* to investigate the effects on virus replication, transmission and host viability.

References

- Anderson, J.F., Ferrandino, F.J., Dingman, D.W., Main, A.J., Andreadis, T.G. & Becnel, J.J. (2011). Control of mosquitoes in catch basins in Connecticut with *Bacillus thuringiensis israelensis*, *Bacillus sphaericus*, [corrected] and spinosad. *J Am Mosq Control Assoc*, 27(1), 45-55.
- Bakonyi, T., Ferenczi, E., Erdelyi, K., Kutasi, O., Csorgo, T., Seidel, B., Weissenbock, H., Brugger, K., Ban, E. & Nowotny, N. (2013). Explosive spread of a neuroinvasive lineage 2 West Nile virus in Central Europe, 2008/2009. *Vet Microbiol*, 165(1-2), 61-70.
- Bardos, V., Adamcova, J., Dedei, S., Gjini, N., Rosicky, B. & Simkova, A. (1959). Neutralizing antibodies against some neurotropic viruses determined in human sera in Albania. *J Hyg Epidemiol Microbiol Immunol*, 3, 277-82.
- Bavia, L., Mosimann, A.L., Aoki, M.N. & Duarte Dos Santos, C.N. (2016). A glance at subgenomic flavivirus RNAs and microRNAs in flavivirus infections. *Virology*, 13, 84.
- Becker, N., Petric, D., Zgomba, M., Boase, C., Dahl, C., Madon, M. & Kaiser, A. (2010). *Mosquitoes and Their Control, Second Edition*. (Journal of the European mosquito control association 1). Berlin Heidelberg: Springer-Verlag. <Go to ISI>://WOS:000282534400003
- Benedict, M.Q., Levine, R.S., Hawley, W.A. & Lounibos, L.P. (2007). Spread of the tiger: global risk of invasion by the mosquito *Aedes albopictus*. *Vector Borne Zoonotic Dis*, 7(1), 76-85.
- Best, S.M. (2016). Flaviviruses. *Curr Biol*, 26(24), R1258-R1260.
- Babraham-Bioinformatics, (2021a). *Trim Galore*. Available online: https://www.bioinformatics.babraham.ac.uk/projects/trim_galore/ (accessed on 15 March 2022)
- Babraham-Bioinformatics, (2021b). *FastQC*. Available online: <https://www.bioinformatics.babraham.ac.uk/projects/fastqc/> (accessed on 15 March 2022)
- Blair, C.D. (2011). Mosquito RNAi is the major innate immune pathway controlling arbovirus infection and transmission. *Future Microbiol*, 6(3), 265-77.

- Blitvich, B.J. & Firth, A.E. (2015). Insect-specific flaviviruses: a systematic review of their discovery, host range, mode of transmission, superinfection exclusion potential and genomic organization. *Viruses*, 7(4), 1927-59.
- Bolling, B.G., Eisen, L., Moore, C.G. & Blair, C.D. (2011). Insect-specific flaviviruses from *Culex* mosquitoes in Colorado, with evidence of vertical transmission. *Am J Trop Med Hyg*, 85(1), 169-77.
- Bolling, B.G., Weaver, S.C., Tesh, R.B. & Vasilakis, N. (2015). Insect-Specific Virus Discovery: Significance for the Arbovirus Community. *Viruses*, 7(9), 4911-28.
- Bonds, J.A. (2012). Ultra-low-volume space sprays in mosquito control: a critical review. *Med Vet Entomol*, 26(2), 121-30.
- Brackney, D.E., Scott, J.C., Sagawa, F., Woodward, J.E., Miller, N.A., Schilkey, F.D., Mudge, J., Wilusz, J., Olson, K.E., Blair, C.D. & Ebel, G.D. (2010). C6/36 *Aedes albopictus* cells have a dysfunctional antiviral RNA interference response. *PLoS Negl Trop Dis*, 4(10), e856.
- Breitwieser, F.P. & Salzberg, S.L. (2020). Pavian: interactive analysis of metagenomics data for microbiome studies and pathogen identification. *Bioinformatics*, 36(4), 1303-1304.
- Brien, J.D., Lazear, H.M. & Diamond, M.S. (2013). Propagation, quantification, detection, and storage of West Nile virus. *Curr Protoc Microbiol*, 31, 15D 3 1-15D 3 18.
- Buchfink, B., Xie, C. & Huson, D.H. (2015). Fast and sensitive protein alignment using DIAMOND. *Nat Methods*, 12(1), 59-60.
- Buchman, A., Gamez, S., Li, M., Antoshechkin, I., Li, H.H., Wang, H.W., Chen, C.H., Klein, M.J., Duchemin, J.B., Crowe, J.E., Jr., Paradkar, P.N. & Akbari, O.S. (2020). Broad dengue neutralization in mosquitoes expressing an engineered antibody. *PLoS Pathog*, 16(1), e1008103.
- Calisher, C.H. & Higgs, S. (2018). The Discovery of Arthropod-Specific Viruses in Hematophagous Arthropods: An Open Door to Understanding the Mechanisms of Arbovirus and Arthropod Evolution? *Annu Rev Entomol*, 63, 87-103.
- Calzolari, M., Ze-Ze, L., Ruzek, D., Vazquez, A., Jeffries, C., Defilippo, F., Osorio, H.C., Kilian, P., Ruiz, S., Fooks, A.R., Maioli, G., Amaro, F., Tlusty, M., Figuerola, J., Medlock, J.M., Bonilauri, P., Alves, M.J., Sebesta, O., Tenorio, A., Vaux, A.G.C., Bellini, R., Gelbic, I., Sanchez-Seco, M.P., Johnson, N. & Dottori, M. (2012). Detection of mosquito-only flaviviruses in Europe. *J Gen Virol*, 93(Pt 6), 1215-1225.

- Caminade, C., Medlock, J.M., Ducheyne, E., McIntyre, K.M., Leach, S., Baylis, M. & Morse, A.P. (2012). Suitability of European climate for the Asian tiger mosquito *Aedes albopictus*: recent trends and future scenarios. *J R Soc Interface*, 9(75), 2708-17.
- Caragata, E.P., Dutra, H.L.C., Sucupira, P.H.F., Ferreira, A.G.A. & Moreira, L.A. (2021). Wolbachia as translational science: controlling mosquito-borne pathogens. *Trends Parasitol*, 37(12), 1050-1067.
- Castillo, J.C., Robertson, A.E. & Strand, M.R. (2006). Characterization of hemocytes from the mosquitoes *Anopheles gambiae* and *Aedes aegypti*. *Insect Biochem Mol Biol*, 36(12), 891-903.
- CDC (2016). *Species of dead birds in which West Nile virus has been detected, United States, 1999-2016*. <https://www.cdc.gov/westnile/resources/pdfs/BirdSpecies1999-2016.pdf>
- Ciota, A.T. & Kramer, L.D. (2013). Vector-virus interactions and transmission dynamics of West Nile virus. *Viruses*, 5(12), 3021-47.
- Colpitts, T.M., Barthel, S., Wang, P. & Fikrig, E. (2011). Dengue virus capsid protein binds core histones and inhibits nucleosome formation in human liver cells. *PLoS One*, 6(9), e24365.
- Crochu, S., Cook, S., Attoui, H., Charrel, R.N., De Chesse, R., Belhouchet, M., Lemasson, J.J., de Micco, P. & de Lamballerie, X. (2004). Sequences of flavivirus-related RNA viruses persist in DNA form integrated in the genome of *Aedes* spp. mosquitoes. *J Gen Virol*, 85(Pt 7), 1971-1980.
- Crooks, G.E., Hon, G., Chandonia, J.M. & Brenner, S.E. (2004). WebLogo: a sequence logo generator. *Genome Res*, 14(6), 1188-90.
- Davidson, A.H., Traub-Dargatz, J.L., Rodeheaver, R.M., Ostlund, E.N., Pedersen, D.D., Moorhead, R.G., Stricklin, J.B., Dewell, R.D., Roach, S.D., Long, R.E., Albers, S.J., Callan, R.J. & Salman, M.D. (2005). Immunologic responses to West Nile virus in vaccinated and clinically affected horses. *J Am Vet Med Assoc*, 226(2), 240-5.
- Delatte, H., Desvars, A., Bouetard, A., Bord, S., Gimonneau, G., Vourc'h, G. & Fontenille, D. (2010). Blood-feeding behavior of *Aedes albopictus*, a vector of Chikungunya on La Reunion. *Vector Borne Zoonotic Dis*, 10(3), 249-58.
- Doudna, J.A. & Charpentier, E. (2014). Genome editing. The new frontier of genome engineering with CRISPR-Cas9. *Science*, 346(6213), 1258096.
- Dutra, H.L., Rocha, M.N., Dias, F.B., Mansur, S.B., Caragata, E.P. & Moreira, L.A. (2016). Wolbachia Blocks Currently Circulating Zika Virus

- Isolates in Brazilian *Aedes aegypti* Mosquitoes. *Cell Host Microbe*, 19(6), 771-4.
- Edgar, R.C. (2004). MUSCLE: multiple sequence alignment with high accuracy and high throughput. *Nucleic Acids Res*, 32(5), 1792-7.
- Erasmus, J.H., Auguste, A.J., Kaelber, J.T., Luo, H., Rossi, S.L., Fenton, K., Leal, G., Kim, D.Y., Chiu, W., Wang, T., Frolov, I., Nasar, F. & Weaver, S.C. (2017). A chikungunya fever vaccine utilizing an insect-specific virus platform. *Nat Med*, 23(2), 192-199.
- Etebari, K., Hegde, S., Saldana, M.A., Widen, S.G., Wood, T.G., Asgari, S. & Hughes, G.L. (2017). Global Transcriptome Analysis of *Aedes aegypti* Mosquitoes in Response to Zika Virus Infection. *mSphere*, 2(6).
- Ewels, P.A., Peltzer, A., Fillinger, S., Patel, H., Alneberg, J., Wilm, A., Garcia, M.U., Di Tommaso, P. & Nahnsen, S. (2020). The nf-core framework for community-curated bioinformatics pipelines. *Nat Biotechnol*, 38(3), 276-278.
- Farajollahi, A., Fonseca, D.M., Kramer, L.D. & Marm Kilpatrick, A. (2011). "Bird biting" mosquitoes and human disease: a review of the role of *Culex pipiens* complex mosquitoes in epidemiology. *Infect Genet Evol*, 11(7), 1577-85.
- Ferreira, D.D., Cook, S., Lopes, A., de Matos, A.P., Esteves, A., Abecasis, A., de Almeida, A.P., Piedade, J. & Parreira, R. (2013). Characterization of an insect-specific flavivirus (OCFVPT) co-isolated from *Ochlerotatus caspius* collected in southern Portugal along with a putative new Negev-like virus. *Virus Genes*, 47(3), 532-45.
- Flores, H.A. & O'Neill, S.L. (2018). Controlling vector-borne diseases by releasing modified mosquitoes. *Nat Rev Microbiol*, 16(8), 508-518.
- Franz, A.W., Kantor, A.M., Passarelli, A.L. & Clem, R.J. (2015). Tissue Barriers to Arbovirus Infection in Mosquitoes. *Viruses*, 7(7), 3741-67.
- Fros, J.J., Geertsema, C., Vogels, C.B., Roosjen, P.P., Failloux, A.B., Vlak, J.M., Koenraadt, C.J., Takken, W. & Pijlman, G.P. (2015). West Nile Virus: High Transmission Rate in North-Western European Mosquitoes Indicates Its Epidemic Potential and Warrants Increased Surveillance. *PLoS Negl Trop Dis*, 9(7), e0003956.
- Galiana-Arnoux, D., Dostert, C., Schneemann, A., Hoffmann, J.A. & Imler, J.L. (2006). Essential function in vivo for Dicer-2 in host defense against RNA viruses in drosophila. *Nat Immunol*, 7(6), 590-7.

- Garver, L.S., Dong, Y. & Dimopoulos, G. (2009). Caspar controls resistance to *Plasmodium falciparum* in diverse anopheline species. *PLoS Pathog*, 5(3), e1000335.
- Giraldo-Calderon, G.I., Emrich, S.J., MacCallum, R.M., Maslen, G., Dialynas, E., Topalis, P., Ho, N., Gesing, S., VectorBase, C., Madey, G., Collins, F.H. & Lawson, D. (2015). VectorBase: an updated bioinformatics resource for invertebrate vectors and other organisms related with human diseases. *Nucleic Acids Res*, 43(Database issue), D707-13.
- Girardi, E., Miesen, P., Pennings, B., Frangeul, L., Saleh, M.C. & van Rij, R.P. (2017). Histone-derived piRNA biogenesis depends on the ping-pong partners Piwi5 and Ago3 in *Aedes aegypti*. *Nucleic Acids Res*, 45(8), 4881-4892.
- Giribet, G. & Edgecombe, G.D. (2019). The Phylogeny and Evolutionary History of Arthropods. *Curr Biol*, 29(12), R592-R602.
- Goertz, G.P., Miesen, P., Overheul, G.J., van Rij, R.P., van Oers, M.M. & Pijlman, G.P. (2019). Mosquito Small RNA Responses to West Nile and Insect-Specific Virus Infections in *Aedes* and *Culex* Mosquito Cells. *Viruses*, 11(3).
- Goic, B., Stapleford, K.A., Frangeul, L., Doucet, A.J., Gausson, V., Blanc, H., Schemmel-Jofre, N., Cristofari, G., Lambrechts, L., Vignuzzi, M. & Saleh, M.C. (2016). Virus-derived DNA drives mosquito vector tolerance to arboviral infection. *Nat Commun*, 7, 12410.
- Goic, B., Vodovar, N., Mondotte, J.A., Monot, C., Frangeul, L., Blanc, H., Gausson, V., Vera-Otarola, J., Cristofari, G. & Saleh, M.C. (2013). RNA-mediated interference and reverse transcription control the persistence of RNA viruses in the insect model *Drosophila*. *Nat Immunol*, 14(4), 396-403.
- Goldblum, N., Sterk, V.V. & Paderski, B. (1954). West Nile fever; the clinical features of the disease and the isolation of West Nile virus from the blood of nine human cases. *Am J Hyg*, 59(1), 89-103.
- Habarugira, G., Suen, W.W., Hobson-Peters, J., Hall, R.A. & Bielefeldt-Ohmann, H. (2020). West Nile Virus: An Update on Pathobiology, Epidemiology, Diagnostics, Control and "One Health" Implications. *Pathogens*, 9(7).
- Haddow, A.D., Guzman, H., Popov, V.L., Wood, T.G., Widen, S.G., Haddow, A.D., Tesh, R.B. & Weaver, S.C. (2013). First isolation of *Aedes flavivirus* in the Western Hemisphere and evidence of vertical transmission in the mosquito *Aedes* (*Stegomyia*) *albopictus* (*Diptera: Culicidae*). *Virology*, 440(2), 134-9.

- Hall-Mendelin, S., McLean, B.J., Bielefeldt-Ohmann, H., Hobson-Peters, J., Hall, R.A. & van den Hurk, A.F. (2016). The insect-specific Palm Creek virus modulates West Nile virus infection in and transmission by Australian mosquitoes. *Parasit Vectors*, 9(1), 414.
- Hang, J., Klein, T.A., Kim, H.C., Yang, Y., Jima, D.D., Richardson, J.H. & Jarman, R.G. (2016). Genome Sequences of Five Arboviruses in Field-Captured Mosquitoes in a Unique Rural Environment of South Korea. *Genome Announc*, 4(1).
- Hartley, D.M., Barker, C.M., Le Menach, A., Niu, T., Gaff, H.D. & Reisen, W.K. (2012). Effects of temperature on emergence and seasonality of West Nile virus in California. *Am J Trop Med Hyg*, 86(5), 884-94.
- Hillyer, J.F. & Strand, M.R. (2014). Mosquito hemocyte-mediated immune responses. *Curr Opin Insect Sci*, 3, 14-21.
- Hobson-Peters, J., Harrison, J.J., Watterson, D., Hazlewood, J.E., Vet, L.J., Newton, N.D., Warrilow, D., Colmant, A.M.G., Taylor, C., Huang, B., Piyasena, T.B.H., Chow, W.K., Setoh, Y.X., Tang, B., Nakayama, E., Yan, K., Amarilla, A.A., Wheatley, S., Moore, P.R., Finger, M., Kurucz, N., Modhiran, N., Young, P.R., Khromykh, A.A., Bielefeldt-Ohmann, H., Suhrbier, A. & Hall, R.A. (2019). A recombinant platform for flavivirus vaccines and diagnostics using chimeras of a new insect-specific virus. *Sci Transl Med*, 11(522).
- Horton, A.A., Wang, B., Camp, L., Price, M.S., Arshi, A., Nagy, M., Nadler, S.A., Faeder, J.R. & Luckhart, S. (2011). The mitogen-activated protein kinome from *Anopheles gambiae*: identification, phylogeny and functional characterization of the ERK, JNK and p38 MAP kinases. *BMC Genomics*, 12, 574.
- Houe, V., Bonizzoni, M. & Failloux, A.B. (2019). Endogenous non-retroviral elements in genomes of *Aedes* mosquitoes and vector competence. *Emerg Microbes Infect*, 8(1), 542-555.
- Huhtamo, E., Moureau, G., Cook, S., Julkunen, O., Putkuri, N., Kurkela, S., Uzcategui, N.Y., Harbach, R.E., Gould, E.A., Vapalahti, O. & de Lamballerie, X. (2012). Novel insect-specific flavivirus isolated from northern Europe. *Virology*, 433(2), 471-8.
- Huhtamo, E., Putkuri, N., Kurkela, S., Manni, T., Vaheri, A., Vapalahti, O. & Uzcategui, N.Y. (2009). Characterization of a novel flavivirus from mosquitoes in northern Europe that is related to mosquito-borne flaviviruses of the tropics. *J Virol*, 83(18), 9532-40.

- Hurlbut, H.S., Rizk, F., Taylor, R.M. & Work, T.H. (1956). A study of the ecology of West Nile virus in Egypt. *Am J Trop Med Hyg*, 5(4), 579-620.
- Huson, D.H., Auch, A.F., Qi, J. & Schuster, S.C. (2007). MEGAN analysis of metagenomic data. *Genome Res*, 17(3), 377-86.
- Lundström J.O., Hesson J.C., Blomgren E, Lindström A, Wahlqvist P, Halling A, Hagelin A, Ahlm C, Evander M, Broman T, Forsman M, Persson Vinnersten T. (2013). The geographic distribution of mosquito species in Sweden. *Journal of the European mosquito control association*, 31.
- Jansen, C.C., Webb, C.E., Northill, J.A., Ritchie, S.A., Russell, R.C. & Van den Hurk, A.F. (2008). Vector competence of Australian mosquito species for a North American strain of West Nile virus. *Vector Borne Zoonotic Dis*, 8(6), 805-11.
- Joshi NA, F.J. (2011). *Sickle: A sliding-window, adaptive, quality-based trimming tool for FastQ files* <https://github.com/najoshi/sickle>
- Junglen, S., Korries, M., Grasse, W., Wieseler, J., Kopp, A., Hermanns, K., Leon-Juarez, M., Drosten, C. & Kummerer, B.M. (2017). Host Range Restriction of Insect-Specific Flaviviruses Occurs at Several Levels of the Viral Life Cycle. *mSphere*, 2(1).
- Jupatanakul, N., Sim, S., Anglero-Rodriguez, Y.I., Souza-Neto, J., Das, S., Poti, K.E., Rossi, S.L., Bergren, N., Vasilakis, N. & Dimopoulos, G. (2017). Engineered *Aedes aegypti* JAK/STAT Pathway-Mediated Immunity to Dengue Virus. *PLoS Negl Trop Dis*, 11(1), e0005187.
- Kall, L., Krogh, A. & Sonnhammer, E.L. (2007). Advantages of combined transmembrane topology and signal peptide prediction--the Phobius web server. *Nucleic Acids Res*, 35(Web Server issue), W429-32.
- Katzourakis, A. & Gifford, R.J. (2010). Endogenous viral elements in animal genomes. *PLoS Genet*, 6(11), e1001191.
- Kenney, J.L., Solberg, O.D., Langevin, S.A. & Brault, A.C. (2014). Characterization of a novel insect-specific flavivirus from Brazil: potential for inhibition of infection of arthropod cells with medically important flaviviruses. *J Gen Virol*, 95(Pt 12), 2796-808.
- Kent, R.J., Crabtree, M.B. & Miller, B.R. (2010). Transmission of West Nile virus by *Culex quinquefasciatus* say infected with *Culex* Flavivirus Izabal. *PLoS Negl Trop Dis*, 4(5), e671.

- Kilpatrick, A.M., Daszak, P., Goodman, S.J., Rogg, H., Kramer, L.D., Cedeno, V. & Cunningham, A.A. (2006). Predicting pathogen introduction: West Nile virus spread to Galapagos. *Conserv Biol*, 20(4), 1224-31.
- Kim, M., Lee, J.H., Lee, S.Y., Kim, E. & Chung, J. (2006). Caspar, a suppressor of antibacterial immunity in *Drosophila*. *Proc Natl Acad Sci U S A*, 103(44), 16358-63.
- Kopylova, E., Noe, L. & Touzet, H. (2012). SortMeRNA: fast and accurate filtering of ribosomal RNAs in metatranscriptomic data. *Bioinformatics*, 28(24), 3211-7.
- Kramer, L.D., Styer, L.M. & Ebel, G.D. (2008). A global perspective on the epidemiology of West Nile virus. *Annu Rev Entomol*, 53, 61-81.
- Ku, H.Y. & Lin, H. (2014). PIWI proteins and their interactors in piRNA biogenesis, germline development and gene expression. *Natl Sci Rev*, 1(2), 205-218.
- Kumar, A., Srivastava, P., Sirisena, P., Dubey, S.K., Kumar, R., Shrinet, J. & Sunil, S. (2018). Mosquito Innate Immunity. *Insects*, 9(3).
- Kumar, S., Stecher, G. & Tamura, K. (2016). MEGA7: Molecular Evolutionary Genetics Analysis Version 7.0 for Bigger Datasets. *Mol Biol Evol*, 33(7), 1870-4.
- Kuno, G., Chang, G.J., Tsuchiya, K.R., Karabatsos, N. & Cropp, C.B. (1998). Phylogeny of the genus *Flavivirus*. *J Virol*, 72(1), 73-83.
- Kuwata, R., Isawa, H., Hoshino, K., Sasaki, T., Kobayashi, M., Maeda, K. & Sawabe, K. (2015). Analysis of Mosquito-Borne *Flavivirus* Superinfection in *Culex tritaeniorhynchus* (*Diptera: Culicidae*) Cells Persistently Infected with *Culex Flavivirus* (*Flaviviridae*). *J Med Entomol*, 52(2), 222-9.
- Lanciotti, R.S., Roehrig, J.T., Deubel, V., Smith, J., Parker, M., Steele, K., Crise, B., Volpe, K.E., Crabtree, M.B., Scherret, J.H., Hall, R.A., MacKenzie, J.S., Cropp, C.B., Panigrahy, B., Ostlund, E., Schmitt, B., Malkinson, M., Banet, C., Weissman, J., Komar, N., Savage, H.M., Stone, W., McNamara, T. & Gubler, D.J. (1999). Origin of the West Nile virus responsible for an outbreak of encephalitis in the northeastern United States. *Science*, 286(5448), 2333-7.
- Langmead, B., Trapnell, C., Pop, M. & Salzberg, S.L. (2009). Ultrafast and memory-efficient alignment of short DNA sequences to the human genome. *Genome Biol*, 10(3), R25.
- Le, S.Q. & Gascuel, O. (2008). An improved general amino acid replacement matrix. *Mol Biol Evol*, 25(7), 1307-20.

- Lee, J.H. & Kokas, J.E. (2004). Field evaluation of CDC gravid trap attractants to primary West Nile virus vectors, *Culex* mosquitoes in New York State. *J Am Mosq Control Assoc*, 20(3), 248-53.
- Lee, W.S., Webster, J.A., Madzokere, E.T., Stephenson, E.B. & Herrero, L.J. (2019). Mosquito antiviral defense mechanisms: a delicate balance between innate immunity and persistent viral infection. *Parasit Vectors*, 12(1), 165.
- Lee, Y.M., Tscherne, D.M., Yun, S.I., Frolov, I. & Rice, C.M. (2005). Dual mechanisms of pestiviral superinfection exclusion at entry and RNA replication. *J Virol*, 79(6), 3231-42.
- Lee, Y.S., Nakahara, K., Pham, J.W., Kim, K., He, Z., Sontheimer, E.J. & Carthew, R.W. (2004). Distinct roles for *Drosophila* Dicer-1 and Dicer-2 in the siRNA/miRNA silencing pathways. *Cell*, 117(1), 69-81.
- Lemaitre, B. & Hoffmann, J. (2007). The host defense of *Drosophila melanogaster*. *Annu Rev Immunol*, 25, 697-743.
- Lemaitre, B., Nicolas, E., Michaut, L., Reichhart, J.M. & Hoffmann, J.A. (1996). The dorsoventral regulatory gene cassette spatzle/Toll/cactus controls the potent antifungal response in *Drosophila* adults. *Cell*, 86(6), 973-83.
- Li, C.X., Shi, M., Tian, J.H., Lin, X.D., Kang, Y.J., Chen, L.J., Qin, X.C., Xu, J., Holmes, E.C. & Zhang, Y.Z. (2015a). Unprecedented genomic diversity of RNA viruses in arthropods reveals the ancestry of negative-sense RNA viruses. *Elife*, 4.
- Li, D., Liu, C.M., Luo, R., Sadakane, K. & Lam, T.W. (2015b). MEGAHIT: an ultra-fast single-node solution for large and complex metagenomics assembly via succinct de Bruijn graph. *Bioinformatics*, 31(10), 1674-6.
- Li, M., Xing, D., Su, D., Wang, D., Gao, H., Lan, C., Gu, Z., Zhao, T. & Li, C. (2021). Transcriptome Analysis of Responses to Dengue Virus 2 Infection in *Aedes albopictus* (Skuse) C6/36 Cells. *Viruses*, 13(2).
- Li, M.J., Lan, C.J., Gao, H.T., Xing, D., Gu, Z.Y., Su, D., Zhao, T.Y., Yang, H.Y. & Li, C.X. (2020). Transcriptome analysis of *Aedes aegypti* Aag2 cells in response to dengue virus-2 infection. *Parasit Vectors*, 13(1), 421.
- Liu, P., Dong, Y., Gu, J., Puthiyakunnon, S., Wu, Y. & Chen, X.G. (2016). Developmental piRNA profiles of the invasive vector mosquito *Aedes albopictus*. *Parasit Vectors*, 9(1), 524.
- Luz, P.M., Vanni, T., Medlock, J., Paltiel, A.D. & Galvani, A.P. (2011). Dengue vector control strategies in an urban setting: an economic modelling assessment. *Lancet*, 377(9778), 1673-80.

- Marklewitz, M., Zirkel, F., Kurth, A., Drosten, C. & Junglen, S. (2015). Evolutionary and phenotypic analysis of live virus isolates suggests arthropod origin of a pathogenic RNA virus family. *Proc Natl Acad Sci U S A*, 112(24), 7536-41.
- Matranga, C., Tomari, Y., Shin, C., Bartel, D.P. & Zamore, P.D. (2005). Passenger-strand cleavage facilitates assembly of siRNA into Ago2-containing RNAi enzyme complexes. *Cell*, 123(4), 607-20.
- Meister, S., Kanzok, S.M., Zheng, X.L., Luna, C., Li, T.R., Hoa, N.T., Clayton, J.R., White, K.P., Kafatos, F.C., Christophides, G.K. & Zheng, L. (2005). Immune signaling pathways regulating bacterial and malaria parasite infection of the mosquito *Anopheles gambiae*. *Proc Natl Acad Sci U S A*, 102(32), 11420-5.
- Melnick, J.L., Paul, J.R., Riordan, J.T., Barnett, V.H., Goldblum, N. & Zabin, E. (1951). Isolation from human sera in Egypt of a virus apparently identical to West Nile virus. *Proc Soc Exp Biol Med*, 77(4), 661-5.
- Michel, T., Reichhart, J.M., Hoffmann, J.A. & Royet, J. (2001). Drosophila Toll is activated by Gram-positive bacteria through a circulating peptidoglycan recognition protein. *Nature*, 414(6865), 756-9.
- Miesen, P., Girardi, E. & van Rij, R.P. (2015). Distinct sets of PIWI proteins produce arbovirus and transposon-derived piRNAs in *Aedes aegypti* mosquito cells. *Nucleic Acids Res*, 43(13), 6545-56.
- Mitchell, A.L., Attwood, T.K., Babbitt, P.C., Blum, M., Bork, P., Bridge, A., Brown, S.D., Chang, H.Y., El-Gebali, S., Fraser, M.I., Gough, J., Haft, D.R., Huang, H., Letunic, I., Lopez, R., Luciani, A., Madeira, F., Marchler-Bauer, A., Mi, H., Natale, D.A., Necci, M., Nuka, G., Orengo, C., Pandurangan, A.P., Paysan-Lafosse, T., Pesseat, S., Potter, S.C., Qureshi, M.A., Rawlings, N.D., Redaschi, N., Richardson, L.J., Rivoire, C., Salazar, G.A., Sangrador-Vegas, A., Sigrist, C.J.A., Sillitoe, I., Sutton, G.G., Thanki, N., Thomas, P.D., Tosatto, S.C.E., Yong, S.Y. & Finn, R.D. (2019). InterPro in 2019: improving coverage, classification and access to protein sequence annotations. *Nucleic Acids Res*, 47(D1), D351-D360.
- Moreira, L.A., Iturbe-Ormaetxe, I., Jeffery, J.A., Lu, G., Pyke, A.T., Hedges, L.M., Rocha, B.C., Hall-Mendelin, S., Day, A., Riegler, M., Hugo, L.E., Johnson, K.N., Kay, B.H., McGraw, E.A., van den Hurk, A.F., Ryan, P.A. & O'Neill, S.L. (2009). A *Wolbachia* symbiont in *Aedes aegypti* limits infection with dengue, Chikungunya, and *Plasmodium*. *Cell*, 139(7), 1268-78.

- Murgue, B., Zeller, H. & Deubel, V. (2002). The ecology and epidemiology of West Nile virus in Africa, Europe and Asia. *Curr Top Microbiol Immunol*, 267, 195-221.
- Nag, D.K., Brecher, M. & Kramer, L.D. (2016). DNA forms of arboviral RNA genomes are generated following infection in mosquito cell cultures. *Virology*, 498, 164-171.
- Nag, D.K. & Kramer, L.D. (2017). Patchy DNA forms of the Zika virus RNA genome are generated following infection in mosquito cell cultures and in mosquitoes. *J Gen Virol*, 98(11), 2731-2737.
- Nagy, P.D. (2016). Tombusvirus-Host Interactions: Co-Opted Evolutionarily Conserved Host Factors Take Center Court. *Annu Rev Virol*, 3(1), 491-515.
- Nakatogawa, S., Oda, Y., Kamiya, M., Kamijima, T., Aizawa, T., Clark, K.D., Demura, M., Kawano, K., Strand, M.R. & Hayakawa, Y. (2009). A novel peptide mediates aggregation and migration of hemocytes from an insect. *Curr Biol*, 19(9), 779-85.
- Nasar, F., Gorchakov, R.V., Tesh, R.B. & Weaver, S.C. (2015). Eilat virus host range restriction is present at multiple levels of the virus life cycle. *J Virol*, 89(2), 1404-18.
- Paradkar, P.N., Trinidad, L., Voysey, R., Duchemin, J.B. & Walker, P.J. (2012). Secreted Vago restricts West Nile virus infection in *Culex* mosquito cells by activating the Jak-STAT pathway. *Proc Natl Acad Sci U S A*, 109(46), 18915-20.
- Patro, R., Duggal, G., Love, M.I., Irizarry, R.A. & Kingsford, C. (2017). Salmon provides fast and bias-aware quantification of transcript expression. *Nat Methods*, 14(4), 417-419.
- Piyasena, T.B.H., Setoh, Y.X., Hobson-Peters, J., Newton, N.D., Bielefeldt-Ohmann, H., McLean, B.J., Vet, L.J., Khromykh, A.A. & Hall, R.A. (2017). Infectious DNAs derived from insect-specific flavivirus genomes enable identification of pre- and post-entry host restrictions in vertebrate cells. *Sci Rep*, 7(1), 2940.
- Powell, J.R., Gloria-Soria, A. & Kotsakiozi, P. (2018). Recent History of *Aedes aegypti*: Vector Genomics and Epidemiology Records. *Bioscience*, 68(11), 854-860.
- Ramirez, J.L. & Dimopoulos, G. (2010). The Toll immune signaling pathway control conserved anti-dengue defenses across diverse *Ae. aegypti* strains and against multiple dengue virus serotypes. *Dev Comp Immunol*, 34(6), 625-9.

- Rand, T.A., Petersen, S., Du, F. & Wang, X. (2005). Argonaute2 cleaves the anti-guide strand of siRNA during RISC activation. *Cell*, 123(4), 621-9.
- Rodriguez-Andres, J., Rani, S., Varjak, M., Chase-Topping, M.E., Beck, M.H., Ferguson, M.C., Schnettler, E., Fragkoudis, R., Barry, G., Merits, A., Fazakerley, J.K., Strand, M.R. & Kohl, A. (2012). Phenoloxidase activity acts as a mosquito innate immune response against infection with Semliki Forest virus. *PLoS Pathog*, 8(11), e1002977.
- Rozen, S. & Skaletsky, H. (2000). Primer3 on the WWW for general users and for biologist programmers. *Methods Mol Biol*, 132, 365-86.
- Runtuwene, L.R., Kawashima, S., Pijoh, V.D., Tuda, J.S.B., Hayashida, K., Yamagishi, J., Sugimoto, C., Nishiyama, S., Sasaki, M., Orba, Y., Sawa, H., Takasaki, T., James, A.A., Kobayashi, T. & Eshita, Y. (2020). The *Lethal(2)-Essential-for-Life [L(2)EFL]* Gene Family Modulates Dengue Virus Infection in *Aedes aegypti*. *Int J Mol Sci*, 21(20).
- Sadeghi, M., Altan, E., Deng, X., Barker, C.M., Fang, Y., Coffey, L.L. & Delwart, E. (2018). Virome of >12 thousand *Culex* mosquitoes from throughout California. *Virology*, 523, 74-88.
- Saiyasombat, R., Bolling, B.G., Brault, A.C., Bartholomay, L.C. & Blitvich, B.J. (2011). Evidence of efficient transovarial transmission of *Culex* flavivirus by *Culex pipiens* (Diptera: Culicidae). *J Med Entomol*, 48(5), 1031-8.
- Sanborn, M.A., Klein, T.A., Kim, H.C., Fung, C.K., Figueroa, K.L., Yang, Y., Asafo-Adjei, E.A., Jarman, R.G. & Hang, J. (2019). Metagenomic Analysis Reveals Three Novel and Prevalent Mosquito Viruses from a Single Pool of *Aedes vexans nipponii* Collected in the Republic of Korea. *Viruses*, 11(3).
- Satyavathi, V.V., Minz, A. & Nagaraju, J. (2014). Nodulation: an unexplored cellular defense mechanism in insects. *Cell Signal*, 26(8), 1753-63.
- Schultz, M.J., Frydman, H.M. & Connor, J.H. (2018). Dual Insect specific virus infection limits Arbovirus replication in *Aedes* mosquito cells. *Virology*, 518, 406-413.
- Schurch, N.J., Schofield, P., Gierlinski, M., Cole, C., Sherstnev, A., Singh, V., Wrobel, N., Gharbi, K., Simpson, G.G., Owen-Hughes, T., Blaxter, M. & Barton, G.J. (2016). How many biological replicates are needed in an RNA-seq experiment and which differential expression tool should you use? *RNA*, 22(6), 839-51.
- Seguin, J., Otten, P., Baerlocher, L., Farinelli, L. & Pooggin, M.M. (2016). MISIS-2: A bioinformatics tool for in-depth analysis of small RNAs

- and representation of consensus master genome in viral quasispecies. *J Virol Methods*, 233, 37-40.
- Shi, M., Lin, X.D., Tian, J.H., Chen, L.J., Chen, X., Li, C.X., Qin, X.C., Li, J., Cao, J.P., Eden, J.S., Buchmann, J., Wang, W., Xu, J., Holmes, E.C. & Zhang, Y.Z. (2016). Redefining the invertebrate RNA virosphere. *Nature*, 540(7634), 539-543.
- Shin, D., Civana, A., Acevedo, C. & Smartt, C.T. (2014). Transcriptomics of differential vector competence: West Nile virus infection in two populations of *Culex pipiens quinquefasciatus* linked to ovary development. *BMC Genomics*, 15, 513.
- Shin, S.W., Bian, G. & Raikhel, A.S. (2006). A toll receptor and a cytokine, Toll5A and Spz1C, are involved in toll antifungal immune signaling in the mosquito *Aedes aegypti*. *J Biol Chem*, 281(51), 39388-95.
- Shrinet, J., Srivastava, P. & Sunil, S. (2017). Transcriptome analysis of *Aedes aegypti* in response to mono-infections and co-infections of dengue virus-2 and chikungunya virus. *Biochem Biophys Res Commun*, 492(4), 617-623.
- Simon, F., Savini, H. & Parola, P. (2008). Chikungunya: a paradigm of emergence and globalization of vector-borne diseases. *Med Clin North Am*, 92(6), 1323-43, ix.
- Siomi, M.C., Sato, K., Pezic, D. & Aravin, A.A. (2011). PIWI-interacting small RNAs: the vanguard of genome defence. *Nat Rev Mol Cell Biol*, 12(4), 246-58.
- Smith, C.E. (1956). The history of dengue in tropical Asia and its probable relationship to the mosquito *Aedes aegypti*. *J Trop Med Hyg*, 59(10), 243-51.
- Smithburn, K.C.H., T. P.; Burke, A. W.; Paul, J. H. (1940). A Neurotropic Virus Isolated from the Blood of a Native of Uganda. *American Journal of Tropical Medicine*, 20, 471-473.
- Souza-Neto, J.A., Sim, S. & Dimopoulos, G. (2009). An evolutionary conserved function of the JAK-STAT pathway in anti-dengue defense. *Proc Natl Acad Sci U S A*, 106(42), 17841-6.
- Spigland, I., Jasinska-Klingberg, W., Hofshi, E. & Goldblum, N. (1958). [Clinical and laboratory observations in an outbreak of West Nile fever in Israel in 1957]. *Harefuah*, 54(11), 275-80; English & French abstracts 280-1.
- Sriwichai, P., Karl, S., Samung, Y., Sumruayphol, S., Kiattibutr, K., Payakkapol, A., Mueller, I., Yan, G., Cui, L. & Sattabongkot, J. (2015).

- Evaluation of CDC light traps for mosquito surveillance in a malaria endemic area on the Thai-Myanmar border. *Parasit Vectors*, 8, 636.
- Stollar, V. & Thomas, V.L. (1975). An agent in the *Aedes aegypti* cell line (Peleg) which causes fusion of *Aedes albopictus* cells. *Virology*, 64(2), 367-77.
- Tamura, K., Stecher, G. & Kumar, S. (2021). MEGA11: Molecular Evolutionary Genetics Analysis Version 11. *Mol Biol Evol*, 38(7), 3022-3027.
- Tassetto, M., Kunitomi, M., Whitfield, Z.J., Dolan, P.T., Sanchez-Vargas, I., Garcia-Knight, M., Ribiero, I., Chen, T., Olson, K.E. & Andino, R. (2019). Control of RNA viruses in mosquito cells through the acquisition of vDNA and endogenous viral elements. *Elife*, 8.
- Traver, B.E., Anderson, M.A. & Adelman, Z.N. (2009). Homing endonucleases catalyze double-stranded DNA breaks and somatic transgene excision in *Aedes aegypti*. *Insect Mol Biol*, 18(5), 623-33.
- Turell, M.J., Dohm, D.J., Sardelis, M.R., Oguinn, M.L., Andreadis, T.G. & Blow, J.A. (2005). An update on the potential of north American mosquitoes (*Diptera: Culicidae*) to transmit West Nile Virus. *J Med Entomol*, 42(1), 57-62.
- van den Hurk, A.F., Hall-Mendelin, S., Pyke, A.T., Frentiu, F.D., McElroy, K., Day, A., Higgs, S. & O'Neill, S.L. (2012). Impact of *Wolbachia* on infection with chikungunya and yellow fever viruses in the mosquito vector *Aedes aegypti*. *PLoS Negl Trop Dis*, 6(11), e1892.
- Varjak, M., Donald, C.L., Mottram, T.J., Sreenu, V.B., Merits, A., Maringer, K., Schnettler, E. & Kohl, A. (2017). Characterization of the Zika virus induced small RNA response in *Aedes aegypti* cells. *PLoS Negl Trop Dis*, 11(10), e0006010.
- Vazquez, A., Sanchez-Seco, M.P., Palacios, G., Molero, F., Reyes, N., Ruiz, S., Aranda, C., Marques, E., Escosa, R., Moreno, J., Figuerola, J. & Tenorio, A. (2012). Novel flaviviruses detected in different species of mosquitoes in Spain. *Vector Borne Zoonotic Dis*, 12(3), 223-9.
- Volz, A., Lim, S., Kaserer, M., Lulf, A., Marr, L., Jany, S., Deeg, C.A., Pijlman, G.P., Koraka, P., Osterhaus, A.D., Martina, B.E. & Sutter, G. (2016). Immunogenicity and protective efficacy of recombinant Modified Vaccinia virus Ankara candidate vaccines delivering West Nile virus envelope antigens. *Vaccine*, 34(16), 1915-26.
- Walton, W.E. (2007). Larvivorous fish including *Gambusia*. *J Am Mosq Control Assoc*, 23(2 Suppl), 184-220.

- Weaver, S.C. & Barrett, A.D. (2004). Transmission cycles, host range, evolution and emergence of arboviral disease. *Nat Rev Microbiol*, 2(10), 789-801.
- Xi, Z., Ramirez, J.L. & Dimopoulos, G. (2008). The *Aedes aegypti* toll pathway controls dengue virus infection. *PLoS Pathog*, 4(7), e1000098.
- Yen, J.H. & Barr, A.R. (1973). The etiological agent of cytoplasmic incompatibility in *Culex pipiens*. *J Invertebr Pathol*, 22(2), 242-50.
- Yen, P.S., James, A., Li, J.C., Chen, C.H. & Failloux, A.B. (2018). Synthetic miRNAs induce dual arboviral-resistance phenotypes in the vector mosquito *Aedes aegypti*. *Commun Biol*, 1, 11.
- Zhang, R., Miner, J.J., Gorman, M.J., Rausch, K., Ramage, H., White, J.P., Zuiani, A., Zhang, P., Fernandez, E., Zhang, Q., Dowd, K.A., Pierson, T.C., Cherry, S. & Diamond, M.S. (2016). A CRISPR screen defines a signal peptide processing pathway required by flaviviruses. *Nature*, 535(7610), 164-8.
- Zhang, X., He, Y., Cao, X., Gunaratna, R.T., Chen, Y.R., Blissard, G., Kanost, M.R. & Jiang, H. (2015). Phylogenetic analysis and expression profiling of the pattern recognition receptors: Insights into molecular recognition of invading pathogens in *Manduca sexta*. *Insect Biochem Mol Biol*, 62, 38-50.
- Zhao, L., Pridgeon, J.W., Becnel, J.J., Clark, G.G. & Linthicum, K.J. (2009). Identification of genes differentially expressed during heat shock treatment in *Aedes aegypti*. *J Med Entomol*, 46(3), 490-5.
- Öhlund, P., Delhomme, N., Hayer, J., Hesson, J.C. & Blomstrom, A.L. (2022). Transcriptome Analysis of an *Aedes albopictus* Cell Line Single- and Dual-Infected with Lammi Virus and WNV. *Int J Mol Sci*, 23(2).
- Öhlund, P., Hayer, J., Hesson, J.C. & Blomstrom, A.L. (2021). Small RNA Response to Infection of the Insect-Specific Lammi Virus and Hanko Virus in an *Aedes albopictus* Cell Line. *Viruses*, 13(11).
- Öhlund, P., Hayer, J., Lunden, H., Hesson, J.C. & Blomstrom, A.L. (2019a). Viromics Reveal a Number of Novel RNA Viruses in Swedish Mosquitoes. *Viruses*, 11(11).
- Öhlund, P., Lunden, H. & Blomstrom, A.L. (2019b). Insect-specific virus evolution and potential effects on vector competence. *Virus Genes*, 55(2), 127-137.

Popular science summary

Mosquitoes are considered the deadliest animal in the world because of all the diseases they spread, and are often compared to as flying infection needles. The spread of disease almost exclusively occurs during a blood meal, when the disease-causing pathogen is introduced to the person's blood stream via the mosquito's saliva. Many of you probably know that the single-celled parasite malaria is transmitted by mosquitoes, however, mosquitoes are also a major vector for many viral diseases, such as West Nile virus, Yellow Fever virus and Dengue virus. These mosquito-borne viruses cause a major health burden across the globe, which is predicted to increase due to global trade, urbanization and increased temperatures, that expand the geographical range of the mosquito vectors and their associated disease burden. For many of these arboviruses, there are no preventive vaccines or therapeutic drugs available and to reduce the mosquito associated disease burden the only strategy is to suppress the mosquito populations with insecticides. However, this is very cumbersome and costly, and, with the increase in insecticide resistance, these strategies are becoming less effective. New control strategies are needed, and the development of strategies that target the mosquito's ability to harbor and spread medically important viruses have been suggested. This would mean that a mosquito bite would be harmless, since the mosquito do not harbor or transmit any disease causing pathogen.

In the first study of this thesis, mosquitoes were collected in mid-eastern Sweden to investigate what kind of viruses they harbored. Results revealed that most of the mosquito species studied, harbored a broad range of different viruses from several different viral families. Most if not all of these viruses were predicted to be insect-specific viruses (ISVs). This group of viruses have a strict host-restriction and are only able to infect and replicate in insects. Furthermore, mosquitoes infected with certain ISVs have shown an increased resistance to the medically important mosquito-borne viruses, and

because of this have been suggested to be utilized as biocontrol agents in mosquitoes to interrupt the spread of disease causing viruses.

However, how the ISVs are able to block a secondary viral infection in the mosquito is unknown, and it is hypothesized that ISVs manipulate the immune system of the mosquito. Unlike the human (mammalian) immune system, mosquitoes lack an adaptive immunity such as an antibody response, and instead rely on their innate immune system to fight viral infections. Therefore, the main antiviral immune response in mosquito cells was investigated upon acute infection of two different ISVs (Hanko- and Lammi virus). Results showed that the mosquito cells mounted a robust and specific immune response towards both of these viruses, which indicate that these viruses induce a higher level of immune activity in the mosquito, that could hinder the establishment of a second viral infection

In the third study, one of the investigated ISVs (Lammi virus) was shown to hinder the infection of a pathogenic mosquito-borne virus (West Nile virus). To further study the possible interference effect of the ISV, the overall changes in a mosquito cell line was investigated during infection of both the ISV and a pathogenic virus. Results showed an increase amount of protein coding RNA sequences that are associated with stress in the cell and help in the production of proteins. furthermore, an increased amount of protein coding RNA sequences that has been proven important for virus production in the cell was observed. The up-regulated protein coding sequences observed in this study could potentially be modified in the mosquito to block the spread of medically important viruses. However, further evaluations are needed to draw any conclusions.

Overall, this thesis provides knowledge of the ISV interaction with the mosquito host, that could aid in the development of novel control strategies that aim to reduce the spread of medically important viruses by mosquitoes.

Populärvetenskaplig sammanfattning

Myggor anses vara det dödligaste djuret i världen på grund av alla sjukdomar de sprider, och kan jämföras med flygande injektionsnålar. Spridningen av sjukdomar sker nästan uteslutande när myggan tar ett blodmål, då den sjukdomsalstrande patogenen förs in i personen/djurets blodomlopp via myggans saliv. Många av er känner säkert till att den encelliga parasiten malaria sprids av myggor, dock är myggor även en väldigt potent spridare av olika virussjukdomar såsom West-Nile-virus, Gulafebern virus och Denguevirus. Alla dessa myggburna virus orsakar en stor hälsobörda över hela världen, som förutspås att öka på grund av den globala handeln, urbaniseringen och de stigande temperaturena, som utökar det geografiska område där potenta myggarter kan frodas och sprida sjukdomar. För många av dessa virus finns det inga förebyggande vacciner eller antivirala läkemedel och den enda strategi för att minska den myggrelaterade sjukdomsbördan är att bekämpa och minska myggpopulationerna med olika kemikalier (insekticider). Dessa metod är dock väldigt besvärliga och dyra och har blivit mindre effektiv då myggans motståndskraft mot insekticiderna har ökat. Nya kontrollstrategier behövs och utveckling av strategier som inriktar sig på myggans förmåga att bära och sprida dessa virus har föreslagits. Detta skulle innebära att myggbetten blir ofarliga då myggorna är inkapabel att bära och sprida virussjukdomar.

I avhandlingens första studie så samlades myggor in i östra Svealand för att undersöka vilken typ av virus som de bar på. Resultaten visade att de flesta myggarter som studerades bar på ett brett spektrum av olika virus från flera olika virusfamiljer. De flesta om inte alla av dessa virus förutspåddes vara insekts-specifika virus (ISVs). Denna grupp av virus kan endast infektera och replikera i insekter. Dessutom finns det studier som har visat att myggor som är infekterade av vissa ISVs har haft en ökad motståndskraft

mot dem sjukdomsframkallande virusen och på grund av detta har ISVs föreslagits att användas i myggor för att minska spridningen av dessa.

Dock är det okänt hur dessa ISVs kan blockera en sekundär virusinfektion i myggan och en hypotes är att dem manipulerar myggans immunförsvar på något sätt. Till skillnad från det mänskliga immunsystemet så saknar myggor ett adaptivt immunförsvar såsom ett antikroppsvar, istället förlitar sig myggan på deras medfödda immunförsvar för att bekämpa virusinfektioner. Därför så undersöktes det huvudsakliga antivirala immunsvaret i myggceller vid akut infektion av två olika ISVs (Hanko- och Lammi virus). Resultaten visade att myggcellerna svarade med ett robust och specifikt immunsvaret mot bägge virusen, vilket indikerar på att dem ISVs inducerar en högre nivå av immunaktivitet i myggan, vilken kan hindra etablering av en sekundär virusinfektion.

I den tredje studien visades att en av dem studerade ISV (Lammi virus) hindrade infektionen av ett sjukdomsframkallande virus (West Nile virus). För att ytterligare studera hur det ISV motverkar den sekundära virusinfektionen, så undersöktes de övergripande förändringar i myggceller infekterade av både ett ISV och ett sjukdomsframkallande virus. Resultaten visade en ökad mängd proteinkodande RNA sekvenser som är associerade med stress i cellen och hjälper till att producera proteiner under dessa förhållanden. Dessutom så visades en ökad mängd proteinkodande RNA sekvenser som är viktiga för virusproduktionen i cellen. Dessa proteinkodade sekvenser skulle potentiellt kunna modifieras i myggor för att blockera spridningen av sjukdomsframkallande myggburna virus. Dock, krävs ytterligare studier för att utvärdera detta.

Sammantaget har denna avhandling get mer kunskap om de effekter ISVs har på myggvärden och potentiella mekanismer som öka myggans motståndskraft mot dem sjukdomsframkallande virusen, vilket kan hjälpa till i utvecklingen av nya kontrollstrategier som syftar till att minska spridningen av myggburna virus.

Acknowledgements

The studies presented in this doctoral thesis were mainly performed at the section of Virology, **Department of Biomedical Sciences and Veterinary Public Health (BVF)**, Swedish University of Agricultural Sciences (SLU). Financial support was provided by the **Swedish research Council VR (2016-01251)**, **The Royal Swedish Academy of Agriculture and Forestry (GFS2016-0033)**, **Konung Carl XVI Gustafs 50-årsfond för Vetenskap, Teknik och miljö**. I sincerely have a lot of people to thank for my accomplishments during these years, whom all I wish to thank here, in the hopes that I do not forget anyone.

This thesis have involved many areas of expertise and would not have been possible without my dedicated team of supervisors. **Anne-Lie**, thank you for accepting me as your first PhD-student and entrusting me with this exciting project. You have been a great guide, motivator and a constant source of support. You have also provided a good working environment, where mistakes can happen, questions can be asked and differences can be discussed, which I am very thankful for. **Jenny**, thank you for introducing me to the world of mosquitoes, I still remember our field trip to Flen to scavenge for good spots to place mosquito traps, which were successful. You have always cheered me up and been supportive. **Juliette**, you have been a very patient teacher in bioinformatics, some scripts and loops were not logical to me, but I have kept them all because they work. You are a problem solver and source of comfort. **Mikael**, You have been the calm and steady tutor that you can always ask, and get a good answer. You have a great taste in music, which I have missed during the pandemic when you were mostly working from home. Thank you.

To my co-workers at the **section of Virology**, thank you for making these years such a great time! **Hari**, thank you for the lab support, lunch conversations, ping-pong games and the future Nobel prize that we will share. **Hedvig**, thank you for the nice conversations and small debates, you have been a great office-mate (when you are in the office), good luck with the PhD and everything. **Hanna**, thank you for the help in the lab and being a good colleague, good luck with the research and everything else. **Emeli**, you were a spark of joy that spread good energy, it feels like we didn't have a proper goodbye before you left. **Sara**, yes I see you as a fellow virologist, you are full of energy and fun to talk to, good luck with the post doc. **Maja**, **Fredrik**, **Giorgi** and **Ylva** thank you for the virology fikas, conversations and inspirations.

To the people at the **Department of Medical Biochemistry and Microbiology/Zoonosis Science Center**, Uppsala University. Thank you for the warm welcome and introduction to the BSL-3 facility. Especially thanks to you **Dario Akaberi** for all the help in the lab, but also **Janina** and **Tove**. Thank you **Åke Lundkvist** for inviting me and providing the WNV strain used in Paper III.

All studies in this thesis have involved high-throughput sequencing and massive amounts of computational resources to analyse all data. So I would like to thank and acknowledge the support of the **National Genomics Infrastructure** for assistance with massively parallel sequencing, funded by Science for Life Laboratory, the Knut and Alice Wallenberg Foundation, the Swedish Research Council. The computations/data handling were enabled by resources in project SNIC 2017/7-290 provided by the **Swedish National Infrastructure for computing (SNIC)** at the **Multidisciplinary Center for Advanced Computational Science (UPPMAX)**, partially funded by the Swedish Research Council through gran agreement no. 2018-05973. I would also like to acknowledge the **SLU Bioinformatics Infrastructure (SLUBI)** for help and support with the bioinformatics analyses. Especially, **Nicolas Delhomme** for all the help with analyses of transcriptomic data.

There are many people at **BVF** and **VHC** that I am thankful for. **Ivar Vågsholm** as head of BVF for accepting me as PhD student. Many thanks to the **team at VHC Godsmottagningen** for all the help with deliveries, autoclave and small talk. To the **section of immunology, Magnus** you are a very wise man and I always feel a bit calmer after talking with you. **Stina**, my fellow infection biologist, you are a “Doer” and very fun to be around. **Bernt**, for all the fishing trip talks. **Caroline**, for checking in on me from time to time.

To the **toxicologists, Stefan Örn**, for keeping an eye on me and always initiating small talks. To the massive wave of fun **toxicologists, Johannes, Erica, Maria, Jennifer, Geeta, Sebastian, and Kim**, thank you for involving me in your lunches, fikas and AWs, and of course all the “end of the world” discussions. Also thank for joining the PhD council out of pity. While speaking of it, to all the ambitious people in the PhD council, **Daniel, Torun, Hadrien, Emma, Hanna, Julie**, I do like to think that we made a difference.

Thanks to all of my **friends** in and outside of academia for being supportive and in some cases sceptical to why money should be spent on some research.

Tack till min familj som har stöttat, hjälp och trott på mig, **Mamma, Pappa, stora syster, svåger** och deras **barn**. Jag vill även tacka min extra familj som har hjälp och stöttat, **Lasse, Carina, Caroline** och **Micke**. Sist men inte minst så vill jag tacka min underbara fästmö **Jennifer** för att du har försökt förstå och lösa mina problem, stöttat och hjälpt mig samt att du har stått ut med mig när jag är stressad, trött och gnällig.

Also, thanks to all the Swedish mosquitoes.

Article

Viromics Reveal a Number of Novel RNA Viruses in Swedish Mosquitoes

Pontus Öhlund ^{1,*}, Juliette Hayer ², Hanna Lundén ¹, Jenny C. Hesson ³ and Anne-Lie Blomström ¹

¹ Department of Biomedical Sciences and Veterinary Public Health, Swedish University of Agricultural Sciences, Box 7028, 750 07 Uppsala, Sweden; Hanna.lundén@slu.se (H.L.); anne-lie.blomstrom@slu.se (A.-L.B.)

² Department of Animal Breeding and Genetics, Swedish University of Agricultural Sciences, SLU-Global Bioinformatics Centre, Box 7023, 750 07 Uppsala, Sweden; juliette.hayer@slu.se

³ Department of Medical Biochemistry and Microbiology/Zoonosis Science Center, Uppsala University, Box 582, 751 23 Uppsala, Sweden; jenny.hesson@imbim.uu.se

* Correspondence: pontus.ohlund@slu.se; Tel.: +46-18-672-409

Received: 15 October 2019; Accepted: 2 November 2019; Published: 5 November 2019



Abstract: Metagenomic studies of mosquitoes have revealed that their virome is far more diverse and includes many more viruses than just the pathogenic arboviruses vectored by mosquitoes. In this study, the virome of 953 female mosquitoes collected in the summer of 2017, representing six mosquito species from two geographic locations in Mid-Eastern Sweden, were characterized. In addition, the near-complete genome of nine RNA viruses were characterized and phylogenetically analysed. These viruses showed association to the viral orders *Bunyavirales*, *Picornavirales*, *Articulavirales*, and *Tymovirales*, and to the realm Ribovira. Hence, through this study, we expand the knowledge of the virome composition of different mosquito species in Sweden. In addition, by providing viral reference genomes from wider geographic regions and different mosquito species, future in silico recognition and assembly of viral genomes in metagenomic datasets will be facilitated.

Keywords: insect-specific virus; metagenomics; virome; mosquitoes

1. Introduction

Mosquitoes are known to host and transmit numerous arthropod-borne viruses (arboviruses) that cause disease both in humans and animals, such as West Nile virus (WNV) [1], Zika virus [2], chikungunya virus [3], and dengue virus [4]. However, mosquitoes can harbour more than pathogenic arboviruses. Large metagenomic surveys of invertebrates, enabled via the use of high-throughput sequencing and advanced bioinformatics, have led to the discovery of numerous novel viruses [5–10]. Hence, these studies have shown that the mosquito virome is highly diverse and includes viruses restricted to arthropods, more commonly known as insect-specific viruses (ISVs). Although these viruses are harmless to humans and animals and have no direct impact on public health, they are interesting for multiple reasons. Several studies have shown that ISVs could potentially alter the mosquito's susceptibility to carry and transmit pathogens of concern for animal and human health [11–16]. Furthermore, some of the ISVs belong to viral families associated with arboviruses such as *Peribunyaviridae*, *Flaviviridae*, *Reoviridae*, and *Togaviridae* and are thought to be ancestral to arboviruses. With this in mind, ISVs could be a potential source of new arboviruses if they acquire dual-host tropism [7,17,18]. Therefore, by studying the virome of mosquitoes from different regions and from different mosquito species, we will not only have the opportunity to discover new viruses but can also learn more about viral evolution and the factors influencing vector competence.

The majority of the metagenomic surveys of mosquitoes have been conducted in countries where arboviruses of human and animal health concern circulate, such as China, Australia, Mozambique, and the US [5,6,19,20]. In Sweden, two mosquito-borne viruses circulate: the arthralgia-associated Sindbis virus (SINV) [21] and Inkoo virus (INKV), which in rare cases, may cause mild encephalitis [22,23]. Further, it has been discussed whether WNV can be introduced to Sweden as it circulates in Southern and Central Europe, and the mosquito vector species, such as *Culex* (*Cx.*) *pipiens* and *Cx. torrentium*, are already present in the country [24,25].

In this study, we aimed to provide additional knowledge of viruses circulating in Northern Europe, as well as investigate the virome composition of different mosquito species in this region by using a viral metagenomic approach. In total, the virome composition of six different mosquito species collected in two locations in Mid-Eastern Sweden were investigated. In addition, we have further genetically characterised nine near-complete viral genomes associated with the orders *Bunyavirales*, *Picornavirales*, *Articulavirales*, and *Tymovirales*, and the realm *Ribovira*.

2. Materials and Methods

2.1. Mosquito Collection, Species Separation and Pool Design

Mosquitoes were collected in the summer of 2017 at two different geographic locations in Mid-Eastern Sweden, close to the small town Flen (coordinate: 59°04′08.6″ N 16°31′14.1″ E) and in the nature reserve Hammarskog (coordinate: 59°46′31.9″ N 17°35′01.3″ E) close to the city of Uppsala. In the location close to Flen, mosquitoes were collected once every second week from May to the end of August, using dry-ice-baited Centers for Disease Control and Prevention (CDC) miniature light traps and CDC gravid traps (John W. Hock company, Gainesville, FL, USA). In Hammarskog, a Mosquito Magnet® was placed close to a bird breeding ground from Monday to Friday every second week, from July to the end of August. The Mosquito Magnet® was emptied every 24 h. The mosquitoes were euthanized and stored at −80 °C after collection. Female mosquitoes were determined to species based on morphological character, using a taxonomic key [26], stereomicroscope, and a cold table. *Culex* (*Cx.*) *torrentium* and *Cx. pipiens* were identified to species using a molecular method previously described [27]. Eight to twelve female mosquitoes were pooled based on mosquito species, time of collection, and location. The most abundant species collected (*Coquillettidia* (*Cq.*) *richardii*, *Aedes* (*Ae.*) *communis*, *Ae. annulipes*, *Ae. cantans* and all *Cx. pipiens* and *Cx. torrentium*) were used in further analyses.

2.2. Homogenisation, Nucleic acid Extraction, Pre-Sequencing Preparation and Sequencing

Prior to homogenisation, all mosquitoes were washed once in 70% ethanol and then twice in milliQ water to remove potential surface microorganisms. The mosquitoes in each pool were then transferred to Precellys tubes (soft tissue homogenization CK14) and 700 µL PBS supplemented with Amphotericin (250 µg/mL) and Penicillin-Streptomycin (100 U penicillin/mL + 100 µg streptomycin/mL) was added. Homogenisation was performed mechanically with a Precellys® evolution (Bertin instruments, Paris, France) at two cycles of 5500 RPM for 30 s with a 40 s pause between each cycle. In addition, to keep the temperature at 10 °C a Cryolys (Bertin instruments, Paris, France) cooled with liquid nitrogen was coupled to the Precellys® evolution. The homogenates were centrifuged at 8000× *g* for 5 min at 4 °C and the supernatant was collected for future analysis. Total RNA was extracted with TRIzol™ according to the manufacturer's protocol. The aqueous phase obtained after the addition of chloroform and the subsequent centrifugation step was collected and diluted 1:1 with freshly prepared 70% ethanol and purified with GeneJet spin columns. The purified RNA was further pooled with RNA from the same mosquito species, location, and time point, resulting in a total of 12 pools (Table 1). These pools were subjected to DNase treatment using RNAeasy mini elute kit and RNase-Free DNase set (Qiagen, Hilden, Germany), following the manufacturer's recommended protocol. Ribosomal RNA was removed using the Ribo-Zero Gold (epidemiology) rRNA Removal Kit (Illumina, San Diego, USA) and the non-ribosomal RNA was randomly amplified with the Ovation® RNA-Seq System V2

(NuGEN Technology, San Carlos, CA, USA), following the manufacture's instruction. The amplified RNA was submitted to SciLifeLab for library preparation and sequencing using the Ion 530™ Chip kit (Thermo Fisher scientific, Massachusetts, USA). The 12 pools were divided on four Ion 530™ chips and sequencing was carried out with an Ion S5 XL sequencing system running the protocol for 400 bp-long reads.

2.3. Metagenomics Data Analysis

The Ion S5 XL sequence data were analysed in a metagenomics pipeline starting with quality control using FastQC (v1.2.1). Reads of low quality were trimmed with sickle (version 1.210) using a cut-off PHRED score of 20. The mean reads length after trimming was 359–380 nt. The good quality reads were de-novo assembled using MEGAHIT (v1.1.2). Both the good quality reads and the de-novo assembled contigs were taxonomically assigned in separate runs using Diamond version 0.9.10 with the blastx option using the default settings (e-value cutoff 0.001 and one top hit) and the NCBI database from October 2018. In order to visualize the results with the R-package Pavian (v0.8.4), the output format taxonomy (102) was used in Diamond. This option performs a LCA (Last Common Ancestor) algorithm to assign the taxonomy of each read and output a tabulated file (https://github.com/bbuchfink/diamond/blob/master/diamond_manual.pdf). For the de-novo assembled contigs, an additional Diamond run was performed to output a DAA (Direct Access Archive) format that could be imported into MEGAN6 (version 6.15.2) for further investigation. Potential viral sequences were analysed with NCBI's ORF finder (<https://www.ncbi.nlm.nih.gov/orffinder/>), functional annotation of the ORFs was performed using NCBI's BLASTp, EMBL-EBI's protein sequence analysis and classification tool InterProScan [28] and Phobius [29]. Phylogenetic analyses were performed on the RNA-dependent RNA polymerase (RdRp) amino acid sequences for the novel viruses and related sequences in the GenBank database with >20% amino acid (aa) identity. Sequence alignment and phylogenetic tree building were performed in MEGA 7 [30]. MUSCLE was used for multiple sequence alignment of the amino acid (aa) sequences [31]. The phylogenetic trees were computed with the maximum-likelihood method using 500 bootstraps replicates.

2.4. PCR Gap Closure of Viral Genome

We further investigated the Hammarskog picorna-like virus (HPLV) with PCR and Sanger sequencing. Viral hits were inspected and retrieved in Megan, overlapping contigs that mapped to the same virus were manually assembled into longer sequences. The extended sequences were subsequently used to design primers pairs to fill gaps and cover as much as possible of the genome using the primer3 software. The original RNA extractions of interest were reverse transcribed to cDNA using SuperScript® III (Invitrogen, Carlsbad CA, USA). PCR reactions were carried out with KAPA2G Robust Hotstart ReadyMix (KAPABiosystems, Wilmington, MA, USA). PCR products were analysed with electrophoresis and bands of correct size were cut out and extracted with a GenJet gel extraction kit (Thermo Fisher Scientific, Waltham, MA USA). Purified PCR products were sent to Macrogen for Sanger sequencing and the returning sequences were analysed in DNASTAR, SeqMan Pro (Version 2.1.0.97).

2.5. Accession Numbers

The raw sequence reads generated in this study are available at the NCBI sequence read archive (SRA) database under Bioproject accession (PRJNA574583). All virus genome sequences retrieved in this study have been deposited in GenBank under the accession numbers: MN513369–MN513382.

3. Results

3.1. Mosquito Collection

In total, 1428 mosquitoes of at least 12 different species were collected at the two different locations; 920 mosquitoes in Flen and 508 mosquitoes in Uppsala. The most abundant mosquito species were *Cq. richardii* (433), *Ae. cantans* (407), *Ae. communis* (106) and *Ae. annulipes* (72). The less abundant mosquito species out of those collected were *Ae. vexans* (45), *Ae. intrudens* (44), *Ae. punctor* (29), *Cx. pipiens* (22) and *Cx. torrentium* (4) (Figure 1).

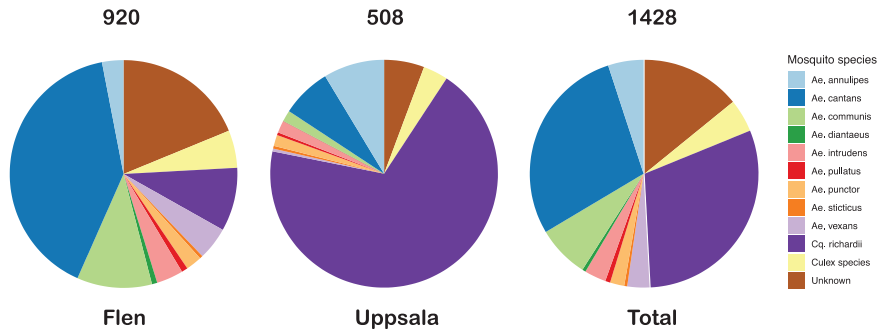


Figure 1. Distribution of all mosquito species collected in Flen and Uppsala. Mosquito species are represented by different colors. *Aedes* (*Ae.*), *Coquillettidia* (*Cq.*).

Table 1. Summary of the mosquito pools that were sequenced. Mix of sample location means that mosquitoes in this pool were collected both in Flen and Uppsala. Mix of sample time point means that mosquitoes in this pool were collected over several time points. *Culex* (*Cx.*).

Pool Name	Mosquito spp	Sample Location	Sample Time Point	Raw Reads	Diptera Reads (%)	Microbial Reads (%)	Viral Reads (%)
1	<i>Cx. pipiens</i>	Mix	Mix	2 985 629	7.6%	27.55%	8.76%
2	<i>Cx. torrentium</i>	Mix	Mix	4 713 173	42.65%	56.21%	4.86%
3	<i>Ae. communis</i>	Mix	Mix	8 590 873	1.43%	13.78%	1.44%
4	<i>Ae. annulipes</i>	Mix	Mix	1 842 681	5.42%	27.65%	12.47%
5	<i>Ae. cantans</i>	Flen	May and June	1 427 446	5.35%	24.75%	11.00%
6	<i>Ae. cantans</i>	Flen	July	5 877 722	3.3%	13.23%	5.43%
7	<i>Ae. cantans</i>	Flen	August	2 269 961	5.11%	19.73%	8.48%
8	<i>Ae. cantans</i>	Uppsala	mix	1 238 350	6.5%	23.54%	8.00%
9	<i>Cq. richardii</i>	Uppsala	June	5 201 595	14.02%	26.8%	3.13%
10	<i>Cq. richardii</i>	Uppsala	July	8 889 584	12.6%	26.37%	5.39%
11	<i>Cq. richardii</i>	Uppsala	August	4 821 295	9.19%	27.73%	10.4%
12	<i>Cq. richardii</i>	Flen	Mix	4 247 080	12.2%	29.19%	5.81%

3.2. The Mosquito Viromes

We have characterized the RNA viromes of 953 female mosquitoes, divided into 12 pools, representing six mosquito species from two geographic locations in Mid-Eastern Sweden. For each mosquito pool, between 1.4–9.2 million reads were obtained, of these 1.4–42.6% mapped to diptera and 13.2–56.2% were microbial reads, of which 1.44–12.5% of the reads were classified as viral (Table 1). A large proportion of the viral reads were labelled as unclassified RNA viruses (Figure 2A). In the unclassified virus group, the majority of the viral sequences showed close to distant similarity (28–96% amino acids (aa) identity) to various viruses previously identified through different large metagenomic surveys of invertebrates [5–7]. The classified viral reads belonged to the families *Flaviviridae*, *Nodaviridae*, *Orthomyxoviridae*, *Partitiviridae*, *Peribunyaviridae*, *Phasmaviridae*, *Reoviridae*, *Rhabdoviridae*, *Solemoviridae*,

and *Tombusviridae* (Figure 2B). De novo assembly of the viral reads produced the near-complete genomes of nine viruses in the orders *Picornavirales*, *Tymovirales*, *Bunyavirales*, and *Articulavirales*, and the realm *Riboviria*.

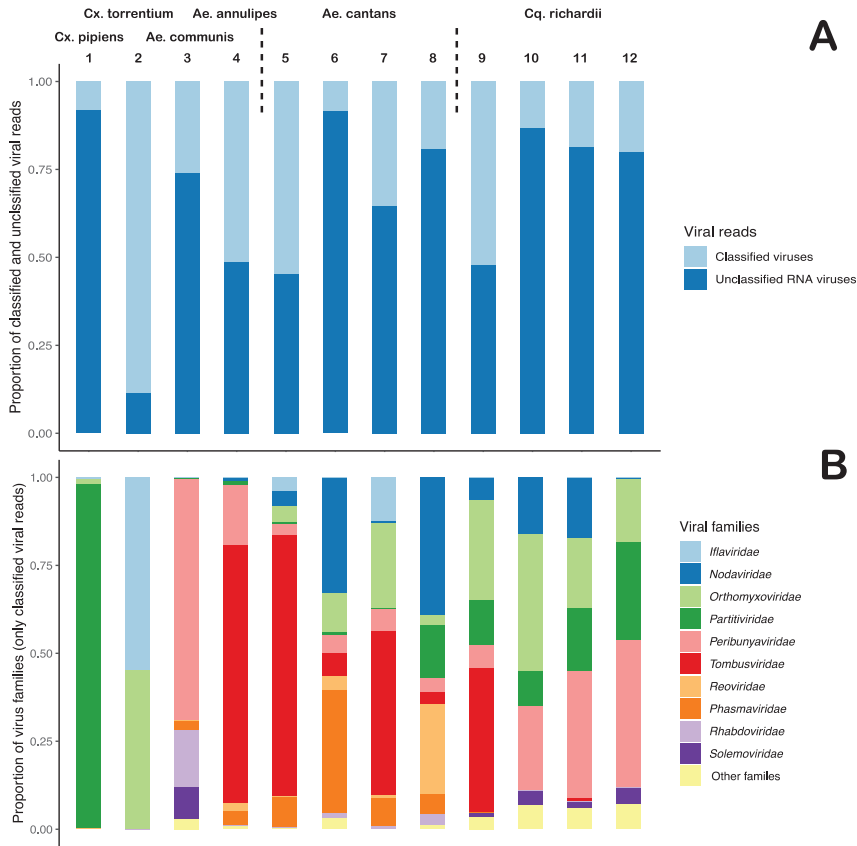


Figure 2. Annotation of viral reads in the different pools of mosquitoes. Each bar represents a mosquito pool—designated 1–12 and are described in Table 1. (A) Proportion of classified viral reads and unclassified RNA viral read. (B) Proportion of virus families of the classified viral reads.

3.3. Diverse Distribution of Viral Reads

The viromes analysed in this study were diverse and many viral families were represented (Figure 1 and Table 2). Differences between mosquito species and the types of viruses they harboured were observed, however, a large number of viral hits were observed across more than one species and genera. For example, viral reads that mapped to the *Culex mononega*-like virus 2 (CMLV2) were observed in all pools except in the *Cx. pipiens* mosquitoes and in one pool of *Ae. cantans*, collected late in the season. Reads that mapped to CMLV2 were particularly abundant in the *Cx. torrentium* (0.216% total reads (TR)), *Ae. communis* (0.112% TR) and *Ae. annulipes* mosquitoes (0.721% TR) (Table 2). In terms of mosquito genera, many similarities could be observed. For example, the *Aedes* mosquitoes had many common negative-sense RNA viral hits, such as those showing similarity to Yongsan bunyavirus 1 (YBV1) (0.016–2.844% TR), Xincheng anphevirus (0.004–0.142% TR), Anopheles darlingi virus (0.001–0.381% TR), and Wuhan mosquito orthophasmavirus 2 (0.003–0.215%

TR) (Table 2). However, the *Culex* mosquito species only shared one viral hit, the *Culex* Iflavi-like virus 3, which was exceptionally abundant in the *Cx. torrentium* (2.3% TR) compared to the *Cx. pipiens* (0.003% TR). Many of the viral hits were restricted to one mosquito species, such as similarity hits to the Hubei virga-like virus 21, which was only observed in the *Cx. pipiens* mosquitoes and in those, represented more than half of the viral reads in that pool (4.916% TR) (Table 2). Moreover, several of the unclassified RNA virus hits were only observed in the *Cq. richardii* pools, such as, Hubei noda-like virus 12 (0.023–4.22% TR), Hubei diptera virus 13 (0.022–0.074% TR), Hubei sobemo-like virus 8 and 9 (0.02–0.064%, 0.022–0.069% TR) and the Hubei tetragnatha maxillosa virus 8 (0.015–0.48% TR) (Table 2). Viral reads showing similarity to the positive-sense RNA virus Yongsan picorna-like virus 3 (YPLV3) were also only observed in the *Cq. richardii* pools, with high abundance in those collected in Uppsala (0.124–1.279% TR) and lower abundance in those collected in Flen (0.002% TR) (Table 2). The *Ae. cantans* mosquitoes shared most of its viral hits with other mosquito species, except four viruses; two positive-sense RNA viruses, Wuhan mosquito virus 3 (0.006–0.119% TR) and the Whidbey virus (0.007–0.102% TR) and two negative-sense RNA viruses, Kinkell virus (0.087–0.109% TR) and the unclassified virus Shuangao insect virus 12 (0.024–0.166% TR). Comparing the virus composition and abundance between the species and genera in this dataset, one can observe some differences. The *Aedes* genus seems to harbour a more diverse negative-sense RNA virome compared to the *Culex* and *Coquillettidia* genera. The *Culex* mosquitoes had few but very abundant viruses, one that represented more than half of the total viral reads in the *Cx. pipiens* pool. Many viral hits could only be observed in one of the mosquito species, indicating a host restriction. No significant differences could be observed comparing the locations or time point of collection in the *Cq. richardii* pools and *Ae. cantans* pool (Table 2).

Table 2. Cont.

	Abundance of Viruses (% of Total Reads)														
Hubei tetragnatha maxillosa virus 8	0	0	0	0	0	0	0	0	0	0	0	0.015	0.054	0.054	0.48
Wuhan insect virus 13	0	0.29	0	0	0	0	0	0	0	0	0	0	0	0	0
Wuhan fly virus 4	0	0	0	0	0	0.612	0	1.05	0	0	0	0	0	0.001	0.003
Wenzhou sobemo-like virus 4	0	0	0.034	0	0	0	0	0	0	0	0	0	0	0	0
Saxxia water strider virus 17	0	0	0	0	0	0	0	0	0	0	0	0	0	0.035	0.052
Shuangao insect virus 12	0	0	0	0	0	0.024	0	0.166	0	0	0	0	0	0	0
Renna virus	0	0	0.038	0	0	0	0	0.001	0	0	0	0	0	0	0
Culex mononega-like virus 2	0	0.216	0.112	0	0.721	0.091	0.017	0	0.189	0.005	0.004	0.004	0.004	0.002	0.002
Culex mononega-like virus 1	0	0	0.006	0.112	0.112	0.012	0.003	0	0.018	0	0	0	0	0	0
Ae camptorhynchus negev-like virus	0	0	0	0	0	0.359	0.11	0.654	1.902	0	0	0	0	0	0
Ae alboannulatus orthomyxo-like virus	0	0	0	0	0	0.183	0.038	0.323	0.015	0	0	0	0.002	0	0
Ae camptorhynchus reo-like virus	0	0	0.046	0	0	0	0	0	0	0	0	0	0	0	0
Salarivirus Mos8CM0	0	0	0.018	0.707	0.707	0.597	0.19	0.819	0.326	0.01	0.009	0.015	0.04	0.04	0.04
Chaq virus-like 1	0	0	0	0	0	0	0	0	0	0	0.126	0.032	0.025	0.366	0.366
uncultured virus	0	0	0.021	0.032	0.032	0.128	0.015	0.071	0.021	0.251	0.347	0.434	0.485	0.485	0.485
Caninivirus sp.	0	0	0	0	0	0.068	0.082	0	0.096	0	0	0	0	0	0
Total reads in table (%)	4.93	4.7	0.52	7.02	7.02	5.64	3.32	4.71	4.97	1.32	2.74	2.74	7	2.11	2.11
Other viral reads (%)	3.83	0.16	0.92	5.45	5.45	5.36	2.11	3.77	3.03	1.81	2.66	3.4	3.7	3.7	3.7
Total viral reads (%)	8.76	4.86	1.44	12.47	12.47	11	5.43	8.48	8	3.13	5.4	10.4	5.81	5.81	5.81

3.4. Positive-Sense RNA Viruses

The positive-sense RNA viruses observed in our mosquitoes were within the viral families/orders *Iflaviridae*, *Nodaviridae*, *Tombusviridae*, *Solemoviridae*, and *Picornavirales* and represented between 0.03–47% of the viral reads in the mosquito pools. Four of the positive-sense RNA viruses detected were further characterized and phylogenetically analysed and fell within the viral orders *Picornavirales* and *Tymovirales*.

The analysed high-throughput data from the three pools of *Cq. richardii* mosquitoes collected in Uppsala showed many contigs that mapped to the Yongsan picorna-like virus 3 (YPLV3) (NC_040584.1). Using these contigs, combined with PCR and Sanger sequencing, the near-complete genome of a picorna-like virus, that we named “Hammarskog picorna-like virus” (HPLV) (Figure 3A), was recovered. This near-complete genome was 10,818 nt long and the sequence was further confirmed by mapping raw reads from the respective pools to the retrieved sequence. BLASTn analysis confirmed that the YPLV3 (NC_040584.1) had the closest similarity to the picorna-like sequence identified in this study with a nucleotide (nt) identity of 69.71%. YPLV3 was discovered in *Ae. vexans nipponii* mosquitoes collected in the Republic of Korea [32] and has a genome of 11,291 nt with four described ORFs coding for three small hypothetical proteins and a polyprotein. Analysing the HPLV genome with NCBI’s ORF finder software resulted in five ORFs, i.e., one extra ORF of 202 aa was identified between the first and the second ORF described by Sanborn et al. [32]. However, analysing the YPLV3 (NC_040584.1) genome with NCBI’s ORF finder showed that it also contained this additional ORF (191 aa). Sequence comparison of these two ORF sequences showed that they share a 62% aa identity to each other. No function of the protein could be predicted. Furthermore, the first ORF of our sequence translated to a protein of 194 aa and is predicted to code for a viral coat protein subunit (IPR029053). The third and fourth ORF code for proteins of 271 aa and 376 aa with no predicted functions. The fifth ORF had no stop codon, which suggests that our sequence is incomplete, in addition to lacking a 3’ UTR. Moreover, the fifth ORF is predicted to code for a polyprotein of 2402 aa that would be processed into a peptidase S1 (IPR009003), Helicase super family 3 (IPR000605, IPR014759) and an RNA-directed RNA polymerase (RdRp) (IPR001205) from the N- to C-terminus direction. BLASTp analyses of HPLV’s hypothetical proteins showed an aa identity of 58.55%, 74.17%, 60.95%, and 66.54% to each respective hypothetical protein of YPLV3. Phylogenetic analysis of the polyprotein and related sequences showed that our sequence clustered with picorna-like viruses discovered in insects, such as the Hubei picorna-like virus 82 (YP_009330058) (Figure 3A).

Further, two near-complete genomes showing 67.63% and 75.17% nt identity to the Yongsan tombus-like virus 1 (YTLV1) (NC_040725) were identified. One of the genomes was found in the *Ae. cantans* collected late in the season in Flen and one genome was found in the *Cq. richardii* mosquitoes collected early in the season in Uppsala. The tombus-like viral contig retrieved from *Ae. cantans* mosquitoes was 4520 nt long and the virus was named Flen tombus-like virus (FTLV), while the tombus-like viral contig retrieved from the *Cq. richardii* mosquitoes was 4166 nt long and this virus was named Hammarskog tombus-like virus (HTLV) (Figure 3B). Sequence comparison between FTLV and HTLV showed that they are different tombus-like viruses as they only showed an nt identity of 64.5% to each other. Using NCBI’s ORF finder, it was predicted that both genomes had three ORFs of similar size and position as the YTLV1 (Table 3).

Table 3. Summary of the BLASTp analysis of each ORF of FTLV and HTLV.

ORFs	FTLV Protein	HTLV Protein	aa Identity between FTLV and HTLV	aa Identity to YPLV1 (FTLV)	aa Identity to YPLV1 (HTLV)	Accession Number
ORF 1	411 aa	379 aa	46.88%	43.98%	70.59%	YP_009553260
ORF 2	479 aa	482 aa	65.13%	66.6%	81.17%	YP_009553261
ORF 3	412 aa	409 aa	62.77%	64.63%	87.5%	YP_009553263

The InterProScan analysis of each ORF's aa sequences revealed no predicted function for the first ORF, the second ORF showed a detailed signature match of a RdRp, hepatitis C virus (IPR002166) and the third ORF resulted in a detailed signature match of the Nodavirus capsid (IPR024292). Phylogenetic analysis of the two predicted RdRp sequences of the second ORF showed that our sequences cluster to the YTLV1 (YP_009553261) and the Wenzhou tombus-like virus 11 (YP_009342051). Based on this, we classified our near-complete viruses as tombus-like (Figure 3B).

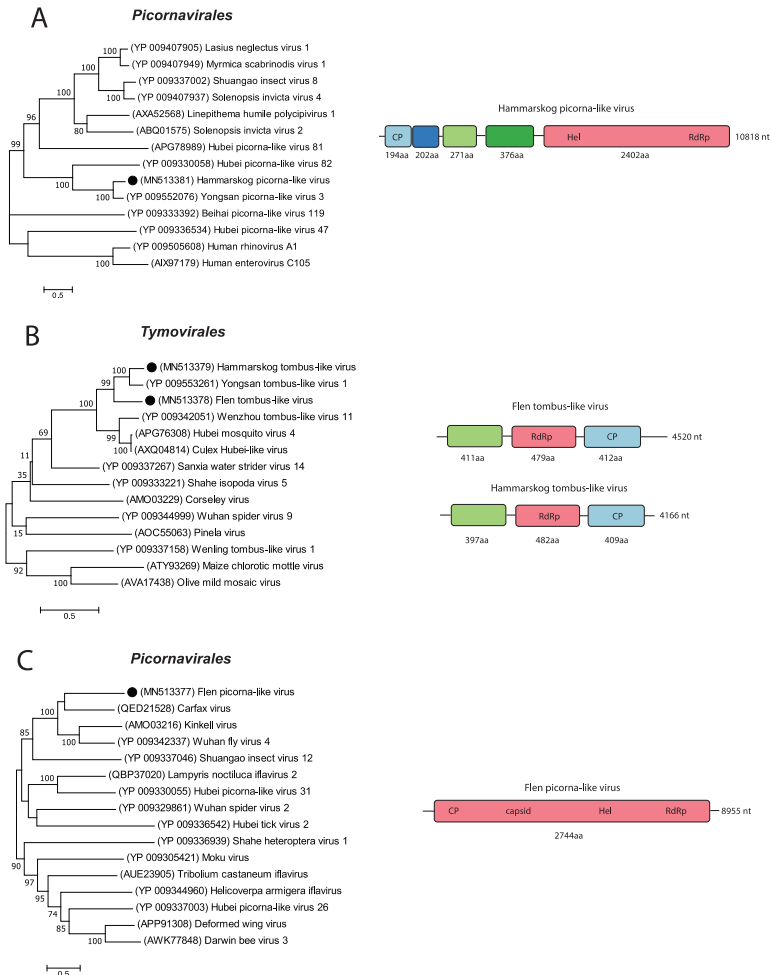


Figure 3. Phylogenetic analysis and genomic features of the positive-sense RNA viruses discovered in this study. The maximum-likelihood phylogenetic trees show the positions of newly discovered viruses (solid black circles) in the context of representatives of their closest relatives. The genome structures of viruses discovered in this study are shown next to their corresponding phylogenies. (A) The phylogenetic tree was generated using the translation of the fifth ORF. (B) Phylogenetic tree was generated using the translation of the second ORF for both FTLV and HTLV. (C) The phylogenetic tree was generated using the aa sequence of the complete polyprotein. RNA-dependent RNA polymerase (RdRp).

Two pools of the *Ae. cantans* mosquitoes, collected early and late in the summer, had many viral hits corresponding to the unclassified RNA virus Wuhan fly virus 4 (WV4) (Table 2). From one of these pools, we retrieved an 8955 nt long contig. BLASTn analysis of the sequence yielded the Carfax virus (MIN167498) as the top hit, with 68.19% nt identity; however, the query cover was only 8%. The second top hit was the WV4 (KX883891), with 65.79% nt identity, and similar to the Carfax virus, the query cover was only 10%. The low query cover indicates that our sequence is probably highly divergent from any other in the database. Further, analysing our sequence with NCBI's ORF finder revealed one ORF coding for a protein of 2744 aa. A BLASTp search of the aa sequence displayed the polyprotein of the Carfax virus (QED21528) as the top hit with 34.59% aa identity and 92% query cover. The hypothetical protein of WV4 (YP_009342337) was the third top hit, with 34.14% aa identity and 96% query cover. Analysing our polyprotein with InterProScan showed detailed signature matches of a calicivirus coat protein (IPR004005), Picornavirus capsid (IPR001676), dicistrovirus capsid-polyprotein C-terminal (IPR014872), helicase superfamily 3 single-stranded RNA virus (IPR014759), peptidase S1 PA clan (IPR009003) and a RdRp C-terminal domain (IPR001205), in the N- to C-terminal direction. Based on the detailed signature matches of the polyprotein, this virus follows many of the hallmarks of the order *Picornavirales* [33]. The phylogenetic analysis of the polyprotein showed that our sequence clusters with viruses, such as, the Carfax virus (QED21528) and Kinkell virus (AMO03216) in the viral order *Picornavirales*. Therefore, the near-complete virus was classified as a picorna-like virus and due to the high divergence, we named it Flen picorna-like virus after the location of collection (Figure 3C).

3.5. Negative-Sense RNA Viruses

The negative-sense RNA viruses observed in our mosquitoes belonged to the viral families/orders *Orthomyxoviridae*, *Peribunyaviridae*, *Phasmaviridae*, *Mononegavirales*, *Articulavirales*, and *Bunyavirales* and represented between 0.1-39% of the viral reads in the mosquitoes pools. Two of the negative-sense RNA viruses detected were further characterized and phylogenetically analysed and fell within the viral orders *Bunyavirales* and *Articulavirales*.

A partial genome similar to the Wuhan mosquito virus 4 (WMV4) was detected in the *Cx. torrentium* mosquitoes (Figure 4A). WMV4 is an unclassified *Quarantjavirus* with a single-stranded, negative-sense segmented RNA genome. To date, only four segments of generally six segments have been identified, coding for the replicative polymerase complex PB1, PB2, and PA and for the nucleocapsid protein (NP), respectively [7,34]. The length of the segments detected in this study were 2517 nt (PB1), 2574 nt (PB2), 2228 nt (PA), and 1892 nt (NP). BLASTn analysis of the four segments showed 86.86% nt identity to the PB1, 84.30% nt identity to the PB2, 84.92% to the PA and 81.6% nt identity to the NP of WMV4. Analysing each segment with NCBI's ORF finder, revealed one ORF of 770 aa (PB1), one ORF of 786 aa (PB2), one ORF of 717 aa (PA), and one ORF of 579 aa for segment NP. BLASTp analysis of each ORF showed that the proteins had a high aa similarity to those of WMV4: 95.58% for PB1, 91.22% for PB2, 93.31% for PA and 82.21% for NP. Phylogenetic analysis of the ORF's aa sequence of the PA segment showed that our sequence clusters with the unclassified *Quarantjaviruses* Wuhan mosquito virus 4 and 6 (KX883866 and MF176380). Based on the characterization of each segment and the phylogenetic analysis, our partial genome was classified as orthomyxo-like and named the *Culex* orthomyxo-like virus after the mosquito genera it was found in (Figure 4A).

In the *Ae. cantans* mosquitoes collected early in the summer in Flen, we identified near-full-length genome segments with high similarity to the Yongsan bunyavirus 1 (YBV1). The YBV1 is an unclassified bunyavirus with a linear single-stranded, negative-sense genome divided into three segments [32]. The segments are named small, medium, and large, where the small segment codes for the nucleocapsid protein (NP), the medium segment codes for the glycoprotein (GP), and the large segment codes for the RdRp. The retrieved near-complete genome segments from this study were 1040 nt (small), 2095 nt (medium), and 6596 nt (large) (Figure 4B). BLASTn analysis of each segment, showed a 77.46% nt identity to the NP segment of YBV1, but only with a query cover of 6%. The medium segment showed 66.80% nt identity to the GP segment of YBV1, with a query cover of 35% and the large segment showed

66.37% nt identity to the RdRp segment of YBV1, with a query cover of 59%. Analysing each segment with NCBI's ORF finder showed one ORF of 341 aa (small segment) with no stop codon, one ORF of 490 aa (medium segment), and one ORF of 2145 aa for the large segment. A BLASTp search of each segment revealed 42.77% aa identity to the YBV1 NP, 55.19% aa identity to the YBV1 GP, and 53.34% aa identity to the YBV1 RdRp. The phylogenetic analysis of the aa sequence of the protein-coding region of the large segment showed that our sequence cluster with the unclassified Bunyavirales YBV1 (YP_009553313), the Orthophasmavirus Wuhan mosquito virus 2 (YP_009305135), and the unclassified virus *Culex phasma-like virus* (ASA4765) (Figure 4B). Based on the characterization of each segment and the phylogenetic analysis, we classified our near-complete genome as bunya-like and named it Flen bunya-like virus.

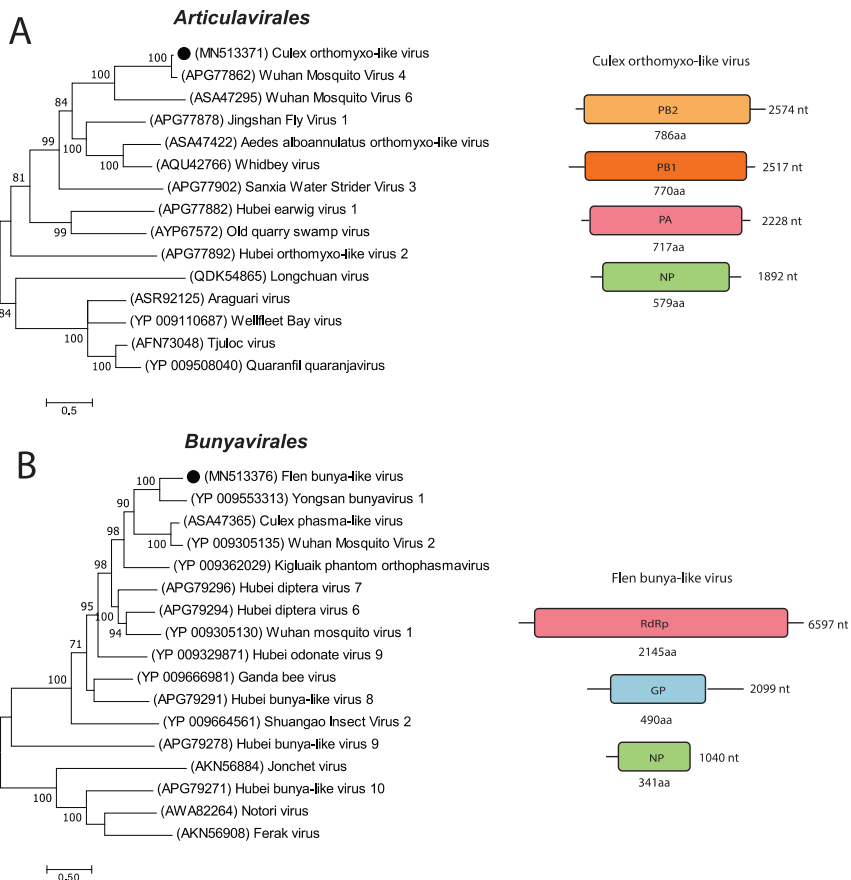


Figure 4. Phylogenetic analysis of the predicted and genomic features of the negative-sense RNA viruses discovered in this study. The maximum-likelihood phylogenetic trees show the positions of newly discovered viruses (solid black circles) in the context of representatives of their closest relatives. The genome structures of the viruses discovered in this study are shown next to their corresponding phylogenies. (A) The phylogenetic tree was generated using the translation of the ORF of the PA segment. (B) The phylogenetic tree was generated using the translation of the ORF of the large segment.

3.6. Unclassified Viruses

A large proportion of all viral reads were labelled as unclassified RNA viruses (Figure 2A). By investigating these viral reads in greater detail, we detected the near-complete genomes of three unclassified RNA viruses. Almost all pools had viral reads that mapped to the *Culex mononega*-like virus 2 (CMLV2), and by assembling overlapping contigs, a near-complete genome of 13,105 nt was identified in the *Cx. torrentium* mosquitoes (Figure 5A). BLASTn of the consensus sequence showed that it had a high nt identity (95.76–96%) to six different strains of CMLV2 (MF176318, MF176377, MF176247, MF176332, MF176268, and MF176298). The top hit (MF176318) has a linear RNA genome of 13,277 nt that codes for six hypothetical proteins. Analysing our CMLV2 sequence with NCBI's ORF finder software showed similar ORFs coding for similar proteins. Starting from the 5' end, the first ORF codes for a 508 aa-long protein, BLASTp showed 96.65% identity to a hypothetical protein of CMLV2 (YP_009388617). The second ORF codes for a small protein of 99 aa that shows 98.99% identity to a hypothetical CMLV2 protein (YP_009388618). Analysing the sequence with Phobius showed that it is probably a transmembrane signaling peptide. The third ORF codes for a 445 aa protein with 95.51% nt identity to a hypothetical protein of CMLV2 (ASA47289). The fourth ORF codes for a protein of 638 aa, BLASTp analysis showed high aa identity 97.96% to the glycoprotein of CMLV2 (YP_009388620). The fifth ORF codes for a small protein of 74 aa, with an aa identity of 90% to a hypothetical protein (ASA47321) of CMLV2. Analysing the sequence in Phobius predicted a transmembrane domain. The last and sixth ORF codes for a long protein of 2074 aa with no stop codon, suggesting that our sequence is not complete. BLASTp analysis showed that the protein has a high aa identity of 96% to the RdRp (ASA47413) of CMLV2. InterProScan revealed detailed signature matches to *Mononegavirales* RdRp (IPR014023), *Mononegavirales* mRNA-capping domain V (IPR026890), and mononegavirus L protein 2-O-ribose methyltransferase (IPR025786). Phylogenetic analysis of the 2074 aa sequence containing the RdRp gene showed the closest association to the CMLV2 (ASA47413), which is an unclassified virus. Two more distant associations were to the unclassified Anphevirus, *Anopheles marajoara* virus (QBK47216) and the drosophilid anphevirus, *Drosophila unispina* virus 1 (YP_009666282). As our near-complete genome showed such close genetic identity to other strains of CMLV2 (96% nt identity) [35], we consider this a genotype of CMLV2 (Figure 5A).

All pools of *Cq. richardii* mosquitoes had viral reads mapping to the unclassified RNA virus Hubei noda-like virus 12 (HNLV 12). However, most of the reads were found in the pool of *Cq. richardii* mosquitoes collected late in the season in Uppsala (Table 2). From this pool, a near-complete genome of 4027 nt was retrieved and BLASTn analysis showed that the sequence had 75.98% nt identity to the HNLV 12 (KX883125). This virus has a linear RNA genome of 4727 nt coding for two hypothetical proteins [5]. Analysing our sequence with NCBI's ORF finder also revealed two ORFs. The first ORF codes for a protein of 1007 aa, BLASTp search of the aa sequence showed 81% aa identity to the hypothetical protein 1 (APG76311) of Hubei noda-like virus 12. InterProScan showed a signature of a DNA/RNA polymerase (SSF56672). The second ORF codes for a 352 aa protein, with 88.92% aa identity to the hypothetical protein 2 (APG76312) of HNLV 12 and no function could be predicted. Phylogenetic analysis of the 1007 aa sequence, containing the DNA/RNA polymerase, showed that our sequence clusters with viruses in the realm Riboviria, such as the HNLV 12 (APG76311) and the Sanxia water strider virus 17 (YP_009337232). A more distant association in the cluster showed the virus Alphanodavirus HB-2007/CHN (ADF97523), which is an unclassified Alphanodavirus. Our near-complete genome was classified in the realm Riboviria and named Hammarskog noda-like virus based on the characterisation and phylogenetic analysis [36] (Figure 5B).

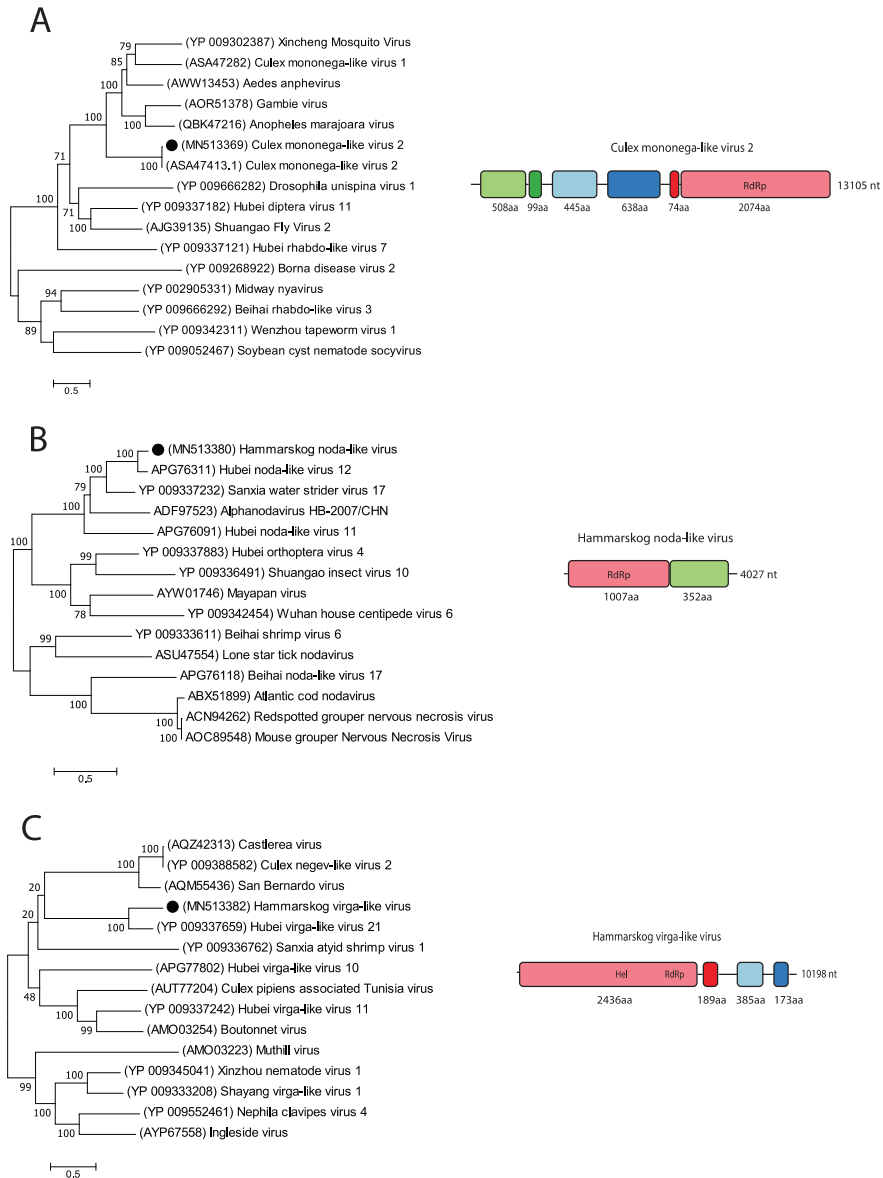


Figure 5. Phylogenetic analysis and genomic features of the unclassified RNA viruses discovered in this study. The maximum-likelihood phylogenetic trees show the positions of newly discovered viruses (solid black circles) in the context of representatives of their closest relatives. The genome structures of viruses discovered in this study are shown next to their corresponding phylogenies. (A) The phylogenetic tree was generated using the translation of the sixth ORF. (B) The phylogenetic tree was generated using the translation of the first ORF. (C) The phylogenetic tree was generated using the translation of the first ORF.

In the *Cx. pipiens* pool, a sequence of 10 200 nt was detected with 65.63% nt identity to the Hubei virga-like virus 21 (HVLV 21) (KX883775.1). The HVLV 21 has a linear RNA genome of 10,072 nt, with four ORFs coding for one larger hypothetical polyprotein and three smaller hypothetical proteins [5]. Analysing our sequence with NCBI's ORF finder showed four ORFs with similarity to HVLV 21 (KX883775). The first ORF codes for the large protein of 2436 aa, with 47.20% aa identity to HVLV 21 (YP_009337659), the second ORF codes for a 189 aa protein with 48.15% aa identity to HVLV 21 (YP_009337660), the third ORF codes for a protein of 385 aa with 36.57% aa identity to HVLV 21 (YP_009337661) and the fourth ORF code for a 173 aa protein with 45.56% aa identity to HVLV 21 (YP_009337662). Analysing the aa sequences with InterProScan predicted that the protein of the first ORF could possess an Alphavirus-like methyltransferase (MT) domain (IPR002588), (+)RNA virus helicase core domain (IPR027351), Tymovirus, RdRp (IPR001788), and a RdRp, catalytic domain (IPR007094). No function or domain could be predicted for the other ORFs. Phylogenetic analysis of the aa sequence of the first ORF showed that our sequence only clusters with the HVLV 21 (YP_009337659). More distant associations were to the unclassified viruses Boutonnet virus (AMO03254) and Sanxia atyid shrimp virus 1 (YP_009336762). Our near-complete genome was classified in the realm Riboviria and named Hammarskog virga-like virus based on the characterisation and phylogenetic analysis [37] (Figure 5C).

4. Discussion

We have used a viral metagenomic approach to characterize the virome of mosquitoes collected at two geographic locations in Mid-Eastern Sweden representing six mosquito species. A homology search of the viral reads showed that most of the mosquito viromes were highly diverse, representing multiple viral families (Table 2, Figure 2). Comparing viral hits across the mosquito species and genera, some similarities could be observed, such as viral hits to the CMLV2 and Zhee mosquito virus in almost all pools (Table 2). We could also observe similarities within mosquito genera, such as viral hits to the *Culex* Iflavi-like virus 3 in the *Culex* mosquitoes and viral hits to the Yongsan bunyavirus 1 in the *Aedes* mosquitoes. Further, many viral hits could only be observed in one of the mosquito species, indicating a host restriction. One example is that only the *Coquillettidia* mosquitoes had viral reads that mapped to the YPLV3 (Table 2). Overall, from our data, we can observe indications that the *Aedes* genera seem to harbour a more diverse negative-sense RNA virome compared to the *Culex* and *Coquillettidia* genera. The *Coquillettidia* mosquitoes had more viral hits among the unclassified RNA viruses compared to the others and the *Culex* mosquitoes had few but very abundant viruses, one that represented more than half of the total viral reads in the *Cx. pipiens* pool (Table 2). However, the mosquito sampling was biased between the species collected and the location, e.g., 350/433 of the *Cq. richardii* were collected in Uppsala and 371/407 of the *Ae. cantans* were collected in Flen (Figure 1). If this reflects the species present at the different locations, the environment of the locations or the different traps used in Flen and Uppsala is hard to say. To draw any conclusions regarding local differences of the viromes, we would need a larger sampling, covering more geographic regions of Sweden and bigger sampling size of each mosquito species from each location. Neither have the different sequence depth and number of mosquitoes in each pool been accounted for in this comparison.

The near-complete genomes of nine RNA viruses were characterized and phylogenetically analysed in greater detail. Four of these viruses were associated to (+)ssRNA viruses in the orders *Picornavirales* and *Tymovirales*. Two viruses were associated to (-)ssRNA viruses in the orders *Bunyavirales* and *Articulavirales* and three viruses could not be classified to an order and have instead been classified in the realm Riboviria, which is the basal rank for RNA viruses [38]. Phylogenetic analyses of these nine viruses showed the closest association to viruses previously detected in mosquitoes or other invertebrates (Figures 3–5). This could indicate that these viruses are potentially insect-specific, however, to confirm host specificity, we would need to perform infection studies in different animals or vertebrate cell-lines. Many of the viral reads in our study, especially those unclassified, showed similarity to viruses identified in a metagenomic study from China, by Shi et al. [5], that investigated

220 invertebrate species and discovered 1445 novel viruses. Moreover, four of the near-complete viruses detected in this study were closely associated to the Yongsan picorna-like virus 3, Yongsan bunyavirus 1, and Yongsan tombus-like virus 1. These viruses were found in metagenomic studies of mosquitoes collected at the Yongsan U.S Army Garrison, in the Republic of Korea [32,39]. Further, the CMLV2 detected in this study showed close genetic identity (95.76–96% nt identity) to the CMLV2 discovered in mosquitoes collected in Australia [20]. The majority of viral sequences that our viral reads and near-complete genomes mapped to, have been discovered in mosquitoes far from Northern Europe and Sweden. Providing reference genomes from wider geographic regions and different mosquito species will facilitate future in silico recognition and assembly of viral genomes in metagenomic datasets.

Two of the nine characterized viruses in this study showed association to a viral family related to plant viruses. The FTLV and HTLV were closely associated to the *Tombusviridae* virus YTLV1 (NC_040725), with 67.63% and 75.17% nt identity. The family *Tombusviridae* is currently associated with plant viruses [40]. Assigning host tropism in metagenomic analysis of whole mosquitoes is hard, as it may include plant viruses from their diet and viruses of parasitic or commensal organisms residing inside or on the mosquito. However, when mapping the reads from respective pools to the FTLV or HTLV sequences, 27,318 reads mapped to HTLV and 48,980 reads mapped to FTLV. This could indicate high abundance of the virus in the mosquito and possibly replication. Further work is needed to confirm replication of these two viruses in mosquito cells.

This study expands the knowledge of viruses circulating in different mosquito species in Northern Europe. It provides information on the diversity of the viromes of the respective mosquito species investigated, as well as shows the presence of a number of viruses not known to circulate in this region and that are highly divergent to previously characterized viruses. Whether any of these viruses have any direct or indirect potential veterinary or public health-relevance remains to be further investigated.

Author Contributions: P.Ö., J.H., J.C.H. and A.-L.B. conceived and designed the experiments; P.Ö. and H.L. performed the experiments; P.Ö., J.H. and A.-L.B. analysed the data; P.Ö. wrote and prepared the original draft; H.L., J.H., J.C.H. and A.-L.B. reviewed and edited the manuscript.

Funding: This study was supported by the Swedish research Council VR (2016-01251), the Kungl. Skogs- och Lantbruksakademien (GFS2016-0033) and Konung Carl XVI Gustafs 50-årsfond för Vetenskap, Teknik och miljö.

Acknowledgments: The authors would like to acknowledge support of the National Genomics Infrastructure (NGI)/Uppsala Genome Center and UPPMAX for providing assistance in massive parallel sequencing and computational infrastructure. Work performed at NGI/Uppsala Genome Center has been funded by RFI/VR and Science for Life Laboratory, Sweden. The SNIC through Uppsala Multidisciplinary Center for Advanced Computational Science (UPPMAX) under project SNIC 2017/7-290 is acknowledged for providing the computational resources.

Conflicts of Interest: The authors declare no conflict of interest. The founding sponsors had no role in the design of the study; in the collection, analyses, or interpretation of data; in the writing of the manuscript; or in the decision to publish the results.

References

1. Rizzoli, A.; Jimenez-Clavero, M.A.; Barzon, L.; Cordioli, P.; Figuerola, J.; Koraka, P.; Martina, B.; Moreno, A.; Nowotny, N.; Pardigon, N.; et al. The challenge of West Nile virus in Europe: Knowledge gaps and research priorities. *Eurosurveillance* **2015**, *20*. [[CrossRef](#)] [[PubMed](#)]
2. Fauci, A.S.; Morens, D.M. Zika Virus in the Americas—Yet Another Arbovirus Threat. *N. Engl. J. Med.* **2016**, *374*, 601–604. [[CrossRef](#)] [[PubMed](#)]
3. Silva, L.A.; Dermody, T.S. Chikungunya virus: Epidemiology, replication, disease mechanisms, and prospective intervention strategies. *J. Clin. Investig.* **2017**, *127*, 737–749. [[CrossRef](#)] [[PubMed](#)]
4. Messina, J.P.; Brady, O.J.; Scott, T.W.; Zou, C.; Pigott, D.M.; Duda, K.A.; Bhatt, S.; Katzelnick, L.; Howes, R.E.; Battle, K.E.; et al. Global spread of dengue virus types: Mapping the 70 year history. *Trends Microbiol.* **2014**, *22*, 138–146. [[CrossRef](#)]
5. Shi, M.; Lin, X.D.; Tian, J.H.; Chen, L.J.; Chen, X.; Li, C.X.; Qin, X.C.; Li, J.; Cao, J.P.; Eden, J.S.; et al. Redefining the invertebrate RNA virosphere. *Nature* **2016**, *540*, 539–543. [[CrossRef](#)]

6. Sadeghi, M.; Altan, E.; Deng, X.; Barker, C.M.; Fang, Y.; Coffey, L.L.; Delwart, E. Virome of >12 thousand Culex mosquitoes from throughout California. *Virology* **2018**, *523*, 74–88. [[CrossRef](#)]
7. Li, C.X.; Shi, M.; Tian, J.H.; Lin, X.D.; Kang, Y.J.; Chen, L.J.; Qin, X.C.; Xu, J.; Holmes, E.C.; Zhang, Y.Z. Unprecedented genomic diversity of RNA viruses in arthropods reveals the ancestry of negative-sense RNA viruses. *Life* **2015**, *4*. [[CrossRef](#)]
8. Frey, K.G.; Biser, T.; Hamilton, T.; Santos, C.J.; Pimentel, G.; Mokashi, V.P.; Bishop-Lilly, K.A. Bioinformatic Characterization of Mosquito Viromes within the Eastern United States and Puerto Rico: Discovery of Novel Viruses. *Evol. Bioinform. Online* **2016**, *12*, 1–12. [[CrossRef](#)]
9. Junglen, S.; Drosten, C. Virus discovery and recent insights into virus diversity in arthropods. *Curr. Opin. Microbiol.* **2013**, *16*, 507–513. [[CrossRef](#)]
10. Webster, C.L.; Longdon, B.; Lewis, S.H.; Obbard, D.J. Twenty-Five New Viruses Associated with the Drosophilidae (Diptera). *Evol. Bioinform. Online* **2016**, *12*, 13–25. [[CrossRef](#)]
11. Bolling, B.G.; Olea-Popelka, F.J.; Eisen, L.; Moore, C.G.; Blair, C.D. Transmission dynamics of an insect-specific flavivirus in a naturally infected Culex pipiens laboratory colony and effects of co-infection on vector competence for West Nile virus. *Virology* **2012**, *427*, 90–97. [[CrossRef](#)] [[PubMed](#)]
12. Hobson-Peters, J.; Yam, A.W.; Lu, J.W.; Setoh, Y.X.; May, F.J.; Kurucz, N.; Walsh, S.; Prow, N.A.; Davis, S.S.; Weir, R.; et al. A new insect-specific flavivirus from northern Australia suppresses replication of West Nile virus and Murray Valley encephalitis virus in co-infected mosquito cells. *PLoS ONE* **2013**, *8*, e56534. [[CrossRef](#)] [[PubMed](#)]
13. Kenney, J.L.; Solberg, O.D.; Langevin, S.A.; Brault, A.C. Characterization of a novel insect-specific flavivirus from Brazil: Potential for inhibition of infection of arthropod cells with medically important flaviviruses. *J. Gen. Virol.* **2014**, *95*, 2796–2808. [[CrossRef](#)] [[PubMed](#)]
14. Goenaga, S.; Kenney, J.L.; Duggal, N.K.; Delorey, M.; Ebel, G.D.; Zhang, B.; Levis, S.C.; Enria, D.A.; Brault, A.C. Potential for Co-Infection of a Mosquito-Specific Flavivirus, Nhumirim Virus, to Block West Nile Virus Transmission in Mosquitoes. *Viruses* **2015**, *7*, 5801–5812. [[CrossRef](#)]
15. Nasar, F.; Erasmus, J.H.; Haddow, A.D.; Tesh, R.B.; Weaver, S.C. Eilat virus induces both homologous and heterologous interference. *Virology* **2015**, *484*, 51–58. [[CrossRef](#)]
16. Hall-Mendelin, S.; McLean, B.J.; Bielefeldt-Ohmann, H.; Hobson-Peters, J.; Hall, R.A.; van den Hurk, A.F. The insect-specific Palm Creek virus modulates West Nile virus infection in and transmission by Australian mosquitoes. *Parasit. Vectors* **2016**, *9*, 414. [[CrossRef](#)]
17. Marklewitz, M.; Zirkel, F.; Kurth, A.; Drosten, C.; Junglen, S. Evolutionary and phenotypic analysis of live virus isolates suggests arthropod origin of a pathogenic RNA virus family. *Proc. Natl. Acad. Sci. USA* **2015**, *112*, 7536–7541. [[CrossRef](#)]
18. Crochu, S.; Cook, S.; Attoui, H.; Charrel, R.N.; De Chesse, R.; Belhouchet, M.; Lemasson, J.J.; de Micco, P.; de Lamballerie, X. Sequences of flavivirus-related RNA viruses persist in DNA form integrated in the genome of Aedes spp. mosquitoes. *J. Gen. Virol.* **2004**, *85*, 1971–1980. [[CrossRef](#)]
19. Cholleti, H.; Hayer, J.; Abilio, A.P.; Mulandane, F.C.; Verner-Carlsson, J.; Falk, K.I.; Fafetine, J.M.; Berg, M.; Blomstrom, A.L. Discovery of Novel Viruses in Mosquitoes from the Zambezi Valley of Mozambique. *PLoS ONE* **2016**, *11*, e0162751. [[CrossRef](#)]
20. Shi, M.; Neville, P.; Nicholson, J.; Eden, J.S.; Imrie, A.; Holmes, E.C. High-Resolution Metatranscriptomics Reveals the Ecological Dynamics of Mosquito-Associated RNA Viruses in Western Australia. *J. Virol.* **2017**, *91*. [[CrossRef](#)]
21. Ahlm, C.; Eliasson, M.; Vapalahti, O.; Evander, M. Seroprevalence of Sindbis virus and associated risk factors in northern Sweden. *Epidemiol. Infect.* **2014**, *142*, 1559–1565. [[CrossRef](#)] [[PubMed](#)]
22. Lwande, O.W.; Bucht, G.; Ahlm, C.; Ahlm, K.; Naslund, J.; Evander, M. Mosquito-borne Inkoo virus in northern Sweden-isolation and whole genome sequencing. *Virol. J.* **2017**, *14*, 61. [[CrossRef](#)] [[PubMed](#)]
23. Putkuri, N.; Kantele, A.; Levanov, L.; Kivisto, I.; Brummer-Korvenkontio, M.; Vaheri, A.; Vapalahti, O. Acute Human Inkoo and Chatanga Virus Infections, Finland. *Emerg. Infect. Dis.* **2016**, *22*, 810–817. [[CrossRef](#)] [[PubMed](#)]
24. Lundstrom, J.O. Mosquito-borne viruses in western Europe: A review. *J. Vector Ecol.* **1999**, *24*, 1–39. [[PubMed](#)]
25. Hubalek, Z. Mosquito-borne viruses in Europe. *Parasitol. Res.* **2008**, *103* (Suppl. 1), S29–S43. [[CrossRef](#)]
26. Becker, N.; Petric, D.; Zgomba, M.; Boase, C.; Dahl, C.; Madon, M.; Kaiser, A. *Mosquitoes and Their Control*, 2nd ed.; Springer: Berlin/Heidelberg, Germany, 2010; Volume 1, pp. 1–577.

27. Hesson, J.C.; Lundstrom, J.O.; Halvarsson, P.; Erixon, P.; Collado, A. A sensitive and reliable restriction enzyme assay to distinguish between the mosquitoes *Culex torrentium* and *Culex pipiens*. *Med. Vet. Entomol.* **2010**, *24*, 142–149. [[CrossRef](#)] [[PubMed](#)]
28. Mitchell, A.L.; Attwood, T.K.; Babbitt, P.C.; Blum, M.; Bork, P.; Bridge, A.; Brown, S.D.; Chang, H.Y.; El-Gebali, S.; Fraser, M.I.; et al. InterPro in 2019: Improving coverage, classification and access to protein sequence annotations. *Nucleic Acids Res.* **2019**, *47*, D351–D360. [[CrossRef](#)]
29. Kall, L.; Krogh, A.; Sonnhammer, E.L. Advantages of combined transmembrane topology and signal peptide prediction—the Phobius web server. *Nucleic Acids Res.* **2007**, *35*, W429–W432. [[CrossRef](#)]
30. Kumar, S.; Stecher, G.; Tamura, K. MEGA7: Molecular Evolutionary Genetics Analysis Version 7.0 for Bigger Datasets. *Mol. Biol. Evol.* **2016**, *33*, 1870–1874. [[CrossRef](#)]
31. Le, S.Q.; Gascuel, O. An improved general amino acid replacement matrix. *Mol. Biol. Evol.* **2008**, *25*, 1307–1320. [[CrossRef](#)]
32. Sanborn, M.A.; Klein, T.A.; Kim, H.C.; Fung, C.K.; Figueroa, K.L.; Yang, Y.; Asafo-Adjei, E.A.; Jarman, R.G.; Hang, J. Metagenomic Analysis Reveals Three Novel and Prevalent Mosquito Viruses from a Single Pool of *Aedes vexans nipponii* Collected in the Republic of Korea. *Viruses* **2019**, *11*, 222. [[CrossRef](#)] [[PubMed](#)]
33. Koonin, E.V.; Wolf, Y.I.; Nagasaki, K.; Dolja, V.V. The Big Bang of picorna-like virus evolution antedates the radiation of eukaryotic supergroups. *Nat. Rev. Microbiol.* **2008**, *6*, 925–939. [[CrossRef](#)] [[PubMed](#)]
34. Contreras-Gutierrez, M.A.; Nunes, M.R.T.; Guzman, H.; Uribe, S.; Suaza Vasco, J.D.; Cardoso, J.F.; Popov, V.L.; Widen, S.G.; Wood, T.G.; Vasilakis, N.; et al. Sinu virus, a novel and divergent orthomyxovirus related to members of the genus *Thogotovirus* isolated from mosquitoes in Colombia. *Virology* **2017**, *501*, 166–175. [[CrossRef](#)] [[PubMed](#)]
35. Maes, P.; Amarasinghe, G.K.; Ayllon, M.A.; Basler, C.F.; Bavari, S.; Blasdel, K.R.; Briese, T.; Brown, P.A.; Bukreyev, A.; Balkema-Buschmann, A.; et al. Taxonomy of the order Mononegavirales: Second update 2018. *Arch. Virol.* **2019**, *164*, 1233–1244. [[CrossRef](#)] [[PubMed](#)]
36. Sahul Hameed, A.S.; Ninawe, A.S.; Nakai, T.; Chi, S.C.; Johnson, K.L.; ICTV Report Consortium. ICTV Virus Taxonomy Profile: Nodaviridae. *J. Gen. Virol.* **2019**, *100*, 3–4. [[CrossRef](#)]
37. Adams, M.J.; Adkins, S.; Bragard, C.; Gilmer, D.; Li, D.; MacFarlane, S.A.; Wong, S.M.; Melcher, U.; Ratti, C.; Ryu, K.H.; et al. ICTV Virus Taxonomy Profile: Virgaviridae. *J. Gen. Virol.* **2017**, *98*, 1999–2000. [[CrossRef](#)]
38. Walker, P.J.; Siddell, S.G.; Lefkowitz, E.J.; Mushegian, A.R.; Dempsey, D.M.; Dutilh, B.E.; Harrach, B.; Harrison, R.L.; Hendrickson, R.C.; Junglen, S.; et al. Changes to virus taxonomy and the International Code of Virus Classification and Nomenclature ratified by the International Committee on Taxonomy of Viruses (2019). *Arch. Virol.* **2019**, *164*, 2417–2429. [[CrossRef](#)]
39. Hang, J.; Klein, T.A.; Kim, H.C.; Yang, Y.; Jima, D.D.; Richardson, J.H.; Jarman, R.G. Genome Sequences of Five Arboviruses in Field-Captured Mosquitoes in a Unique Rural Environment of South Korea. *Genome Announc.* **2016**, *4*. [[CrossRef](#)]
40. Nagy, P.D. Tombusvirus-Host Interactions: Co-Opted Evolutionarily Conserved Host Factors Take Center Court. *Annu. Rev. Virol.* **2016**, *3*, 491–515. [[CrossRef](#)]



Article

Small RNA Response to Infection of the Insect-Specific Lammi Virus and Hanko Virus in an *Aedes albopictus* Cell Line

Pontus Öhlund ^{1,*}, Juliette Hayer ², Jenny C. Hesson ³ and Anne-Lie Blomström ¹

¹ Department of Biomedical Sciences and Veterinary Public Health, Swedish University of Agricultural Sciences, P.O. Box 7028, 750 07 Uppsala, Sweden; anne-lie.blomstrom@slu.se

² Department of Animal Breeding and Genetics, Swedish University of Agricultural Sciences, SLU-Global Bioinformatics Centre, P.O. Box 7023, 750 07 Uppsala, Sweden; juliette.hayer@slu.se

³ Department of Medical Biochemistry and Microbiology, Zoonosis Science Center, Uppsala University, P.O. Box 582, 751 23 Uppsala, Sweden; jenny.hesson@imbim.uu.se

* Correspondence: pontus.ohlund@slu.se; Tel.: +46-18-672-409

Abstract: RNA interference (RNAi)-mediated antiviral immunity is believed to be the primary defense against viral infection in mosquitoes. The production of virus-specific small RNA has been demonstrated in mosquitoes and mosquito-derived cell lines for viruses in all of the major arbovirus families. However, many if not all mosquitoes are infected with a group of viruses known as insect-specific viruses (ISVs), and little is known about the mosquito immune response to this group of viruses. Therefore, in this study, we sequenced small RNA from an *Aedes albopictus*-derived cell line infected with either Lammi virus (LamV) or Hanko virus (HakV). These viruses belong to two distinct phylogenetic groups of insect-specific flaviviruses (ISFVs). The results revealed that both viruses elicited a strong virus-derived small interfering RNA (vsiRNA) response that increased over time and that targeted the whole viral genome, with a few predominant hotspots observed. Furthermore, only the LamV-infected cells produced virus-derived Piwi-like RNAs (vpiRNAs); however, they were mainly derived from the antisense genome and did not show the typical ping-pong signatures. HakV, which is more distantly related to the dual-host flaviviruses than LamV, may lack certain unknown sequence elements or structures required for vpiRNA production. Our findings increase the understanding of mosquito innate immunity and ISFVs' effects on their host.

Keywords: insect-specific flaviviruses; Hanko virus; Lammi virus; small interfering RNA; Piwi-interacting RNA



Citation: Öhlund, P.; Hayer, J.; Hesson, J.C.; Blomström, A.-L. Small RNA Response to Infection of the Insect-Specific Lammi Virus and Hanko Virus in an *Aedes albopictus* Cell Line. *Viruses* **2021**, *13*, 2181. <https://doi.org/10.3390/v13112181>

Academic Editor: A. Lorena Passarelli

Received: 22 September 2021

Accepted: 27 October 2021

Published: 29 October 2021

Publisher's Note: MDPI stays neutral with regard to jurisdictional claims in published maps and institutional affiliations.



Copyright: © 2021 by the authors. Licensee MDPI, Basel, Switzerland. This article is an open access article distributed under the terms and conditions of the Creative Commons Attribution (CC BY) license (<https://creativecommons.org/licenses/by/4.0/>).

1. Introduction

Most of our current knowledge on virus interactions with the mosquito vector has come from studies on human pathogenic arboviruses such as West Nile virus (WNV), Dengue virus (DENV), and Chikungunya virus (CHIKV). However, mosquitoes are often naturally and persistently infected with a group of viruses that are known as insect-specific viruses (ISVs). This group of viruses are unable to infect vertebrates and are maintained in the mosquito population through vertical transmission from mother to offspring [1–4]. Moreover, phylogenetic analyses have shown that many ISVs belong to viral families associated with pathogenic arboviruses such as *Flaviviridae*, *Togaviridae*, and *Peribunyaviridae* [5,6]. Insect-specific flaviviruses (ISFVs) can further be divided into two distinct phylogenetic subgroups. Those of the first subgroup are phylogenetically distinct from all other known flaviviruses and are referred to as classical ISFVs. The ISFVs of the other subgroup are phylogenetically affiliated with the medically important dual-host flaviviruses but have the insect-restriction phenotype and are referred to as dual-host affiliated ISFVs [7]. Two members of the insect-specific flavivirus group are Lammi virus (LamV) and Hanko virus (HakV), which were both isolated from mosquitoes in Finland. LamV was isolated from *Aedes cinereus* mosquitoes and belongs to the dual-host affiliated

ISFV category [8], and HakV was isolated from *Aedes caspius* mosquitoes and belongs to the classical ISFV category [9]. Little is known about how these ISFVs interact with the mosquito and whether they trigger an antiviral immune response in the host.

The main antiviral immune response in mosquitoes is believed to be the RNA interference (RNAi) pathway, which includes three major classes of regulatory small RNAs (sRNAs): Small interfering RNA (siRNA), microRNA (miRNA), and P-element-induced wimpy testis (Piwi)-interacting RNA (piRNA) [10]. The siRNA pathway is possibly the most important one with regards to antiviral defense in the mosquito. Upon a viral infection, double-stranded RNA (dsRNA) will form as replicative intermediates in the cytoplasm. These foreign (exogenous) dsRNAs are recognized and processed by the Dcr2–R2D2 complex into siRNAs of 21 nucleotides (nt) in length. Furthermore, the siRNA is incorporated into the RNA-induced silencing complex (RISC), where one of the strands is degraded and the remaining guide strand is used as a template to recognize complementary target RNAs, which are subsequently cleaved and degraded by Ago2 [11–13]. Functional Dcr2, R2D2, and Ago2 are crucial for limiting virus replication and dissemination in the mosquito, as demonstrated by many studies [14–18].

The miRNA pathway is similar to the siRNA pathway in the sense that dsRNAs are processed into smaller dsRNAs that are loaded into an RISC complex and facilitate target-specific cleavage. In the miRNA pathway, Dcr1 and Ago1 are analogous to Dcr2 and Ago2, respectively, in the siRNA pathway. However, the primary function of the miRNA pathway is post-transcriptional gene regulation, and the miRNAs (20–25 nt) come from endogenous hairpin transcripts [19,20]. The miRNA pathway has been shown to play a critical role in modulating host genes to control viral infection, e.g., the *Aae-miR-2940-5p* miRNA was found to be selectively downregulated in C6/36 cells as a response to WNV infection. This resulted in a lower expression of the metalloprotease m41 FtsH gene, which has been shown to be important for WNV replication [21]. Other studies have observed miRNA-driven gene modulation during the active viral infection of Zika virus (ZIKV) [22], DENV [23], and WNV [24].

The primary roles of the piRNA pathway are to silence transposons and maintain the integrity of the germline [25]. The key proteins of this pathway are members of the PIWI and Argonaut superfamilies, and the *Aedes albopictus* genome is known to encode seven PIWI proteins (Piwi 1–6 and Ago3) [26]. The piRNAs are 24–30 nt in length and usually show specific signature features such as a uracil (U) bias at the first position of the antisense strand and an adenine (A) at the 10th position of the sense strand. Recent studies on mosquitoes have suggested a possible role of the piRNA pathway in antiviral defense. For example, the production of ping-pong-dependent virus-derived piRNAs (vpiRNAs) by the PIWI-5 and Ago3 proteins has been observed during viral infection, suggesting an antiviral function [27]. Furthermore, the knockdown of the PIWI-4 proteins in mosquito cell lines has been found to increase the viral titers in comparison to controls [28–30]. The exact antiviral mechanisms of the piRNA pathway are still unknown.

In this study, we infected the *Aedes albopictus* U4.4 cell line with either of two ISFVs from two distinct phylogenetic groups, LamV or HakV, to investigate the small RNA response. We found that both LamV and HakV elicited a strong virus-derived small interfering RNA (vsiRNA) response that increased over time and targeted the whole viral genome. However, only the LamV-infected cells produced viral pi-like RNAs (vpi-like RNAs), which were mainly derived from the antisense genome and did not show the characteristic ping-pong signatures.

2. Materials and Methods

2.1. Cell Culture

Aedes albopictus U4.4 cells (kindly provided by Associate Professor G. Pijlman, Wageningen University, Wageningen, The Netherlands) and C6/36 cells (Sigma-Aldrich, Darmstadt, Germany) were cultured at 28 °C in a Leibovitz L-15 medium (Gibco, Paisley, UK) supplemented with 10% fetal bovine serum (FBS) (Gibco, Paisley, UK), 10% tryptose

phosphate broth (TPB) (Gibco, Paisley, UK), amphotericin (250 µg/mL) (Gibco, Grand Island, NY, USA), and Pen Strep (100 U penicillin/mL and 100 µg streptomycin/mL) (Gibco, Grand Island, NY, USA).

2.2. Virus Stocks and Virus Titration

The ISFVs LamV (Strain: 2009/FI/Original) and HakV (Strain: 2005/FI/UNK) were obtained from the European Virus Archive—Global (EVAg). Virus stocks were propagated in C6/36 *Aedes albopictus* cells until a clear cytopathic effect (CPE) was shown (4 days post infection (d.p.i.)), and then supernatant was collected, centrifuged, and frozen at -80°C . We did not obtain any reliable virus stock titers with the traditional methods. Thus, to quantify the ISFV stocks, plasmid standards containing the PCR target region of the virus were ordered (GeneScript Biotech, Leiden, The Netherlands). The plasmids were used to construct a qPCR standard curve, and a stock concentration was calculated as RNA copies/µL. RNA extractions and qRT-PCR protocols are described below.

2.3. In Vitro Infection

On the day of infection, U4.4 cells grown in 24-well plates to a confluence of 85–90% were used (approximately 350,000 cells per well). The cells were infected as triplicates for each timepoint. In brief, per infection, 35,000 RNA copies of either LamV or HakV were mixed with 200 µL of infection medium (Leibovitz L-15 medium containing 2% FBS and 10% TPB) and added to the respective wells. After one hour of incubation at 28°C , the inoculum was discarded, and 500 µL of Leibovitz L-15 medium supplemented with 5% FBS, 10% TPB, and PEST were added. Mock infected cells were used as controls. The U4.4 cells were sampled every 24 h until 72 h post-infection (p.i.) for small RNA sequencing, and the supernatant was collected from 24 to 96 h p.i. for qPCRs.

2.4. RNA Extractions

The RNA used for growth curves and virus titration was extracted from 200 µL of supernatant/virus stocks in 750 µL of TRIzol™ (Thermo Fisher Scientific, Carlsbad, CA, USA) and homogenized. The aqueous phase obtained after the addition of chloroform and the subsequent centrifugation step was collected, diluted to 1:1 with freshly prepared 70% ethanol, and purified with GeneJet spin columns (Thermo Fisher Scientific, Vilnius, Lithuania). The RNA was eluted in 40 µL of nuclease-free water and stored at -80°C until further processing.

Small RNA used for high-throughput sequencing was isolated from cells that were collected by adding 750 µL of TRIzol™ to respective wells. The aqueous phase was obtained in the same manner as described above, and the RNA was further purified using the mirVana™ PARIS™ Kit (Thermo Fisher Scientific, Vilnius, Lithuania) according to the protocol to isolate small RNA (<200 nt) provided by the manufacturer.

2.5. qPCR

First-strand cDNA was generated using the SuperScript™ III Reverse Transcription kit (Thermo Fisher Scientific, Carlsbad, CA, USA) with Random Hexamers (Thermo Fisher Scientific, Carlsbad, CA, USA) following the manufacturer's instructions, with an input of 5 µL of RNA in a total reaction volume of 20 µL. The qPCR was performed using the iTaq Universal SYBR® Green Supermix (Bio-Rad laboratories Inc., Hercules, CA, USA) with 2 µL of template cDNA and 0.5 µM of each corresponding virus primer (Table 1) in a total volume of 20 µL per reaction. The qPCR was carried out using the Bio-Rad® CFX96 real-time PCR system (Bio-Rad laboratories Inc., Hercules, CA, USA), with amplification conditions consisting of an initial denaturation at 95°C for 30 s, followed by 40 cycles of denaturation at 95°C for 7 s, and finally annealing/extension and plate reading at 60°C for 30 s. A melt curve was generated starting at 60°C with a 0.5°C increase up to 96°C .

Primer pairs for the qPCR were designed using the software Primer3 [31] to generate a product between 170 and 200 bp long and a T_m of 60°C . Virus reference genomes were

obtained from the NCBI database and are listed together with the primer sequences in Table 1.

Table 1. Primer pairs used for the qPCR analysis.

Primers	Binding Site	Sequence (5' → 3')	Ref
LamV-F	4659–4678	TGGGTGTTACCGGTTATGT	FJ606789
LamV-R	4845–4864	ACGTTCCATTCAAGTTTCCAT	
HakV-F	4655–4674	TGTGTTACGGTGGAAACTGG	NC030401
HakV-R	4842–4861	CAACTGGTTCCTCCGTTGACA	

2.6. High-Throughput Sequencing of Small RNA

Small RNA isolated from the infected U4.4 cells was quantified and quality-controlled with the 4150 TapeStation System using the RNA ScreenTape Analysis kit (Agilent Technologies, Santa Clara, CA, USA). Triplicates for each timepoint (24–72 h) were pooled and submitted to SciLifeLab (Stockholm, Sweden) for library preparation using the QIAseq miRNA low input kit (QIAGEN, Hilden, Germany), and libraries were sequenced on one flow cell of the NextSeq 2000 with a 101nt(Read1)-8nt(Index1) setup using the ‘P2’ flow cell, which generated 10–20 million reads per sample with a read length of 1 × 100 base-pairs (bps).

2.7. Small RNA Sequence Analysis

The generated small RNA sequence data (FASTQ files) were analyzed with a pipeline including the trimming of adaptors and the removal of bad quality reads using Trim Galore! (v0.6.6), with a setting to discard all reads below 17 nt and above 40 nt. The trimmed reads were mapped to the LamV (FJ606789) genome and the HakV (NC030401) genome using Bowtie (v1.2.3) [32], allowing for one mismatch. We used the *-a*, *-best*, *-strata*, and *-all* flags, which instructed Bowtie to only report those alignments in the best alignment stratum and to generate a FASTQ file of the mapped reads in addition to the SAM file. The FASTQ files were used to analyze the size distribution of the mapped reads, which was visualized with the R package ggplot2. The SAM output files were further analyzed with the MISIS-2 software (v2.6) to visualize the alignment and polarity distribution of small RNA to the viral genomes [33]. The ping-pong signatures of 27–30 nt piRNA were analyzed with WebLogo [34].

2.8. Data Availability

All sequencing data have been made publicly available at the NCBI Sequence Read Archive (SRA) under accession number PRJNA761074.

3. Results

To investigate the RNAi response to ISFV infection in mosquitoes, we infected the *Aedes albopictus* U4.4 cell line with LamV or HakV at a concentration of 175,000 RNA copies/mL. Mock infections were used as controls. Cells were collected at 24, 48, and 72 h p.i. and processed for small RNA sequencing. The retrieved sequence data were trimmed from adaptors and bad quality reads, resulting in 10.4–16.9 million reads per sample, with read lengths between 17 and 40 nt. The size distributions of small RNAs were similar between all samples, with the highest peak observed at 21 nt (22.3–26.3% of total reads) and the second highest peak observed at 22 nt (13.7–15.3% of total reads) (Figure 1). These two peaks most likely corresponded to the populations of siRNAs and miRNAs in the cell. We could also observe an elevation in the proportion of reads between 26 and 30 nt, which is in the size range of piRNAs (Figure 1).

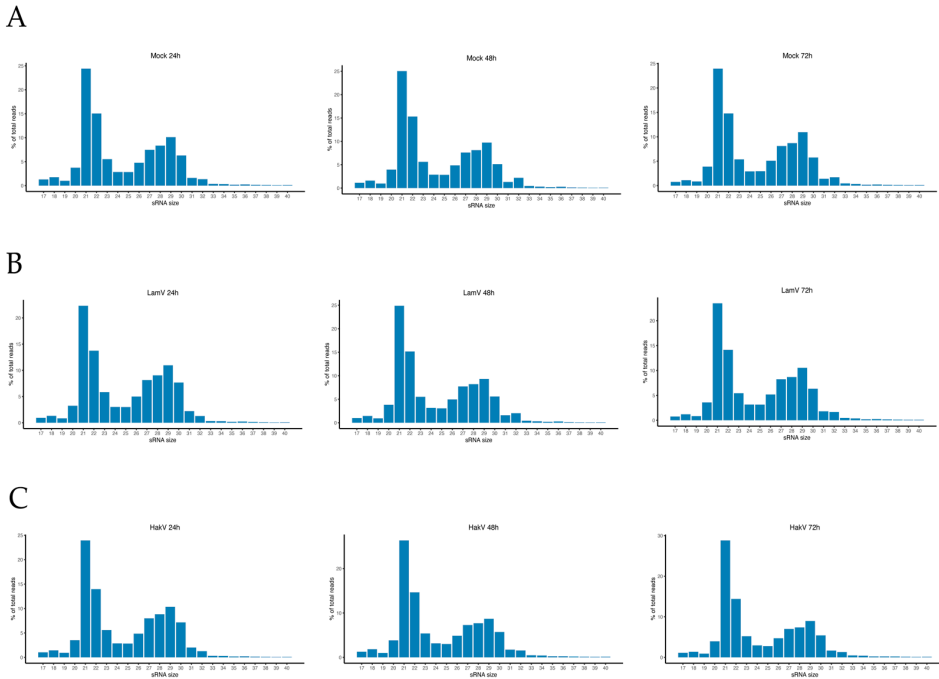


Figure 1. Small RNA profiles of U4.4 cells at 24, 48, and 72 h. (A) Small RNA profile of total reads in mock infected cells; (B) small RNA profile of total read in LamV-infected cells; (C) small RNA profile of total reads in HakV-infected cells.

To confirm active viral infection and replication, the supernatant was collected, further processed by RNA extraction and cDNA synthesis, and analyzed with qPCR. The data were used to calculate a growth curve over time (Figure 2). Both LamV and HakV showed steep virus growth during the first 48 h before plateauing. Furthermore, LamV showed a higher replication compared to HakV, with approximately one log more RNA copies at 48 h p.i. and the later timepoints recorded (Figure 2).

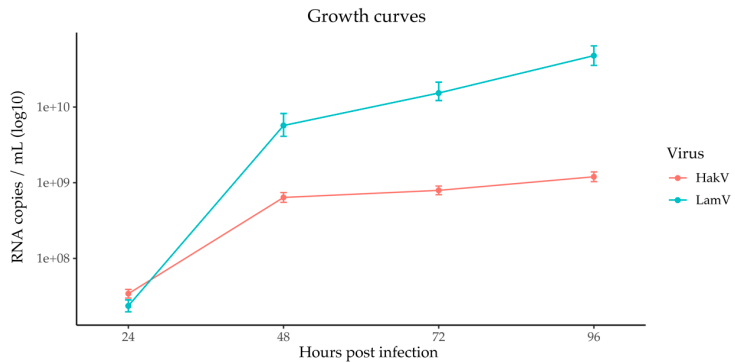


Figure 2. Growth curves of LamV and HakV in U4.4 cells, shown as RNA copies over time. Dots show the mean RNA copy numbers with a standard deviation between the biological triplicates.

3.1. Viral Small RNA Profiles in U4.4 Infected with LamV

To further investigate the production of virus-derived small RNAs (vsRNAs), the trimmed sequence data were mapped to the viral genomes. Results from U4.4 cells infected with LamV showed that few reads were virus-specific at 24 h p.i.: only 0.001% ($n = 270$) of the reads mapped to the LamV genome. However, the proportion of virus-specific reads increased over time, with 0.06% ($n = 6096$) observed at 48 h p.i. and 0.17% ($n = 24,179$) observed at 72 h p.i. The majority of the mapped reads had a read length of 21 nt and most likely corresponded to vsRNA (32.2% at 24 h, 36.7% at 48 h, and 32.9% at 72 h) (Figure 3). At 48 and 72 h p.i. a shoulder of reads in the size range of 27–30 nt that resembled vpiRNA was observed (Figure 3c,d). These 27–30 nt long reads were examined for ping-pong signatures, with antisense piRNA having a 1U bias (shown as T in this dataset) and the sense piRNA having a 10A bias. The 1U characteristics for Piwi-5-bound piRNAs were identified; however, the 10A bias was not observed (Figure 4a–d).

The vsRNAs from the LamV-infected cells mapped across the entire LamV genome, with a few predominant hotspots with a higher coverage. These hotspots were most distinct at 72 h p.i. (Figure 3d) and included four positions in the genome. Starting from the 5' end of the LamV genome, the first hotspot was at position 423, which was in the gene encoding for the capsid protein. The second hotspot was at position 3854, i.e., in the NS2A gene. The third hotspot at position 6808 was located in the NS4A protein, and the fourth hotspot at position 10,437 was positioned in the 3'-UTR of the genome. Moreover, the fourth hotspot had a coverage of over 900 reads, mainly at the size of 39 nt, which could be seen as a small hump in the read length distribution (Figure 3d). These reads were extracted and analyzed with WebLogo, and it was found that the majority consisted of the same sequence (Figure 4e). This suggested that these 39 nt long reads were not degraded products; however, their function and biogenesis are uncertain. Interestingly, a large majority of the vsRNA mapped to the sense strand of the LamV genome: 79.2% at 48 h and 82.4% at 72 h p.i. (Figure 3, left panel). This suggests that Ago-2 has a preferred bias for the antisense strand as a template and that the RISC complex mainly targets and degrades the sense genomes during LamV infection.

3.2. Viral Small RNA Profiles in U4.4 Infected with HakV

The results from HakV-infected U4.4 cells showed a slightly higher production of vsRNAs at 24 h p.i. compared to LamV-infected cells, where 0.01% ($n = 1296$) of the reads mapped to the HakV genome. The observed proportion of vsRNAs was similar at 48 h p.i., 0.06% ($n = 7324$), and lower at 72 h p.i., 0.08% ($n = 11,179$) compared to LamV-infected cells. Moreover, when analyzing the read length distribution, a high proportion of the reads was in the size range of siRNA (21 nt), with 48.4% observed at 24 h p.i., 60.9% observed at 48 h p.i., and 66.5% observed at 72 h p.i. The shoulder of piRNAs (27–30 nt) observed in the LamV-infected cells was absent in those cells infected with HakV (Figure 5). The lack of vpiRNA suggests that HakV does not trigger the proteins responsible for vpiRNA amplification such as Ago3 and PIWI-5. An analysis of the read alignment showed that the vsRNA mapped across the entire HakV genome, with slightly more coverage observed at the 3' end (7840–10,158 nt), which corresponded to the RNA-dependent RNA polymerase (NS5) gene region. The strand polarity showed a more even distribution between sense (68.6%) and antisense (31.4%) compared to LamV-infected U4.4 cells.

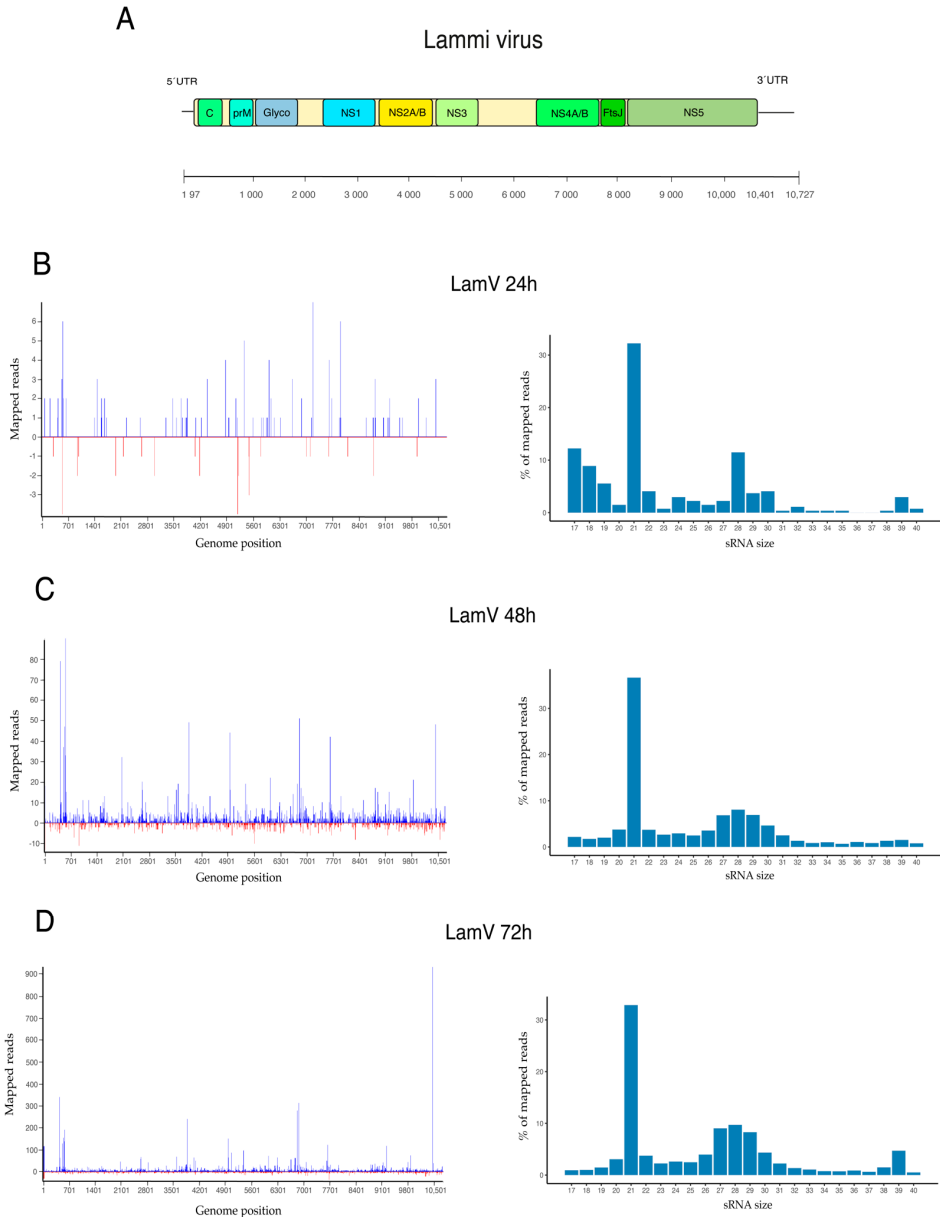


Figure 3. Viral small RNA profiles of U4.4 cells after LamV infection. **(A)** Schematic representation of the LamV genome and vsRNA profiles at 24 h **(B)**, 48 h **(C)**, and 72 h **(D)** p.i. Figures to the left show vsRNA reads along the LamV genome as a histogram. The positive values (blue) are counts of sRNAs mapped to the sense strand, and the negative values (red) are those mapped to the antisense strand. Figures to the right show the size distribution of reads that mapped to the LamV genome.

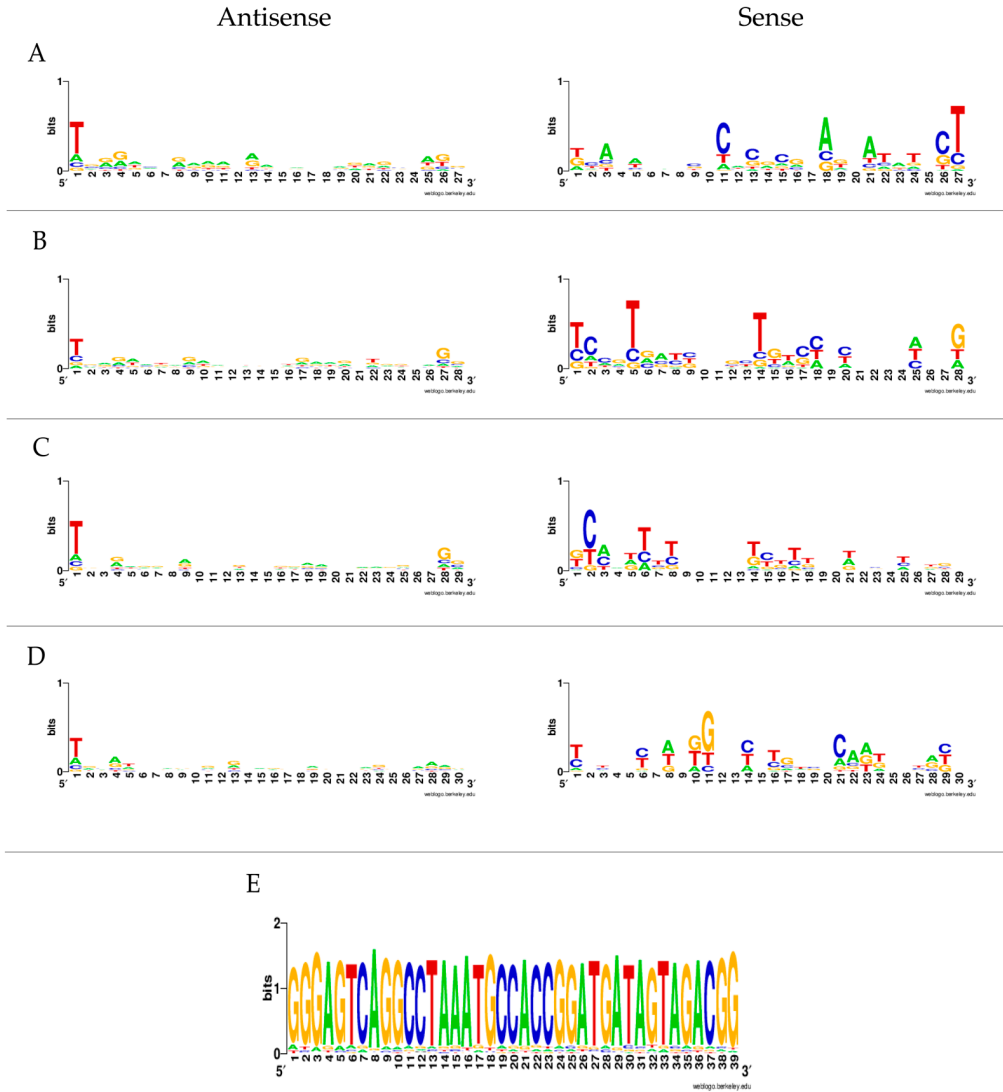


Figure 4. Nucleotide biases of the 27–30 and 39 nt long reads at 72 h p.i. of LamV. The sequences are in DNA format, so U is written as T. Reads derived from the antisense are shown in the left panel. Reads derived from sense strand are shown in the right panel: (A) 27 nt reads, (B) 28 nt reads, (C) 29 nt reads, (D) 30 nt reads, and (E) 39 nt long reads from the fourth hotspot in the LamV genome.

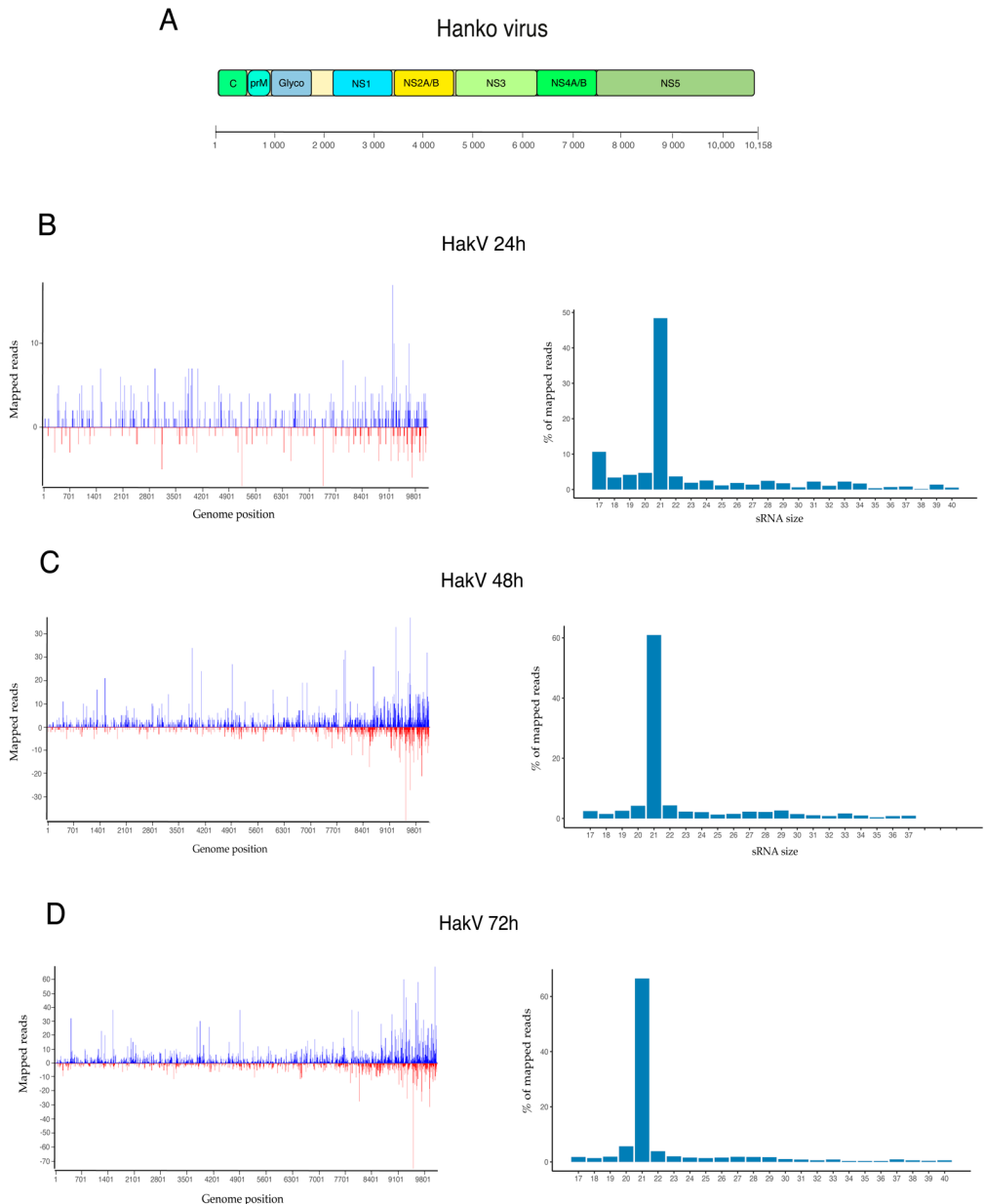


Figure 5. Viral small RNA profiles of U4.4 cells after HakV infection. **(A)** Schematic representation of the HakV genome. vsRNA profiles at 24 h **(B)**, 48 h **(C)**, and 72 h **(D)** p.i. Figures to the left show vsRNA reads along the HakV genome as a histogram. The positive values are counts of vsRNAs mapped to the sense strand, and the negative values are those mapped to the antisense strand. Figures to the right show the size distribution of reads that mapped to the HakV genome.

4. Discussion

RNAi-mediated antiviral immunity is thought to be key in the defense against viral infection in mosquitoes. The production of virus-specific small RNAs has been demonstrated in mosquitoes and mosquito-derived cell lines for viruses in all of the major arbovirus families: *Peribunyaviridae*, *Togaviridae*, and *Flaviviridae* [18,35–40]. However, although mosquitoes and mosquito-derived cell lines are often persistently infected with this group of viruses, the RNAi response to ISVs is not as well-studied. To our knowledge, only a handful of studies have investigated the effect of ISVs on the RNAi response in mosquitoes. One study developed an integrated mosquito small RNA genomics resource and included data from mosquito cell lines persistently infected with ISVs, including the ISFV cell-fusing agent virus [41]. Another study investigated the RNAi response of the mosquito U4.4 (*Aedes albopictus*), Aag2 (*Aedes aegypti*), and CT (*Culex tarsalis*) cell lines, which were shown to be persistently infected with different ISVs. For example, the U4.4 cells were persistently infected with Culex Y virus (CYV) and displayed a potent siRNA response against it [42]. In the present study, we investigated the RNAi response to acute ISFV infection over time in the aforementioned U4.4 cells. At the early time point (24 h p.i.), both the LamV- and HakV-infected U4.4 cells showed low amounts of vsRNAs (0.01–0.001% of total reads), which could have been because of the relatively low amount of virus or because the siRNA and piRNA pathways had not yet responded. Results from the qPCR analysis of the supernatant showed the replication of both LamV and HakV at this time point (Figure 2). Moreover, the proportion of vsRNA steadily increased over time, with 0.06% observed at 48 h p.i. and 0.17–0.08% observed at 72 h p.i. Interestingly, the increasing proportion of vsRNA correlated with the plateau of the virus growth curves (Figure 2) and might have been a sign of RNAi-induced interference with the virus replication.

The siRNA pathway is regarded as the most important antiviral defense mechanism, and in line with this, our experiments showed that it was the most abundant population of sRNAs between all groups and time points. Hence, this was observed in the general sRNA distribution—including the mock infected cells, most likely due to the persistent CYV infection (Figure 1)—and in the distribution of ISFV-specific sRNAs (Figures 3 and 5). The LamV-infected cells had proportions of between 32.2 and 36.7% of vsiRNAs, and the HakV-infected cells had slightly higher proportions of between 48.4 and 66.5%. The vsiRNAs from LamV-infected cells mapped along the whole genome, with no particular coldspots but one predominant hotspot that correspond to the NS4AB proteins (Figure S1). We also observed that most of the vsiRNAs mapped to the sense strand of the genome, which could be a strategy for the efficient restriction of virus replication. The vsiRNAs of HakV-infected cells also mapped to the whole genome, with a slightly higher coverage at the 3' end (7840–10,158 nt) corresponding to the gene coding for the NS5 protein (Figure S1). The strand polarity distribution was close to even, with slightly more vsiRNAs mapping to the sense strand. Although the siRNA response is regarded as the main antiviral immune response, it has also been postulated that siRNA is necessary for a persistent viral infection in mosquitoes [43,44]. The hypothesis behind this is that the siRNA response keeps the viral load in the host cell at a tolerable level, thereby sustaining a persistent infection. Many of the ISVs have been shown to not only persistently infect mosquitoes but also vertically transmit from mother to offspring [2–4]. Our data showed that the mosquito U4.4 cell line is able to elicit a strong virus-specific siRNA response to the studied ISFVs, which could support lifelong infection in mosquitoes.

In the LamV-infected cells, we observed a hotspot positioned in the 3'-UTR with a coverage of 900 reads, mainly at the size of 39 nt. These reads mainly consisted of the same sequence (5'GGGAGTCAGGCCTAAATGCCACCGGATGATAGTAGACGG), suggesting that the reads were not degraded products (Figure 4e). The BLASTn search of the consensus sequence showed that this sequence could also be found in the 3'-UTR of another ISFV named Chaoyang virus (NC 017086), indicating that it may be a conserved sequence that can exist in the UTR of other ISFVs as well. However, the origin, function, and biogenesis of these 39 nt reads are uncertain.

Apart from the detection of vsiRNAs, putative vpiRNAs were identified in the LamV-infected cells. Earlier studies in an *Aedes aegypti* cell line have shown that the production of ping-pong-dependent vpiRNA relies on the PIWI-5 and Ago-3 proteins. The knockdown of either of these proteins in the Aag2 cell line infected with Sindbis virus or DENV-2 showed a massive decrease in vpiRNAs [27,45]. The ping-pong amplification of piRNAs is a two-step amplification mechanism where the PIWI-5 protein, loaded with a primary piRNA, cleaves a complementary target RNA. The 3' cleavage product is transferred to the protein Ago-3 and used as a template to cleave a complementary target RNA. This generates a new piRNA precursor for the Piwi-5 protein, which gives rise to the same primary piRNA sequence that initiated the amplification. Therefore, this type of amplification predicts an even distribution of piRNAs derived from both strands [27,46].

In the data from our U4.4 cells infected with LamV, we did not observe equal amounts of vpiRNA from both strands. The majority of the putative vpiRNAs (26–30 nt) were derived from the antisense strand, with the ping-pong characteristic nucleotide bias of an U at the first position. However, the few putative vpiRNAs derived from the sense strand did not show the nucleotide bias of an A in the tenth position characteristic for Ago-3 bound piRNA. Moreover, because of the unequal strand distribution, we could not analyze the overlap probability and look for the 10 nt overlap, which is significant for ping-pong-amplified piRNA (Figures 3 and 4 and Figure S2). Similar observations have been made in studies where U4.4 cells were infected with WNV [42] and where Aag2 cells were infected with ZIKV [47]. In these studies, reads in the size range of 25–30 nt mainly mapped to the sense strand but with no 1U bias. These observations suggest that the identified putative LamV vpiRNAs are not ping-pong-dependent, and we hypothesize that they could be primary vpiRNAs cleaved by an ortholog to the zucchini proteins in *Drosophila* or some unknown endonuclease using either exogenous viral RNA or pre-primary RNA transcribed from viral-derived cDNA (vDNA) [30,48]. Further evaluation is needed to understand their function and biogenesis, as well as whether they interact with any of the PIWI proteins. Surprisingly, U4.4 cells infected with HakV did not elicit any production of these putative vpiRNAs (Figure 5), which suggests that the production of vpiRNAs is virus-dependent. HakV belongs to the group of classical ISFVs that are very distinct from all known flaviviruses [7]. It would be interesting to further investigate whether other viruses in the classical ISFV group show similar results, which could reveal factors important for putative vpiRNA production. We speculate that virus-specific sequence elements or structures trigger the production of vpiRNAs by an unknown Piwi-dependent amplification mechanism.

5. Conclusions

In conclusion, we showed that two ISFVs from two distinct phylogenetic groups can trigger the RNAi response during an acute infection of the *Aedes albopictus* U4.4 cell line. Both viruses elicited a strong vsiRNA response that increased over time and targeted the whole viral genome. Furthermore, infection with LamV (which is closely related to the pathogenic dual-host flaviviruses) triggered the production of putative primary piRNAs, while infection with HakV, which is more distantly related, did not. This suggests that the mosquito piRNA pathway is virus-specific and might need specific sequence elements or structures. These results contribute to our understanding of mosquito antiviral immunity, small RNA machineries, and how ISVs affect mosquitoes.

Supplementary Materials: The following are available online at <https://www.mdpi.com/article/10.3390/v13112181/s1>: Figure S1: Mapping of viral siRNA 72 h after ISFVs infection; Figure S2: Distribution of virus-derived piRNAs 72 h after LamV infection.

Author Contributions: P.Ö., J.H., J.C.H. and A.-L.B. conceived and designed the experiments; P.Ö. performed the experiments; P.Ö., J.H. and A.-L.B. analyzed the data; P.Ö. wrote and prepared the original draft; J.H., J.C.H. and A.-L.B. reviewed and edited the manuscript. All authors have read and agreed to the published version of the manuscript.

Funding: This study was supported by the Swedish research Council VR (2016-01251), the Swedish University of Agricultural Sciences (SLU), the Vice-chancellor junior career grant awarded to A.L.B., and the Kungl. Skogs- och Lantbruksakademien (GFS2016-0033).

Data Availability Statement: All sequencing data have been made publicly available at the NCBI Sequence Read Archive (SRA) under accession number PRJNA761074.

Acknowledgments: The authors would like to acknowledge the support of the National Genomics Infrastructure in Stockholm funded by Science for Life Laboratory, the Knut and Alice Wallenberg Foundation, the Swedish Research Council, and the SNIC/Uppsala Multidisciplinary Center for Advanced Computational Science for assistance with massively parallel sequencing and access to the UPPMAX computational infrastructure. The SNIC through Uppsala Multidisciplinary Center for Advanced Computational Science (UPPMAX) under project SNIC 2017/7-290 is acknowledged for providing computational resources. This publication was supported by the European Virus Archive goes Global (EVAg) project, which has received funding from the European Union's Horizon 2020 research and innovation program under grant agreement No 653316.

Conflicts of Interest: The authors declare no conflict of interest.

References

- Nasar, F.; Gorchakov, R.V.; Tesh, R.B.; Weaver, S.C. Eilat virus host range restriction is present at multiple levels of the virus life cycle. *J. Virol.* **2015**, *89*, 1404–1418. [[CrossRef](#)]
- Saiyasombat, R.; Bolling, B.G.; Brault, A.C.; Bartholomay, L.C.; Blitvich, B.J. Evidence of efficient transovarial transmission of *Culex flavivirus* by *Culex pipiens* (Diptera: Culicidae). *J. Med. Entomol.* **2011**, *48*, 1031–1038. [[CrossRef](#)]
- Bolling, B.G.; Eisen, L.; Moore, C.G.; Blair, C.D. Insect-specific flaviviruses from *Culex* mosquitoes in Colorado, with evidence of vertical transmission. *Am. J. Trop. Med. Hyg.* **2011**, *85*, 169–177. [[CrossRef](#)]
- Haddow, A.D.; Guzman, H.; Popov, V.L.; Wood, T.G.; Widen, S.G.; Haddow, A.D.; Tesh, R.B.; Weaver, S.C. First isolation of *Aedes flavivirus* in the Western Hemisphere and evidence of vertical transmission in the mosquito *Aedes* (*Stegomyia*) *albopictus* (Diptera: Culicidae). *Virology* **2013**, *440*, 134–139. [[CrossRef](#)] [[PubMed](#)]
- Marklewitz, M.; Zirkel, F.; Kurth, A.; Drosten, C.; Junglen, S. Evolutionary and phenotypic analysis of live virus isolates suggests arthropod origin of a pathogenic RNA virus family. *Proc. Natl. Acad. Sci. USA* **2015**, *112*, 7536–7541. [[CrossRef](#)]
- Li, C.X.; Shi, M.; Tian, J.H.; Lin, X.D.; Kang, Y.J.; Chen, L.J.; Qin, X.C.; Xu, J.; Holmes, E.C.; Zhang, Y.Z. Unprecedented genomic diversity of RNA viruses in arthropods reveals the ancestry of negative-sense RNA viruses. *eLife* **2015**, *4*. [[CrossRef](#)]
- Blitvich, B.J.; Firth, A.E. Insect-specific flaviviruses: A systematic review of their discovery, host range, mode of transmission, superinfection exclusion potential and genomic organization. *Viruses* **2015**, *7*, 1927–1959. [[CrossRef](#)] [[PubMed](#)]
- Huhtamo, E.; Putkuri, N.; Kurkela, S.; Manni, T.; Vaehri, A.; Vapalahti, O.; Uzcategui, N.Y. Characterization of a novel flavivirus from mosquitoes in northern Europe that is related to mosquito-borne flaviviruses of the tropics. *J. Virol.* **2009**, *83*, 9532–9540. [[CrossRef](#)]
- Calzolari, M.; Ze-Ze, L.; Ruzek, D.; Vazquez, A.; Jeffries, C.; Defilippo, F.; Osorio, H.C.; Kilian, P.; Ruiz, S.; Fooks, A.R.; et al. Detection of mosquito-only flaviviruses in Europe. *J. Gen. Virol.* **2012**, *93*, 1215–1225. [[CrossRef](#)]
- Blair, C.D. Mosquito RNAi is the major innate immune pathway controlling arbovirus infection and transmission. *Future Microbiol.* **2011**, *6*, 265–277. [[CrossRef](#)] [[PubMed](#)]
- Galiana-Arnoux, D.; Dostert, C.; Schneemann, A.; Hoffmann, J.A.; Imler, J.L. Essential function in vivo for Dicer-2 in host defense against RNA viruses in drosophila. *Nat. Immunol.* **2006**, *7*, 590–597. [[CrossRef](#)]
- Matranga, C.; Tomari, Y.; Shin, C.; Bartel, D.P.; Zamore, P.D. Passenger-strand cleavage facilitates assembly of siRNA into Ago2-containing RNAi enzyme complexes. *Cell* **2005**, *123*, 607–620. [[CrossRef](#)] [[PubMed](#)]
- Rand, T.A.; Petersen, S.; Du, F.; Wang, X. Argonaute2 cleaves the anti-guide strand of siRNA during RISC activation. *Cell* **2005**, *123*, 621–629. [[CrossRef](#)] [[PubMed](#)]
- Campbell, C.L.; Keene, K.M.; Brackney, D.E.; Olson, K.E.; Blair, C.D.; Wilusz, J.; Foy, B.D. *Aedes aegypti* uses RNA interference in defense against Sindbis virus infection. *BMC Microbiol.* **2008**, *8*, 47. [[CrossRef](#)]
- Sanchez-Vargas, I.; Scott, J.C.; Poole-Smith, B.K.; Franz, A.W.; Barbosa-Solomieu, V.; Wilusz, J.; Olson, K.E.; Blair, C.D. Dengue virus type 2 infections of *Aedes aegypti* are modulated by the mosquito's RNA interference pathway. *PLoS Pathog* **2009**, *5*, e1000299. [[CrossRef](#)] [[PubMed](#)]
- Keene, K.M.; Foy, B.D.; Sanchez-Vargas, I.; Beaty, B.J.; Blair, C.D.; Olson, K.E. RNA interference acts as a natural antiviral response to O'nyong-nyong virus (Alphavirus; Togaviridae) infection of *Anopheles gambiae*. *Proc. Natl. Acad. Sci. USA* **2004**, *101*, 17240–17245. [[CrossRef](#)]
- Franz, A.W.; Sanchez-Vargas, I.; Adelman, Z.N.; Blair, C.D.; Beaty, B.J.; James, A.A.; Olson, K.E. Engineering RNA interference-based resistance to dengue virus type 2 in genetically modified *Aedes aegypti*. *Proc. Natl. Acad. Sci. USA* **2006**, *103*, 4198–4203. [[CrossRef](#)]

18. Brackney, D.E.; Beane, J.E.; Ebel, G.D. RNAi targeting of West Nile virus in mosquito midguts promotes virus diversification. *PLoS Pathog.* **2009**, *5*, e1000502. [[CrossRef](#)]
19. Lee, Y.S.; Nakahara, K.; Pham, J.W.; Kim, K.; He, Z.; Sontheimer, E.J.; Carthew, R.W. Distinct roles for Drosophila Dicer-1 and Dicer-2 in the siRNA/miRNA silencing pathways. *Cell* **2004**, *117*, 69–81. [[CrossRef](#)]
20. Puthiyakunnon, S.; Yao, Y.; Li, Y.; Gu, J.; Peng, H.; Chen, X. Functional characterization of three MicroRNAs of the Asian tiger mosquito, *Aedes albopictus*. *Parasit Vectors* **2013**, *6*, 230. [[CrossRef](#)]
21. Slonchak, A.; Hussain, M.; Torres, S.; Asgari, S.; Khromykh, A.A. Expression of mosquito microRNA Aae-miR-2940-5p is downregulated in response to West Nile virus infection to restrict viral replication. *J. Virol.* **2014**, *88*, 8457–8467. [[CrossRef](#)] [[PubMed](#)]
22. Saldana, M.A.; Etebari, K.; Hart, C.E.; Widen, S.G.; Wood, T.G.; Thangamani, S.; Asgari, S.; Hughes, G.L. Zika virus alters the microRNA expression profile and elicits an RNAi response in *Aedes aegypti* mosquitoes. *PLoS Negl. Trop. Dis.* **2017**, *11*, e0005760. [[CrossRef](#)] [[PubMed](#)]
23. Campbell, C.L.; Harrison, T.; Hess, A.M.; Ebel, G.D. MicroRNA levels are modulated in *Aedes aegypti* after exposure to Dengue-2. *Insect Mol. Biol.* **2014**, *23*, 132–139. [[CrossRef](#)]
24. Skalsky, R.L.; Vanlandingham, D.L.; Scholle, F.; Higgs, S.; Cullen, B.R. Identification of microRNAs expressed in two mosquito vectors, *Aedes albopictus* and *Culex quinquefasciatus*. *BMC Genom.* **2010**, *11*, 119. [[CrossRef](#)] [[PubMed](#)]
25. Rozhkov, N.V.; Hammell, M.; Hannon, G.J. Multiple roles for Piwi in silencing Drosophila transposons. *Genes Dev.* **2013**, *27*, 400–412. [[CrossRef](#)] [[PubMed](#)]
26. Marconcini, M.; Hernandez, L.; Iovino, G.; Houe, V.; Valerio, F.; Palatini, U.; Pischedda, E.; Crawford, J.E.; White, B.J.; Lin, T.; et al. Polymorphism analyses and protein modelling inform on functional specialization of Piwi clade genes in the arboviral vector *Aedes albopictus*. *PLoS Negl. Trop. Dis.* **2019**, *13*, e0007919. [[CrossRef](#)]
27. Miesen, P.; Girardi, E.; van Rij, R.P. Distinct sets of PIWI proteins produce arbovirus and transposon-derived piRNAs in *Aedes aegypti* mosquito cells. *Nucleic Acids Res.* **2015**, *43*, 6545–6556. [[CrossRef](#)] [[PubMed](#)]
28. Schnettler, E.; Donald, C.L.; Human, S.; Watson, M.; Siu, R.W.C.; McFarlane, M.; Fazakerley, J.K.; Kohl, A.; Fragkoudis, R. Knockdown of piRNA pathway proteins results in enhanced Semliki Forest virus production in mosquito cells. *J. Gen. Virol.* **2013**, *94*, 1680–1689. [[CrossRef](#)] [[PubMed](#)]
29. Varjak, M.; Maringer, K.; Watson, M.; Sreenu, V.B.; Fredericks, A.C.; Pondeville, E.; Donald, C.L.; Sterk, J.; Kean, J.; Vazeille, M.; et al. *Aedes aegypti* Piwi4 Is a Noncanonical PIWI Protein Involved in Antiviral Responses. *mSphere* **2017**, *2*, e00144-17. [[CrossRef](#)]
30. Tassetto, M.; Kunitomi, M.; Whitfield, Z.J.; Dolan, P.T.; Sanchez-Vargas, I.; Garcia-Knight, M.; Ribiero, I.; Chen, T.; Olson, K.E.; Andino, R. Control of RNA viruses in mosquito cells through the acquisition of vDNA and endogenous viral elements. *eLife* **2019**, *8*, e41244. [[CrossRef](#)]
31. Rozen, S.; Skaletsky, H. Primer3 on the WWW for general users and for biologist programmers. *Methods Mol. Biol.* **2000**, *132*, 365–386.
32. Langmead, B.; Trapnell, C.; Pop, M.; Salzberg, S.L. Ultrafast and memory-efficient alignment of short DNA sequences to the human genome. *Genome Biol.* **2009**, *10*, R25. [[CrossRef](#)]
33. Seguin, J.; Otten, P.; Baerlocher, L.; Farinelli, L.; Pooggin, M.M. MISIS-2: A bioinformatics tool for in-depth analysis of small RNAs and representation of consensus master genome in viral quasispecies. *J. Virol. Methods* **2016**, *233*, 37–40. [[CrossRef](#)]
34. Crooks, G.E.; Hon, G.; Chandonia, J.M.; Brenner, S.E. WebLogo: A sequence logo generator. *Genome Res.* **2004**, *14*, 1188–1190. [[CrossRef](#)] [[PubMed](#)]
35. Leger, P.; Lara, E.; Jagla, B.; Sismeiro, O.; Mansuroglu, Z.; Coppee, J.Y.; Bonnefoy, E.; Bouloy, M. Dicer-2- and Piwi-mediated RNA interference in Rift Valley fever virus-infected mosquito cells. *J. Virol.* **2013**, *87*, 1631–1648. [[CrossRef](#)] [[PubMed](#)]
36. Morazzani, E.M.; Wiley, M.R.; Murreddu, M.G.; Adelman, Z.N.; Myles, K.M. Production of virus-derived ping-pong-dependent piRNA-like small RNAs in the mosquito soma. *PLoS Pathog.* **2012**, *8*, e1002470. [[CrossRef](#)]
37. Siu, R.W.; Fragkoudis, R.; Simmonds, P.; Donald, C.L.; Chase-Topping, M.E.; Barry, G.; Attarzadeh-Yazdi, G.; Rodriguez-Andres, J.; Nash, A.A.; Merits, A.; et al. Antiviral RNA interference responses induced by Semliki Forest virus infection of mosquito cells: Characterization, origin, and frequency-dependent functions of virus-derived small interfering RNAs. *J. Virol.* **2011**, *85*, 2907–2917. [[CrossRef](#)]
38. Hess, A.M.; Prasad, A.N.; Pitsyn, A.; Ebel, G.D.; Olson, K.E.; Barbacioru, C.; Monighetti, C.; Campbell, C.L. Small RNA profiling of Dengue virus-mosquito interactions implicates the PIWI RNA pathway in anti-viral defense. *BMC Microbiol.* **2011**, *11*, 45. [[CrossRef](#)]
39. Myles, K.M.; Morazzani, E.M.; Adelman, Z.N. Origins of alphavirus-derived small RNAs in mosquitoes. *RNA Biol.* **2009**, *6*, 387–391. [[CrossRef](#)] [[PubMed](#)]
40. Dietrich, I.; Shi, X.; McFarlane, M.; Watson, M.; Blomstrom, A.L.; Skelton, J.K.; Kohl, A.; Elliott, R.M.; Schnettler, E. The Antiviral RNAi Response in Vector and Non-vector Cells against Orthobunyaviruses. *PLoS Negl. Trop. Dis.* **2017**, *11*, e0005272. [[CrossRef](#)] [[PubMed](#)]
41. Ma, Q.; Srivastav, S.P.; Gamez, S.; Dayama, G.; Feitosa-Suntheimer, F.; Patterson, E.I.; Johnson, R.M.; Matson, E.M.; Gold, A.S.; Brackney, D.E.; et al. A mosquito small RNA genomics resource reveals dynamic evolution and host responses to viruses and transposons. *Genome Res.* **2021**, *31*, 512–528. [[CrossRef](#)]

42. Goertz, G.P.; Miesen, P.; Overheul, G.J.; van Rij, R.P.; van Oers, M.M.; Pijlman, G.P. Mosquito Small RNA Responses to West Nile and Insect-Specific Virus Infections in *Aedes* and *Culex* Mosquito Cells. *Viruses* **2019**, *11*, 271. [[CrossRef](#)] [[PubMed](#)]
43. Goic, B.; Stapleford, K.A.; Frangeul, L.; Doucet, A.J.; Gausson, V.; Blanc, H.; Schemmel-Jofre, N.; Cristofari, G.; Lambrechts, L.; Vignuzzi, M.; et al. Virus-derived DNA drives mosquito vector tolerance to arboviral infection. *Nat. Commun.* **2016**, *7*, 12410. [[CrossRef](#)] [[PubMed](#)]
44. Poirier, E.Z.; Goic, B.; Tome-Poderti, L.; Frangeul, L.; Boussier, J.; Gausson, V.; Blanc, H.; Vallet, T.; Loyd, H.; Levi, L.I.; et al. Dicer-2-Dependent Generation of Viral DNA from Defective Genomes of RNA Viruses Modulates Antiviral Immunity in Insects. *Cell Host Microbe* **2018**, *23*, 353–365 e8. [[CrossRef](#)]
45. Miesen, P.; Ivens, A.; Buck, A.H.; van Rij, R.P. Small RNA Profiling in Dengue Virus 2-Infected *Aedes* Mosquito Cells Reveals Viral piRNAs and Novel Host miRNAs. *PLoS Negl. Trop. Dis.* **2016**, *10*, e0004452. [[CrossRef](#)] [[PubMed](#)]
46. Brennecke, J.; Aravin, A.A.; Stark, A.; Dus, M.; Kellis, M.; Sachidanandam, R.; Hannon, G.J. Discrete small RNA-generating loci as master regulators of transposon activity in *Drosophila*. *Cell* **2007**, *128*, 1089–1103. [[CrossRef](#)]
47. Varjak, M.; Donald, C.L.; Mottram, T.J.; Sreenu, V.B.; Merits, A.; Maringer, K.; Schnettler, E.; Kohl, A. Characterization of the Zika virus induced small RNA response in *Aedes aegypti* cells. *PLoS Negl. Trop. Dis.* **2017**, *11*, e0006010. [[CrossRef](#)]
48. Mohn, F.; Handler, D.; Brennecke, J. Noncoding RNA. piRNA-guided slicing specifies transcripts for Zucchini-dependent, phased piRNA biogenesis. *Science* **2015**, *348*, 812–817. [[CrossRef](#)]

Supplementary Material

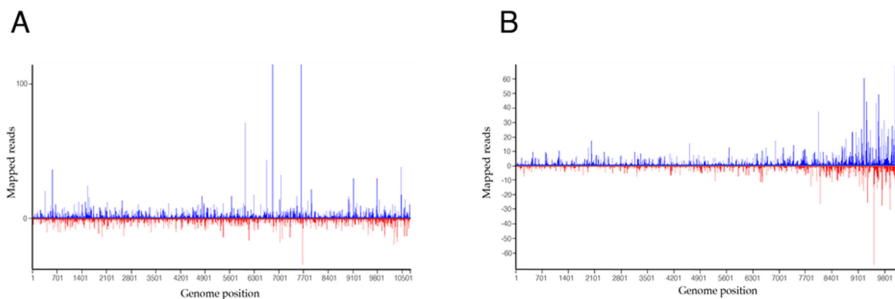


Figure S1. Mapping of viral siRNA at 72 h after ISFVs infection. (A) Distribution of 21 nt long reads to the LamV genome; (B) distribution of 21 nt-long reads to the HakV genome. The positive values are counts of vsRNAs mapped to the sense strand, and the negative values are those mapped to the antisense strand.

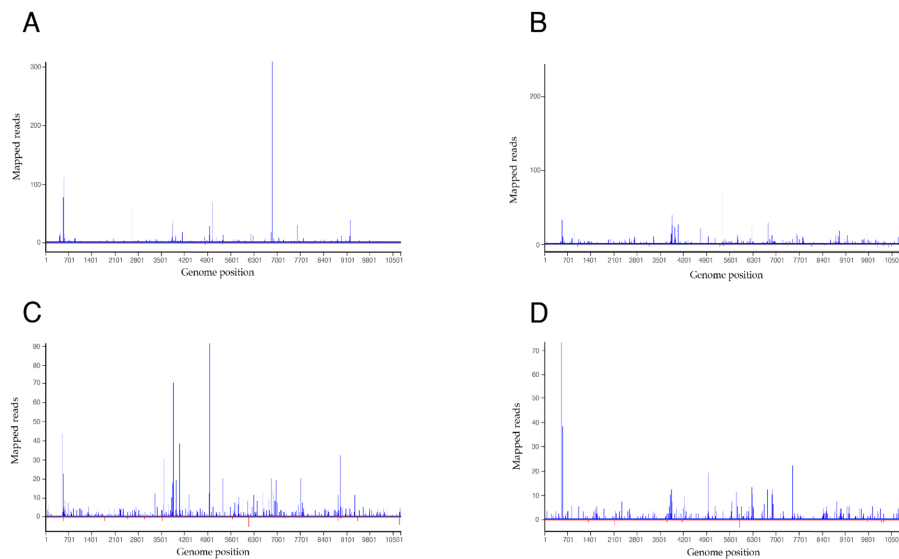


Figure S2. Distribution of virus-derived piRNAs of U4.4 cells at 72 h after LamV infection. (A) vpi-like RNA of 27 nt, (B) vpi-like RNA of 28 nt, (C) vpi-like RNA of 29 nt, and (D) vpi-like RNA of 30 nt. The positive values are counts of vpi-like RNAs mapped to the sense strand, and the negative values are those mapped to the antisense strand.



Article

Transcriptome Analysis of an *Aedes albopictus* Cell Line Single- and Dual-Infected with Lammi Virus and WNV

Pontus Öhlund ^{1,*}, Nicolas Delhomme ², Juliette Hayer ^{3,4}, Jenny C. Hesson ⁵ and Anne-Lie Blomström ¹

- ¹ Department of Biomedical Sciences and Veterinary Public Health, Swedish University of Agricultural Sciences, Box 7028, 750 07 Uppsala, Sweden; anne-lie.blomstrom@slu.se
 - ² Umeå Plant Science Centre (UPSC), Department of Forest Genetics and Plant Physiology, Swedish University of Agricultural Sciences, 901 83 Umeå, Sweden; nicolas.delhomme@slu.se
 - ³ MIVEGEC, IRD, CNRS, University of Montpellier, 34394 Montpellier, France; juliette.hayer@ird.fr
 - ⁴ SLU-Global Bioinformatics Centre, Department of Animal Breeding and Genetics, Swedish University of Agricultural Sciences, Box 7023, 750 07 Uppsala, Sweden
 - ⁵ Department of Medical Biochemistry and Microbiology / Zoonosis Science Center, Uppsala University, Box 582, 751 23 Uppsala, Sweden; jenny.hesson@imbim.uu.se
- * Correspondence: pontus.ohlund@slu.se; Tel.: +46-18-672-409



Citation: Öhlund, P.; Delhomme, N.; Hayer, J.; Hesson, J.C.; Blomström, A.-L. Transcriptome Analysis of an *Aedes albopictus* Cell Line Single- and Dual-Infected with Lammi Virus and WNV. *Int. J. Mol. Sci.* **2022**, *23*, 875. <https://doi.org/10.3390/ijms23020875>

Academic Editor: Hartmut Schlüter

Received: 16 December 2021

Accepted: 12 January 2022

Published: 14 January 2022

Publisher's Note: MDPI stays neutral with regard to jurisdictional claims in published maps and institutional affiliations.



Copyright: © 2022 by the authors. Licensee MDPI, Basel, Switzerland. This article is an open access article distributed under the terms and conditions of the Creative Commons Attribution (CC BY) license (<https://creativecommons.org/licenses/by/4.0/>).

Abstract: Understanding the flavivirus infection process in mosquito hosts is important and fundamental in the search for novel control strategies that target the mosquitoes' ability to carry and transmit pathogenic arboviruses. A group of viruses known as insect-specific viruses (ISVs) has been shown to interfere with the infection and replication of a secondary arbovirus infection in mosquitoes and mosquito-derived cell lines. However, the molecular mechanisms behind this interference are unknown. Therefore, in the present study, we infected the *Aedes albopictus* cell line U4.4 with either the West Nile virus (WNV), the insect-specific Lammi virus (LamV) or an infection scheme whereby cells were pre-infected with LamV 24 h prior to WNV challenge. The qPCR analysis showed that the dual-infected U4.4 cells had a reduced number of WNV RNA copies compared to WNV-only infected cells. The transcriptome profiles of the different infection groups showed a variety of genes with altered expression. WNV-infected cells had an up-regulation of a broad range of immune-related genes, while in LamV-infected cells, many genes related to stress, such as different heat-shock proteins, were up-regulated. The transcriptome profile of the dual-infected cells was a mix of up- and down-regulated genes triggered by both viruses. Furthermore, we observed an up-regulation of signal peptidase complex (SPC) proteins in all infection groups. These SPC proteins have shown importance for flavivirus assembly and secretion and could be potential targets for gene modification in strategies for the interruption of flavivirus transmission by mosquitoes.

Keywords: insect-specific flaviviruses; West Nile virus; *Aedes albopictus*; transcriptome; viral interference

1. Introduction

Mosquitoes serve as vectors for many viral pathogens, and their associated diseases cause a major health burden across the globe. Flaviviruses, such as the West Nile virus (WNV), Dengue virus (DENV) and Zika virus (ZIKV), impose huge burdens on human and animal health [1–3]. For many of these arboviruses, there are no preventive vaccines or therapeutic drugs available and the reduction in transmission relies on traditional methods, e.g., suppressing mosquito populations with insecticides [4]. However, this is very cumbersome and costly, and, with the increase in insecticide resistance, these strategies are becoming less effective [5]. Novel control strategies are needed and the development of transgenic mosquitoes for either population suppression or population replacement with reduced vector competence (the ability of a mosquito to carry and transmit a virus) are among the proposed methods [6,7]. However, to find gene modification targets that interfere with the transmission of viral pathogens, we must first study the mechanisms that contribute to vector competence and viral dissemination in the mosquito vector.

Most mosquito-borne viruses persist in nature through transmission cycles between the mosquito and a vertebrate reservoir [8]. Once the mosquito has taken up the virus through a blood meal and has subsequently been infected, the innate antiviral immune response mounts an array of molecular signaling pathways and immune effector proteins to control the infection. Mosquitoes lack an adaptive immunity, and the main immune pathways are thought to be the RNA interference (RNAi) pathway, the toll pathway, the immune deficiency (Imd) pathway and the Janus kinase-signal transducer (JAK/STAT) pathway [9–11]. The RNAi pathway generates small RNAs from viral double-stranded RNA which are used as template to target and degenerate complementary viral RNA, therefore inhibiting viral replication [12]. The other three are signaling pathways activated upon recognition of pathogen-associated molecular patterns (PAMPs) by pattern-recognition receptors (PRRs), which trigger a signaling cascade leading to the production of effector proteins such as antimicrobial peptides (AMPs) [13]. There are several PRRs in mosquitoes, including peptidoglycan-recognition protein, fibrinogen-related proteins, scavenger receptors and C-type lectins. PRRs play important roles by binding invading pathogens and mediating immune responses, such as melanization and phagocytosis [14,15]. AMPs are potent immune-effectors with antimicrobial activities and consist of several classes, such as defensins, cecropins, gambicin, dipterin and attacins, categorized based on their structure, function and specificity [16–20]. Other important immune proteins in insects are the serine proteases, such as the CLIP proteases; these are present in the hemolymph and act in cascade pathways initiated by different stimuli, such as PAMPs. Activated CLIP-C cleaves and activates CLIP-B, which, in turn, cleaves and activates the toll-ligand Spätzle or prophenoloxidase, which is required for the melanization response [21].

Gene expression profiling in response to arbovirus infection in mosquitoes and mosquito-derived cell lines has revealed not only the alteration of immune-related genes, but also biological processes, such as metabolic pathways, stress, translation and more. Transcriptomics studies have been conducted to investigate the response for major arboviruses such as WNV, ZIKV, DENV and Chikungunya virus (CHIKV) [22–28]. However, mosquitoes are often naturally and persistently infected with a group of viruses that are known as insect-specific viruses (ISVs) [29]. This group of viruses is unable to infect vertebrates and are maintained in the mosquito population through vertical transmission, from mother to offspring [30–33]. ISVs are interesting for several reasons; one is that many of these viruses are thought to be ancestors to the pathogenic arboviruses [34]. Another reason is that a primary infection of certain ISVs can block or interfere with a secondary infection of a pathogenic arbovirus. The insect-specific Palm Creek virus has been shown to reduce infection and replication of WNV [35,36], while similar results were observed with the insect-specific Nhumirim virus [37,38]. The Lammi virus (LamV) is an insect-specific flavivirus (ISFV) that was first isolated from *Aedes cinereus* mosquitoes in Finland [39]. LamV is phylogenetically affiliated with the medically important dual-host flaviviruses, but presents the insect-restriction phenotype and is referred to as dual-host affiliated ISFV [40]. Recently, we have shown that LamV induces a strong small RNA response in the *Aedes albopictus* cell line U4.4 [41].

In the present study, we analyzed the transcriptomic data of *Ae. albopictus* cells infected with either WNV, insect-specific LamV or an infection scheme whereby cells were pre-infected with LamV prior to challenge with WNV. Our aim is to improve the understanding of the ISFV interaction and its effects on the host. Furthermore, we investigated the possible interfering effects of a prior LamV infection on WNV replication.

2. Results

RNA-sequencing was conducted on poly(A)-enriched RNA extracted from the *Ae. albopictus* cell line U4.4 infected with either WNV, insect-specific LamV or an infection scheme whereby cells were pre-infected with LamV 24 h before being challenged with WNV. Cells from the different infection groups, including mock-infected cells, were collected between 24 and 72 hpi as biological triplicates. A total of 30 RNA-seq libraries were created,

generating between 31.1 and 50.9 million paired-end reads per sample. The data were of good quality and the samples clustered as expected when analyzed with a principal component analysis (PCA) (Figure S1).

2.1. qPCR Results of Supernatant

To investigate the possible interfering effect of LamV on WNV replication, RNA from the supernatant was used to follow the infection over time (Figure 1). The results show that the level of LamV RNA copies were similar between cells infected only with LamV and cells challenged with WNV (Figure 1A). However, the level of WNV RNA copies were significantly lower in those cells pre-infected with LamV than in cells infected with WNV only (Figure 1B). The statistical significance differences were calculated using Student's *t*-test.

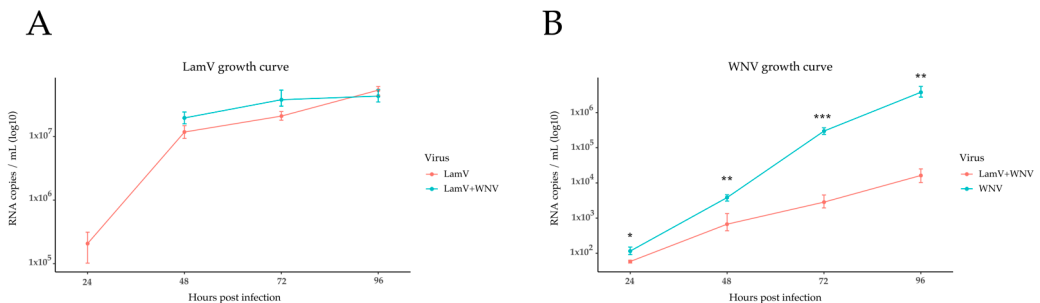


Figure 1. Growth curves of LamV and WNV in U4.4 cells, shown as RNA copies/mL over time. **(A)** LamV growth curve. **(B)** WNV growth curve. Dots show the mean RNA copy number per mL with a standard deviation among the biological replicates. * $p < 0.05$, ** $p < 0.01$, *** $p < 0.001$.

2.2. Transcripts Differentially Expressed (DE) in LamV-Infected U4.4 Cells

The analysis and comparison of mRNA expression profiles of *Ae. albopictus* U4.4 cells at different time points following LamV infection revealed that 13 (13 up-regulated), 102 (84 up- and 18 down-regulated) and 359 (180 up- and 179 down-regulated) transcripts were significantly differentially expressed (DE) at 24 h, 48 h and 72 hpi, respectively. The comparison of the transcriptome profiles showed two overlapping transcripts among all time points, both coding for the 40S ribosomal protein S21—AALF005471 (7.08–11.38-fold change) and AALF002626 (8–10.94-fold change) (Figure 2 and Table S1). Among the 56 overlapping transcripts between the two later time points (Figure 2 and Table S1), we observed an up-regulation of genes related to protein processes in the endoplasmic reticulum (ER), such as BiP/GRP78 (AALF021835), lethal(2) essential for life protein (AALF005663 and AALF015016), endoplasmic (AALF011939) and Signal peptidase complex subunit 3 (AALF003192). Among the down-regulated transcripts, we observed genes related to DNA replication, such as three DNA helicases (AALF015599, AALF022735 and AALF020651), and DNA replication licensing factor MCM7 (AALF006549). The GO enrichment analysis for biological processes resulted in three, five and ten GO slim terms for the up-regulated transcripts at 24 hpi, 48 hpi and 72 hpi, while the down-regulated transcripts at 48 hpi and 72 hpi resulted in five and eight GO slim terms (Figure 3).

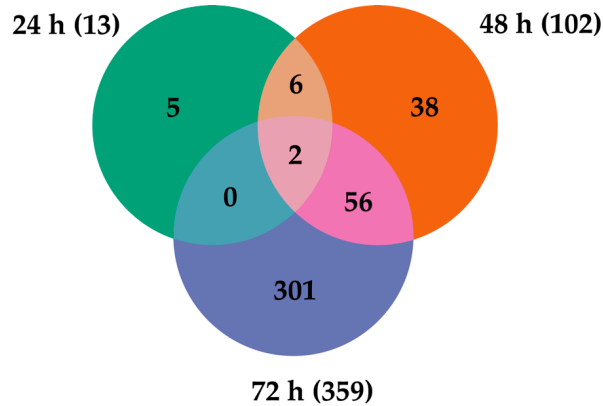


Figure 2. Venn diagram representing the number of differentially expressed transcripts at the different time points post-infection with LamV.

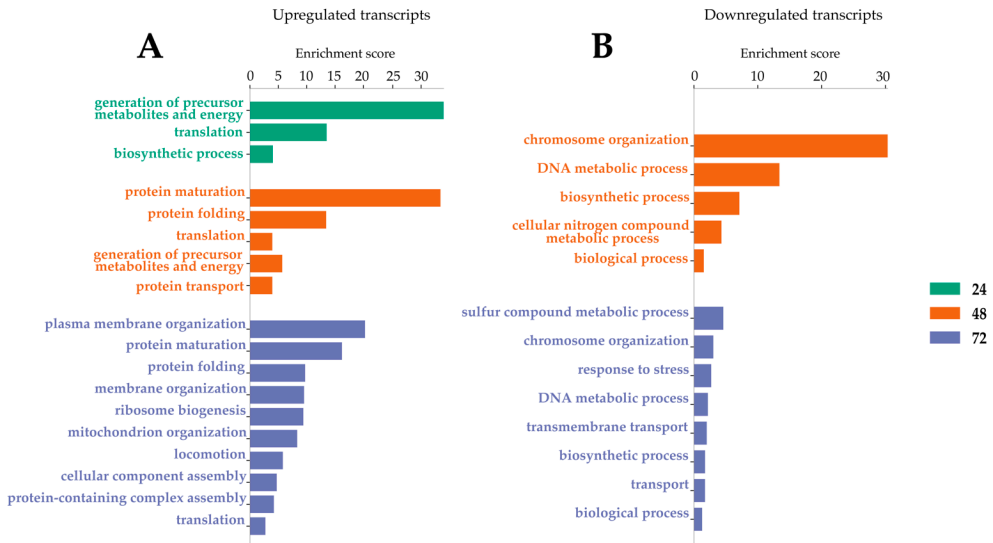


Figure 3. Gene ontology enrichment analysis for biological processes after LamV infection. (A) GO slim terms for up-regulated transcripts. (B) GO slim terms for down-regulated transcripts.

2.3. Transcripts Differentially Expressed in WNV-Infected U4.4 Cells

When comparing WNV-infected U4.4 cells to mock controls, there were 108 (65 up- and 43 down-regulated) and 138 (85 up- and 53 down-regulated) transcripts that were significantly DE at 24 hpi and 48 hpi. The comparison of the transcriptome profiles showed 23 overlapping transcripts that were DE at both time points (Figure 4). Among these transcripts, many of the up-regulated genes were related to immune activity, such as C-type lectin (AALF016234), clip-domain serine protease family B (AALF019859), Defensin (AALF008821) and peptidoglycan-recognition protein (AALF020799) (Table 1 and Table S2). The GO enrichment analysis for biological processes of the up- and down-regulated genes

at 24 hpi and 48 hpi revealed six different GO slim terms for the up-regulated genes and one and seven GO slim terms for the down-regulated transcripts (Figure 5).

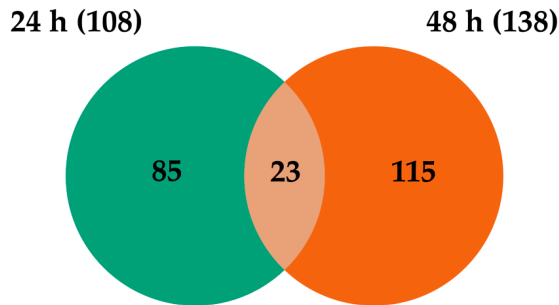


Figure 4. Venn diagram representing the number of differentially expressed transcripts at the different time points post-infection with WNV.

Table 1. List of *Ae. albopictus* overlapping differentially expressed transcripts following WNV infection. Functional categories are based on GO terms for biological processes. The cut-offs used were *p*-adjusted value of ≤ 0.01 and \log_2 FC of ≥ 0.5 .

Transcript ID	Functional Categories	Gene Description	Fold Change 24 hpi	Fold Change 48 hpi
AALF016234	Immune response	C-type lectin	82.89	17.75
AALF013298		Unspecified product	69.1	14.16
AALF003774	Immune response	Fibrinogen and fibronectin	52.23	18.48
AALF019859	Immune response	Clip-Domain Serine Protease family B	49.51	9.26
AALF008821	Immune response	Defensin antimicrobial peptide	45.85	57.72
AALF026731		Unspecified product	22.22	98.88
AALF008229		Unspecified product	19.82	7.04
AALF025212	Ion homeostasis	Transferrin	15.95	20.69
AALF020799	Immune response	Peptidoglycan-Recognition Protein	14.48	10.23
AALF001195		Unspecified product	12.68	9.79
AALF008452		Unspecified product	12.07	10.83
AALF002418	Metabolic process	Imaginal disc growth factor	10.45	10.37
AALF019963		Unspecified product	9.01	4.88
AALF009200		Unspecified product	8.65	5.95
AALF005588	Metabolic process	L-lactate dehydrogenase	8.11	7.45
AALF004727	Metabolic process	Lipase	7.49	5.5
AALF012590		Unspecified product	7.38	4.56
AALF015711	DNA replication	DNA helicase	6.43	-12.12
AALF022735	DNA replication	DNA helicase	5.48	-13.63
AALF009419		Unspecified product	5.14	4.47
AALF028505		Unspecified product	-13.71	-12.83
AALF008879	Metabolic process	Type IV inositol 5-phosphatase	-16.64	-10.21
AALF015015		Unspecified product	-230.7	22.72

2.4. Transcripts Differentially Expressed in Dual-Infected U4.4 Cells

The analysis and comparison of mRNA expression profiles of U4.4 cells dual-infected with WNV 24 h post-infection with LamV revealed that 117 (70 up- and 47 down-regulated) and 577 (300 up- and 277 down-regulated) transcripts were significantly DE at 24 h and 48 h post-infection with WNV. Comparing the two transcriptome profiles showed 55 overlapping transcripts between the two time points (Figure 6). Similar to the WNV-only infected cells, many of the up-regulated transcripts were related to immune activity, namely C-type lectin (AALF016234), clip-domain serine protease family B (AALF019859), Defensin

(AALF008821), peptidoglycan-recognition protein (AALF020799) and Peptidylprolyl isomerase (AALF012257). Some immune genes were up-regulated at 24 h post-infection with WNV but down-regulated at 48 hpi, such as prophenoloxidase (AALF012716) and clip-domain serine protease family B (AALF020197). Furthermore, among the up-regulated transcripts we observed two signal peptide processing genes, putative microsomal signal peptidase 25 kDa subunit (AALF006247) and signal peptidase complex subunit 3 (AALF003192) (Table 2 and Table S3). The GO enrichment analysis for biological processes resulted in seven and sixteen GO slim terms for the up-regulated transcripts and one and eight GO slim terms for the down-regulated transcript (Figure 7).

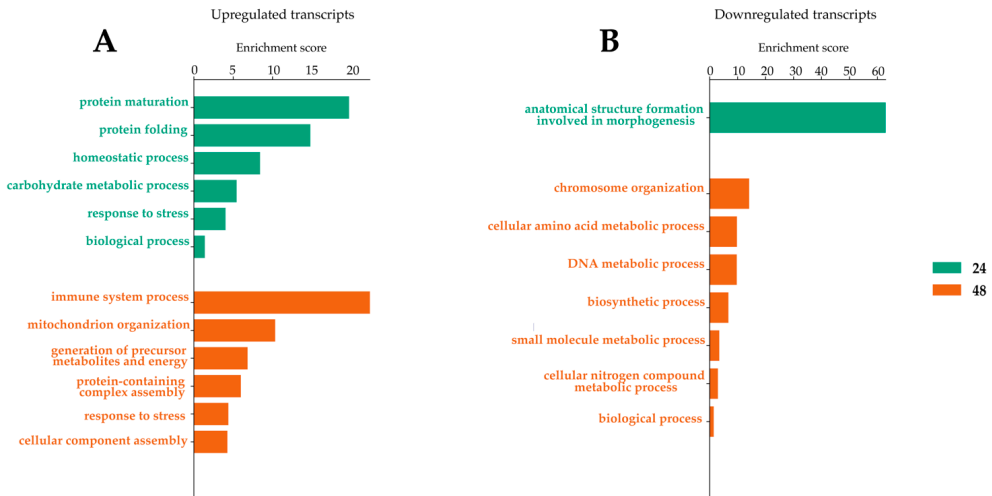


Figure 5. Gene ontology enrichment analysis for biological processes after WNV infection. (A) GO Slim terms for up-regulated transcripts. (B) GO slim terms for down-regulated transcripts.

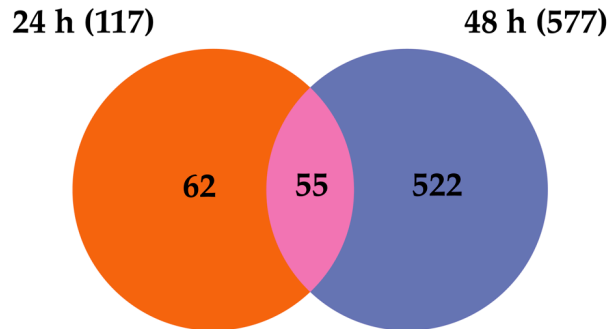


Figure 6. Venn diagram representing the number of differentially expressed transcripts at the different time points of dual-infected U4.4 cells. Timepoints 24 h and 48 h indicate time post-infection with WNV.

Table 2. List of *Ae. albopictus* overlapping differentially expressed transcripts following LamV infection and WNV challenge. Functional categories are based on GO terms for biological processes. Fold changes are shown in hours post-challenge with WNV. The cut-offs used were *p*-adjusted value of ≤ 0.01 and \log_2 FC of ≥ 0.5 .

Transcript ID	Functional Categories	Gene Description	Fold Change 24 hpi	Fold Change 48 hpi
AALF016234	Immune response	C-type lectin	82.76	22.12
AALF013298		Unspecified product	69.07	23.19
AALF003774	Immune response	Fibrinogen and fibronectin	52.19	9.14
AALF019859	Immune response	Clip-Domain Serine Protease family B	49.47	7.65
AALF008821	Immune response	Defensin antimicrobial peptide	45.81	16.18
AALF026731		Unspecified product	22.2	12.95
AALF020197	Immune response	Clip-Domain Serine Protease family B	15.24	-6.49
AALF020799	Immune response	Peptidoglycan-Recognition Protein	14.47	8.03
AALF007525		Unspecified product	12.61	23.73
AALF016365	Granules fusion	Munc13-4	10.03	6.05
AALF004571		Unspecified product	9.85	122.64
AALF012716	Immune response	Prophenoloxidase	9.77	-5.54
AALF006247	Signal peptide processing	Putative microsomal signal peptidase 25 kDa subunit	8.72	20.65
AALF021835	Response to stress	BiP/GRP78	8.37	31.7
AALF005588	Metabolic process	L-lactate dehydrogenase	8.1	28.92
AALF019952		Unspecified product	7.65	6.1
AALF003990	Metabolic process	Mannosyltransferase	7.13	88.65
AALF027716	Metabolic process	Cytochrome P450	6.64	9.16
AALF003192	Signal peptide processing	Signal peptidase complex subunit 3	6.58	20.26
AALF012257		Peptidylprolyl isomerase	6.55	7.31
AALF019397		Putative reticulocalbin calumenin DNA supercoiling factor	5.97	-4.99
AALF022020	Response to stress	Chaperonin-60kD	5.38	6.94
AALF002466	Response to stress	Protein disulfide-isomerase A6 precursor	5.2	11.04
AALF011939	Response to stress	Endoplasmic	5.12	12.98
AALF002534	Response to stress	Putative heat-shock protein	5.08	8.67
AALF020666	Protein degradation	Ubiquitin	-4.79	-4.99
AALF026911		GPCR Orphan/Putative Class B Family	-7.02	-15.17
AALF016818		Unspecified product	-8.1	-5.85
AALF025231		Unspecified product	-9.13	-20.68
AALF028121		Unspecified product	-9.15	-7.13
AALF015500	DNA/RNA binding	Zinc finger protein	-9.41	-7.58
AALF008709	Transport	Mfs transporter	-10.8	-7.4
AALF011706		Unspecified product	-10.79	-26.44
AALF028505		Unspecified product	-13.72	-65.33
AALF020168		Unspecified product	-13.93	-22.6
AALF008099		Endothelin-converting enzyme	-15.39	-66.8
AALF000742		Unspecified product	-15.81	-54.52
AALF008879	Metabolic process	Type IV inositol 5-phosphatase	-16.65	-60.51
AALF004114		No-mechanoreceptor potential a	-24.69	-45.32
AALF011390		Putative ecdysone-induced protein	-26.61	-21.06
AALF020798		Unspecified product	-29.45	-10.58
AALF009909		Unspecified product	-32.33	-140.61
AALF001259		Unspecified product	-36.13	-36.84
AALF012770	Metabolic process	Aldehyde oxidase	-37.85	-39.12
AALF001105		Unspecified product	-40.91	-26.97
AALF002857		Unspecified product	-42.81	-133.32
AALF002636		Unspecified product	-43.27	-11.27
AALF025810		Unspecified product	-51.86	-28.39
AALF013937	Immune-related	Serine protease	-52.04	-60.31

Table 2. Cont.

Transcript ID	Functional Categories	Gene Description	Fold Change 24 hpi	Fold Change 48 hpi
AALF014375		Unspecified product	−57.5	−72.13
AALF013936		Unspecified product	−78.5	−156.98
AALF006472		Unspecified product	−86.08	−193.34
AALF015014	Immune-related	Clip-Domain Serine Protease family D	−245.49	−75.47
AALF016295			−249.88	−269.15
AALF014395			−605.75	−300.78

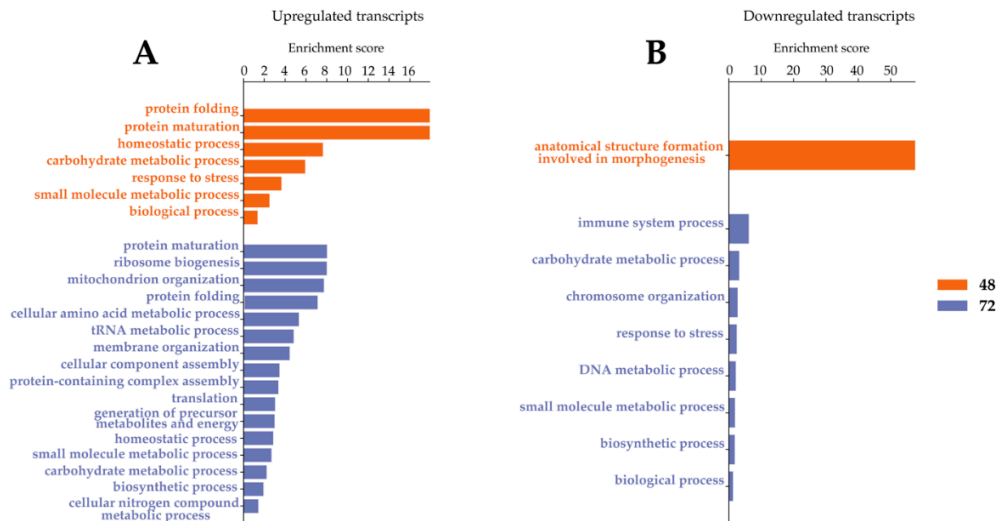


Figure 7. Gene ontology enrichment analysis for biological processes after LamV and WNV infection. (A) GO slim terms for up-regulated transcripts. (B) GO slim terms for down-regulated transcripts.

2.5. Transcripts Differentially Expressed among All Infection Groups

Comparing the transcriptome profiles among all different infection groups at 24 h post-infection with WNV and 48 h post-infection with LamV revealed eight overlapping transcripts (Figure 8A). Many of the up-regulated transcripts are genes involved in protein processes in the ER, such as BiP/GRP78 (AALF021835), Putative microsomal signal peptidase 25 kDa subunit (AALF006247), Signal peptidase complex subunit 3 (AALF003192) and protein disulfide-isomerase A6 precursor (AALF002466) (Table 3). Interestingly, out of the eight overlapping transcripts, the only down-regulated genes could be observed in LamV-infected U4.4 cells. One of those down-regulated genes most likely encodes for a serine protease (AALF009419) and the other one encodes for the innate immune effector protein prophenoloxidase (AALF012716) (Table 3). Furthermore, the WNV-only and dual-infected U4.4 cells shared 94 DE transcripts at this time point and showed similar fold changes of the up-regulated transcripts common among all infections (Figure 8A and Table 3). The comparison of the same infection groups at 48 h post-infection with WNV and 72 h post-infection with LamV showed that the dual-infected cells were more similar to the LamV-infected cells, with 291 DE transcripts in common (Figure 8B). At these time points, 23 overlapping transcripts among all different infection groups were observed. All these transcripts showed similar up- and down-regulation, except for one transcript coding for the fibrinogen C-terminal domain-containing protein (AALF010275), which was down-regulated in the WNV-infected U4.4 cells but up-regulated in cells infected with LamV

or the dual-infection scheme (Table 4). Among the up-regulated genes, the majority was uncharacterized, except for the C-type lectin domain-containing protein (AALF022151), L-lactate dehydrogenase (AALF005588) and Pyrroline-5-carboxylate reductase (AALF003871). The down-regulated genes were mainly involved in DNA replication—DNA helicase (AALF015599, AALF020651 and AALF022735), DNA replication licensing factor MCM7 (AALF006549) and Ribonucleoside-diphosphate reductase (AALF015929 and AALF024232).

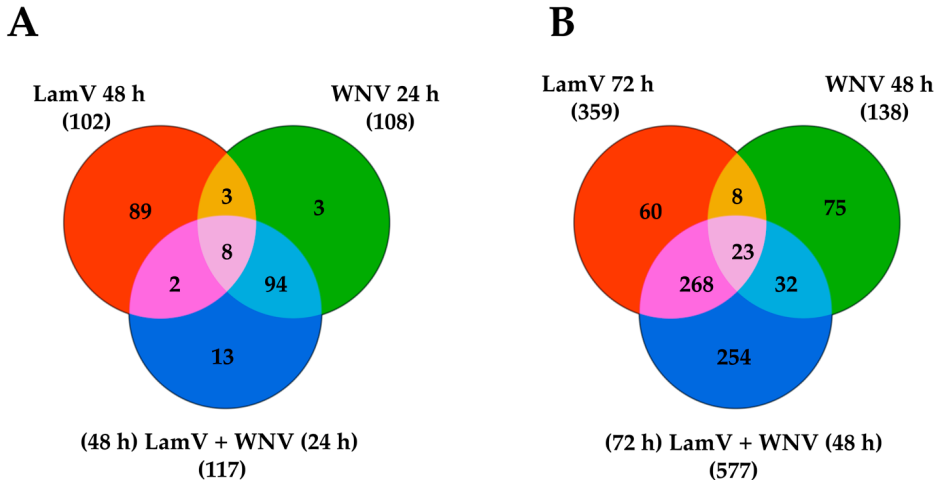


Figure 8. Venn diagram representing the number of differentially expressed transcripts among the different infection groups of U4.4 cells. (A) LamV at 48 hpi, WNV at 24 hpi and the dual infection 48 h post-infection with LamV and 24 h post-infection with WNV. (B) LamV at 72 hpi, WNV at 48 hpi and the dual infection 72 h post-infection with LamV and 48 h post-infection with WNV.

Table 3. List of *Ae. albopictus* overlapping differentially expressed transcripts among LamV at 48 hpi, WNV at 24 hpi and dual-infected cells 24 h post-challenge with WNV. Functional categories are based on GO terms for biological processes. The cut-offs used were *p*-adjusted value of ≤ 0.01 and \log_2 FC of ≥ 0.5 .

Transcript ID	Functional Categories	Gene Description	Fold Change 48 hpi with LamV	Fold Change 24 hpi with WNV	Fold Change Dual Infection 24 hpi with WNV
AALF004571		DUF3456 domain-containing protein	55.17	9.85	8.86
AALF021835	Response to stress	BiP/GRP78	21.95	8.37	8.37
AALF006247	Signal peptide processing	Putative microsomal signal peptidase 25 kDa subunit	19.29	8.73	8.72
AALF003192	Signal peptide processing	Signal peptidase complex subunit 3	15.78	6.58	6.58
AALF011939	Response to stress	Endoplasmic protein disulfide-isomerase A6 precursor	11.87	5.12	5.12
AALF002466	Response to stress	protein disulfide-isomerase A6 precursor	8.33	5.2	5.2
AALF009419		Unspecified product	−4.9	5.14	5.13
AALF012716	Immune response	Prophenoloxidase	−12.04	9.78	9.77

Table 4. List of *Ae. albopictus* overlapping differentially expressed transcripts among LamV at 72 hpi, WNV 48 hpi and dual-infected cells 48 h post-challenge with WNV. Functional categories are based on GO terms for biological processes. The cut-offs used were *p*-adjusted value of ≤ 0.01 and \log_2 FC of ≥ 0.5 .

Transcript ID	Functional Categories	Gene Description	Fold Change 72 hpi with LamV	Fold Change 48 hpi with WNV	Fold Change Dual Infection 48 hpi with WNV
AALF010887		Unspecified product	9.29	23.96	13.02
AALF020693		Unspecified product	27.96	16.03	40.21
AALF019136		Unspecified product	6.81	14.5	10.28
AALF014826		Unspecified product	12.18	11.12	22.82
AALF007397		Unspecified product	8.27	7.88	9.94
AALF022151	Immune response	C-type lectin domain-containing protein	7.5	7.47	7.91
AALF005588	Metabolic process	L-lactate dehydrogenase	8.74	7.45	28.92
AALF017030		Unspecified product	9.79	6.86	14.3
AALF007472		Unspecified product	7.8	6.68	13.9
AALF004337		Unspecified product	5.06	5.93	6.77
AALF003871	Metabolic process	Pyroline-5-carboxylate reductase	14.48	5.21	24.79
AALF010275		Fibrinogen C-terminal domain-containing protein	-6.44	5.05	-6.27
AALF015929	DNA replication	Ribonucleoside-diphosphate reductase	-7.38	-6.52	-9.17
AALF024232	DNA replication	Ribonucleoside-diphosphate reductase	-7.4	-7.42	-9.81
AALF015599	DNA replication	DNA helicase	-6.85	-10.3	-8.42
AALF020651	DNA replication	DNA helicase	-5.72	-10.51	-8.23
AALF000130		dNK domain-containing protein	-12.04	-12.54	-16.06
AALF019880	Oxidationreduction process	Dihydropyrimidine dehydrogenase NADP(+)	-14.35	-12.85	-35.91
AALF013610	Oxidationreduction process	Dihydropyrimidine dehydrogenase NADP(+)	-16.22	-13.14	-42.04
AALF022735	DNA replication	DNA helicase	-5.24	-13.63	-8.08
AALF013129	Metabolic process	Trehalose-6-phosphate synthase	-15.42	-14.88	-23.66
AALF006549	DNA replication	DNA replication licensing factor MCM7	-6.56	-15.21	-9.89
AALF000129	Reverse transcription	Reverse transcriptase domain-containing protein	-21.58	-20	-15.36

3. Discussion

Understanding the mosquito–virus interactions and identifying factors important for viral replication in mosquitoes is fundamental in the search for novel arboviruses control strategies. In the present study, we analyzed the altered gene expression upon infection with WNV, the insect-specific LamV and upon a dual-infection scheme, whereby U4.4 cells were pre-infected with LamV 24 h before being challenged with WNV. The qPCR analysis of the supernatant showed that the dual-infected U4.4 cells had a reduced number of WNV RNA copies compared to WNV-only infected cells, which suggest that a prior LamV infection restrain the secondary WNV infection.

When focusing on immune-related genes in WNV-infected U4.4 cells, we observed a cascade of up-regulated immune genes that have previously been described during flavivirus infection of mosquitoes or mosquito-derived cell lines [22–26]. Among the most up-regulated immune-related genes, we observed C-type lysozyme (AALF016234), defensin (AALF008821), leucine-rich immune protein (AALF016505), Cecropin-A2 (AALF000656), prophenoloxidase (AALF012716), Clip-Domain Serine Protease family B (AALF019859 and AALF020197) and peptidoglycan-Recognition Protein (AALF020799) (Table S2). Furthermore, among the down-regulated transcripts, we observed proteins that belong to the same protein family as the up-regulated immune proteins

but with very low similarity to each other, such as C-type lectin (AALF009202), serine protease (AALF013937) and Clip-Domain Serine Protease family D (AALF015014). Many of the immune-related proteins have regulating counterparts in the same protein family and we speculate that these down-regulated transcripts could have a regulatory function. A down-regulation of negative regulators can increase the expression or activity of an effector protein, or contrariwise if up-regulated. Furthermore, the initial immune response was strong, with a high expression of the immune genes at 24 hpi, which was then dampened with a decreased expression at 48 hpi (Table S2). Although we observed this great increase of immune-related genes, it did not seem to halt the WNV infection, with an increasing growth curve over time (Figure 1B). It is hypothesized that the mosquito antiviral immunity limit viral replication, but is unable to effectively clear the virus. This keeps the viral load at a tolerable level and therefore sustaining a persistent infection [13].

LamV-infected U4.4 cells did not induce the same amount of known immune effector proteins as those cells infected with WNV. However, when focusing on 10-fold or higher DE genes in either direction, we observed an up-regulation of different heat-shock proteins (HSPs). These proteins are known to be induced during stress, such as during a pathogen infection or a heat shock, and act as chaperones to guide misfolded proteins [42]. Among these, we observed endoplasmic reticulum chaperone (AALF011939), also known as HSP-90, which is connected to the innate immunity of humans [43,44]. We also observed two J-domain-containing proteins, known as HSP-40 (AALF010569 and AALF013640); one BiP/GRP-78 protein, which is an HSP-70 (AALF021835); and two proteins of the GRP-E family (AALF026344 and AALF026694) (Table S1). The HSP-40 and GRP-E proteins both act as co-chaperons for the HSP-70, to increase its activity. Furthermore, we observed two genes within the *lethal(2)-essential-for-life l(2)efl* family (AALF005663 and AALF015016), which encodes HSP-20. The *l(2)efl* family have been shown to be up-regulated upon DENV-2 infection in *Ae. aegypti* mosquitoes [45]. Furthermore, suppression of the *l(2)efl* genes in the CCL-125 cell line showed increased replication of DENV-2, while enhanced expression of the *l(2)efl* genes in the same cell line reduced DENV-2 replication [45]. Among the most down-regulated genes at 72 h post-infection with LamV, we observed two histone H2A (AALF007138 and AALF010649) and three histone H2B genes (AALF010137, AALF014537 and AALF010648) that were down-regulated between 85.16 and 344.4-fold (Table S1). The opposite was observed in a study where the DENV capsid protein was shown to bind the core histone proteins in liver cells and act as a histone mimic, possibly to favor viral replication and repressing the host's gene transcription; then, liver cells responded to this by initiating an increased production of histones [46]. In summary, the insect-specific LamV did not trigger as prominent immune response as WNV. However, the active viral infection induced a strong stress response in the cell with an increased expression of different HSPs.

U4.4 cells pre-infected with LamV and then challenged with WNV showed the highest amount of DE transcripts among all infection groups. The transcriptome profile of these cells was a mix of genes triggered by both LamV and WNV. Interestingly, although these cells were pre-infected with LamV 24 h before being challenged with WNV, their transcriptome profile was the most similar to the one of WNV-only infected cells at 24 hpi. The same immune effector proteins were expressed at similar levels to those of WNV-only infected cells (Table S3). However, at 48 h post-challenge with WNV, we observed a shift, with a transcriptome profile similar to the one of LamV-infected U4.4 cells at 72 hpi, with an up-regulation of HSPs and down-regulation of the Histone H2A and H2B (Table S3). Furthermore, at this time point, we observed 254 DE transcripts not overlapping with any of the other infections (Figure 8B). Among these transcripts, the most abundant genes observed were two Mitogen-activated protein kinases (MAPK) (AALF018203 and AALF011886). The MAPK is a serine-threonine protein kinase that regulates a broad spectrum of cellular processes, such as growth, metabolism, apoptosis and innate immune responses; however, the understanding of the MAPK signaling cascades in mosquitoes is limited [47]. Unfortunately, for a large proportion of the DE transcripts, we were unable to infer a functional role, due to a lack of annotation in the database. This was especially problematic for the

dual-infected cells, where many of the most up- or down-regulated transcripts are currently uncharacterized. However, with such large amount of DE genes in the dual-infected cells, we can assume that the cell viability is decreased.

The RNAi is considered the main antiviral immune response in mosquitoes; however, we did not observe any significant altered gene expression of the main genes involved in the RNAi pathways such as PIWI, Dicer or Ago. This is in line with existing transcriptomics studies performed on viral infections of mosquitoes or mosquito-derived cell lines [22–26]. Surprisingly, these genes seem to have a stable expression during viral infection.

Interestingly, among the genes in common to all infections, we discovered that many of the up-regulated genes are associated with ER functions, including a group of ER-associated signal peptidase complex (SPC) proteins, such as the SPC 25 kDa subunit (AALF006247), the SPC subunit 3 (AALF003192) and the SPC subunit SEC11 (AALF019423). The SPC proteins have shown to be important for proper cleavage of the flavivirus structural proteins (PrM and E) and secretion of viral particles [48]. The silencing of either SPC-1, 2 or 3 in *Drosophila* DL1 cells reduced the infection of WNV and DENV-2 without affecting cell viability; furthermore, gene silencing of SPC-2 in the *Ae. aegypti* cell line Aag2, also reduced WNV infection [48]. The up-regulated SPC genes observed in this study could potentially be targets of choice for gene modification in mosquitoes to reduce transmission of flaviviruses. Other potential targets for modification are the up-regulated HSPs observed in LamV- and dual-infected U4.4 cells. This study provides an overview of the transcriptional response to acute infection of LamV, WNV and the dual-infection scheme in cell culture. Further in vitro and in vivo studies are needed to investigate the effects on the transmission of WNV, of either a prior LamV infection or of the gene modification targets brought up in this discussion.

4. Materials and Methods

4.1. Cell Culture

Ae. albopictus U4.4 mosquito cells (kindly provided by Associate Professor G. Pijlman, Wageningen University) and C6/36 cells (Sigma-Aldrich, Darmstadt, Germany) were cultured at 28 °C without CO₂ in Leibovitz L-15 medium (Gibco, Paisley, UK) supplemented with 10% fetal bovine serum (FBS; Gibco, Paisley, UK), 10% tryptose phosphate broth (TPB; Gibco, Paisley, UK), Amphotericin (250 µg/mL; Gibco, Grand Island, NY, USA) and Pen Strep (penicillin 100 U/mL and streptomycin 100 µg/mL; Gibco, Grand Island, NY, USA). Vero E6 cells were cultured at 37 °C with 5% CO₂ in Dulbecco's modified Eagle medium (Gibco, Paisley, UK) supplemented with 10% FBS, Pen Strep and 2 mM L-Glutamine (Gibco, Paisley, UK).

4.2. Virus Stocks and Virus Titration

The ISFV LamV (2009/Fl/Original) was obtained from the European Virus Archive—Global (EVAg). Virus stocks were propagated in C6/36 cells until clear cytopathic effect (CPE) was observed (4 dpi); then, the supernatant was collected, centrifuged and frozen at –80 °C. LamV stock titer could not be obtained with traditional methods. Thus, to quantify the LamV stocks, plasmid standards containing the PCR target region of the virus were ordered (GeneScript Biotech, Leiden, The Netherlands). The plasmids were used to construct a qPCR standard curve and a stock concentration was calculated as RNA copies/mL. RNA extraction and qRT-PCR protocols are described below. WNV (lineage 1) was kindly provided by Professor Åke Lundkvist (Department of Medical Biochemistry and Microbiology/Zoonosis Science Center, Uppsala University, Uppsala, Sweden). WNV stock was grown in Vero E6 cells and the supernatant was collected when clear CPE (3 dpi) was observed. The titer of the WNV stock was determined by a plaque assay, as described in [49].

4.3. In Vitro Infection

On the day of infection, 24-well plates with U4.4 cells at a confluency of 85–90% (approximately 350,000 cells per well) were used. Each infection and timepoint were performed in triplicate. For LamV infections, we added 175,000 RNA copies per well, mixed with 200 μ L infection medium (Leibovitz L-15 medium containing 2% FBS and 10% TPB). For WNV infections, the cells were infected at a MOI of 0.1 in 200 μ L of infection medium. After one hour of incubation, the inoculum was discarded and 500 μ L of Leibovitz L-15 medium supplemented with 5% FBS, 10% TPB and Pen Strep was added. Mock-infected cells were used as control. The supernatant and cells were sampled every 24 h post-infection (hpi) for qPCR and sequencing (Figure 9). All experiments were performed in the BSL-3 facility at the Zoonosis Science Center, Uppsala University, Uppsala, Sweden.

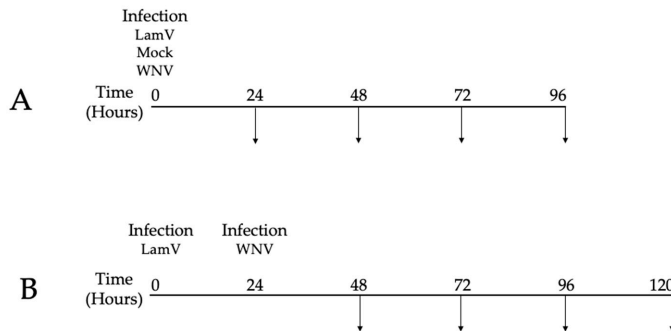


Figure 9. Schematic representation of the experiment schedule. (A) Time scheme for single infections. (B) Time scheme for cells pre-infected with LamV and challenged with WNV. Arrows represent sampling of cells and supernatant. Cells were only collected between the timepoints 24 to 72 hpi.

4.4. Quantitative PCR

First-strand cDNA was generated using the SuperScript™ III Reverse Transcription kit (Thermo Fisher Scientific, Carlsbad, CA, USA) with Random Hexamers (Thermo Fisher Scientific, Carlsbad, CA, USA), following the manufacturer's instructions with an input of 5 μ L of RNA in a total volume of 20 μ L. The qPCR was performed using the iTaq Universal SYBR® Green supermix (Bio-Rad laboratories Inc, Hercules, CA, USA) with 2 μ L of template cDNA and 0.5 μ M each corresponding virus primer (Table 1) in a total volume of 20 μ L per reaction. The qPCR was carried out using the Bio-Rad® CFX96 real-time PCR system (Bio-Rad laboratories Inc, Hercules, CA, USA) with amplification conditions consisting of an initial denaturation at 95 °C for 30 s, followed by 40 cycles of denaturation at 95 °C for 7 s and annealing/extension and plate read at 60 °C 30 s. A melt curve was generated starting at 60 °C with a 0.5 °C increase up to 96 °C.

Primer pairs for the qPCR were designed using the software primer 3 [50] to generate a product between 170 and 200 bp long and T_m of 60 °C. Virus reference genomes were obtained from the NCBI database and are listed, together with the primer sequences, in Table 5. The statistical significance differences were calculated using Student's *t*-test.

Table 5. Primer pairs used for qPCR analysis.

Primers	Binding Site	Sequence (5' → 3')	Ref
qLamV-F	4659–4678	TGGGTGTTACCGGGTTATGT	FJ606789
qLamV-R	4845–4864	ACGTTCCATTTCAGTTTCCAT	
qWNV-F	10490–10508	GAAGTCAGGCCGAAAGTT	AF260968
qWNV-R	10668–10689	TCTCCGCAGAGTGGCACGCC	

4.5. RNA Extractions

RNA used for growth curves and virus titration was extracted from 200 μL of supernatant/virus stocks in 750 μL of TRIzol™ (Thermo Fisher Scientific, Carlsbad, CA, USA). The aqueous phase obtained after the addition of chloroform and the subsequent centrifugation step was collected and diluted (1:1) with freshly prepared 70% ethanol and purified with GeneJet spin columns (Thermo Fisher Scientific, Vilnius, Lithuania). RNA was eluted in 40 μL of nuclease free water and stored at $-80\text{ }^{\circ}\text{C}$ until further processed.

RNA used for high-throughput sequencing was isolated from cells that were collected by adding 750 μL of TRIzol™ to the respective wells. The aqueous phase was obtained in the same manner as described above and the RNA was further purified using the mirVana™ PARIS™ Kit (Thermo Fisher Scientific, Vilnius, Lithuania), according to the protocol to isolate large RNA (>200 nt) provided by the manufacturer.

4.6. Sequencing of mRNA

Large RNA isolated from infected U4.4 cells was quantified and quality-controlled with the 4150 TapeStation System using the RNA ScreenTape Analysis kit (Agilent Technologies, Santa Clara, CA, USA). Triplicates for each infection and timepoint were submitted to SciLifeLab for library preparation using the Illumina Truseq Stranded mRNA (poly-A selection) kit (San Diego, CA, USA). The libraries were sequenced on an Illumina NovaSeq 6000 sequencer using one lane of a S4 flow cell to a depth of 30–40 million reads per sample with a read length of 2×151 bp.

4.7. RNA-Seq Data Analysis

The raw transcriptomic FASTQ files were analyzed with bioinformatic Nextflow pipeline `nf-core/rnaseq` (v3.0) [51]. The pipeline included quality control (FastQC v0.11.9) [52], adapter and quality trimming (Trim Galore! V0.6.6) [53], removal of ribosomal RNA (SortMeRNA v4.2.0) [54] and pseudo-alignment and quantification (Salmon v1.4.0) [55], using the reference *Ae. albopictus* Foshan genome sequence and annotation (version Aalo1.2) retrieved from Vectorbase [56]. The resulting Salmon `quant.sf` files were further analyzed with an inhouse script in R (doi:10.5281/zenodo.5786479). This script includes a quality control of the data, normalization and DESeq2 analysis. Every infection group was compared with mock-infected cells at the corresponding time point, using the parameters of *p*-adjusted value of ≤ 0.01 and \log_2 FC of ≥ 0.5 as cut-offs, following the recommendations found in reference [57]. Lists of significant differentially expressed (DE) transcripts were further analyzed and transcripts IDs were transferred to VectorBase [56] for gene description and Gene Ontology (GO) enrichment analysis. The latter was focused on the sole biological process aspect.

4.8. Data Availability

All sequencing data were made publicly available at the NCBI Sequence Read Archive (SRA) under accession number Bioproject ID PRJNA786637.

5. Conclusions

This study provides an overview of the transcriptional response to acute infection of WNV, the insect-specific LamV and a dual-infection scheme in an *Ae. albopictus* cell line. The transcriptome profiles of the different infection groups showed a variety of genes with altered expression. WNV-infected cells had an up-regulation of a broad range of immune-related genes, while in LamV-infected cells, many genes related to stress, such as different HSPs, were up-regulated. The transcriptome profile of the dual-infected cells was a mix of up- and down-regulated genes triggered by both viruses, which was more similar to the one of WNV-infected cells in the early time point but shifted towards the one of LamV-infected cells in the later time point.

Since a prior LamV infection seemed to restrain the secondary WNV infection, one of the goals of this study was to find potential gene targets for modification in mosquitoes

to reduce transmission of flaviviruses. Interestingly, we observed an up-regulation of SPC proteins in all infection groups. These SPC proteins have shown importance for flavivirus assembly and secretion and could be potential targets for gene modification. Other potential targets for gene modification could be the HSP *l(2)efl* observed in the LamV and dual-infected cells. Further knockdown or overexpression experiments in mosquito-derived cell lines and mosquitoes are needed to study the potential effects on the host and virus transmission.

Supplementary Materials: The following are available online at <https://www.mdpi.com/article/10.3390/ijms23020875/s1>.

Author Contributions: P.Ö., J.H., J.C.H. and A.-L.B. conceived and designed the experiments; P.Ö. performed the experiments; P.Ö., N.D., J.H. and A.-L.B. analyzed the data; P.Ö. wrote and prepared the original draft; J.H., N.D., J.C.H. and A.-L.B. reviewed and edited the manuscript. All authors have read and agreed to the published version of the manuscript.

Funding: This study was supported by the Swedish research Council VR (2016-01251) and the Swedish University of Agricultural Sciences (SLU), as well as the Vice-chancellor junior career grant awarded to A.-L.B.

Data Availability Statement: All sequencing data were made publicly available at the NCBI Sequence Read Archive (SRA) under accession number Bioproject ID PRJNA786637.

Acknowledgments: The authors would like to acknowledge the support of the National Genomics Infrastructure in Stockholm funded by Science for Life Laboratory, the Knut and Alice Wallenberg Foundation, the Swedish Research Council and the SNIC/Uppsala Multidisciplinary Center for Advanced Computational Science for assistance with massively parallel sequencing and access to the UPPMAX computational infrastructure. The SNIC through Uppsala Multidisciplinary Center for Advanced Computational Science (UPPMAX) under project SNIC 2017/7-290 is acknowledged for providing computational resources. The authors would also like to acknowledge the SLU Bioinformatics Infrastructure (SLUBI) for help and support with the bioinformatics analyses of the data. This publication was supported by the European Virus Archive goes Global (EVAg) project, which has received funding from the European Union's Horizon 2020 research and innovation program under grant agreement No 653316.

Conflicts of Interest: The authors declare no conflict of interest. The founding sponsors had no role in the design of the study; in the collection, analyses, or interpretation of data; in the writing of the manuscript; or in the decision to publish the results.

References

1. David, S.; Abraham, A.M. Epidemiological and clinical aspects on West Nile virus, a globally emerging pathogen. *Infect. Dis.* **2016**, *48*, 571–586. [[CrossRef](#)]
2. Guo, C.; Zhou, Z.; Wen, Z.; Liu, Y.; Zeng, C.; Xiao, D.; Ou, M.; Han, Y.; Huang, S.; Liu, D.; et al. Global Epidemiology of Dengue Outbreaks in 1990–2015: A Systematic Review and Meta-Analysis. *Front. Cell Infect. Microbiol.* **2017**, *7*, 317. [[CrossRef](#)] [[PubMed](#)]
3. Ferraris, P.; Yssel, H.; Misse, D. Zika virus infection: An update. *Microbes Infect.* **2019**, *21*, 353–360. [[CrossRef](#)]
4. WHO. *Global Strategy for Dengue Prevention and Control, 2012–2020*; WHO Report; WHO: Geneva, Switzerland, 2012.
5. Luz, P.M.; Vanni, T.; Medlock, J.; Paltiel, A.D.; Galvani, A.P. Dengue vector control strategies in an urban setting: An economic modelling assessment. *Lancet* **2011**, *377*, 1673–1680. [[CrossRef](#)]
6. Sinkins, S.P.; Gould, F. Gene drive systems for insect disease vectors. *Nat. Rev. Genet.* **2006**, *7*, 427–435. [[CrossRef](#)] [[PubMed](#)]
7. Terenius, O.; Marinotti, O.; Sieglaff, D.; James, A.A. Molecular genetic manipulation of vector mosquitoes. *Cell Host Microbe* **2008**, *4*, 417–423. [[CrossRef](#)]
8. Wu, P.; Yu, X.; Wang, P.; Cheng, G. Arbovirus lifecycle in mosquito: Acquisition, propagation and transmission. *Expert Rev. Mol. Med.* **2019**, *21*, e1. [[CrossRef](#)]
9. Cheng, G.; Liu, Y.; Wang, P.; Xiao, X. Mosquito Defense Strategies against Viral Infection. *Trends Parasitol.* **2016**, *32*, 177–186. [[CrossRef](#)]
10. Kumar, A.; Srivastava, P.; Sirisena, P.; Dubey, S.K.; Kumar, R.; Shrinet, J.; Sunil, S. Mosquito Innate Immunity. *Insects* **2018**, *9*, 95. [[CrossRef](#)]
11. Prasad, A.N.; Brackney, D.E.; Ebel, G.D. The role of innate immunity in conditioning mosquito susceptibility to West Nile virus. *Viruses* **2013**, *5*, 3142–3170. [[CrossRef](#)]

12. Goic, B.; Stapleford, K.A.; Frangeul, L.; Doucet, A.J.; Gausson, V.; Blanc, H.; Schemmel-Jofre, N.; Cristofari, G.; Lambrechts, L.; Vignuzzi, M.; et al. Virus-derived DNA drives mosquito tolerance to arboviral infection. *Nat. Commun.* **2016**, *7*, 12410. [[CrossRef](#)]
13. Lee, W.S.; Webster, J.A.; Madzokere, E.T.; Stephenson, E.B.; Herrero, L.J. Mosquito antiviral defense mechanisms: A delicate balance between innate immunity and persistent viral infection. *Parasit. Vectors* **2019**, *12*, 165. [[CrossRef](#)]
14. Xia, X.; You, M.; Rao, X.J.; Yu, X.Q. Insect C-type lectins in innate immunity. *Dev. Comp. Immunol.* **2018**, *83*, 70–79. [[CrossRef](#)]
15. Dziarski, R. Peptidoglycan recognition proteins (PGRPs). *Mol. Immunol.* **2004**, *40*, 877–886. [[CrossRef](#)]
16. Chalk, R.; Albuquerque, C.M.; Ham, P.J.; Townson, H. Full sequence and characterization of two insect defensins: Immune peptides from the mosquito *Aedes aegypti*. *Proc. Biol. Sci.* **1995**, *261*, 217–221. [[CrossRef](#)]
17. Cho, W.L.; Fu, Y.C.; Chen, C.C.; Ho, C.M. Cloning and characterization of cDNAs encoding the antibacterial peptide, defensin A, from the mosquito, *Aedes aegypti*. *Insect. Biochem. Mol. Biol.* **1996**, *26*, 395–402. [[CrossRef](#)]
18. Lowenberger, C.; Bulet, P.; Charlet, M.; Hetru, C.; Hodgeman, B.; Christensen, B.M.; Hoffmann, J.A. Insect immunity: Isolation of three novel inducible antibacterial defensins from the vector mosquito, *Aedes aegypti*. *Insect. Biochem. Mol. Biol.* **1995**, *25*, 867–873. [[CrossRef](#)]
19. Xiao, X.; Liu, Y.; Zhang, X.; Wang, J.; Li, Z.; Pang, X.; Wang, P.; Cheng, G. Complement-related proteins control the flavivirus infection of *Aedes aegypti* by inducing antimicrobial peptides. *PLoS Pathog.* **2014**, *10*, e1004027. [[CrossRef](#)]
20. Bartholomay, L.C.; Fuchs, J.F.; Cheng, L.L.; Beck, E.T.; Vizioli, J.; Lowenberger, C.; Christensen, B.M. Reassessing the role of defensin in the innate immune response of the mosquito, *Aedes aegypti*. *Insect. Mol. Biol.* **2004**, *13*, 125–132. [[CrossRef](#)] [[PubMed](#)]
21. Kanost, M.R.; Jiang, H. Clip-domain serine proteases as immune factors in insect hemolymph. *Curr. Opin. Insect. Sci.* **2015**, *11*, 47–55. [[CrossRef](#)] [[PubMed](#)]
22. Shin, D.; Civana, A.; Acevedo, C.; Smartt, C.T. Transcriptomics of differential vector competence: West Nile virus infection in two populations of *Culex pipiens quinquefasciatus* linked to ovary development. *BMC Genom.* **2014**, *15*, 513. [[CrossRef](#)]
23. Etebari, K.; Hegde, S.; Saldana, M.A.; Widen, S.G.; Wood, T.G.; Asgari, S.; Hughes, G.L. Global Transcriptome Analysis of *Aedes aegypti* Mosquitoes in Response to Zika Virus Infection. *mSphere* **2017**, *2*, e00456-17. [[CrossRef](#)]
24. Li, M.; Xing, D.; Su, D.; Wang, D.; Gao, H.; Lan, C.; Gu, Z.; Zhao, T.; Li, C. Transcriptome Analysis of Responses to Dengue Virus 2 Infection in *Aedes albopictus* (Skuse) C6/36 Cells. *Viruses* **2021**, *13*, 343. [[CrossRef](#)] [[PubMed](#)]
25. Li, M.J.; Lan, C.J.; Gao, H.T.; Xing, D.; Gu, Z.Y.; Su, D.; Zhao, T.Y.; Yang, H.Y.; Li, C.X. Transcriptome analysis of *Aedes aegypti* Aag2 cells in response to dengue virus-2 infection. *Parasit. Vectors* **2020**, *13*, 421. [[CrossRef](#)] [[PubMed](#)]
26. Shrinet, J.; Srivastava, P.; Sunil, S. Transcriptome analysis of *Aedes aegypti* in response to mono-infections and co-infections of dengue virus-2 and chikungunya virus. *Biochem. Biophys. Res. Commun.* **2017**, *492*, 617–623. [[CrossRef](#)] [[PubMed](#)]
27. Dong, S.; Behura, S.K.; Franz, A.W.E. The midgut transcriptome of *Aedes aegypti* fed with saline or protein meals containing chikungunya virus reveals genes potentially involved in viral midgut escape. *BMC Genom.* **2017**, *18*, 382. [[CrossRef](#)]
28. Zhao, L.; Alto, B.W.; Jiang, Y.; Yu, F.; Zhang, Y. Transcriptomic Analysis of *Aedes aegypti* Innate Immune System in Response to Ingestion of Chikungunya Virus. *Int. J. Mol. Sci.* **2019**, *20*, 3133. [[CrossRef](#)]
29. Ohlund, P.; Lunden, H.; Blomstrom, A.L. Insect-specific virus evolution and potential effects on vector competence. *Virus Genes* **2019**, *55*, 127–137. [[CrossRef](#)]
30. Nasar, F.; Gorchakov, R.V.; Tesh, R.B.; Weaver, S.C. Eilat virus host range restriction is present at multiple levels of the virus life cycle. *J. Virol.* **2015**, *89*, 1404–1418. [[CrossRef](#)]
31. Saiyasombat, R.; Bolling, B.G.; Brault, A.C.; Bartholomay, L.C.; Blitvich, B.J. Evidence of efficient transovarial transmission of *Culex* flavivirus by *Culex pipiens* (Diptera: Culicidae). *J. Med. Entomol.* **2011**, *48*, 1031–1038. [[CrossRef](#)]
32. Bolling, B.G.; Eisen, L.; Moore, C.G.; Blair, C.D. Insect-specific flaviviruses from *Culex* mosquitoes in Colorado, with evidence of vertical transmission. *Am. J. Trop. Med. Hyg.* **2011**, *85*, 169–177. [[CrossRef](#)] [[PubMed](#)]
33. Haddow, A.D.; Guzman, H.; Popov, V.L.; Wood, T.G.; Widen, S.G.; Haddow, A.D.; Tesh, R.B.; Weaver, S.C. First isolation of *Aedes* flavivirus in the Western Hemisphere and evidence of vertical transmission in the mosquito *Aedes* (*Stegomyia*) *albopictus* (Diptera: Culicidae). *Virology* **2013**, *440*, 134–139. [[CrossRef](#)]
34. Marklewitz, M.; Zirkel, F.; Kurth, A.; Drosten, C.; Junglen, S. Evolutionary and phenotypic analysis of live virus isolates suggests arthropod origin of a pathogenic RNA virus family. *Proc. Natl. Acad. Sci. USA* **2015**, *112*, 7536–7541. [[CrossRef](#)]
35. Hobson-Peters, J.; Yam, A.W.; Lu, J.W.; Setoh, Y.X.; May, F.J.; Kurucz, N.; Walsh, S.; Prow, N.A.; Davis, S.S.; Weir, R.; et al. A new insect-specific flavivirus from northern Australia suppresses replication of West Nile virus and Murray Valley encephalitis virus in co-infected mosquito cells. *PLoS ONE* **2013**, *8*, e56534. [[CrossRef](#)]
36. Hall-Mendelin, S.; McLean, B.J.; Bielefeldt-Ohmann, H.; Hobson-Peters, J.; Hall, R.A.; van den Hurk, A.F. The insect-specific Palm Creek virus modulates West Nile virus infection in and transmission by Australian mosquitoes. *Parasit. Vectors* **2016**, *9*, 414. [[CrossRef](#)]
37. Kenney, J.L.; Solberg, O.D.; Langevin, S.A.; Brault, A.C. Characterization of a novel insect-specific flavivirus from Brazil: Potential for inhibition of infection of arthropod cells with medically important flaviviruses. *J. Gen. Virol.* **2014**, *95*, 2796–2808. [[CrossRef](#)]
38. Goenaga, S.; Kenney, J.L.; Duggal, N.K.; Delorey, M.; Ebel, G.D.; Zhang, B.; Levis, S.C.; Enria, D.A.; Brault, A.C. Potential for Co-Infection of a Mosquito-Specific Flavivirus, Nhumirim Virus, to Block West Nile Virus Transmission in Mosquitoes. *Viruses* **2015**, *7*, 5801–5812. [[CrossRef](#)]

39. Huhtamo, E.; Putkuri, N.; Kurkela, S.; Manni, T.; Vaheri, A.; Vapalahti, O.; Uzcategui, N.Y. Characterization of a novel flavivirus from mosquitoes in northern Europe that is related to mosquito-borne flaviviruses of the tropics. *J. Virol.* **2009**, *83*, 9532–9540. [[CrossRef](#)]
40. Blitvich, B.J.; Firth, A.E. Insect-specific flaviviruses: A systematic review of their discovery, host range, mode of transmission, superinfection exclusion potential and genomic organization. *Viruses* **2015**, *7*, 1927–1959. [[CrossRef](#)] [[PubMed](#)]
41. Ohlund, P.; Hayer, J.; Hesson, J.C.; Blomstrom, A.L. Small RNA Response to Infection of the Insect-Specific Lammi Virus and Hanko Virus in an *Aedes albopictus* Cell Line. *Viruses* **2021**, *13*, 2181. [[CrossRef](#)] [[PubMed](#)]
42. Zhao, L.; Pridgeon, J.W.; Becnel, J.J.; Clark, G.G.; Linthicum, K.J. Identification of genes differentially expressed during heat shock treatment in *Aedes aegypti*. *J. Med. Entomol.* **2009**, *46*, 490–495. [[CrossRef](#)]
43. Randow, F.; Seed, B. Endoplasmic reticulum chaperone gp96 is required for innate immunity but not cell viability. *Nat. Cell Biol.* **2001**, *3*, 891–896. [[CrossRef](#)]
44. Yang, Y.; Liu, B.; Dai, J.; Srivastava, P.K.; Zammit, D.J.; Lefrancois, L.; Li, Z. Heat shock protein gp96 is a master chaperone for toll-like receptors and is important in the innate function of macrophages. *Immunity* **2007**, *26*, 215–226. [[CrossRef](#)]
45. Runtuwene, L.R.; Kawashima, S.; Pijoh, V.D.; Tuda, J.S.B.; Hayashida, K.; Yamagishi, J.; Sugimoto, C.; Nishiyama, S.; Sasaki, M.; Orba, Y.; et al. The Lethal(2)-Essential-for-Life [L(2)EFL] Gene Family Modulates Dengue Virus Infection in *Aedes aegypti*. *Int. J. Mol. Sci.* **2020**, *21*, 7520. [[CrossRef](#)]
46. Colpitts, T.M.; Barthel, S.; Wang, P.; Fikrig, E. Dengue virus capsid protein binds core histones and inhibits nucleosome formation in human liver cells. *PLoS ONE* **2011**, *6*, e24365. [[CrossRef](#)]
47. Horton, A.A.; Wang, B.; Camp, L.; Price, M.S.; Arshi, A.; Nagy, M.; Nadler, S.A.; Faeder, J.R.; Luckhart, S. The mitogen-activated protein kinase from *Anopheles gambiae*: Identification, phylogeny and functional characterization of the ERK, JNK and p38 MAP kinases. *BMC Genom.* **2011**, *12*, 574. [[CrossRef](#)]
48. Zhang, R.; Miner, J.J.; Gorman, M.J.; Rausch, K.; Ramage, H.; White, J.P.; Zuiani, A.; Zhang, P.; Fernandez, E.; Zhang, Q.; et al. A CRISPR screen defines a signal peptide processing pathway required by flaviviruses. *Nature* **2016**, *535*, 164–168. [[CrossRef](#)] [[PubMed](#)]
49. Brien, J.D.; Lazear, H.M.; Diamond, M.S. Propagation, quantification, detection, and storage of West Nile virus. *Curr. Protoc. Microbiol.* **2013**, *31*, 15D-3. [[CrossRef](#)] [[PubMed](#)]
50. Rozen, S.; Skaletsky, H. Primer3 on the WWW for general users and for biologist programmers. *Methods Mol. Biol.* **2000**, *132*, 365–386. [[CrossRef](#)]
51. Ewels, P.A.; Peltzer, A.; Fillinger, S.; Patel, H.; Alneberg, J.; Wilm, A.; Garcia, M.U.; Di Tommaso, P.; Nahnsen, S. The nf-core framework for community-curated bioinformatics pipelines. *Nat. Biotechnol.* **2020**, *38*, 276–278. [[CrossRef](#)] [[PubMed](#)]
52. Babraham Bioinformatics. FastQC. Available online: <https://www.bioinformatics.babraham.ac.uk/projects/fastqc/> (accessed on 8 December 2021).
53. Babraham Bioinformatics. Trim Galore. Available online: https://www.bioinformatics.babraham.ac.uk/projects/trim_galore/ (accessed on 8 December 2021).
54. Kopylova, E.; Noe, L.; Touzet, H. SortMeRNA: Fast and accurate filtering of ribosomal RNAs in metatranscriptomic data. *Bioinformatics* **2012**, *28*, 3211–3217. [[CrossRef](#)] [[PubMed](#)]
55. Patro, R.; Duggal, G.; Love, M.I.; Irizarry, R.A.; Kingsford, C. Salmon provides fast and bias-aware quantification of transcript expression. *Nat. Methods* **2017**, *14*, 417–419. [[CrossRef](#)] [[PubMed](#)]
56. Giraldo-Calderon, G.I.; Emrich, S.J.; MacCallum, R.M.; Maslen, G.; Dialynas, E.; Topalis, P.; Ho, N.; Gesing, S.; VectorBase, C.; Madey, G.; et al. VectorBase: An updated bioinformatics resource for invertebrate vectors and other organisms related with human diseases. *Nucleic Acids Res.* **2015**, *43*, D707–D713. [[CrossRef](#)] [[PubMed](#)]
57. Schurch, N.J.; Schofield, P.; Gierlinski, M.; Cole, C.; Sherstnev, A.; Singh, V.; Wrobel, N.; Gharbi, K.; Simpson, G.G.; Owen-Hughes, T.; et al. How many biological replicates are needed in an RNA-seq experiment and which differential expression tool should you use? *RNA* **2016**, *22*, 839–851. [[CrossRef](#)] [[PubMed](#)]

We have detected a mistake in our published article “**Transcriptome Analysis of an *Aedes albopictus* Cell Line Single- and Dual-Infected with Lammi Virus and WNV**” (Paper III) and have therefore requested a correction that is currently under process. The mistake comprise fold-change values in tables that were accidentally mistaken for Log10 instead of log2. This error do not affect which genes are significantly differently expressed, if they are up- or down-regulated nor which genes are mostly expressed. It only affect the actual magnitude of the fold-change. The final conclusions are not changed.

Correction in text

- Page 3 Location: 2.2 line 4-6.
Is now: The comparison of the transcriptome profiles showed two overlapping transcripts among all time points, both coding for the 40S ribosomal protein S21—AALF005471 (**7.08–11.38 fold change**) and AALF002626 (**8–10.94 fold change**) (Figure 2 and Table S1).
Should be: The comparison of the transcriptome profiles showed two overlapping transcripts among all time points, both coding for the 40S ribosomal protein S21—AALF005471 (**0.85–1.13 log-2-fold change**) and AALF002626 (**0.9–1.04 log-2-fold change**) (Figure 2 and Table S1).
- Page 11 Location: Line 14-15.
Is now: However, when focusing on **10-fold or higher** DE genes in either direction, we observed an up-regulation of different heat-shock proteins (HSPs).
Should be: However, when focusing on **highly** DE genes in either direction, we observed an up-regulation of different heat-shock proteins (HSPs).
- Page 12 Location: Line 28-31
Is now: Among the most down-regulated genes at 72 h post-infection with LamV, we observed two histone H2A (AALF007138 and AALF010649) and three histone H2B genes (AALF010137, AALF014537 and AALF010648) that were down-regulated between **85.16 and 344.4-fold** (Table S1).
Should be: Among the most down-regulated genes at 72 h post-infection with LamV, we observed two histone H2A (AALF007138 and AALF010649) and three histone H2B genes (AALF010137, AALF014537 and AALF010648) that were down-regulated between **-1.93 and -2.54 log-2-fold** (Table S1).

Corrected tables and supplementary tables below.

Correct tables

Table 1. List of *Ae. albopictus* overlapping differentially expressed transcripts following WNV infection. Functional categories are based on GO terms for biological processes. The cut-offs used were *p*-adjusted value of ≤ 0.01 and \log_2 FC of ≥ 0.5 .

Transcript ID	Functional Categories	Gene Description	Log 2 Fold Change 24 hpi	Log 2 Fold Change 48 hpi
AALF016234	Immune response	C-type lectin	1.9185	1.2493
AALF013298		Unspecified product	1.8395	1.1512
AALF003774	Immune response	Fibrinogen and fibronectin	1.7179	1.2668
AALF019859	Immune response	Clip-Domain Serine Protease family B	1.6947	0.9666
AALF008821	Immune response	Defensin antimicrobial peptide	1.6614	1.7614
AALF026731		Unspecified product	1.3467	1.9951
AALF008229		Unspecified product	1.2970	0.8473
AALF025212	Ion homeostasis	Transferrin	1.2028	1.3158
AALF020799	Immune response	Peptidoglycan-Recognition Protein	1.1608	1.0099
AALF001195		Unspecified product	1.1031	0.9906
AALF008452		Unspecified product	1.0816	1.0348
AALF002418	Metabolic process	Imaginal disc growth factor	1.0189	1.0159
AALF019963		Unspecified product	0.9549	0.6882
AALF009200		Unspecified product	0.9370	0.7745
AALF005588	Metabolic process	L-lactate dehydrogenase	0.9089	0.8721
AALF004727	Metabolic process	Lipase	0.8743	0.7402
AALF012590		Unspecified product	0.8683	0.6585
AALF015711	DNA replication	DNA helicase	0.8084	-1.0837
AALF022735	DNA replication	DNA helicase	0.7384	-1.1344
AALF009419		Unspecified product	0.7106	0.6502
AALF028505		Unspecified product	-1.1371	-1.1084
AALF008879	Metabolic process	Type IV inositol 5-phosphatase	-1.2212	-1.0088
AALF015015		Unspecified product	-2.3631	1.3564

Table 2. List of *Ae. albopictus* overlapping differentially expressed transcripts following LamV infection and WNV challenge. Functional categories are based on GO terms for biological processes. Fold changes are shown in hours post-challenge with WNV. The cut-offs used were *p*-adjusted value of ≤ 0.01 and \log_2 FC of ≥ 0.5 .

Transcript ID	Functional Categories	Gene Description	Log 2 Fold Change 24 hpi	Log 2 Fold Change 48 hpi
AALF016234	Immune response	C-type lectin	1.9178	1.3448

AALF013298		Unspecified product	1.8393	1.3653
AALF003774	Immune response	Fibrinogen and fibronectin	1.7176	0.9609
AALF019859	Immune response	Clip-Domain Serine Protease family B	1.6943	0.8838
AALF008821	Immune response	Defensin antimicrobial peptide	1.6609	1.2091
AALF026731		Unspecified product	1.3463	1.1124
AALF020197	Immune response	Clip-Domain Serine Protease family B	1.1829	-0.8121
AALF020799	Immune response	Peptidoglycan-Recognition Protein	1.1605	0.9047
AALF007525		Unspecified product	1.101	1.3752
AALF016365	Granules fusion	Munc13-4	1.001	0.7821
AALF004571		Unspecified product	0.9935	2.0886
AALF012716	Immune response	Prophenoloxidase	0.9898	-0.7435
AALF006247	Signal peptide processing	Putative microsomal signal peptidase 25 kDa subunit	0.9406	1.315
AALF021835	Response to stress	BiP/GRP78	0.9225	1.5011
AALF005588	Metabolic process	L-lactate dehydrogenase	0.9084	1.4612
AALF019952		Unspecified product	0.8835	0.7852
AALF003990	Metabolic process	Mannosyltransferase	0.8532	1.9477
AALF027716	Metabolic process	Cytochrome P450	0.8222	0.9619
AALF003192	Signal peptide processing	Signal peptidase complex subunit 3	0.8181	1.3067
AALF012257		Peptidylprolyl isomerase	0.8162	0.8641
AALF019397		Putative reticulocalbin calumenin DNA supercoiling factor	0.7763	-0.6983
AALF022020	Response to stress	Chaperonin-60kD	0.7307	0.8416
AALF002466	Response to stress	Protein disulfide-isomerase A6 precursor	0.7157	1.0431
AALF011939	Response to stress	Endoplasmic	0.7090	1.1134
AALF002534	Response to stress	Putative heat-shock protein	0.7058	0.9378
AALF020666	Protein degradation	Ubiquitin	-0.6806	-0.6982
AALF026911		GPCR Orphan/Putative Class B Family	-0.8465	-1.4008
AALF016818		Unspecified product	-0.9540	-0.7674
AALF025231		Unspecified product	-0.9606	-1.3155
AALF028121		Unspecified product	-0.9615	-0.8528
AALF015500	DNA/RNA binding	Zinc finger protein	-0.9737	-0.8797
AALF008709	Transport	Mfs transporter	-1.0332	-0.869
AALF011706		Unspecified product	-1.0328	-1.4222
AALF028505		Unspecified product	-1.1374	-1.8151
AALF020168		Unspecified product	-1.144	-1.354
AALF008099		Endothelin-converting enzyme	-1.1874	-1.8248

AALF000742		Unspecified product	-1.1988	-1.7366
AALF008879	Metabolic process	Type IV inositol 5-phosphatase	-1.2245	-1.7818
AALF004114		No-mechanoreceptor potential a	-1.3925	-1.6563
AALF011390		Putative ecdysone-induced protein	-1.4251	-1.3234
AALF020798		Unspecified product	-1.4691	-1.0245
AALF009909		Unspecified product	-1.5097	-2.148
AALF001259		Unspecified product	-1.5578	-1.5663
AALF012770	Metabolic process	Aldehyde oxidase	-1.578	-1.5924
AALF001105		Unspecified product	-1.6119	-1.4308
AALF002857		Unspecified product	-1.6315	-2.1249
AALF002636		Unspecified product	-1.6362	-1.0520
AALF025810		Unspecified product	-1.7148	-1.4532
AALF013937	Immune-related	Serine protease	-1.7163	-1.7804
AALF014375		Unspecified product	-1.76	-1.8581
AALF013936		Unspecified product	-1.8949	-2.1958
AALF006472		Unspecified product	-1.9349	-2.2863
AALF015014	Immune-related	Clip-Domain Serine Protease family D	-2.39	-1.8778
AALF016295		Unspecified product	-2.3977	-2.43
AALF014395		Unspecified product	-2.7823	-2.4783

Table 3. List of *Ae. albopictus* overlapping differentially expressed transcripts among LamV at 48 hpi, WNV at 24 hpi and dual-infected cells 24 h post-challenge with WNV. Functional categories are based on GO terms for biological processes. The cut-offs used were *p*-adjusted value of ≤ 0.01 and \log_2FC of ≥ 0.5 .

Transcript ID	Functional Categories	Gene Description	Log 2 Fold Change 48 hpi with LamV	Log 2 Fold Change 24 hpi with WNV	Log 2 Fold Change Dual Infection 24 hpi with WNV
AALF004571		DUF3456 domain-containing protein	1.7417	0.9937	0.9935
AALF021835	Response to stress	BIP/GRP78	1.3414	0.9229	0.9225
AALF006247	Signal peptide processing	Putative microsomal signal peptidase 25 kDa subunit	1.2853	0.9409	0.9406
AALF003192	Signal peptide processing	Signal peptidase complex subunit 3	1.1982	0.8185	0.8181
AALF011939	Response to stress	Endoplasmic protein disulfide-isomerase A6 precursor	1.0744	0.71	0.7091
AALF002466	Response to stress	protein disulfide-isomerase A6 precursor	0.9204	0.7162	0.7157
AALF009419		Unspecified product	-0.6904	0.7107	0.7103
AALF012716	Immune response	Prophenoloxidase	-1.0807	0.9904	0.9898

Table 4. List of *Ae. albopictus* overlapping differentially expressed transcripts among LamV at 72 hpi, WNV 48 hpi and dual-infected cells 48 h post-challenge with WNV. Functional categories are based on GO terms for biological processes. The cut-offs used were *p*-adjusted value of ≤ 0.01 and \log_2 FC of ≥ 0.5 .

Transcript ID	Functional Categories	Gene Description	Log 2 Fold Change 72 hpi with LamV	Log 2 Fold Change 48 hpi with WNV	Log 2 Fold Change Dual Infection 48 hpi with WNV
AALF010887		Unspecified product	0.9678	1.3795	1.1146
AALF020693		Unspecified product	1.4466	1.205	1.6044
AALF019136		Unspecified product	0.8331	1.1614	1.0122
AALF014826		Unspecified product	1.0857	1.0462	1.3583
AALF007397		Unspecified product	0.9174	0.8965	0.9974
AALF022151	Immune response	C-type lectin domain-containing protein	0.8748	0.8735	0.8979
AALF005588	Metabolic process	L-lactate dehydrogenase	0.9417	0.8721	1.4612
AALF017030		Unspecified product	0.9909	0.8362	1.1554
AALF007472		Unspecified product	0.8941	0.8249	1.1430
AALF004337		Unspecified product	0.7041	0.7732	0.8306
AALF003871	Metabolic process	Pyrraline-5-carboxylate reductase	1.1609	0.7165	1.3943
AALF010275		Fibrinogen C-terminal domain-containing protein	-0.8091	0.7032	-0.7975
AALF015929	DNA replication	Ribonucleoside-diphosphate reductase	-0.8683	-0.814	-0.9624
AALF024232	DNA replication	Ribonucleoside-diphosphate reductase	-0.8692	-0.8703	-0.9916
AALF015599	DNA replication	DNA helicase	-0.8358	-1.0128	-0.9251
AALF020651	DNA replication	DNA helicase	-0.7573	-1.0216	-0.9155
AALF000130		dNK domain-containing protein	-1.0807	-1.0982	-1.2058
AALF019880	Oxidationreduction process	Dihydropyrimidine dehydrogenase NADP(+)	-1.1569	-1.1089	-1.5552
AALF013610	Oxidationreduction process	Dihydropyrimidine dehydrogenase NADP(+)	-1.2102	-1.1187	-1.6237
AALF022735	DNA replication	DNA helicase	-0.719	-1.1344	-0.9076
AALF013129	Metabolic process	Trehalose-6-phosphate synthase	-1.1882	-1.1725	-1.374
AALF006549	DNA replication	DNA replication licensing factor MCM7	-0.8167	-1.1821	-0.9951
AALF000129	Reverse transcription	Reverse transcriptase domain-containing protein	-1.3339	-1.301	-1.1863

Corrected supplementary tables

Supplementary Table 1. List of *Ae. albopictus* highly differentially expressed transcripts post-infection with LamV. Bold numbers have p-adjust value ≤ 0.01 .

Transcript ID	Gene description	Log2fold change 24 hpi with LamV	Log2fold change 48 hpi with LamV	Log2fold change 72 hpi with LamV
AALF020879	Unspecified product	1.1007825	0.8807227	0.3866261
AALF012914	Unspecified product	1.076227	0.8998677	0.5763329
AALF005471	40S ribosomal protein S21	1.0561793	1.1301156	0.8499839
AALF002626	40S ribosomal protein S21	1.0391225	0.9034112	0.9353855
AALF017826	COX6C domain-containing protein	1.003273	1.1100965	0.6565772
AALF005278	Unspecified product	1.070659	8.383706	1.470771
AALF010569	J domain-containing protein	1.423451	3.762497	3.089864
AALF004571	DUF3456 domain-containing protein	0.369584	1.741722	1.934055
AALF010775	CHCH domain-containing protein	-0.2322116	1.698708	1.851144
AALF003990	Mannosyltransferase	0.4896979	1.540506	1.624327
AALF005663	Lethal(2)essential for life protein	0.4409692	1.3782	1.239109
AALF006960	Derlin	0.4897895	1.353837	1.159904
AALF011414	Unspecified product	0.6123769	1.348851	1.485332
AALF021835	BiP/GRP78	0.0521019	1.341346	1.256646
AALF006247	Putative microsomal signal peptidase 25 kDa subunit	0.2287779	1.285252	1.245623
AALF004828	Putative secreted protein	0.1948594	1.279856	0.7969391
AALF025486	Unspecified product	0.07664198	1.267016	1.478177
AALF013670	Unspecified product	0.6266047	1.261473	1.126339
AALF014036	DUF4536 domain-containing protein	0.6570504	1.255597	1.063209
AALF002158	Unspecified product	0.8851927	1.242752	0.6221746
AALF005738	Unspecified product	0.2372859	1.226492	1.488199
AALF010933	Unspecified product	0.5663689	1.211847	0.4072971
AALF003192	Signal peptidase complex subunit 3	0.3584623	1.198195	1.085948
AALF021815	Sulfhydryl oxidase	0.4858074	1.173338	1.42583
AALF009959	UDP-galactose transporter	0.2799828	1.155953	0.7264897
AALF002306	Unspecified product	0.3867898	1.154484	1.010245
AALF020693	Unspecified product	0.6484965	1.152027	1.446582
AALF013715	Unspecified product	0.3637135	1.116227	1.486534
AALF026819	Unspecified product	0.24784	1.105091	0.6976028
AALF002752	Unspecified product	0.1249299	1.097932	1.290456
AALF005644	Protein KRTCAP2 homolog	0.7297483	1.093221	1.292127
AALF017325	Unspecified product	0.7063908	1.076691	1.090357
AALF011939	Endoplasmic reticulum chaperone protein	-	1.074381	0.7869695
AALF023162	Sep15_SelM domain-containing protein	0.01247764	1.062401	0.774628

AALF012595	EGF-like domain-containing protein	0.2309633	1.03551	0.7731769
AALF002612	Putative mitochondrial respiratory chain complex i	0.7860392	1.033104	0.4602109
AALF005815	Unspecified product	0.7577992	1.027366	0.6114254
AALF012691	Dolichyl-diphosphooligosaccharide--protein glycosyltransferase subunit DAD1	0.4385175	1.003161	0.7334291
AALF021504	Unspecified product	0.05690824	1.000615	0.8290051
AALF013722	DNA polymerase	-0.1758396	-1.030878	- 0.7074312
AALF012716	Prophenoloxidase	- 0.00328026	-1.080676	-1.158936
AALF003040	Unspecified product	- 0.07732382	-1.128587	- 0.872005
AALF016470	Carboxylic ester hydrolase	-0.2525955	-1.228183	- 1.941993
AALF013640	J domain-containing protein	0.2058961	1.454135	2.219441
AALF012753	CHCH domain-containing protein	- 0.0848552	1.094434	1.618056
AALF003110	Unspecified product	0.1726768	0.9771449	1.595991
AALF003128	4-nitrophenylphosphatase	0.2800827	1.130961	1.506854
AALF011149	LITAF domain-containing protein	0.5978697	0.5813468	1.474247
AALF007387	Unspecified product	0.3064848	0.4136308	1.397007
AALF022006	Belongs to the HAD-like hydrolase superfamily	0.03553227	0.9656749	1.37911
AALF026344	Belongs to the GrpE family	0.276744	0.6026283	1.352243
AALF026694	GrpE protein homolog	0.2328192	0.7674576	1.343766
AALF028423	Poly [ADP-ribose] polymerase	0.2564356	0.9403602	1.320982
AALF019485	Brix domain-containing protein	0.298015	0.5606408	1.293807
AALF024199	HSP-70 binding protein	0.2911548	0.937389	1.285139
AALF015016	Lethal(2)essential for life protein, l2efl	0.1448895	0.9515613	1.262915
AALF019596	Unspecified product	0.3491548	0.9800304	1.24109
AALF023086	sil1	0.2884911	0.9257331	1.230209
AALF024273	39S ribosomal protein L34	0.7704319	0.6254313	1.204776
AALF007525	LITAF domain-containing protein	0.08092908	0.6450121	1.203538
AALF027170	Unspecified product	-0.1976002	0.09772569	1.200941
AALF017272	60S ribosome subunit biogenesis protein NIP7 homolog	0.491903	0.2173325	1.180087
AALF026705	Putative mitochondrial import inner membrane translocase subunit tim8	0.5790996	0.8504171	1.162328
AALF008938	Putative vesicle coat complex copi zeta subunit	0.5591313	0.9633468	1.16147
AALF003871	Pyrroline-5-carboxylate reductase	0.200374	0.66144	1.160881
AALF019391	Unspecified product	0.3202892	0.8789991	1.16038
AALF001937	Unspecified product	-0.0548677	- 0.0161363	1.158324
AALF028288	Unspecified product	-0.0135346	0.6634267	1.136348
AALF015083	Unspecified product	0.223505	0.472875	1.13188
AALF009537	Unspecified product	0.6068302	0.7303727	1.130737
AALF005816	ER membrane protein complex subunit 4	0.4202528	0.7919172	1.1298
AALF020200	Mitochondrial ornithine transporter	0.0001999	0.657188	1.101382

AALF017894	Pyrroline-5-carboxylate reductase	0.3309345	0.6657954	1.100626
AALF018519	Nudix hydrolase domain-containing protein	0.5294038	0.8126458	1.099751
AALF027267	39S ribosomal protein L22	0.5799748	0.7631426	1.09169
AALF014826	Unspecified product	0.2878033	0.6764529	1.085734
AALF001439	F-box domain-containing protein	0.06645684	0.3154198	1.082065
AALF016188	Eukaryotic translation initiation factor	0.06100736	0.5592943	1.081972
AALF002862	39S mitochondrial ribosomal protein L28	0.2910054	0.5870734	1.069795
AALF020008	Putative growth hormone-induced protein	-0.006332	0.7761615	1.062631
AALF019423	Signal peptidase complex catalytic subunit SEC11	0.2625324	0.9980706	1.061741
AALF001336	Putative selenoprotein g	0.2460123	0.8840983	1.058822
AALF017936	Unspecified product	0.00503888	0.4404364	1.049836
AALF016828	Unspecified product	0.2801819	0.6978125	1.039622
AALF022971	RING-CH-type domain-containing protein	-0.0489947	0.5155786	1.029267
AALF023408	Unspecified product	0.2667787	0.2500093	1.0214
AALF001047	Unspecified product	0.7860621	0.8913614	1.010322
AALF000279	PHB domain-containing protein	-0.1072049	0.6288148	1.00996
AALF020872	Putative secreted protein	0.4933395	0.2566414	1.00956
AALF015963	Unspecified product	0.3890462	0.588934	1.005786
AALF003447	Unspecified product	0.3968716	0.6264433	1.005658
AALF002436	DUF155 domain-containing protein	0.2132055	0.474343	1.000329
AALF015692	Unspecified product	-0.2445191	-0.5983319	-1.000702
AALF008397	ANK_REP_REGION domain-containing protein	-0.3622025	-0.3768843	-1.00432
AALF028546	GH16 domain-containing protein	0.08596353	-0.7611696	-1.007024
AALF017425	VWFC domain-containing protein	-0.2377081	-0.5222454	-1.023797
AALF013861	Unspecified product	-0.3352368	-0.6561688	-1.031227
AALF006764	Reverse transcriptase domain-containing protein	-0.339622	-0.5631402	-1.044918
AALF016175	Matrix metalloproteinase	-0.0487227	-0.6250816	-1.045732
AALF008809	Nidogen	-0.0576379	-0.5538478	-1.046655
AALF022970	Unspecified product	-0.1540925	-0.2983582	-1.050129
AALF002486	Reverse transcriptase Ty1/copia-type domain-containing protein	-0.3677937	-0.2913728	-1.05021
AALF025212	Transferrin	-0.0235114	-0.3430315	-1.0533
AALF023670	Unspecified product	0.07874719	-0.3262371	-1.057191
AALF021839	Sodium/solute symporter	-0.0432109	-0.3285024	-1.060132
AALF025224	Integrase catalytic domain-containing protein	0.1379983	-0.2584586	-1.060825
AALF023157	Tyrosinase_Cu-bd domain-containing protein	-0.1244129	-0.5119304	-1.063361
AALF003039	Prophenoloxidase	-0.0932836	-0.5654061	-1.068579
AALF000130	dNK domain-containing protein	0.1161716	-0.4901234	-1.080715
AALF011858	Vitellogenin domain-containing protein	-0.4364447	-0.4191864	-1.085945
AALF017340	RGS domain-containing protein	-0.205529	-0.3564582	-1.107644
AALF008038	Y-box binding protein	-0.3709235	-0.4420188	-1.113271
AALF005743	Reverse transcriptase Ty1/copia-type domain-containing protein	-0.0664089	-0.7695397	-1.119569

AALF021923	Gamma-glutamyl hydrolase	-0.0156154	-0.7932295	-1.130118
AALF008037	Unspecified product	-0.2542754	-0.6514822	-1.133915
AALF018011	Unspecified product	-0.1230375	-0.3236634	-1.13611
AALF007570	Clip-Domain Serine Protease family B	-0.0063752	-0.7162002	-1.140533
AALF004790	Unspecified product	-0.1600798	-0.5565066	-1.144223
AALF012770	Aldehyde oxidase	-0.1185153	-0.2976834	-1.149121
AALF005637	Belongs to the short-chain dehydrogenases/reductases (SDR) family	0.3816711	-0.2149534	-1.153221
AALF019880	Dihydropyrimidine dehydrogenase [NADP(+)]	-0.1997018	-0.16973	-1.15694
AALF011617	Unspecified product	-0.0601377	-0.4961643	-1.162532
AALF023601	Peroxidasin	-0.3605996	-0.6109085	-1.162776
AALF013089	tRNA_NucTransf2 domain-containing protein	-0.029201	-0.3629525	-1.187594
AALF013129	Trehalose-6-phosphate synthase	-0.3021912	-0.2940175	-1.188147
AALF001667	Unspecified product	-0.1173959	-0.5123251	-1.200283
AALF006674	Integrase catalytic domain-containing protein	-0.1045049	-0.3527618	-1.200592
AALF013610	Dihydropyrimidine dehydrogenase [NADP(+)]	-0.288467	-0.2416942	-1.210148
AALF008099	Endothelin-converting enzyme	-0.1692418	-0.3668569	-1.213919
AALF006673	Retrotrans_gag domain-containing protein	-0.2346717	-0.248288	-1.219057
AALF016666	FHA domain-containing protein	-0.1639121	-0.5361408	-1.227832
AALF004114	No-mechanoreceptor potential a	-0.0880921	-0.640587	-1.236066
AALF024124	Cytochrome P450	-0.0405503	-0.3416231	-1.253808
AALF011816	Integrase catalytic domain-containing protein	0.05181979	-0.1891046	-1.256912
AALF007569	Peptidase S1 domain-containing protein	0.1836759	-0.5385332	-1.282594
AALF016566	Unspecified product	-0.4462772	-0.5411715	-1.295623
AALF000129	Reverse transcriptase domain-containing protein	-0.0227107	-0.450496	-1.333944
AALF019918	Unspecified product	-0.1753625	-0.5397008	-1.356561
AALF016286	B box-type domain-containing protein	-0.1289051	-0.6169772	-1.373966
AALF014933	Prophenoloxidase	-0.050841	-0.5672947	-1.468056
AALF004309	Putative sodium/potassium-transporting atpase subunit beta-2	-0.0218463	-0.5307739	-1.494088
AALF006581	CHK domain-containing protein	0.05218336	-0.4413908	-1.50691
AALF012955	Serine protease	0.126381	-0.7453164	-1.580942
AALF022750	Unspecified product	-0.6364584	-0.9838494	-1.678908
AALF020600	RT_RNaseH domain-containing protein	-0.3410249	-0.4177124	-1.84908
AALF007138	Histone H2A	0.1922345	0.2182378	-1.930249
AALF003951	Reverse transcriptase Ty1/copia-type domain-containing protein	-0.052237	-0.4257642	-2.018862
AALF010649	Histone H2A	0.6116419	0.1365626	-2.08943
AALF010137	Histone H2B	0.3630782	-0.3503547	-2.173293
AALF014537	Histone H2B	0.05754468	-0.4322638	-2.348725
AALF024096	Unspecified product	-0.1082195	-0.4999374	-2.534106
AALF010648	Histone H2B	0.148153	-0.3245741	-2.537068
AALF028233	Unspecified product	-0.6222383	0.3145327	-5.994889

Supplementary Table 2. List of *Ae. albopictus* highly differentially expressed transcripts post-infection with WNV. Bold numbers have p-adjust value ≤ 0.01 .

Transcript ID	Gene description	Log 2 Fold change 24 hpi with WNV	Log 2 Fold change 48 hpi with WNV
AALF021807	C-Type Lysozyme (Lys-E)	2.6372037	0.8025715
AALF003252	Unspecified product	2.1519817	1.300595
AALF016234	C-Type Lectin	1.9184949	1.249253
AALF010414	Beta-hexosaminidase b	1.864307	0.2724963
AALF026511	Carbonic anhydrase	1.8476415	0.1142675
AALF013298	Unspecified product	1.8394748	1.151182
AALF022426	Unspecified product	1.7650766	0.01971445
AALF009966	Unspecified product	1.7598895	0.6423143
AALF003774	Fibrinogen and fibronectin	1.7178943	1.266782
AALF019859	Clip-Domain Serine Protease family B	1.6947263	0.966631
AALF008821	Defensin anti-microbial peptide	1.6613609	1.761353
AALF008776	Aromatic amino acid decarboxylase	1.6518397	0.4000478
AALF022425	Unspecified product	1.4825905	0.3589861
AALF009414	Putative secreted protein	1.438856	0.6759361
AALF026731	Unspecified product	1.3467243	1.995125
AALF001194	Unspecified product	1.3249252	0.7166746
AALF008229	Unspecified product	1.2970297	0.8472885
AALF001093	Calreticulin	1.2731894	-0.1958079
AALF007742	Unspecified product	1.2648141	0.3556404
AALF020341	Unspecified product	1.2636761	0.5916352
AALF023135	Unspecified product	1.2568938	0.4868306
AALF016505	Leucine-rich immune protein	1.2260744	0.4717319
AALF025212	Transferrin	1.2027562	1.315821
AALF020197	Clip-Domain Serine Protease family B	1.1833156	-0.07211203
AALF020799	Peptidoglycan Recognition Protein	1.1608113	1.0099
AALF000812	Unspecified product	1.1569915	0.2970094
AALF001195	Unspecified product	1.1031906	0.9905867
AALF007525	Unspecified product	1.1011041	0.6134934
AALF008452	Unspecified product	1.0815722	1.034753
AALF003040	Unspecified product	1.0629233	0.4579892
AALF015567	Cystathionine beta-synthase	1.0595983	0.3060131
AALF014689	Fibrinogen and fibronectin	1.0296858	0.281372
AALF002418	Imaginal disc growth factor	1.0188928	1.015853
AALF023540	Unspecified product	1.017626	-0.03019209
AALF001232	Pyruvate carboxylase	1.0104643	-0.4878112
AALF016365	Munc13-4	1.0016484	0.239946
AALF011706	Unspecified product	-1.033549	0.03868099
AALF028505	Unspecified product	-1.137095	-1.108366

AALF020168	Unspecified product	-1.143613	-0.09368173
AALF025541	Unspecified product	-1.184193	0.1421991
AALF008099	Endothelin-converting enzyme	-1.186822	-0.5916785
AALF000742	Unspecified product	-1.199468	0.1120206
AALF008879	Type IV inositol 5-phosphatase	-1.221238	-1.008826
AALF016756	Sugar transporter	-1.221253	0.00056474
AALF022022	cdk11/4	-1.372345	-0.1809358
AALF004114	No-mechanoreceptor potential a	-1.391372	0.1187877
AALF011390	Putative ecdysone-induced protein	-1.422543	-0.3419561
AALF020798	Unspecified product	-1.468631	-0.1163336
AALF000142	Unspecified product	-1.494117	-0.422724
AALF009909	Unspecified product	-1.510331	-0.4373976
AALF001259	Unspecified product	-1.557639	-0.01361896
AALF014478	Heat shock protein HSP70	-1.570458	0.6253193
AALF012770	Aldehyde oxidase	-1.578028	-0.3088155
AALF001105	Unspecified product	-1.611167	0.2682663
AALF002857	Unspecified product	-1.631311	-0.6544968
AALF002636	Unspecified product	-1.635795	-0.01411748
AALF014479	Unspecified product	-1.65992	0.815089
AALF025810	Unspecified product	-1.713488	-0.267314
AALF013937	Serine protease	-1.715828	-0.3631766
AALF014375	Unspecified product	-1.759671	-0.5510356
AALF014481	Unspecified product	-1.785452	0.71727
AALF027745	Microtubule-associated protein	-1.791805	0.2014485
AALF009202	C-Type Lectin (CTL)	-1.815209	0.19416
AALF006472	Unspecified product	-1.934769	-0.5821929
AALF015015	Unspecified product	-2.363056	1.356423
AALF015014	Clip-Domain Serine Protease family D	-2.391395	-0.4717112
AALF016295	Unspecified product	-2.397042	-0.6990839
AALF014395	Unspecified product	-2.782113	-0.6543776
AALF028496	Unspecified product	-4.895226	0.1240877
AALF005731	Zinc finger protein	-5.038072	0.2833406
AALF009658	Unspecified product	-0.1134117	1.493714
AALF019759	Unspecified product	0.2583801	1.465533
AALF000656	Cecropin-A2	1.225066	1.442737
AALF010887	Unspecified product	-0.031884	1.379511
AALF011779	Unspecified product	0.5846527	1.334395
AALF005659	Unspecified product	-0.1387396	1.214115
AALF020693	Unspecified product	-0.405231	1.205022
AALF005658	Unspecified product	-0.5381896	1.174924
AALF019136	Unspecified product	-0.2241327	1.161433
AALF015016	Lethal(2)essential for life protein, l2efl	-0.9658264	1.124133
AALF011176	Acylphosphatase	0.06477895	1.119349

AALF000457	Unspecified product	0.1633997	1.112949
AALF023579	Unspecified product	0.05319677	1.104375
AALF026129	UPF0184 protein	0.2845786	1.064956
AALF025560	c4b-binding protein beta chain	0.8701129	1.057865
AALF014826	Unspecified product	0.2497668	1.046224
AALF013319	Unspecified product	0.6984156	1.045979
AALF018157	Unspecified product	0.7260884	1.015808
AALF002626	40S ribosomal protein S21	-0.1750513	1.00806
AALF006531	Unspecified product	0.8157919	1.007922
AALF016228	Dolichol-phosphate mannosyltransferase subunit 3	0.3953703	1.005824
AALF015599	Unspecified product	0.4818058	-1.012842
AALF015221	Unspecified product	0.293846	-1.01462
AALF020651	Unspecified product	0.4533418	-1.021637
AALF014559	Unspecified product	0.7006329	-1.022585
AALF021818	Unspecified product	-0.2146883	-1.031931
AALF016237	Unspecified product	0.4733015	-1.042688
AALF024446	Unspecified product	0.5832255	-1.072474
AALF015711	Unspecified product	0.8083658	-1.083662
AALF000130	Unspecified product	0.5508883	-1.098217
AALF019880	Unspecified product	0.09564294	-1.108888
AALF009765	Unspecified product	-0.2477456	-1.111471
AALF013917	Unspecified product	0.7310686	-1.116179
AALF013610	Unspecified product	0.1027376	-1.118646
AALF020871	Unspecified product	0.5122051	-1.12258
AALF022735	Unspecified product	0.7383496	-1.134409
AALF006220	Unspecified product	0.414661	-1.134671
AALF017380	Unspecified product	0.6320428	-1.14621
AALF013129	Unspecified product	-0.2855924	-1.172501
AALF006549	Unspecified product	0.5887173	-1.182078
AALF022033	Unspecified product	0.01514515	-1.184795
AALF018633	Unspecified product	-0.4998514	-1.214489
AALF008765	Unspecified product	-0.07212149	-1.21789
AALF025208	Unspecified product	0.6698941	-1.242304
AALF013096	Unspecified product	0.2124903	-1.285949
AALF020652	Unspecified product	0.5726187	-1.290996
AALF000129	Unspecified product	0.6656714	-1.301079
AALF021783	Unspecified product	0.8720385	-1.358839
AALF013722	Unspecified product	0.7220427	-1.389258
AALF013353	Unspecified product	0.7780424	-1.464347

Supplementary Table 3. List of *Ae. albopictus* highly differentially expressed transcripts post dual-infection. Fold change is shown post WNV challenge. Bold numbers have p-adjust value ≤ 0.01

Transcript ID	Gene description	Log 2 Fold change 24 hpi with WNV	Log 2 Fold change 48 hpi with WNV
AALF021807	C-Type Lysozyme (Lys-E)	2.6371611	0.7203514
AALF003252	Unspecified product	2.1516682	0.8378027
AALF016234	C-Type Lectin	1.9178303	1.344769
AALF010414	Beta-hexosaminidase b	1.8640928	0.109577
AALF013298	Unspecified product	1.8392713	1.365333
AALF022426	Unspecified product	1.7647536	0.0916418
AALF009966	Unspecified product	1.7595648	0.5794698
AALF003774	Fibrinogen and fibronectin	1.717618	0.9609377
AALF019859	Clip-Domain Serine Protease family B	1.6943265	0.8838267
AALF008821	Defensin anti-microbial peptide	1.6609376	1.209078
AALF008776	Aromatic amino acid decarboxylase	1.6513976	0.3277108
AALF022425	Unspecified product	1.4823759	0.5397199
AALF009414	Putative secreted protein	1.438657	0.682217
AALF026731	Unspecified product	1.3463197	1.112376
AALF001194	Unspecified product	1.3245046	-0.0090203
AALF008229	Unspecified product	1.2966794	0.05213324
AALF001093	Calreticulin	1.2727314	0.170624
AALF007742	Unspecified product	1.2644508	-0.6028099
AALF020341	Unspecified product	1.2633052	-0.04071043
AALF023135	Unspecified product	1.2565623	-0.111073
AALF016505	Leucine-rich immune protein	1.2257511	-0.1558631
AALF025212	Transferrin	1.2022837	-0.03396152
AALF020197	Clip-Domain Serine Protease family B	1.1829333	-0.8121424
AALF020799	Peptidoglycan Recognition Protein	1.1604789	0.9046648
AALF000812	Unspecified product	1.1566901	-0.4478676
AALF001195	Unspecified product	1.1027901	0.08780285
AALF007525	Unspecified product	1.1005816	1.375204
AALF008452	Unspecified product	1.08121	0.07771275
AALF015567	Cystathionine beta-synthase	1.0593735	0.3151985
AALF014689	Fibrinogen and fibronectin	1.0292969	-0.3256825
AALF002418	Imaginal disc growth factor	1.0181351	0.4970238
AALF023540	Unspecified product	1.0172458	0.0020
AALF023089	Serine--pyruvate aminotransferase	1.0131823	0.4110143
AALF001232	Pyruvate carboxylase	1.0099912	-0.1621548
AALF016365	Munc13-4	1.0012583	0.7820547
AALF011706	Unspecified product	-1.0328208	-1.422239
AALF008709	Mfs transporter	-1.0332126	-0.868967
AALF028505	Unspecified product	-1.1374374	-1.815143

AALF020168	Unspecified product	-1.1439461	-1.354041
AALF025541	Unspecified product	-1.1853102	-0.8665145
AALF008099	Endothelin-converting enzyme	-1.1873574	-1.82479
AALF000742	Unspecified product	-1.1988357	-1.736559
AALF010788	Unspecified product	-1.2092883	-0.4826923
AALF008879	Type IV inositol 5-phosphatase	-1.2214493	-1.781791
AALF016756	Sugar transporter	-1.2214661	-0.5646973
AALF005838	Unspecified product	-1.2858563	-0.5469924
AALF022022	cdk1l/4	-1.3726316	-0.5772162
AALF004114	No-mechanoreceptor potential a	-1.3925384	-1.656296
AALF011390	Putative ecdysone-induced protein	-1.4251159	-1.323415
AALF020798	Unspecified product	-1.4690903	-1.024524
AALF000142	Unspecified product	-1.494289	-0.9575368
AALF009909	Unspecified product	-1.5096536	-2.148011
AALF001259	Unspecified product	-1.5578043	-1.566307
AALF014478	Heat shock protein HSP70	-1.5706274	-0.3475951
AALF012770	Aldehyde oxidase	-1.5780432	-1.592426
AALF001105	Unspecified product	-1.6118557	-1.430825
AALF002857	Unspecified product	-1.6315333	-2.12488
AALF002636	Unspecified product	-1.6361542	-1.05204
AALF014479	Unspecified product	-1.6606975	-0.6525477
AALF025810	Unspecified product	-1.7148038	-1.453152
AALF013937	Serine protease	-1.7163273	-1.780422
AALF014375	Unspecified product	-1.7596912	-1.858132
AALF014481	Unspecified product	-1.786233	-0.6557541
AALF027745	Microtubule-associated protein	-1.7923202	-1.093662
AALF009202	C-Type Lectin (CTL)	-1.8149303	-1.139927
AALF013936	Unspecified product	-1.8948828	-2.195835
AALF006472	Unspecified product	-1.934909	-2.286312
AALF018782	Unspecified product	-2.148395	-0.8497697
AALF015015	Unspecified product	-2.3632105	-0.4439168
AALF015014	Clip-Domain Serine Protease family D	-2.39003	-1.877799
AALF016295	Unspecified product	-2.3977265	-2.429996
AALF014395	Unspecified product	-2.7822935	-2.478255
AALF028496	Unspecified product	-4.892907	-0.4011087
AALF005731	Zinc finger protein	-5.0366567	-0.4863022
AALF010569	Unspecified product	1.740684	3.808917
AALF001962	Unspecified product	-1.062751	2.784968
AALF013640	Unspecified product	0.4174449	2.241564
AALF018203	Mitogen-activated protein kinase	0.2227864	2.167032
AALF004571	Unspecified product	0.9935221	2.088632
AALF013285	Unspecified product	-0.0400942	2.029161
AALF019759	Unspecified product	0.2578946	1.948348

AALF003990	Mannosyltransferase	0.853202	1.947694
AALF003128	4-nitrophenylphosphatase	0.8776709	1.82398
AALF003110	Unspecified product	0.4680416	1.762361
AALF005738	Unspecified product	0.5153181	1.72073
AALF013715	Unspecified product	0.7617375	1.652631
AALF025486	Unspecified product	0.6192941	1.650474
AALF011149	Unspecified product	0.1360631	1.644787
AALF011886	Mitogen-activated protein kinase	0.5438541	1.637723
AALF010775	Unspecified product	1.627517	1.634653
AALF011414	Unspecified product	0.4331776	1.607814
AALF020693	Unspecified product	-0.4049599	1.604364
AALF022006	Unspecified product	1.162805	1.599921
AALF003569	Unspecified product	0.9762325	1.596865
AALF002752	Unspecified product	0.5514676	1.579261
AALF001937	Unspecified product	0.647978	1.576332
AALF021815	Sulfhydryl oxidase	0.2615741	1.523302
AALF027170	Unspecified product	-0.07099947	1.505943
AALF026344	Unspecified product	0.4067483	1.501238
AALF021835	BiP/GRP78	0.9225128	1.501091
AALF027168	Pcdc2/rp-8	0.8273775	1.466495
AALF005588	L-lactate dehydrogenase	0.9084434	1.461238
AALF026694	GrpE protein homolog	0.6782464	1.460043
AALF023086	Sil1	0.1769638	1.456167
AALF012753	Unspecified product	1.081563	1.452282
AALF024273	39S ribosomal protein L34	0.4278898	1.427921
AALF019596	Unspecified product	0.4443897	1.427778
AALF007470	Unspecified product	0.1976043	1.402671
AALF003871	Unspecified product	0.4446915	1.394271
AALF005644	Protein KRTCAP2 homolog	-0.02129383	1.377517
AALF017272	60S ribosome subunit biogenesis protein NIP7 homolog	0.4204127	1.375071
AALF028423	Poly [ADP-ribose] polymerase	0.04549477	1.374508
AALF019485	Unspecified product	0.5563411	1.374462
AALF007387	Unspecified product	0.5142646	1.37176
AALF003976	Unspecified product	1.017919	1.369269
AALF014826	Unspecified product	0.2494335	1.358271
AALF006960	Derlin	0.3679644	1.339335
AALF014725	Unspecified product	0.7405399	1.33051
AALF008938	Putative vesicle coat complex copI zeta subunit	0.4739701	1.328079
AALF006247	Putative microsomal signal peptidase 25 kDa subunit	0.940603	1.314961
AALF003192	Signal peptidase complex subunit 3	0.8180742	1.306711
AALF019423	Signal peptidase complex catalytic subunit SEC11	0.7220617	1.297388
AALF026705	Putative mitochondrial import inner membrane translocase subunit tim8	0.07451373	1.296001
AALF005816	ER membrane protein complex subunit 4	0.5836886	1.269729

AALF018519	Unspecified product	0.3752417	1.267043
AALF017894	Pyrroline-5-carboxylate reductase	0.2383656	1.266109
AALF010277	L-lactate dehydrogenase	0.6285311	1.265367
AALF017936	Unspecified product	0.08214152	1.26359
AALF027267	39S ribosomal protein L22	0.4062505	1.261865
AALF019139	Hect E3 ubiquitin ligase	0.09166593	1.24913
AALF021211	Unspecified product	0.6587264	1.212402
AALF018192	Kinase	0.566552	1.208745
AALF006811	Metaxin	0.8366219	1.207895
AALF023408	Unspecified product	0.4289006	1.204661
AALF013670	Unspecified product	0.8006446	1.202066
AALF017066	Unspecified product	0.2050764	1.200726
AALF002862	39S mitochondrial ribosomal protein L28	0.5056599	1.190748
AALF028288	Unspecified product	0.194947	1.189041
AALF016188	Eukaryotic translation initiation factor	0.7354959	1.185777
AALF012726	Unspecified product	0.4295454	1.175719
AALF015083	Unspecified product	0.3610579	1.170427
AALF023527	Unspecified product	0.2127	1.169133
AALF025878	Unspecified product	0.4748845	1.165725
AALF002306	Unspecified product	0.7093045	1.165664
AALF002436	Unspecified product	0.263209	1.165386
AALF016399	Unspecified product	0.581796	1.164069
AALF015963	Unspecified product	-0.0169975	1.160791
AALF017030	Unspecified product	0.4822692	1.15538
AALF010131	Unspecified product	0.6806408	1.153957
AALF017935	Stearoyl-coa desaturase	-0.02939566	1.146435
AALF024308	Unspecified product	0.4689312	1.145748
AALF007472	Unspecified product	0.1699452	1.143047
AALF003428	Unspecified product	1.032048	1.141519
AALF027123	Long-chain-fatty-acid coa ligase	0.5172992	1.138998
AALF001336	Putative selenoprotein g	0.4797149	1.136878
AALF023156	tRNA (adenine(58)-N(1))-methyltransferase catalytic subunit TRMT61A	0.4250858	1.129128
AALF002987	Unspecified product	0.1813468	1.124039
AALF008836	Unspecified product	0.1985597	1.122516
AALF017325	Unspecified product	0.1050834	1.1178
AALF020872	Putative secreted protein	0.3686121	1.115598
AALF021933	Unspecified product	0.1182372	1.115378
AALF010887	Unspecified product	-0.03252791	1.114611
AALF008678	Choline-phosphate cytidyltransferase a, b	0.9927097	1.113623
AALF011939	Endoplasmic	0.7090556	1.11336
AALF021504	Unspecified product	0.3848204	1.106931
AALF015904	Unspecified product	0.5454898	1.106172
AALF026342	Unspecified product	0.4879757	1.105911

AALF001505	Cell adhesion molecule	0.103493	1.105461
AALF006812	Short-chain dehydrogenase	0.3044513	1.091256
AALF010373	Phosphoglycerate mutase	0.1338896	1.091255
AALF008913	Unspecified product	0.4315325	1.084558
AALF006680	Unspecified product	0.3917734	1.080363
AALF020200	Mitochondrial ornithine transporter	0.5108838	1.079608
AALF009639	Unspecified product	0.7827637	1.073397
AALF012016	Dnaj homolog subfamily B member 11 precursor	0.3118379	1.070781
AALF020282	Unspecified product	0.4982286	1.069055
AALF002846	Putative cpj005033 nucleolar protein nhp2	0.6466115	1.068664
AALF001439	Unspecified product	0.1340644	1.068367
AALF000613	Unspecified product	0.3972053	1.066201
AALF014036	Unspecified product	0.3548569	1.063397
AALF016160	Activating signal cointegrator 1 complex subunit 3, helc1	0.2648123	1.05902
AALF013787	Unspecified product	-0.02808245	1.055177
AALF016639	Unspecified product	-0.03593101	1.050282
AALF026969	Unspecified product	0.3458147	1.044093
AALF002466	Protein disulfide-isomerase A6 precursor	0.7157289	1.043132
AALF003447	Unspecified product	0.2911015	1.038312
AALF013154	Unspecified product	0.6795145	1.037396
AALF019760	Unspecified product	0.8736492	1.018174
AALF020008	Putative growth hormone-induced protein	0.7987033	1.016941
AALF019136	Unspecified product	-0.2243095	1.012166
AALF001501	Phosphoglucomutase	0.3496378	1.011161
AALF022744	Mitochondria associated granulocyte macrophage csf signaling molecule	0.01735893	1.009088
AALF014037	Cle7	0.3943556	1.002068
AALF009537	Unspecified product	-0.01112283	1.00013
AALF003854	Repressor of RNA polymerase III transcription MAF1	-0.06328337	-1.002003
AALF023601	Peroxidasin	0.6720596	-1.005328
AALF013429	Unspecified product	-0.7905049	-1.005731
AALF006047	Unspecified product	-0.49561	-1.007391
AALF026258	DNA helicase	-0.4060362	-1.008038
AALF023157	Unspecified product	-0.1218915	-1.020093
AALF003039	Prophenoxidase	-0.1814269	-1.020292
AALF015542	Unspecified product	0.3121525	-1.023989
AALF008037	Unspecified product	0.03058438	-1.027351
AALF016899	Unspecified product	-0.2230217	-1.029382
AALF023425	Unspecified product	-0.458523	-1.030735
AALF011299	Gamma glutamyl transpeptidases	-0.8400709	-1.038228
AALF017425	Unspecified product	0.6683729	-1.038664
AALF021839	Sodium/solute symporter	-0.5671954	-1.045419
AALF027385	Adenylate cyclase	-0.3352958	-1.045712
AALF005533	Unspecified product	-0.584051	-1.060107

AALF011858	Unspecified product	-0.933535	-1.066504
AALF008809	Nidogen	0.3225722	-1.076963
AALF024686	Unspecified product	-0.5250034	-1.078654
AALF015269	Unspecified product	-0.5795056	-1.088378
AALF020706	Bifunctional purine biosynthesis protein	-0.2469478	-1.098325
AALF019525	Unspecified product	-0.9502853	-1.099509
AALF000395	Unspecified product	0.150742	-1.135805
AALF018338	F-spondin	0.1487004	-1.143845
AALF003944	Unspecified product	-0.7981504	-1.155032
AALF025462	Unspecified product	-1.194596	-1.168561
AALF000129	Unspecified product	0.6643426	-1.186293
AALF008893	Unspecified product	-0.4251912	-1.193101
AALF024829	Brain chitinase and chia	-0.3246557	-1.196701
AALF011491	Unspecified product	0.2616987	-1.19972
AALF015943	Methylenetetrahydrofolate dehydrogenase	0.3172626	-1.200496
AALF008765	Glutamate synthase	-0.07316092	-1.204769
AALF000130	Unspecified product	0.5505672	-1.205756
AALF022389	Unspecified product	-0.1332124	-1.211223
AALF007615	Unspecified product	-0.9829718	-1.213565
AALF005637	Unspecified product	-0.4658423	-1.214647
AALF007101	Unspecified product	-0.2902726	-1.230073
AALF019868	F-spondin	0.4292185	-1.23676
AALF007246	Unspecified product	-0.09800467	-1.239226
AALF009035	Cyclin a	-0.6483297	-1.239941
AALF007570	Clip-Domain Serine Protease family B. Protease homologue	0.2176238	-1.24319
AALF009765	Glutamate synthase	-0.2481691	-1.251454
AALF027905	Prophenoloxidase	0.2514348	-1.256435
AALF023670	Unspecified product	-0.4726193	-1.256462
AALF005743	Unspecified product	-0.6574452	-1.259283
AALF012739	Alpha-mannosidase	-0.4013183	-1.263318
AALF027708	Unspecified product	-0.4274602	-1.263785
AALF013089	Unspecified product	-0.4472785	-1.274875
AALF021923	Gamma-glutamyl hydrolase	0.1039451	-1.275234
AALF012022	Sodium-dependent phosphate transporter	-0.1964669	-1.280561
AALF016175	Matrix metalloproteinase	-0.4403291	-1.291947
AALF014285	Unspecified product	-0.9509276	-1.296985
AALF002486	Unspecified product	-1.170651	-1.303498
AALF006132	Unspecified product	-0.8459656	-1.311609
AALF025231	Unspecified product	-0.9606379	-1.315466
AALF017372	Translin associated factor x	-0.8760226	-1.315683
AALF016456	Unspecified product	-1.094728	-1.323887
AALF003366	Unspecified product	-1.13667	-1.329196
AALF027074	Unspecified product	-0.8744154	-1.33458

AALF028546	Unspecified product	-0.7905111	-1.339157
AALF016286	Unspecified product	-0.4487126	-1.339759
AALF012694	Putative apolipoprotein d/lipocalin	-0.5927993	-1.350955
AALF022970	Unspecified product	-0.3027337	-1.35262
AALF024663	GPCR Octopamine/Tyramine Family	-1.333525	-1.356435
AALF002599	Unspecified product	-0.3874404	-1.358903
AALF011816	Unspecified product	-0.302958	-1.365927
AALF018011	Unspecified product	-0.2103318	-1.372786
AALF013129	Trehalose-6-phosphate synthase	-0.2856851	-1.373976
AALF003849	Unspecified product	-0.8035338	-1.386232
AALF016501	Unspecified product	-0.8882556	-1.390952
AALF016566	Unspecified product	-0.3666516	-1.39953
AALF026911	GPCR Orphan/Putative Class B Family	-0.8464737	-1.400814
AALF020305	Carboxylic ester hydrolase	-0.7280262	-1.402937
AALF027964	Unspecified product	-1.071808	-1.40415
AALF023403	Unspecified product	-0.8521671	-1.410698
AALF028503	Defense repressor	-0.7520397	-1.417701
AALF012970	Unspecified product	0.2860433	-1.420927
AALF021548	GPCRG astrin/Bombesin Family	-1.129069	-1.427167
AALF021556	Unspecified product	-1.425896	-1.452462
AALF025810	Unspecified product	-1.714804	-1.453152
AALF010876	Unspecified product	-0.716625	-1.461977
AALF008397	Unspecified product	-0.9517475	-1.470575
AALF006674	Unspecified product	-1.075791	-1.472462
AALF006581	Unspecified product	0.1347496	-1.473683
AALF006673	Unspecified product	-0.7910587	-1.500617
AALF010019	Brain chitinase and chia	-0.5632531	-1.525798
AALF004309	Putative sodium/potassium-transporting atpase subunit beta-2	0.6131738	-1.533361
AALF019880	Dihydropyrimidine dehydrogenase [NADP(+)]	0.09513857	-1.555219
AALF010137	Histone H2B	0.12636	-1.581001
AALF014933	Prophenoxidase	0.5348487	-1.584833
AALF020399	Unspecified product	-1.584096	-1.593888
AALF013610	Dihydropyrimidine dehydrogenase [NADP(+)]	0.1022718	-1.623649
AALF022513	Unspecified product	-0.3718985	-1.646279
AALF016111	Unspecified product	-0.9792314	-1.649723
AALF012955	Serine protease	-0.592814	-1.653365
AALF014537	Histone H2B	0.3143672	-1.700164
AALF003951	Unspecified product	-0.8910649	-1.726523
AALF010648	Histone H2B	0.2815907	-1.735993
AALF005415	Unspecified product	-1.435357	-1.758952
AALF020202	Unspecified product	-0.9642724	-1.766137
AALF024124	Cytochrome P450	0.5791274	-1.799292
AALF004118	Unspecified product	-0.9426208	-1.815528

AALF010649	Histone H2A	-0.1002183	-1.937962
AALF011637	Unspecified product	-0.7200285	-1.982807
AALF012023	Unspecified product	-0.9125271	-2.005426
AALF016470	Carboxylic ester hydrolase	-0.07487092	-2.101836
AALF019822	Unspecified product	-1.907426	-2.183592
AALF010790	Unspecified product	-0.4404848	-2.226252
AALF022750	Unspecified product	-1.008224	-2.321371
AALF019479	Unspecified product	-1.597264	-2.50655
AALF013172	Alpha-amylase	-0.6848346	-2.569293
AALF012014	Unspecified product	-1.288233	-2.753047
AALF023401	Unspecified product	-2.11558	-2.809923
AALF018987	Unspecified product	-0.04404843	-3.468187

Supplementary figure

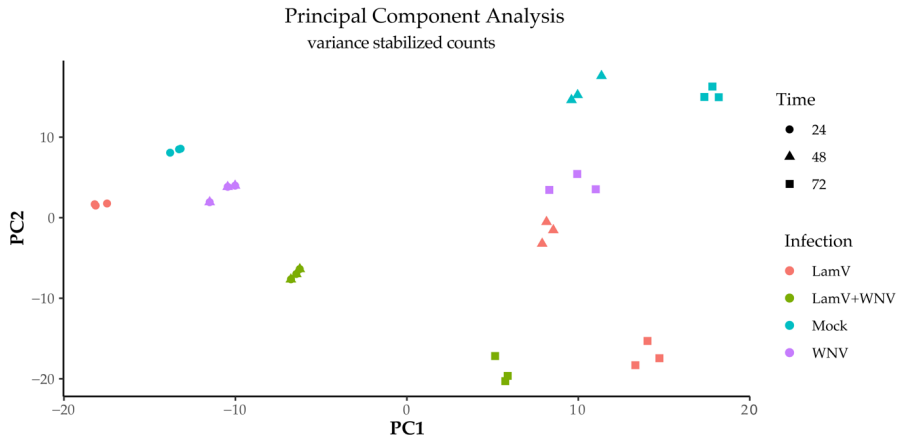


Figure S1. Principal component analysis (PCA) of biological triplicates infected with either LamV, WNV, mock or a dual-infection scheme. The different infection groups are shown as a color and hours post infection are shown as geometrical figures.

ACTA UNIVERSITATIS AGRICULTURAE SUECIAE

DOCTORAL THESIS NO. 2022:18

Mosquitoes serve as vector for many medically important viruses and their associated diseases cause a major health burden across the globe. This thesis has investigated a group of viruses known as insect-specific flaviviruses (ISFVs) with the focus on how they affect the mosquito host and if ISFVs can be used to manipulate the mosquito antiviral immunity to increase host's resistance to infection of medically important arboviruses, with a specific focus on WNV.

Pontus Öhlund received his doctoral education at the Department of Biomedical Sciences and Veterinary Public Health, Swedish University of Agricultural Sciences. His bachelor's and master's degrees were obtained at Uppsala University.

Acta Universitatis Agriculturae Sueciae presents doctoral theses from the Swedish University of Agricultural Sciences (SLU).

SLU generates knowledge for the sustainable use of biological natural resources. Research, education, extension, as well as environmental monitoring and assessment are used to achieve this goal.

Online publication of thesis summary: <http://pub.epsilon.slu.se/>

ISSN 1652-6880

ISBN (print version) 978-91-7760-911-7

ISBN (electronic version) 978-91-7760-912-4